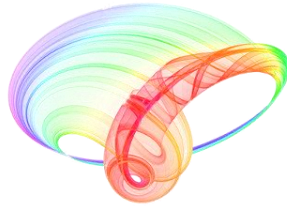


Book of abstracts



PHOTONICA2017

The Sixth International School and Conference on Photonics

& COST actions: MP1406 and MP1402



&H2020-MSCA-RISE-2015 CARDIALLY workshop



28 August – 1 September 2017

Belgrade, Serbia

Editors

Marina Lekić and Aleksandar Krmpot

Institute of Physics Belgrade, Serbia

Belgrade, 2017

ABSTRACTS OF TUTORIAL, KEYNOTE, INVITED LECTURES,
PROGRESS REPORTS AND CONTRIBUTED PAPERS

of

The Sixth International School and Conference on Photonics
PHOTONICA2017

28 August – 1 September 2017
Belgrade Serbia

Editors

Marina Lekić and Aleksandar Krmpot

Technical assistance

Marko Nikolić and Danica Pavlović

Publisher

Institute of Physics Belgrade
Pregrevica 118
11080 Belgrade, Serbia

Printed by

Serbian Academy of Sciences and Arts

Number of copies

300

ISBN 978-86-82441-46-5

PHOTONICA 2017 (The Sixth International School and Conference on Photonica - www.photonica.ac.rs) is organized by Institute of Physics Belgrade, University of Belgrade (www.ipb.ac.rs), Serbian Academy of Sciences and Arts (www.sanu.ac.rs), and Optical Society of Serbia (www.ods.org.rs).



Other institution that helped the organization of this event are: Vinča Institute of Nuclear Sciences, University of Belgrade (www.vinca.rs), Faculty of Electrical Engineering, University of Belgrade (www.etf.bg.ac.rs), Institute of Chemistry, Technology and Metallurgy, University of Belgrade (www.ihtm.bg.ac.rs), Faculty of Technical Sciences, University of Novi Sad (www.ftn.uns.ac.rs), Faculty of Physics, University of Belgrade (www.ff.bg.ac.rs), and Faculty of Biology, University of Belgrade (www.bio.bg.ac.rs).

PHOTONICA 2017 is organized under auspices and with support of the Ministry of Education, Science and Technological Development, Serbia (www.mpn.gov.rs). PHOTONICA 2017 is supported and recognized by The Integrated Initiative of European Laser Research Infrastructures LaserLab-Europe (www.laserlab-europe.eu) and European Physical Society (www.eps.org).



The support of the sponsors of PHOTONICA 2017 is gratefully acknowledged:



Committees

Scientific Committee

Aleksandar Krmpot, Serbia
Antun Balaž, Serbia
Arlene D. Wilson-Gordon, Israel
Bojan Resan, Switzerland
Boris Malomed, Israel
Branislav Jelenković, Serbia
Dejan Gvozdić, Serbia
Detlef Kip, Germany
Dragan Indjin, United Kingdom
Edik Rafailov, United Kingdom
Feng Chen, China
Francesco Cataliotti, Italy
Giannis Zacharakis, Greece
Goran Isić, Serbia
Goran Mašanović, United Kingdom
Isabelle Philippa Staude, Germany
Jelena Radovanović, Serbia
Jerker Widengren, Sweden
Jovana Petrović, Serbia
Laurent Sanchez, France
Ljupčo Hadžievski, Serbia
Marco Santagiustina, Italy
Milan Mashanović, United States of America
Milan Trtica, Serbia
Miloš Živanov, Serbia
Milutin Stepić, Serbia
Milivoj Belić, Qatar
Nikola Stojanović, Germany
Pavle Andus, Serbia
Peđa Mihailović, Serbia
Radoš Gajić, Serbia
Schaaf Peter, Germany
Sergei Turitsyn, United Kingdom
Suzana Petrović, Serbia
Ticijana Ban, Croatia
Vladana Vukojević, Sweden
Zoran Jakšić, Serbia
Željko Šljivančanin, Serbia

Organizing Committee

Aleksandar Krmpot, (Chair)
Marina Lekić (Secretary)
Stanko Nikolić (webmaster)
Marko Nikolić,
Vladimir Veljić
Danica Pavlović

Technical Organizer



Dear Colleagues, friends of photonics,

We are honored by your participation at our PHOTONICA 2017 and your contribution to the tradition of this event. It is our pleasure to host you in Belgrade and in Serbia. Welcome to the world of photonics.

The International School and Conference on Photonics- PHOTONICA, is a biennial event held in Belgrade since 2007. The first meeting in the series was called ISCOM (International School and Conference on Optics and Optical Materials), but it was later renamed to PHOTONICA to reflect more clearly the aims of the event as a forum for education of young scientists, exchanging new knowledge and ideas, and fostering collaboration between scientists working within emerging areas of photonic science and technology. A particular educational feature of the program is to enable students and young researchers to benefit from the event, by providing introductory lectures preceding most recent results in many topics covered by the regular talks. In other words, tutorial and keynote speakers will give lectures specifically designed for students and scientists starting in this field. Apart from the oral presentations PHOTONICA hosts vibrant poster sessions. A significant number of best posters will be selected and the authors will have opportunity to present their work through short oral presentations – contributed talks.

The wish of the organizers is to provide a platform for discussing new developments and concepts within various disciplines of photonics, by bringing together researchers from academia, government and industrial laboratories for scientific interaction, the showcasing of new results in the relevant fields and debate on future trends.

This PHOTONICA 2017 will include two COST Action meetings and one workshop with the main objective to promote knowledge in various disciplines of photonics. In addition, the representatives of the companies related to photonics will have significant role at the event by presenting the new trends in research and development sector.

Following the official program, the participants will also have plenty of opportunities to mix and network outside of the lecture theatre with planned free time and social events. Participating in the social program of PHOTONICA 2017, visiting the attractions of Belgrade like the Nikola Tesla museum or simply walking around the city center, the participants will have opportunity to meet Belgrade and Serbia and to learn useful facts about culture and history of the region.

This book contains 216 abstracts of all presentations at the VI International School and Conference on Photonics, PHOTONICA2017. Authors from all around the world, from all the continents, will present their work at this event. There will be five tutorial and seven keynote lectures to the benefits of students and early stage researches. The most recent results in various research fields of photonics will be presented through twenty one invited lectures and nine progress reports of early stage researchers. Within the two poster sessions and a number of contributed talks, authors will present 174 their new results in a cozy atmosphere of the building of Serbian Academy of Science and Arts.

Belgrade, July 2017

Editors

PHOTONICA 2017 Timetable (Serbian Academy of Sciences and Arts - Main Hall)

Monday, August 28 th	Tuesday, August 29 th	Wednesday, August 30 th	Thursday, August 31 st	Friday, September 1 st
08.00-17.00 Registration	08.00-17.00 Registration	08.00-12.00 Registration	08.00-12.00 Registration	
08.30-09.00 Opening				
09.00-09.35 Krolikowski	09.00-09.35 Chichkov	09.00-09.35 Zalevsky	09.00-09.35 Weis	09.00 – 09.45 Pernice
09.35-09.45 Discussion break	09.35-09.45 Discussion break	09.35-09.45 Discussion break	09.35-09.45 Discussion break	
09.45-10.20 Krolikowski	09.45-10.20 Chichkov	09.45-10.20 Zalevsky	09.45-10.20 Weis	09.45– 10.30 Belić
10.20-10.40 Coffee break	10.20-10.40 Coffee break	10.20-10.40 Coffee break	10.20-10.40 Coffee break	10.30 – 10.50 Coffee break
10.40-11.25 Hingerl	10.40-11.25 Jerker	10.40-11.25 Kralj	10.40-11.25 Adhikari	10.50 – 11.35 Barry
11.25-11.35 Discussion break	11.25-11.35 Discussion break	11.25-11.35 Discussion break	11.25-11.35 Discussion break	
11.35-12.05 Pasiskevicius	11.35-12.05 Jakovcevski	11.35-12.05 Artemyev	11.35-12.05 Pelster	11.35-11.45 Discussion break
12.05-12.35 Fratalochi	12.05-12.35 Štrancar	12.05-12.35 Teichert	12.05-12.35 Salasnich	11.45 - 12.15 Leisher
12.35-14.30 LUNCH BREAK	12.35-14.30 LUNCH BREAK	12.35-14.30 LUNCH BREAK	12.35-14.30 LUNCH BREAK	12.15 - 12.45 Gerharth
				12.45-14.30 LUNCH BREAK
14.30-15.05 Radić	14.30-15.00 Luning	14.30-15.00 Rakich	14.30-15.00 Loew	14.30-15.00 van Oosten
15.05-15.10 Discussion break	15.00-15.30 Dučić	15.00-15.30 Baronio	15.00-15.30 Affolderbach	15.00-15.30 Zamfiresku
15.10-15.45 Radić	15.30-15.45 CT3	15.30-16.00 Setzpfandt	15.30-15.45 CT6	15.30-15.45 CT8
15.45-16.00 CT1	15.45-16.00 CT4		15.45-16.00 CT7	15.45-16.00 CT9
16.00-16.20 Coffee break	16.00-16.20 Coffee break	18.00 – 20.00 Excursion (boat trip and sightseeing from Belgrade rivers)	16.00-16.20 Coffee break	16.00-16.20 Coffee break
16.20-16.50 Slavik	16.20-16.50 Borzsonyi		16.30 – 18.30 Posters & Industrial talks	16.20-16.50 Longo
16.50-17.10 Tarasov	16.50-17.10 Krešić			16.50-17.10 Stupar
17.10-17.30 Chernysheva	17.10-17.30 Mladenović			17.10-17.30 Bajić
17.30-17.50 Popovic	17.30-17.50 Ralević			17.30-17.50 Obradov
17.50-18.05 CT2	17.50-18.05 CT5			17.50 -18.05 CT10
				18.05-18.20 CT11
18.30 -20.00 Cocktail	18.15 – 20.00 Posters &Industrial talks			18.20 Closing
			20.00 ---- Conference dinner (bohemian quarter Skadarlija)	

Tutorial lecture	2x35 min	Keynote lecture	45 min	Invited lecture	30 min	Special invited lecture	30 min	Progress report	20 min	Contributed talk -CT	15 min
---------------------	-------------	--------------------	-----------	--------------------	-----------	-------------------------------	-----------	--------------------	-----------	-------------------------	-----------

Conference Topics

1. Quantum optics and ultracold systems
2. Nonlinear optics
3. Optical materials
4. Biophotonics
5. Devices and components
6. Optical communications
7. Laser spectroscopy and metrology
8. Ultrafast optical phenomena
9. Laser - material interaction
10. Optical metamaterials and plasmonics
11. Other topics in photonics

Table of Contents

Tutorial lectures

T.1	A fully algebraic approach to magneto-optical effect in atoms:.....2 Lecture 1: "Stokes parameters, atomic multipole moments and their interaction" Lecture 2: "Atom light interactions in the presence of magnetic fields" <i>Antoine Weis</i>	2
T.2	Lecture 1: "3D laser printing of polymers, nanoparticles, and living cells"3 Lecture 2: "3D laser printing of polymers, nanoparticles, and living cells" <i>Boris Chichkov</i>	3
T.3	Beyond the myth of nonlinear capacity limits in fiber optic transmission.....4 <i>S. Radic and N. Alic</i>	4
T.4	Self-organization of light in media with competing nonlocal nonlinearities.....5 <i>F. Maucher, T.Poh, S.Skupin and W.Krolikowski</i>	5
T.5	Translation of remote photons based sensing into virtual tactile and hearing senses.....6 <i>Yevgeny Beiderman, Yafim Beiderman, Sergey Agdarov and Zeev Zalevsky</i>	6

Keynote lectures

K.1	Ultrasensitive and ultrahigh resolution fluorescence spectroscopy and imaging for fundamental biomolecular studies and towards clinical diagnostics.....8 <i>Jerker Widengren</i>	8
K.2	A classical model for depolarization by temporal and spatial decoherence.....9 <i>Kurt Hingerl</i>	9
K.3	Developing high capacity fibre transmission systems employing spectrally efficient super-channel technology.....10 <i>Vidak Vujicic, Cosimo Calò, Colin Browning, Kamel Merghem, Anthony Marlinez, Abderrahim Ramdane, Liam P Barry</i>	10
K.4	In situ visual observation of 2D materials growth and modifications, and characterization of their optical properties.....11 <i>Marko Kralj</i>	11
K.5	Rogue waves, Talbot carpets and accelerating beams.....12 <i>M.R. Belic, S. Nikolic, O. Ashour, and Y.Q. Zhang</i>	12
K.6	All-optical processing using phase-change nanophotonics.....13 <i>Wolfram Pernice</i>	13
K.7	Three-dimensional "solitons" in Bose-Einstein condensates and nonlinear optics.....14 <i>Sadhan K. Adhikari</i>	14

Invited lectures

I.1	Metal free structural colors via disordered nanostructures with nm resolution and full CYMK color spectrum.....16 <i>V. Mazzone, M. Bonifazi and A. Fratalocchi</i>	16
I.2	Two Intriguing Examples for Topological Effects in Ultracold Atoms.....17 <i>Axel Pelster</i>	17

I.3	Organic crystalline nanoneedles on 2D materials and their optoelectronic properties.....	18
	<i>Christian Teichert</i>	
I.4	Precision measurements for compact vapor-cell atomic clocks.....	19
	<i>C. Affolderbach, M. Gharavipour, F. Gruet, W. Moreno, M. Pellaton, and G. Mileti</i>	
I.5	Time-resolved studies of femtosecond laser surface ablation of dielectrics and Semiconductors(in air).....	20
	<i>Dries van Oosten</i>	
I.6	Dark Line, Lump and X-solitary Waves in Optical Media.....	21
	<i>F. Baronio and S. Wabnitz</i>	
I.7	Spontaneous parametric down-conversion in periodically structured media.....	22
	<i>Frank Setzpfandt</i>	
I.8	Confocal synaptology - a simple method for the assessment of synaptic re-arrangements in neurodegenerative disorders and upon nervous system injury.....	23
	<i>Igor Jakovcevski</i>	
I.9	Single Photons: Hong-Ou-Mandel Experiments and beyond.....	24
	<i>Mohammad Rezaei, Jörg Wrachtrup and Ilja Gerhardt</i>	
I.10	Probing Ultrafast Magnetization Dynamics with Resonant X-ray Scattering Techniques.....	25
	<i>Jan Luning</i>	
I.11	Lipid wrapping as a molecular initiating event in nanotoxicology through fluorescence microspectroscopy and super-resolution microscopy.....	26
	<i>I. Urbančič, M. Garvas, B. Kokot, H. Majaron, P. Umek, M. Škarabot, F. Schneider, S. Galiani, Z. Arsov, T. Koklič, A. Mertelj, I. Muševič, C. Eggeling and J. Štrancar</i>	
I.12	Bright solitons in ultracold atoms.....	27
	<i>Luca Salasnich</i>	
I.13	Applications of 3D laser lithography.....	28
	<i>M. Zamfirescu, B. Calin, F. Jipa and Irina Paun</i>	
I.14	Optical properties of 2D colloidal semiconductor quantum wells and hybrid structures.....	29
	<i>Mikhail Artemyev</i>	
I.15	Advancements in high efficiency semiconductor lasers for high power applications.....	30
	<i>Paul O. Leisher</i>	
I.16	Stimulated Brillouin Scattering in Silicon Photonics.....	31
	<i>Peter Rakich</i>	
I.17	Signal Propagation Time through Hollow-Core Fibres and its Low Sensitivity to Temperature.....	32
	<i>R. Slavík, E. Numkam Fokoua, M. N. Petrovich, N. V. Wheeler, T. Bradley, F. Poletti, and D.J. Richardson</i>	
I.18	Hot Rydberg atoms and more.....	33
	<i>Robert Löw</i>	
I.19	Synchrotron light based spectro-microscopies: illumination of cellular disorders in neuro-degenerative diseases.....	34
	<i>Tanja Dučić</i>	
I.20	Backward-wave optical parametric interactions in structured nonlinear media.....	35
	<i>V. Pasiskevicius, C. Canalias, A. Zukauskas</i>	

Special invited lecture

S.1	Research opportunities within LaserLab Europe and ELI.....	36
	<i>Adam Borzsonyi</i>	

Progress reports

P.1	Development and application of an electronic sensing system by using polymer optical fibre with sensitive zone.....	38
	<i>D. Stupar, J. Bajić and M. Živanov</i>	
P.2	Frequency comb cooling of rubidium atoms.....	39
	<i>N. Šantić, I. Krešić, A. Cipriš, T. Ban and D. Aumiler</i>	
P.3	Low cost optical sensors for absolute rotary position measurement.....	40
	<i>Jovan S. Bajić, Dragan Z. Stupar, Ana Joža, Branislav Batinić, Nikola Laković, Miloš B. Živanov</i>	
P.4	Mid-infrared fibre laser sources and their application for vibrational spectroscopy.....	41
	<i>Maria Chernysheva</i>	
P.5	Photoacoustic response of an transmission photoacoustic configuration for two-layer samples with thermal memory.....	42
	<i>M.N. Popovic, M. Nesic, D. Markushev, M. Zivanov, S. Galovic</i>	
P.6	Electronic Properties of Interfaces between Domains in Organic Semiconductors.....	43
	<i>M. Mladenovic and N. Vukmirovic</i>	
P.7	Plasmonics for infrared detectors.....	44
	<i>Marko Obradov</i>	
P.8	Instabilities in nonlinear systems.....	45
	<i>N. Tarasov, A. M. Perego and S. K. Turitsyn</i>	
P.9	Surface enhanced Raman spectroscopy of thiocyanine coated silver nanoparticle clusters.....	46
	<i>U. Ralević, G. Isić, B. Laban, D. Vasić Aničijević, V. Vodnik, U. Bogdanović, V. Vasić, V. M. Lazović and R. Gajić</i>	

1. Quantum optics and ultracold systems

Q.O.1	Ultraslow propagation of optical pulses in hot potassium vapor.....	48
	<i>B. Zlatković, A. J. Krmpot, D. Arsenović, I. S. Radojičić, M. M. Čurčić, Z. Nikitović, and B. M. Jelenković</i>	
Q.O.2	Parallel solvers for dipolar Gross-Pitaevskii equation.....	49
	<i>V. Lončar, D. Vudragović, S. K. Adhikari, and A. Balaž</i>	
Q.O.3	Effect of conduction band Non-parabolicity on the intersubband transitions in ZnO/Mg _x Zn _{1-x} O Quantum Well Heterostructures.....	50
	<i>Y. Chrafić, L. Moudou, K. Rahmani, I. Zorkani</i>	
Q.O.4	Deformation of the Fermi Surface.....	51
	<i>Vladimir Veljić, Antun Balaž and Axel Pelster</i>	
Q.O.5	Transport dynamics in optical lattices with flux.....	52
	<i>A. Hudomal, I. Vasić, H. Buljan, W. Hofstetter, and A. Balaž</i>	
Q.O.6	Quantum phase gate based on quantum Zeno dynamics.....	53
	<i>H. V. Do, C. Lovecchio, S. Gherardini, M. Muller, F. Caruso and F. S. Cataliotti</i>	
Q.O.7	Open-Dissipative Gross-Pitaevski Approach to Photon BEC Dynamics.....	54
	<i>Enrico Stein, Axel Pelster</i>	
Q.O.8	Excitation spectra of a Bose-Einstein condensate with an angular spin-orbit coupling.....	55
	<i>I. Vasić and A. Balaž</i>	
Q.O.9	A distinguishable single excited-impurity in a Bose-Einstein condensate.....	56
	<i>Javed Akram</i>	
Q.O.10	Photonic simulation of open quantum systems with various exchange statistics.....	57
	<i>Milan Radonjić and Philip Walther</i>	

Q.O.11	Electromagnetically induced transparency in degenerate 3-level ladder-type system.....	58
	<i>Lj. Stevanović, N. Filipović and V. Pavlović</i>	
Q.O.12	Husimi function for time-frequency analysis in optical, microwave and plasmonics applications.....	59
	<i>Milena D Davidović, Miloš D Davidović, Ljubica D Davidović, Vladimir A Andreev, Dragomir M Davidović</i>	
 2. Nonlinear optics		
N.O.1	Quasi-stable rotating solitons supported by a single spiral waveguide.....	60
	<i>Aleksandra I. Strinić, Milan S. Petrović, Najdan B. Aleksić and Milivoj R. Belić</i>	
N.O.2	Routing of optical beams by asymmetric defects in (non)linear waveguide arrays.....	61
	<i>M. Stojanović Krasić, S. Jovanović, A. Mančić and M. Stepić</i>	
N.O.3	Four wave mixing in potassium vapor with off-resonant double lambda system.....	62
	<i>D. Arsenović, M. M. Ćurčić, B. Zlatković, A. J. Krmpot, I. S. Radojičić, T. Khalifa and B. M. Jelenković</i>	
N.O.4	Towards the fully developed statistical approach of vector rogue waves.....	63
	<i>A. Mančić, A. Maluckov, F. Baronio, Lj. Hadzievski, S. Wabnitz</i>	
N.O.5	Signatures of non-quenched disorder in the wave pattern's spreading in flat band geometries.....	64
	<i>G. Gligorić, A. Maluckov</i>	
N.O.6	Molecules in a bicircular strong laser field.....	65
	<i>D. Habibović, A. Čerkić, M. Busuladžić, A. Gazibegović-Busuladžić, S. Odžak, E. Hasović, and D. B. Milošević</i>	
N.O.7	Enhanced second harmonic generation in lithium niobate photonic crystal cavities.....	66
	<i>Reinhard Geiss, Séverine Diziain, Michael Steinert and Thomas Pertsch</i>	
N.O.8	Solitons generated by self-organization in bismuth germanium oxide single crystals during the interaction with laser beam.....	67
	<i>V. Skarka, M. Lekić, A. Kovačević, B. Zarkov, and N. Z. Romčević</i>	
N.O.9	Broad-band femtosecond pulses, λ^3 type diffraction and X-waves. Evolution and management.....	68
	<i>V. Slavchev, A. Dakova, D. Dakova, K. Kovachev and L. Kovachev</i>	
N.O.10	Sum frequency conversion of compact Q-switched cryogenic slab RF discharge CO laser radiation in nonlinear ZnGeP ₂ crystal.....	69
	<i>A. Ionin, I. Kinyaevskiy, Yu. Klimachev, Yu. Kochetkov, A. Kozlov, L.V. Seleznev, D. Sinitsyn, D. Zemtsov</i>	
N.O.11	Realizing aperiodic photonic lattices by synthesized Mathieu-Gauss beams.....	70
	<i>J. M. Vasiljević, Alessandro Zannotti, D. V. Timotijević, Cornelia Denz, D. M. Jović Savić</i>	
N.O.12	Measurement of powerful ultrashort UV pulse parameters.....	71
	<i>A.A. Ionin, D.V. Mokrousova, D.A. Piterimov, L.V. Seleznev, A.V. Shutov, E.S. Sunchugasheva, N.N. Ustinovskii, V.D. Zvorykin</i>	
N.O.13	Polarization properties of vector solitons in optical fibers.....	72
	<i>A. Dakova, L. Kovachev, D. Dakova, D. Georgieva and V. Slavchev</i>	
N.O.14	Optical-Terahertz Solitons.....	73
	<i>A.N. Bugay and S.V. Sazonov</i>	
N.O.15	Vortices and topological structures in photorefractive materials.....	74
	<i>M. Ćubrović and M. Petrović</i>	
N.O.16	Exact traveling and solitary wave solutions to the generalized Gross-Pitaevskii equation with cylindrical potential.....	75
	<i>Nikola Z. Petrović</i>	
N.O.17	Nonlinear Fourier analysis of a mode-locked laser.....	76

	<i>M. Kamalian, A. M. Perego, J. Prilepsky and S. K. Turitsyn</i>	
N.O.18	Nonlinear light scattering and nonlinear absorption in photorefractive LiNbO ₃ crystals studied by Z-scan technique.....	77
	<i>S.M. Kostritskii, M. Aillerie, E. Kokanyan, O.G. Sevostyanov</i>	
N.O.19	Gain analysis for fiber optical parametric amplifier in presence of attenuation and dispersion fluctuations.....	78
	<i>M. S. Kovacevic, Lj. Kuzmanovic, and A. Djordjevich</i>	
N.O.20	Analytical and dynamical generation of higher-order solitons and breathers of the extended nonlinear Schrödinger equation on different backgrounds.....	79
	<i>S. N. Nikolić, Najdan B. Aleksić, Omar A. Ashour, Milivoj R. Belić, Siu A. Chin</i>	
 3. Optical materials		
O.M.1	Enhancing conductivity of self-assembled transparent graphene films with UV/Ozone Treatment.....	80
	<i>T. Tomasević-Ilić, Đ. Jovanović, J. Pešić, A. Matković, M. Spasenović, R. Gajić</i>	
O.M.2	One-step synthesis of NIR-responsive NaYF ₄ :Yb,Er@Chitosane nanoparticles for biomedical application.....	81
	<i>I. Dinic, A. Djukic-Vukovic, L. Mojovic, M.G. Nikolic, M.D. Rabasovic, A.J. Krmpot, O. Milosevic and L. Mancic</i>	
O.M.3	Defect detection in aluminum using pulse thermography for a sample width periodic structure.....	82
	<i>V. Damnjanović, Lj. Tomić, G. Dikić, B. Milanović and S. Petričević</i>	
O.M.4	Rare-earth enabled silicon light emitting diodes for the near-infrared.....	83
	<i>M. A. Lourenço and K. P. Homewood</i>	
O.M.5	Band edge modified rare-earth doped silicon for efficient mid-infrared photodetectors.....	84
	<i>K. P. Homewood and M. A. Lourenço</i>	
O.M.6	Selection of optical polymers in lens design.....	85
	<i>N. Sultanova, S. Kasarova, I. Nikolov and R. Kasarov</i>	
O.M.7	Photoluminescence spectroscopy of CdSe nanoparticles embedded in transparent glass.....	86
	<i>M. Gilić, R. Kostić, D. Stojanović, M. Romčević, B. Hadžić, Z. Lazarević, J. Trajić, J. Ristić-Đurović, N. Romčević</i>	
O.M.8	Improved thermal and mechanical properties of tot'hema–gelatin eco-friendly films.....	87
	<i>B. Muric, D. Pantelic, D. Vasiljevic and B. Jelenkovic</i>	
O.M.9	Ab-initio calculations of electronic and vibrational properties of Sr and Yb-intercalated grapheme.....	88
	<i>A. Šolajić, J. Pešić and R. Gajić</i>	
O.M.10	Influence of x-ray irradiation on the dielectric properties of YbF ₃ -doped (Ba/Ca)F ₂ crystals.....	89
	<i>M. Stef and I. Nicoara</i>	
O.M.11	Bifurcation in reflection spectra of holographic pullulan diffraction grating.....	90
	<i>S. Savić-Šević, D. Pantelić, V. Damljanović and B. Jelenković</i>	
O.M.12	Discrete and Selective Absorption in Crystalline Molecular Nanofilms.....	91
	<i>M. Vojnović, A.J. Šetrajić – Tomić, S.M. Vučenović, J.P. Šetrajić</i>	
O.M.13	Optical properties of atomic layer deposition prepared Al-doped ZnO for photonic applications.....	92
	<i>N. Bojinov, V. Marinova and D. Z. Dimitrov</i>	
O.M.14	An example of two-dimensional crystal structure with semi-Dirac electronic dispersion.....	93
	<i>V. Damljanović and R. Gajić</i>	
O.M.15	Ab-initio study of optical properties of MoS ₂ and WS ₂ compared to spectroscopic results of liquid phase exfoliated nanoflakes.....	94

	<i>Jelena Pešić, Jasna Vujin, Tijana Tomašević-Ilić, Marko Spasenović Radoš Gajić</i>	
O.M.16	Nanostructured films based on Au nanocrystals of different morphology for SERS.....	95
	<i>T.H. Beinyk, N.A. Matveevskaya, S.V. Dukarov</i>	
O.M.17	Self-polarization effects in spherical core-shell quantum dot.....	96
	<i>D. Stojanović, R. Kostić</i>	
O.M.18	Sb- based phase- change materials.....	97
	<i>D. Z. Dimitrov</i>	
O.M.19	Electronic and optical properties of square HgTe quantum dots.....	98
	<i>D. B. Topalović, V. V. Arsoški, N. A. Čukarić, M. Ž. Tadić and F. M. Peeters</i>	
O.M.20	Polarization holographic gratings with high diffraction efficiency recorded in azopolymer PAZO.....	99
	<i>L. Nedelchev, D. Ivanov, N. Berberova and D. Nazarova</i>	
O.M.21	Optical and microstructural characterization of NiO:K.....	100
	<i>P. Petkova, A. Boukhachem, P. Vasilev and V. Altonyan</i>	
O.M.22	Luminescence thermometry using Gd ₂ Zr ₂ O ₇ :Eu ³⁺	101
	<i>M.G. Nikolic, M.S. Rabasovic, J. Krizan, S. Savic-Sevic, M.D. Rabasovic, B.P. Marinkovic, A. Vlastic and D. Sevic</i>	

4. Biophotonics

B.1	Using infrared radiation for the measurement of arterial blood flow waveform.....	102
	<i>B. Stojadinović, Z. Nestorović, D. Žikić</i>	
B.2	Study on relationship between amyloid-β peptides and metal ions via two-photon excitation fluorescence microscopy.....	103
	<i>S. Jovanić, N. Loncarevic, M. Rabasovic, A. Krmpot, M. Jovic, S. Kanazir, and B. Jelenkovic</i>	
B.3	Two-photon excited hemoglobin fluorescence for <i>ex vivo</i> microscopy analysis of erythrocytes at single cell level.....	104
	<i>I. T. Drvenica, A. Stančić, S. Jovanić, V. Lj. Ilić, M. D. Rabasović, D. V. Pantelić, B. M. Jelenković, B.M. Bugarski, A. J. Krmpot</i>	
B.4	Feasibility study of TPEF, SHG & CFM for soft tissue neoplasia analysis.....	105
	<i>Ts. Genova, E. Borisova, G. Stanciu, D. Tranca, O. Semyachkina-Glushkovskaya, D. Gorin, I. Terziev</i>	
B.5	Phycomyces blakesleeanus hypha cell wall surgery by Ti: Sapphire laser.....	106
	<i>T. Pajić, K. Stevanovic, N. Todorovic, A. Krmpot, M. Rabasovic, V. Lazovic, D. Pantelic, B. Jelenkovic⁴ and M. Zivic</i>	
B.6	Peculiarities of cw laser beam imaging of contrasting small-depth inclusions in highly-scattering media.....	107
	<i>T. Dreischuh, L. Gurdev, O. Vankov, E. Toncheva, L. Avramov, D. Stoyanov</i>	
B.7	Compact lasers for innovative non-invasive biomedical research and diagnostics.....	108
	<i>Karina S. Litvinova, Sergei G. Sokolovski, Edik U. Rafailov</i>	
B.8	Study of acute complications of diabetes mellitus type II by Raman spectroscopy.....	109
	<i>M. Miletić, S. Askračić, D. Popović, M. Djordjević, I. Mrdović and Z. Dohčević-Mitrović</i>	
B.9	Synchrotron based X-ray microscopy for the verification of trace metals and SOD1 protein aggregates in intact astrocytes from arat model of amyotrophic lateral sclerosis.....	110
	<i>S. Stamenković, B. Lai, P. Andjus and T. Dučić</i>	
B.10	Light controllable TiO ₂ -Ru nanocomposite system encapsulated in small unilamellar vesicles for anti-cancer photodynamic therapy.....	111
	<i>M. Matijević, M. Nešić, I. Popović, M. Stepić, M. Radoičić, Z. Šaponjić and M. Petković</i>	
B.11	Application of multiparametric cardiac measurement system in ejection fraction calculation.....	112
	<i>Marjan Miletić, Marija D. Ivanović, Lana Popović Maneski, Boško Bojović</i>	

B.12	Nonlinear microscopy as a novel method for studying insect morphology.....	113
	<i>D. Pavlović, D. Pantelić, A. Krmpot, M. Rabasović, V. Lazović, M. Vrbica, S. Čurčić</i>	
B.13	Confocal image analysis of immunohistochemistry of connexin isoforms during the second trimester of gestation of the human fetal brain development.....	114
	<i>Dušica Kočović, Mandakini B. Singh, Jasmina Tadić, Svetlana Vrzić-Petronijević, Pavle R. Andjus and Srdjan D. Antic</i>	
B.14	Combined photoacoustic and optical microscopy for the detailed description of ciliary body anatomy.....	115
	<i>George J. Tserévelakis, Stella Avtzi, Miltiadis K. Tsilimbaris, and Giannis Zacharakis</i>	
B.15	Analysis of human healthy dentin microstructure by using two photon excitation fluorescence microscopy and second harmonic generation.....	116
	<i>Tijana Lainović, Mihailo Rabasović, Larisa Blažić, Dejan Pantelić, Aleksandar Krmpot, Vladimir Lazović, Branislav Jelenković</i>	
B.16	Second harmonic generation imaging of collagen fibers in the uninvolved human rectal mucosa 10 cm and 20 cm away from the malignant tumor.....	117
	<i>Sanja Despotović, Ivana Lalić, Novica Milićević, Živana Milićević, Mihailo Rabasović, Dejan Pantelić, Svetlana Jovanić and Aleksandar Krmpot</i>	
B.17	Voltage-Sensitive Dye Imaging of Membrane Potential Transients in Thin Dendritic Branches of Cortical Pyramidal Neurons.....	118
	<i>Jesse A. White, Mandakini B. Singh and Srdjan D. Antic</i>	
B.18	Designing Multi-Functional Plasmonic Nanoparticles for Cancer Theranostics.....	119
	<i>E. D. Onal and K. Guven</i>	
B.19	Method of preparing biomedical samples for cancer detection by infrared spectroscopy.....	120
	<i>J. L. Ristić-Djurović, S. T. Čirković, N. Paunović, J. T. Juloski, S. R. De Luka, V. M. Čuk, M. Romčević, A. M. Trbovich and N. Romčević</i>	
B.20	Fetal Actometer Based on Optical Fibre Gratings.....	121
	<i>V. Atanasoski, M. Ivanovic, N. Stojanovic, Lj. Hadzievski and J. Petrovic</i>	
B.21	Time resolved luminescence spectra of greater celandine (<i>Chelidonium majus</i> L.).....	122
	<i>M. S. Rabasovic, D. Sevic, M. D. Rabasovic, M. G. Nikolic and B. P. Marinkovic</i>	
B.22	Quantitative characterization of receptor-receptor interactions in live cells using dual-color fluorescence cross-correlation spectroscopy.....	123
	<i>V. Radoi, A. A. Ghavanini, J. Rüegg, E. Kosek and V. Vukojevic</i>	
B.23	Effect of Size and Geometry of Quantum Dots on Performance of Time Resolved Fluorescence Spectroscopy; A Monte Carlo Study.....	124
	<i>Amid Rahi, Tahereh Tekieh, and Pezhman Sasanpour</i>	
B.24	Optimized Design of Intensity Based Plasmonic Fiber Biosensor; Modeling and Experiment.....	125
	<i>Mitra Abedini, Raheleh Mohammadpour, Mohsen Ahmadi, and Pezhman Sasanpour</i>	
B.25	The effect of short-term fish oil supplementation on Alzheimer disease-like pathology in 5xFAD mouse model.....	126
	<i>Milena Jović, Nataša Lončarević-Vasiljković, Desanka Milanović, Vladimir Avramović, Marjana Brkić, Selma Kanazir</i>	
 5. Devices and components		
D.C.1	A New Method for Multi-Bit and Qudit Transfer Based on Commensurate Waveguide Arrays.....	127
	<i>J. Krsic, P. Veerman and J. Petrovic</i>	
D.C.2	Digital holography of graphene oxide paper acoustic membranes.....	128
	<i>J. Mitrić, D. Abramović, D. Todorović, N. Demoli, M. Spasenović</i>	
D.C.3	Polarized Intensity Reduction of Red-Sea Glint Reflection.....	129

	<i>R. Avrahamy, B. Milgrom, S. Hava</i>	
D.C.4	Self-pulsing in monolithic and external cavity mid-IR QCLs.....	130
	<i>N. Vukovic, J. Radovanovic, V. Milanovic and D.L. Boiko</i>	
D.C.5	Eigenmode and frequency domain analysis of the third-order microring filters.....	131
	<i>M. Radmilović-Radjenović and B. Radjenović</i>	
D.C.6	Analysis of the transmission and tunneling time characteristics in light propagation through anisotropic media.....	132
	<i>N. Opacak, J. Radovanovic and V. Milanovic</i>	
D.C.7	3D finite element eigenmode analysis of coupling mode induced resonance frequency shift in coupled microring resonators.....	133
	<i>B. Radjenović, M. Radmilović-Radjenović and P. Beličev</i>	
D.C.8	Coupled-mode theory approximation of scattering parameters of antisymmetric structures.....	134
	<i>V. Milosevic and B. Jokanovic</i>	
D.C.9	Fabry-Pérot lasers with Al-containing quantum wells in the COBRA generic photonic integration platform.....	135
	<i>F. Lemaître, J. Decobert, H. Ambrosius, G. Binet, N. Lagay, R. Van Veldhoven, F. Pommereau and K. Williams</i>	
D.C.10	Terahertz narrowband transmission filters based on guided mode resonant metallic gratings.....	136
	<i>A. Ferraro, D. C. Zografopoulos, R. Caputo, and R. Beccherelli</i>	
D.C.11	Modeling of aircraft IC signature based on comparative tracking.....	137
	<i>D. Knežević, P. Matavulj and Z Nikolić</i>	
D.C.12	Graphene acoustic diaphragms.....	138
	<i>M. Spasenović, J. Mitrić, D. Abramović, N. Demoli, D. Grujić, D. Pantelić, D. Todorović</i>	
D.C.13	Hybrid organic/inorganic devices for display applications.....	139
	<i>V. Marinova, Y.C. Su, C. C. Chiou, S. Petrov, Ch. Dikov, D. Dimitrov and S. H. Lin</i>	
D.C.14	Laser Fabrication of Diffractive Optical Elements for Two-dimensional Airy Beams.....	140
	<i>Bogdan – Ștefăniță Călin, Liliana Preda, Florin Jiipa, Marian Zamfirescu</i>	
D.C.15	Development of composite wavelength tunable interference wedged structures for laser technology, spectroscopy and optical communications.....	141
	<i>Marin Nenchev, Margarita Deneva and Elena Stoykova</i>	
D.C.16	Temperature Measurement with Ruby gauge.....	142
	<i>M. Nikolic, A. Vlasic and D. Lukic</i>	
D.C.17	Insight into different module options for the electro-absorption modulator.....	143
	<i>M. Trajkovic, F. Blache, H. Debregeas, K. Williams and X. Leijtens</i>	
D.C.18	Optimization of the cleaning properties of fog by means of an optical sensor for control of impurities in	144
	<i>O. Ivanov, P. Todorov, S. Markova, Y. Ralev, J. L. Pérez-Díaz</i>	
D.C.19	Systems for 2-dimensional laser scanning of solid surfaces.....	144
	<i>O. Ivanov, K. Pashev, P. Todorov, Y. Ralev, J. L. Pérez-Díaz, K. Balashev</i>	
6.	Optical communications	
O.C.1	Multiparameter QKD authentication protocol design over optical quantum channel.....	145
	<i>Nemanja Miljković, Aleksandar Stojanović, Rubens Viana Ramos, Petar Matavulj</i>	
O.C.2	Reconfigurable all-optical NAND/NOR logic gate based on dual injection-locked laser diodes.....	146
	<i>M. Lalović, A. Mićević, M. Krstić, J. Crnjanski, A. Totović and D. Gvozdić</i>	
O.C.3	Ultrahigh-speed hybrid VCSEL for short-distance optical interconnects.....	147
	<i>V. Topić, G. C. Park, S. Tandukar, L. Ottaviano and I.-S. Chung</i>	

O.C.4	Improving Quality of Service in four-channel WDM Ethernet Passive Optical Network.....	148
	<i>B. Pajčin, P. Matavulj and M. Radivojević</i>	
O.C.5	Quiescent points of self-seeded RSOA-FCL with Rayleigh backscattering feedback.....	149
	<i>A. Totović, J. Crnjanski, M. Krstić and D. Gvozdić</i>	
O.C.6	Estimation of Rayleigh scattering loss in a double clad photonic crystal fiber.....	150
	<i>M. S. Kovacevic, Lj. Kuzmanovic, and A. Djordjevich</i>	

7. Laser spectroscopy and metrology

L.S.M.1	Relaxation times of population and coherences in Rb vapor.....	151
	<i>Ivan S. Radojičić, Mohammadreza Gharavipour, Aleksandar J. Krmpot, Gaetano Mileti and Brana M. Jelenković</i>	
L.S.M.2	The new system for transferring units of temperature in the optical pyrometry in DMDM	152
	<i>Violeta Stankovic, Boban Zarkov, Slavica Simic</i>	
L.S.M.3	Evaluation of temporal scales of migration of cosmetic ingredients into the human skin by two-dimensional dynamic speckle analysis.....	153
	<i>E. Stoykova, B. Blagoeva, D. Nazarova, L. Nedelchev, T. Nikova, Y.M. Kim, H.J. Kang</i>	
L.S.M.4	The Global Network of Optical Magnetometers for Exotic physics searches.....	154
	<i>T. Scholtes, Z. Grujić, V. Lebedev and A. Weis</i>	
L.S.M.5	Light-shift in pulsed optically pumped Rubidium atomic clock.....	155
	<i>William Moreno, Matthieu Pellaton, Mohammadreza Gharavipour, Florian Gruet, Christoph Affolderbach and Gaetano Mileti</i>	
L.S.M.6	Improving the accuracy of cesium magnetometers.....	156
	<i>Z. D. Grujić, P. A. Koss, J. Piller, V. Lebedev, Y. Shi, V. Dolgovskiy, T. Scholtes, S. Colombo and A. Weis</i>	
L.S.M.7	Europium and Samarium dopant ions as luminescent sensors of Y_2O_3 phase transitions under high pressure.....	157
	<i>Ana Vlašić, Mihailo Rabasović, Branka Murić, Vladan Čelebonović and Marko G. Nikolić</i>	
L.S.M.8	Excitation transfer from the Second to the First resonance line of Potassium observed in a hot atomic vapor.....	158
	<i>C. Andreeva, A. Krasteva, A. Markovski, S. Tsvetkov, S. Gateva, S. Gozzini, S. Cartaleva</i>	
L.S.M.9	H-alpha line broadening in diagnostics of pulsed laser plasma in aqueous aerosol.....	159
	<i>M. Momčilović, J. Ciganović, J. Savović, M. Stoiljković</i>	
L.S.M.10	Frequency-doubled laser sources stabilized to Rb-cell references.....	160
	<i>N. Almat, W. Moreno, M. Pellaton, F. Gruet, C. Affolderbach and G. Mileti</i>	
L.S.M.11	Retrieval of group refractive index in a dense atomic vapor helped by buffer gas-assisted radiation channeling.....	161
	<i>A. Papoyan, S. Shmavonyan, Davit Khachatryan and G. Grigoryan</i>	
L.S.M.12	Application of virtual instrumentation into the metrology system for optical thermometer calibration.....	162
	<i>Boban Zarkov, Slavica Simic</i>	

8. Ultrafast optical phenomena

U.O.1	Second order optical autocorrelator for measuring ultra short laser pulses duration.....	163
	<i>Andreja Vladković, Mihailo Rabasović, Torsten Golz, Nikola Stojanović, Dejan Pantelić, Branislav Jelenković, Aleksandar Krmpot</i>	
U.O.2	Origin of Space-separated Charges in Photoexcited Organic Heterojunctions on	

Subpicosecond Time Scales.....	164
<i>Veljko Janković and Nenad Vukmirović</i>	
U.O.3 High-harmonic generation in bulk diamond irradiated by intense ultrashort laser pulse.....	165
<i>Tzveta Apostolova and Boyan Obreshkov</i>	
U.O.4 En route: single-shot THz characterization technique for THz beamline at FLASH1.....	166
<i>R. Pan, E. Zapolnova, T. Golz, M. Rabasovic, A. Krmpot, A. Vladkovic, J. Petrovic, N. Stojanovic</i>	
U.O.5 Tunable High- field THz source at FLASH: Spectral and spatial characterization.....	167
<i>E. Zapolnova, T. Golz, R. Pan, A. Vladkovic</i>	
U.O.6 Multiphoton imaging with blue-diode-pumped SESAM-modelocked Ti:Sapphireoscillator.....	168
<i>B. Resan, A. Rohrbacher, O. E. Olarte, and P. Loza-Alvarez</i>	

9. Laser - material interaction

L.M.I.1 One Approach to Laser Scanning Problems for Improving Road Condition Diagnostics.....	169
<i>N.Slavkovic, D.Mamula Tartalja and M.Bjelica</i>	
L.M.I.2 Photophoresis-based laser trapping with a line optical trap.....	170
<i>A. Porfirev and S. Fomchenkov</i>	
L.M.I.3 Gold chloride cluster ions generated by vacuum laser ablation.....	171
<i>Boris Rajčić, Silvana B. Dimitrijević, Marijana Petković, Marija Nišavić, Mario Cindrić, Filip Veljković and Suzana Veličković</i>	
L.M.I.4 Effect of the Corrected Ionization Potential on the High-Harmonic Generation transition rate in a linearly polarized laser field.....	172
<i>Violeta Petrović, Hristina Delibašić, Kristina Isaković</i>	
L.M.I.5 Laser ablation of nickel/palladium multilayer thin films by nanosecond pulses.....	173
<i>B. Salatić, S. Petrović, D.Peruško, I. Bogdanović-Radović, M. Čekada, P.Panjan, D.Pantelić and B. Jelenković</i>	
L.M.I.6 Effects of nanosecond laser pulses at 248 nm wavelength on multilayer CrN/(Cr,V)N coatings.....	174
<i>B. Gaković, Suzana Petrović, P. Panjan, J. Kovač, V. Lazović, C. Ristoscu, I. Negut and I. N. Mihailescu</i>	
L.M.I.7 A Laser-based Fabrication Method of Carbonized Polyimide Surfaces for Flexible Devices.....	175
<i>Yong-Won Maand Bo Sung Shin</i>	
L.M.I.8 Tungsten modification induced by femtosecond laser with 10^{14} W/cm ² intensity in vacuum.....	176
<i>M. Trtica, J. Stasic, J. Limpouch, P. Gavrilov</i>	
L.M.I.9 Laser-induced periodic structure on Ti and Ti/Al thin films for photocatalytic application.....	177
<i>D. Pjević, D. Peruško, E. Skoulas, E. Stratakis, Z. Siketić, I. Bogdanović-Radović, T. Savić, M. Čomor, S. Petrović</i>	
L.M.I.10 Calculation of populations of energy levels of sodium interacting with an intense laser pulse and estimation of the resonant dynamic Stark shift.....	178
<i>A. Bunjac, D. B. Popović and N. S. Simonović</i>	
L.M.I.11 Inducing periodic structures on multilayers of Ti and Ta by femtosecond laser beam.....	179
<i>Aleksander G. Kovačević, Suzana M. Petrović, Davor Peruško, Vladimir Lazović, Iva Bogdanović-Radović, Vladimir Pavlović, Dejan Pantelić, Branislav M. Jelenković</i>	
L.M.I.12 Micro-structured biopolymer scaffolds fabricated by femtosecond laser ablation.....	180
<i>A. Daskalova, I. Bliznakova, P. Loukakos, A. Zhelyazkova, E. Kijeńska and C. Fotakis</i>	
L.M.I.13 Laser parameters optimization for the artifacts silver coated surfaces cleaning.....	181
<i>B. Radojkovic, S. Ristic, S. Polic, B. Jegdic and M. Janicijevic</i>	

L.M.I.14 Laser induced mixing in multilayered Ti/Ta thin film structures.....	182
<i>Marko Obradović, Janez Kovač, Suzana Petrović, Vladimir Lazović, Branislav Salatić, Jovan Ciganović, Dejan Pjević, Momir Milosavljević, Davor Peruško</i>	
L.M.I.15 Energy distribution of ejected photoelectrons in $K^{-2}V$ process.....	183
<i>Kristina Isaković, Violeta Petrović, Hristina Delibašić</i>	

10. Optical metamaterials and plasmonics

O.M.P.1 Extending useful spectrum of solar radiation in dye-sensitized solar cells using stochastic surface reliefs in plasmonic materials.....	184
<i>K. Cvetanović Zobenica, Z. Jakšić, M. Obradov, D. Vasiljević Radović, D. Stanisavljev</i>	
O.M.P.2 Influence of graphene and two-dimensional materials on electromagnetic enhancement in silver nanoparticle clusters.....	185
<i>U. Ralević, A. Panarin and G. Isić</i>	
O.M.P.3 Analysis of layer interactions between stacked metasurfaces.....	186
<i>J. Sperrhake, M. Falkner, S. Fasold and T. Pertsch</i>	
O.M.P.4 Spontaneous emission into Tamm plasmon modes on semi-infinite metallodielectric superlattices.....	187
<i>G. Isić, Z. Jakšić, S. Vuković</i>	
O.M.P.5 Influence of a resonance on delay times in terahertz chiral metamaterial slab.....	188
<i>D. B. Stojanović, P. P. Beličev, G. Gligorić, J. Radovanović, V. Milanović, Lj. Hadžievski</i>	
O.M.P.6 Photoemission Electron Microscopy of Airy Surface Plasmon Polaritons.....	189
<i>A. V. Singh, M. Falkner, M. Steinert, C. Menzel and T. Pertsch</i>	
O.M.P.7 Electromagnetic wave propagation through chiral metamaterials composed of twisted closed ring resonators.....	190
<i>D. B. Stojanović, P. P. Beličev, G. Gligorić, Lj. Hadžievski</i>	
O.M.P.8 Metal layers with subwavelength texturing for broadband enhancement of processes in photocatalytic microreactors.....	191
<i>M. Rašljić, Z. Jakšić, Ž. Lazić, M. Obradov, D. Vasiljević Radović, Ž. Čupić, D. Stanisavljev</i>	
O.M.P.9 Optical modulation using gain-assisted metasurfaces.....	192
<i>B. Vasić and R. Gajić</i>	
O.M.P.10 Film-coupled silver nanoparticles on flat and periodically corrugated aluminium substrates.....	193
<i>G. Isić, U. Ralević, S. Aškrabić, S. Graovac, S. Savić-Šević, A. Mikhailov, A. Antanovich, A. Prudnikau, M. Artemyev, I. Fabijanić, V. Janicki, B. Okorn, J. Sancho-Parramon and R. Gajić</i>	
O.M.P.11 Refractive index fluctuations due to multianalyte adsorption in chemical and biological plasmonic sensors of ultralow analyte concentrations.....	194
<i>O. Jakšić, I. Jokić, Z. Jakšić, M. Frantlović, M. Rašljić and K. Cvetanović Zobenica</i>	
O.M.P.12 Controlling silver nanoparticle production by ion-reduction process for tailoring of plasmonic properties.....	195
<i>I. Fabijanić, V. Janicki, B. Okorn, J. Sancho Parramon</i>	
O.M.P.13 Resonant absorption and extrinsic chirality in GaAs-based nanowires.....	196
<i>E. Petronijević, G. Leahu, A. Belardini, M. Centini, R. Li Voti, T. Hakkarainen, E. Koivusalo, M. Rizzo Piton, S. Suomalainen, M. Guina and C. Sibilica</i>	
O.M.P.14 Open Triangular Ring Cavity Resonator Integrating a Nanograting Mirror.....	197
<i>G. Ehrlich, M. Zohar, M. Auslender and S. Hava</i>	
O.M.P.15 All-dielectric metamaterials based on water. Experimental confirmation of the toroidal response.....	198
<i>Ivan Stenishchev, Alexey Basharin</i>	

O.M.P.16 Subwavelength nickel-copper multilayers as an alternative plasmonic material.....	199
<i>Ivana Mladenović, Zoran Jakšić, Marko Obradov, Slobodan Vuković, Goran Isić, Dragan Tanasković, Jelena Lamovec</i>	
O.M.P.17 Nontrivial nonradiating all-dielectric anapole sources.....	200
<i>Nikita A. Nemkov, Ivan V. Stenishchev, Alexey A Basharin</i>	
O.M.P.18 Metamaterials with broken symmetry: general approach, experiment and multipolar decomposition.....	201
<i>Anar K. Ospanova and Alexey A. Basharin</i>	
O.M.P.19 Titanium nitride plasmonic resonator Fabry-Perot for Raman lasing on nanoscale.....	202
<i>A. V. Kharitonov, S. S. Kharintsev and M. Kh. Salakhov</i>	
O.M.P.20 Phase and amplitude tunability in planar THz metamaterials with toroidal response.....	203
<i>Maria V. Cojocari, Kristina Schegoleva, Alexey A. Basharin</i>	
O.M.P.21 Laser induced ultrafast switching processes in diamond.....	204
<i>T. Apostolova and B. Obreshkov</i>	
O.M.P.22 Plasmonic Transmission Gratings for biosensors and atomic physics.....	205
<i>A. Sierant, B. Jany, D. Bartoszek-Bober, J. Fiutowski, J. Adam and T. Kawalec</i>	
O.M.P.23 Flat lenses with continuously graded metamaterials designed using transformation optics: anexact analytical solution of field equations.....	206
<i>M. Dalarsson, R. Mittra and Z. Jakšić</i>	

11. Other topics in photonics

O.P.1 Fresnel diffraction of a Laguerre-Gaussian $LG(l,n)$ laser beam by a combination of a fork-shaped grating and an axicon.....	207
<i>S. Topuzoski</i>	
O.P.2 Manipulation of the topological charges of vortices within large optical vortex lattices: Far-field beam reshaping.....	208
<i>L. Stoyanov, G. Maleshkov, I. Stefanov, A. Dreischuh</i>	
O.P.3 Characterization of liquid-phase epitaxy grown thick GaInAs (Sb)N layers.....	209
<i>V Donchev, I Asenova, M Milanova, D Alonso-Álvarez, K Kirilov, N Shtinkov, I G Ivanov, S Georgiev, E Valcheva and N Ekins-Daukes</i>	
O.P.4 Vertical Raman LIDAR profiling of atmospheric aerosol optical properties over Belgrade.....	210
<i>Z. Mijić, L. Ilić and M. Kuzmanoski</i>	
O.P.5 Planar versus three-dimensional growth of metal nanostructures at 2D heterostructures.....	211
<i>S. Stavrić, M. Belić, Ž. Šljivančanin</i>	
O.P.6 <i>Ab initio</i> study of superconducting properties of $NbSe_2$ monolayer in the DFPT formalism using Wannier interpolation.....	212
<i>Tatjana Agatonović Jovin and Radoš Gajić</i>	
O.P.7 Characterization of magnetron sputtered transparent hole conducting layers for organic solar cells.....	213
<i>M. Sendova-Vassileva, R. Gergova, Hr. Dikov, G. Popkirov, V. Gancheva and G. Grancharov</i>	
O.P.8 Post-processing synchronization and characterization of generated signals by a repetitive Marx generator.....	214
<i>A. Redjimi, Z. Nikolić, D. Knežević and D. Vasiljević</i>	
O.P.9 Cryogenic slab CO laser with RF discharge pumping: sealed-off plasma chemistry of the active medium.....	215
<i>A.A. Ionin, I.V. Kochetov, A.Yu. Kozlov, A.K. Kurnosov, A.P. Napartovich, L.V. Seleznev, D.V. Sinitsyn</i>	
O.P.10 Organic Nanocrystals for Quantum Nanophotonic Applications.....	216

	<i>S.Pazzagli, P. Lombardi, F. S. Cataliotti, C. Toninelli</i>	
O.P.11	Density Matrix Superoperator for Terahertz Quantum Cascade Lasers.....	217
	<i>A. Demić, A. Grier, Z. Ikonić, A. Valavanis, R. Mohandas, L. Li, E. Linfield, A. G. Davies and D. Indjin</i>	
O.P.12	Fluorescence of bio-molecules a simple and quick method: What honey emission speaks about bee society and honey quality.....	218
	<i>M. Stanković, D. Bartolić, B. Šikoparija, D. Spasojević, D. Mutavdžić, M. Natić and K. Radotić</i>	
O.P.13	Tuning exciton and trion population in MoS ₂ with photodoping.....	219
	<i>V. Jadriško, N. Vujičić, D. Čapeta and M. Kralj</i>	
O.P.14	Trajectory based interpretation of the laser light diffraction on a sharp edge	220
	<i>Milena D Davidović, Miloš D Davidović, Angel S Sanz, Mirjana Božić, Darko Vasiljević</i>	

Tutorial lectures

A fully algebraic approach to magneto-optical effect in atoms

A. Weis

University of Fribourg, Physics Department, Chemin du Musée 3, 1700 Fribourg, Switzerland
e-mail: antoine.weis@unifr.ch

In these two tutorial lectures I will give an *ab initio* introduction to the modeling of the interaction of polarized light with polarized multi-level atoms in the presence of static and time-varying magnetic fields.

Part 1: Stokes parameters, atomic multipole moments and their interaction: I start by introducing the parametrization of the interaction of unpolarized light with unpolarized multi-level atoms. I will then introduce the Stokes parameters, S_i , for describing (partially or fully) polarized light, and the atomic multipole moments, $m_{k,q}$, for describing spin polarized atoms. The lecture culminates with the derivation of a master formula that expresses the absorption coefficient, $\kappa(S_i, m_{k,q})$ (and the index of refraction, $n(S_i, m_{k,q})$) of a medium with arbitrary spin polarization interacting with light of arbitrary polarization. I will show that the optical properties (when interrogated by an electric dipole transition) of a medium with an arbitrary angular momentum are fully described by the multipole moments $m_{0,0}$, $m_{1,0}$, $m_{2,0}$, and $m_{2,2}$ (corresponding to 5 real numbers since $m_{2,2}$ is imaginary). I will further show that these relevant multipole moments can all be calculated algebraically by solving a system of rate equations, leading to algebraic expressions for the attenuation and phase shift of light propagating through a polarized medium.

Part 2: Atom light interactions in the presence of magnetic fields: I will first introduce the so-called three step model, which breaks the atom light interaction down into distinct time-sequential steps, viz., (1) multipole moment creation by optical pumping, (2) evolution of the (relaxing) multipole moments in external fields to a steady state, and (3) probing of this steady state by interrogation with the same light as in (1) or with light of a different polarization. Emphasis will be put on the range of validity of the model. I will then demonstrate how perfectly well this model works for making precision predictions of the line shapes of magneto-optical resonances. This will be illustrated by a variety of experimental results, which fully confirm the algebraic predictions.

3D laser printing of polymers, nanoparticles, and living cells

Boris Chichkov

Laser Zentrum Hannover e.V., Hollerithallee 8, 30419 Hannover, Germany
e-mail: b.chichkov@lzh.de

Laser printing can be used for printing very small and delicate objects like 3D nanostructures, nanoparticles, and living cells.

Nowadays, 3D printers can be bought for less than 500 Euros. Here we will report on laser printing of 3D polymer microstructures, nanoparticles, and living cells.

We demonstrate several laser printing techniques allowing the generation of 3D nanostructures and arrangement of spherical metal and dielectric nanoparticles in a very precise manner. For example, laser printed silicon nanoparticles have a predefined size and are characterized by unique optical properties. With sizes in the range of 100-200 nm in diameter they exhibit pronounced electric and magnetic dipole resonances within the visible spectral range. Possible applications of the generated nanoparticle arrays will be discussed.

In a series of publications on laser printing of living cells we proved that cells are not harmed by the printing process. The differentiation behavior and potential of laser printed stem cells are not affected. Stem cells can be printed in defined patterns and then differentiated within these patterns towards bone, cartilage or adipose tissue. Furthermore, fibroblast and keratinocyte cells have been printed layer-by-layer to form 3D skin tissue constructs. The skin tissue formation has been proven by visualizing intercellular junctions and verifying their functionality.

Beyond the myth of nonlinear capacity limits in fiber optic transmission

S. Radic¹ and N. Alic¹

¹Jacobs School of Engineering, University of California San Diego, La Jolla, CA
e-mail: sradic@ucsd.edu

The $\chi^{(3)}$ nonlinear response of the dielectric permittivity of silica has been known ever since the 1960's [1]. Indeed, depending on the application, paradoxically, it has been recognized as either a blessing, or a curse. For example, from a scientific perspective, the Kerr effect has been amply studied and has found its most important applications in all-optical signal processing, as well as in fiber optic parametric amplifiers [2]. In certainly its most important application, silica is the medium of choice for the world-wide transmission of information over fiber optic networks, whereas some 85 billion kilometers of optical fibers have, so far, been laid on Earth to enable unimpeded dissemination of information. When it comes to reliable information transfer, however, a medium whose permittivity is prone to an instantaneous nonlinear response to the transmitted electric field is certainly not a desirable characteristic. In fact, the nature of the Kerr nonlinearity (i.e. modulation of the group index by the field intensity) acts, in a way, as an irregular grating traveling with the transmitted wave, changing locally the index of refraction of the waveguide, (and thus the group velocity) proportionally to the instantaneous peak power. Such condition, certainly spells trouble even for a single wave transmitted through a waveguide, since it, in effect creates a time-varying system, which if observed in Fourier domain is equivalent to (new) frequency generation, and if accompanied with waveguide group velocity dispersion, leads to pulse distortion, since it causes different parts of the pulse(s) to travel at different speeds (in proportion to the local intensity). The situation becomes both worse and significantly more difficult to analyze in modern communication systems which consist of a large number of frequency-allocated information channels. In the latter, again, due to the GVD, the information streams pertinent to different channels effectively walk through each other, thereby continuously changing the local intensity profile, resembling a random process, and ultimately leading to an insurmountable impediment in transmission systems, that since the '90s [3] predicted a strict barrier in power and/or amount of information that can be conveyed in such communication systems. Specifically, in information theoretic terms, this has led to the definition / introduction of the Nonlinear Shannon Limit conjecture [4].

In sharp contrast, we have recently shown in a stream of publications that the formulation of the above limit was only an illusion: The transmission systems based on single mode fibers, although indeed nonlinear, are fully deterministic, whereas the associated governing 1+1 Nonlinear Schrodinger Equation, although non-conservative in the strict sense, is well behaved and (numerically) integrable / invertible. Following the theoretical proposition of the above fact, we have in a series of experiments with unprecedented accuracy demonstrated and proved ability to transmit beyond the previously assumed nonlinear capacity limits, by virtue of applying digital signal processing in according to the inversion of the NLS. As first disclosed in [5] and later rigorously proven in [6], what had been at the root of the 20 years' long misconception in the field was on the one hand due to the complexity of the system, as well as conversion of carrier frequency uncertainty into nonlinear interaction variation which appeared as a random process. We have, furthermore, shown that once this uncertainty is removed from the system, all nonlinear interactions in fiber transmission can be reversed, whereas significantly higher capacities are achievable in transmission system than previously assumed. Indeed, as is well known, reversible deterministic effects cannot lead to capacity limitation.

REFERENCES

- [1] G.P. Agrawal, *Nonlinear Fiber Optics*, 2nd Edition, Academic Press (1995).
- [2] C. J. McKinstrie, S. Radic and A. R. Chraplyvy, *IEEE Sel. Top. Quantum Electron.* 8, 538(2002).
- [3] A. R. Chraplyvy, *J. Lightw. Technol.* 8, 1548 (1990).
- [4] R.-J. Essiambre, et al., *J. Lightwave Technol.* 28(4), 662 (2010).
- [5] N. Alic, et al., *J. Lightwave Technol.*, 32, (2014).
- [6] E. Temprana, et al., *Science* 348 (6242), 1445-1448 (2015).

Self-organization of light in media with competing nonlocal nonlinearities

F. Maucher¹, T.Pohl,² S.Skupin³, W.Krolikowski⁴

¹*Joint Quantum Centre (JQC) Durham-Newcastle, Department of Physics, Durham University, Durham DH1 3LE, United Kingdom; Department of Mathematical Sciences, Durham University, Durham DH1 3LE, UK*

²*Max Planck Institute for the Physics of Complex Systems, 01187 Dresden, Germany*

³*University of Bordeaux, France*

⁴*Science Program, Texas A&M University at Qatar, Doha, Qatar*
e-mail: Wieslaw.krolikowski@qatar.tamu.edu

In nonlocal nonlinear media the nonlinear response induced by propagating electromagnetic wave in a particular location depends on wave's intensity in the certain neighborhood of this location [1-3]. The spatial extent of this neighborhood determines the degree of nonlocality. In this talk I will discuss wave propagation and localisation in nonlocal media. In particular I will show that competition between nonlocal nonlinearities leads to emergence of spatial periodic pattern [4, 5].

Acknowledgement: This work is supported by the Qatar National Research Fund (grant # NPRP 8-246-1-060).

REFERENCES

- [1] D. Suter and T. Blasberg, *Phys. Rev. A* **48**, 4583 (1993).
- [2] F. Dalfovo, S. Giorgini, L. P. Pitaevskii, and S. Stringari, *Rev. Mod. Phys.* **71**, 463 (1999).
- [3] O. Bang, W. Krolikowski, J. Wyller, J.J. Rasmussen, *Phys. Rev. E* **66**, 046619 (2002).
- [4] B. K. Esbensen, A. Wlotzka, M. Bache, O. Bang, and W. Krolikowski, *Phys. Rev. A* **84**, 053854 (2011).
- [5] F. Maucher, T. Pohl, S. Skupin, and W. Krolikowski, *Phys. Rev. Lett.* **116**, 163902 (2016)

Translation of remote photons based sensing into virtual tactile and hearing senses

Yevgeny Beiderman, Yafim Beiderman, Sergey Agdarov and Zeev Zalevsky
Faculty of Engineering and the Nanotechnology Center, Bar Ilan University, Ramat-Gan, 52900, Israel
Email: Zeev.zalevsky@biu.ac.il

In this presentation I will show photons can be used to sense “voice” and how this sensed information can be translated to the used via tactile stimulation. In my presentation I will talk about two technologies. In the first part I will present a technological platform that can be used for remote sensing of biomedical parameters as well as for establishing a directional communication channel. The technology is based upon illuminating a surface with a laser and then using an imaging camera to perform temporal and spatial tracking of secondary speckle patterns in order to have nano metric accurate estimation of the movement of the back reflecting surface. If the back reflecting surface is a skin located close to main blood arteries then biomedical monitoring can be realized. If the surface is close to our neck or head then a directional communication channel can be established. The proposed technology was already applied for remote and continuous estimation of heart beats, breathing, blood pulse pressure, pulse wave velocity, intra ocular pressure and chemicals in the blood stream such as alcohol and glucose and more. It was also experimentally used as invisible photonic mean for remote, directional and noise isolated sensing of speech signals.

In the second part I will present our work on a special device that we have developed which aims to allow blind people or people that are visually impaired to “see” via tactile stimulation of their cornea. A camera that is installed on the spectacles of the user transmits in a wireless way the captured image, after properly processing and encoding it, to special micro mirrors array that converts the visual information into tactile spatial stimulation of the cornea by transmitting ultrasonic waves. After short training the user can recognize the spatial tactile feeling and to associate the visual features with the tactile stimulation. We have conducted preliminary clinical trials and were the first to show that indeed the concept works. We have transmitted simple geometric shapes and the users were able to recognize them with high probability. We were able to clinically characterize the spatial two point discrimination of the cornea and to measure its temporal response time. This technology can also provide additional visual information to well seeing users as our wearable device can allow the conventional visual photons through such that original vision sense can be used in parallel to the tactile information sent by our device.

Keynote lectures

Ultrasensitive and ultrahigh resolution fluorescence spectroscopy and imaging for fundamental biomolecular studies and towards clinical diagnostics

J Widengren

Exp. Biomol. Physics / Applied Physics, Royal Inst. Technology (KTH)

AlbanovaUnivCenter, 106 91 Stockholm, Sweden

e-mail: jwideng@kth.se

The focus of our research group at KTH is to develop ultrasensitive and ultrahigh resolution fluorescence spectroscopy and imaging techniques for detection, identification and characterization of biomolecules, and to apply these techniques for biomolecular diagnostics, screening, and for fundamental dynamic and conformational studies of biomolecules and their interactions.

This presentation will start with an introduction to single-molecule fluorescence spectroscopy, and how fluorescence fluctuation analyses, in particular Fluorescence Correlation Spectroscopy (FCS), can be used to monitor a wide range of molecular dynamic processes down to a single molecule level. Recently developed FCS modalities will be presented, and how the FCS technique can be used to provide new perspectives on proton exchange and biomolecular interactions in biomembranes.

Second, it will first be presented how fluorescence blinking kinetics due to long-lived, photo-induced transient states of organic fluorophores can be exploited as an additional source of fluorescence-based information. By two major approaches, where the transient state information is obtained either from FCS or by recording the time-averaged fluorescence response to a time-modulated excitation, it is possible to combine the detection sensitivity of the fluorescence signal with the environmental sensitivity of the long-lived transient states. Proof-of-principle experiments, advantages, limitations will be discussed, and applications including live cell transient state (TRAST) imaging of cellular metabolism and membrane microfluidity will be presented.

Last, it will be shown how ultrahigh resolution imaging of cellular protein distribution patterns using Stimulated Emission Depletion (STED) microscopy can potentially provide new diagnostic parameters on the level of individual cells, and also give further insights into underlying disease mechanisms. Examples including cultured cells, clinically sampled breast cancer cells and platelets will be given.

A classical model for depolarization by temporal and spatial decoherence

Kurt Hingerl

Center for Surface- and Nanoanalytics, University Linz , Austria
e-mail: kh@jku.at

A finite spectral resolution and/or an imperfectly collimated beam /and or an (areal) extended light source / and or an (areal) extended detector and/ or a sample with a varying thickness can produce depolarization in any ellipsometric or polarization measurement. However, despite these experimental findings, there are to our knowledge no physical models published which trace the origin of depolarization back to the atomic properties. Therefore, in the talk I will explain crosspolarization - and subsequently depolarization by considering the common- not separable- effect between the light beam and the sample, described by coherence length and coherence area.

For inhomogeneous samples with dimensions smaller than the coherence area, the fields have to be added coherently. However, inner and non-planar boundaries give rise to evanescent fields in the vicinity of these boundaries. Parallel and perpendicular field components oscillate and decay differently in the vicinity of the boundaries, therefore cross- polarization (incident s- polarized light excites reflected p-polarized light and vice versa) occurs.[1] In inhomogeneous samples the Fresnel reflectances are not correct any more, these strictly rely on homogeneity (i.e. arbitrary shifts of the sample along any surface direction change the measurement).

However, in optics we never measure the electric fields, because our available detectors are much too slow, but we measure their statistical second moments. In homogeneous samples with thick transparent overlayers it turns out that depolarization arises through the temporal decoherence of photons, and the measured Müller matrix (MM) elements are given by a convolution of the spectral width of the light source and a sample property: the thickness of the transparent overlayer.

For inhomogeneous samples, when the sample sizes or structures are larger than the coherence area, then the different local polarization states in reflection coming from different materials have to be added incoherently- partially depolarized light results.[2] Also here the measured Müller matrix is given by a convolution of a light source property (i.e. the coherence area) and a sample property: the structure size).

For both depolarization mechanisms mathematical models[3,4] will be presented, allowing to predict the polarization response, i.e. all MM elements for periodic structures, metamaterials and thick films.

REFERENCES

- [1] J. -P. Perin, K. Hingerl, Applied Surface Science, in print (2016).
- [2] The mathematical formulations- which will be largely avoided in the talk- are given through the coherency matrix / respectively the Stokes vectors, and decoherence shows up by the Cittert- Zernike theorem (M. Born & E. Wolf, Principles of Optics, chapter X.9).
- [3] K. Hingerl, R. Ossikovski, Opt. Lett., 41, 219, (2016).
- [4] R. Ossikovski, K. Hingerl, Opt. Lett., 41, 4044, (2016).

Developing high capacity fibre transmission systems employing spectrally efficient super-channel technology

Vidak Vujicic, Cosimo Calò, Colin Browning, Kamel Merghem, Anthony Marlinez, Abderrahim Ramdane,

Liam P Barry

¹*School of Electronic Engineering, Dublin City University, Glasnevin, Dublin 9, Ireland*

²*CNRS, Laboratory for Photonics and Nanostructures, Route de Nozay, 91460 Marcoussis, France*
e-mail:liam.barry@dcu.ie

Interfaces operating at 400 Gbit/s or 1 Tbit/s are foreseen as the next standards after 100 Gbit/s systems [1]. In this context, optical super-channels are promising candidates, combining a multitude of sub-channels in a wavelength-division multiplexing (WDM) scheme, while each sub-channel operates at a moderate symbol rate that complies with currently available CMOS driver circuitry. Typically the super-channels use spectrally efficient advanced modulation formats such as quadrature phase shift keying (QPSK) or 16-state quadrature amplitude modulation (QAM) in combination with advanced multiplexing schemes such as orthogonal frequency-division multiplexing (OFDM) [2] or Nyquist WDM [3]. The performance of these transmission schemes depends heavily on the properties of the optical source, in particular on the number of lines, the power per line, the optical carrier-to-noise ratio (OCNR), the optical linewidth, and on the relative intensity noise (RIN). In addition, tunability of emission wavelength and line spacing are important features providing flexibility of the transmission scheme. Terabit/s super-channel transmission has been demonstrated before, using different approaches for realizing the optical source. These approaches include ensembles of independent lasers [4], single-laser concepts with sidebands generated by external modulation [5] or fiber-based spectral broadening [6]. Arrays of independent lasers offer flexibility and do not require filters for spectrally separating the comb lines. However, the achievable spectral efficiency (SE) is limited by the drift of the individual emission wavelengths and the associated guard bands. For modulator based comb sources, the number of comb lines is generally limited by the achievable modulation depth. In this work we demonstrate that gain-switched comb sources (GSCS) [7] and Quantum Dash mode locked laser (QDMLL) comb sources [8] can be used as alternative approaches to generate terabit/s super-channels. The GSCS exploits injection locking of a gain-switched laser diode and features both an electrically tunable free spectral range and an electrically tunable center wavelength, good spectral flatness, high OCNR, low RIN and low optical linewidth. The QDMLL provide a compact comb source with low power consumption and many optical lines. Here we demonstrate various terabit/s super-channel experiments using polarization division multiplexed (PDM) QPSK and 16QAM in combination with Nyquist pulse shaping for efficient use of the available bandwidth using these comb sources. Transmission over various distances of standard single-mode fiber (SSMF) has been tested and we show the influence of the comb source parameters such as phase noise, RIN, etc. on system performance.

REFERENCES

- [1] P. Winzer, *IEEE Commun. Mag.* 48(7), 26–30 (2010).
- [2] W. Shieh and I. Djordjevic, Elsevier Academic Press, 2010.
- [3] H.-C. Chien et al., *J. Lightwave Technol.* 30(24), 3965–3971 (2012).
- [4] Y.-K. Huang et al., in *Asia Communications and Photonics Conference*, (Optical Society of America, 2012), Paper PAF4C.2
- [5] C. Weimann et al., *Opt. Express* 22(3), 3629–3637 (2014).
- [6] D. Hillerkuss et al., *J. Opt. Commun. Netw.* 4(10), 715–723 (2012).
- [7] P. Anandarajah et al., *Optical Fiber Communication Conference* (Optical Society of America, 2013), Paper OTh3I.8
- [8] Vidak Vujicic et al., *Optical Fiber Communication Conference 2015*, (Optical Society of America, (2015)).

In situ visual observation of 2D materials growth and modifications, and characterization of their optical properties

M. Kralj¹

¹Center of Excellence for Advanced Materials and Sensing Devices, Institute of Physics, Zagreb, Croatia
e-mail: mkralj@ifs.hr

The properties of atomically thin two-dimensional (2D) materials are extremely depending on their atomic-scale quality and on their interface with the surrounding. Therefore the ability to control structure, uniformity, doping and other properties of novel 2D materials at the nano-scale provides possibilities for developing various promising applications arising from their electronic properties or mechanical strength. Specifically, while linear bands in semimetallic graphene lead to record mobility, mono- and few-layer transition metal dichalcogenides (TMDs) attract increasing attention due to their intrinsic semiconducting and optoelectronic properties and corresponding advantages over graphene.

In order to demonstrate possibilities of the nano-scale control of 2D materials, first we investigate epitaxial graphene on iridium. This system exhibits intrinsic properties matching that of a freestanding graphene but the presence of a metal substrate in this case introduces superperiodic potential to graphene [1]. We use scanning tunneling microscopy (STM), low energy electron microscopy (LEEM) and electron spectroscopy to study a mechanism and effects of insertion/intercalation of atomic layers between graphene and iridium [2]. Along with a pronounced charge transfer effects, a quasiparticle scattering of doped graphene is directly visualized in low-temperature STM, marking a pseudospin character of electrons in graphene [3]. Furthermore, we demonstrate a way to extend optoelectronic applications of graphene and bypass limited use of graphene in plasmonics only in the mid-infrared range. In the highly doped epitaxial graphene we report a novel optical response of graphene plasmons in visible, showing a strong nonlinear response on a femtosecond time scale as well as THz oscillation of resonance energy [4].

Next, we show how optical visibility of mono- and few-layer TMDs samples on SiO₂ covered silicon wafers at elevated temperatures was exploited to construct chemical vapor deposition system with optical access for real time microscopy that enables observation of TMDs during growth. This provides us a significant level of control and understanding of the growth process, which is crucial for development of TMD materials for large-scale applications [5]. After synthesis, the quality of grown MoS₂ and WS₂ samples and their heterostructures is checked by the characterization of optical response, transport and in particular STM characterization of atomic-scale defects and their typical concentrations at the nano-scale [6]. Finally, we show how macromolecular adsorption strongly enhances photoluminescence response of single layer MoS₂ [7], paving a way for development of sensing applications of TMSs.

REFERENCES

- [1] I. Pletikosić, M. Kralj, P. Pervan, et al., *Phys. Rev. Lett.* 102, 056808 (2009).
- [2] M. Petrović, I. Šrut Rakić, S. Runte, et al., *Nat. Commun.* 4, 2772 (2013).
- [3] D. Dombrowski, W. Jolie, M. Petrović, et al., *Phys. Rev. Lett.* 118, 116401 (2017).
- [4] S. Tanaka, M. Petrović, K. Watanabe, et al., submitted (2017).
- [5] D. Čapeta, I. Šrut Rakić, M. Kralj, et al., in preparation (2017).
- [6] I. Delač Marion, D. Čapeta, B. Pelić, et al., in preparation (2017).
- [7] I. Delač Marion, N. Vujučić, D. Čapeta, et al., in preparation (2017).

Rogue waves, Talbot carpets and accelerating beams

M.R. Belic¹, S. Nikolic¹, O. Ashour¹, and Y.Q. Zhang²

¹*Texas A&M University at Qatar, 23874 Doha, Qatar*

²*Xi'an Jiaotong University, Xi'an 710049, China*

e-mail: milivoj.belic@qatar.tamu.edu

Rogue waves are giant waves that sporadically appear and disappear in oceans and optics. Talbot carpets are elaborate recurrent images of light and plasma waves. Accelerating beams are the beams that, well, accelerate. We put the three together.

All-optical processing using phase-change nanophotonics

W.H.P. Pernice

*¹Institute of Physics, Westfälische Wilhelms-Universität Münster
Münster, Germany*

e-mail: wolfram.pernice@uni-muenster.de

Nanophotonic integrated circuits allow for realizing functional optical devices using efficient design and fabrication routines. Their inherent stability and scalability makes them attractive for applications where optical signal processing is combined with coupling to external light stimuli. A majority of nanophotonic devices is, however, based on passive materials, which do not provide low-power tuning options or convenient knobs for reconfigurability. We address this shortcoming by combining passive silicon nitride photonic devices with tunable phase-change materials (PCMs). PCMs offer attractive material properties such as large optical contrast, durability and high cyclability. In the form of nanoscale patches they can be efficiently integrated with waveguide devices. Such a platform allows realizing both on-chip optical data storage and active photonic components. Multi-level photonic memories with random access would allow for leveraging even greater computational capability. Thus far, photonic memories have been predominantly volatile, meaning that their state is lost once the input power is removed. By using optical near-field coupling within on-chip waveguides, we realize bit storage of up to eight levels in a single device that readily switches between intermediate states. We show that individual memory elements can be addressed using a wavelength multiplexing scheme. Such multi-level, multi-bit devices provide a pathway towards eliminating the von Neumann bottleneck and portend a new paradigm in all-photonic memory and non-conventional computing. We further show that such devices can be operated with short optical pulses, both for write and read operations. Using a pulsed optical scheme then allows for implementing elementary all-optical processing units. In the talk properties, implementations and applications of phase-change photonic components will be discussed.

Three-dimensional "soliton" in Bose-Einstein condensates and nonlinear optics

Sadhan K. Adhikari

Instituto de Física Teórica, UNESP - São Paulo State University, São Paulo, Brazil
e-mail: adhikari@ift.unesp.br

A bright soliton is a self-bound one-dimensional (1D) object that maintains its shape, while traveling at a constant velocity, due to a cancellation of nonlinear attraction and dispersive effects. In our three-dimensional (3D) world only quasi-solitons are observed where a reduced (integrated) 1D density exhibits soliton-like properties. Such solitons have been studied in Bose-Einstein condensates (BEC), water wave, nonlinear optics, among others. In this presentation we consider the possibility of generating a self-bound 3D "soliton" in BEC (matter-wave quantum ball) and in nonlinear optics (spatiotemporal light bullet).

We study the statics and dynamics of a stable, mobile, 3D matter-wave spherical quantum ball or "soliton" created in the presence of an attractive two-body and a very small repulsive three-body interaction. The quantum ball can propagate with a constant velocity in any direction in free space. A small three-body repulsion can stop the collapse of the quantum ball. In absence of this repulsion the quantum ball collapses due to two-body attraction alone. In frontal head-on and angular collisions at large velocities two quantum balls behave like quantum solitons. Such collision is found to be quasi elastic and the quantum balls emerge after collision without any change of direction of motion and velocity and with practically no deformation in shape. However, in a collision at small velocities two quantum balls coalesce to form a larger ball which we call a quantum-ball breather. The present study is based on an analytic variational approximation and a numerical solution of the mean-field Gross-Pitaevskii (GP) equation using the parameters of Li atoms.

However, the mathematical structure of the nonlinear mean-field GP equation is the same as that of the nonlinear Schrödinger (NLS) equation used to study pulse propagation in nonlinear optics, although the physical meaning of the different terms is distinct in two cases. Hence, the above study on matter-wave soliton implies that in a cubic quintic nonlinear medium one can have a stable mobile 3D spatiotemporal light bullet. We study the statics and dynamics of such a light bullet by variational approximation and a numerical solution of the NLS equation. We also demonstrate the formation of such soliton with an angular momentum which we call vortex soliton in BEC and spinning light bullet in nonlinear optics.

For experimental observation of a matter-wave quantum ball, a weak harmonic trap should be used in a BEC to localize it. By increasing the two-body attraction using a Feshbach resonance, the size of a matter-wave quantum ball can be made much smaller than the characteristic length of the harmonic trap. When this happens, the BEC can be identified as a matter-wave quantum ball.

REFERENCES

- [1] S. K. Adhikari, Phys. Rev. A 95, 023606 (2017).
- [2] S. K. Adhikari, Phys. Rev. E 94, 032217 (2016).
- [3] S. K. Adhikari, Laser Phys. Lett. 14, 025501 (2017).
- [4] S. K. Adhikari, Laser Phys. Lett. 14, 065402 (2017).

Invited lectures

Metal free structural colors via disordered nanostructures with nm resolution and full CYMK color spectrum

V. Mazzone¹, M. Bonifazi² and A. Fratalocchi¹

¹PRIMALIGHT, Faculty of Electrical Engineering; Applied Mathematics and Computational Science, King Abdullah University of Science and Technology (KAUST), Thuwal 239955-6900 Saudi Arabia
mail:andrea.fratalocchi@kaust.edu.sa

Engineering colors through optical properties of nanostructures represents a research area of great interest, due to the many applications that can be enabled by this technology, from adaptive camouflage to micro-images for security and biomimetic materials [1-3]. The state of the art technology is represented by the use of metallic periodic structures of 140nm, which can create a limited number of colors of the spectrum [3].

In this work we introduce a new approach, based on a fully metal-free technique that takes advantage from the complex scattering of disordered structures created by a three-dimensional process with EBL (electron beam lithography). Engineering the scattering from complex media already demonstrated to be a successful in creating ultra-black material and new type of sources for optical applications [4].

Our new approach realizes the fundamental colors of the CMYK (Ciano, Magenta, Yellow and Black) system, and therefore is able to represent any color in the spectrum, including variations in intensity. The resolution of each pixel is limited by the EBL only, ranging in the nm scale.

This method is interesting in the field of micro-security, due to the impossibility of counterfeiting a random, three-dimensional pattern of pixels created on a transparent dielectric.

We will discuss the fabrication detail of this color printing technique, many examples of applications and the approaches for large-scale fabrication through nanoimprinting lithography.

REFERENCES

- [1] T. S. Kustandi, H. Y. Low, J. H. Teng, I. Rodriguez and R. Yin, *Small* No. 5, 574-578, (2009).
- [2] M.A. Kats, R. Blanchard, P. Genevet and F. Capasso, *Nat. Mat.*, vol 12, January (2013).
- [3] K. Kumar, H. Duan, R.S. Hedge, S. C. W. Koh, J. N. Wei and J. K. W. Yang *Nat. Natotech.*, vol 7, September (2012).
- [4] Liu, C., et al. *Nat. Nanotech.*, Vol. 11, 60-66, (2016).

Two Intriguing Examples for Topological Effects in Ultracold Atoms

Axel Pelster

*Physics Department and Research Center OPTIMAS, Technical University of Kaiserslautern, Erwin Schrödinger Str. 46,
67663 Kaiserslautern, Germany
e-mail:axel.pelster@physik.uni-kl.de*

The talks discuss two specific bosonic lattice systems where topological effects occur. At first, we analyze the ground-state properties of anyons in a one-dimensional lattice using the Anyon-Hubbard Hamiltonian [1]. To this end we map the hopping dynamics of correlated anyons to an occupation dependent hopping Bose-Hubbard model using the fractional Jordan-Wigner transformation. In particular, we calculate the quasi-momentum distribution of anyons, which interpolates between Bose-Einstein and Fermi-Dirac statistics. Analytically, we apply a modified Gutzwiller mean-field approach, which goes beyond a classical one by including the influence of the fractional phase of anyons within the many-body wave function. Numerically, we use the density-matrix renormalization group by relying on the ansatz of matrix product states. As a result it turns out that the anyonic quasi-momentum distribution reveals both a peak-shift and an asymmetry which mainly originates from the nonlocal string property. In addition, we determine the corresponding quasi-momentum distribution of the Jordan-Wigner transformed bosons, where, in contrast to the hard-core case, we also observe an asymmetry for the soft-core case, which strongly depends on the particle number density.

Afterwards, we investigate the extended hard-core Bose-Hubbard model on the triangular lattice as a function of spatial anisotropy with respect to both hopping and nearest-neighbor interaction strength [2]. At half-filling the system can be tuned from decoupled one-dimensional chains to a two-dimensional solid phase with alternating density order by adjusting the anisotropic coupling. At intermediate anisotropy, however, frustration effects dominate and an incommensurate supersolid phase emerges, which is characterized by incommensurate density order as well as an anisotropic superfluid density. We demonstrate that this intermediate phase results from the proliferation of topological defects in the form of quantum bosonic domain walls. Accordingly, the structure factor has peaks at wave vectors, which are linearly related to the number of domain walls in a finite system in agreement with extensive quantum Monte Carlo simulations. We discuss possible connections with the supersolid behavior in the high-temperature superconducting striped phase.

REFERENCES

- [1] G. Tang, S. Eggert, and A. Pelster: *New J. Phys.* **17**, 123016 (2015).
- [2] X.-F. Zhang, S. Hu, A. Pelster, and S. Eggert, *Phys. Rev. Lett.* **117**, 193210 (2016).

Organic crystalline nanoneedles on 2D materials and their optoelectronic properties

C. Teichert

Institute of Physics, Montanuniversitaet Leoben,

Leoben, Austria

e-mail: teichert@unileoben.ac.at

Crystalline films of small conjugated molecules offer attractive potential for fabricating organic solar cells, organic light emitting diodes, and organic field effect transistors on flexible substrates. Here, the novel two-dimensional (2D) van der Waals materials like graphene (Gr) or ultrathin hexagonal boron nitride (hBN) come into play. We report on the self-assembly of crystalline needles composed of rod-like molecules. The needles are several 10 nm wide and a few nm high, but they can extend to several 10 μm . The needle networks obtained offer the potential to be used as templates for nanoscale patterning of 2D materials.

As a non-polar model molecule, the oligophenylene para-hexaphenyl (6P) was grown by hot-wall epitaxy (HWE) on different Gr substrates. On exfoliated, wrinkle-free graphene, we observed by atomic-force microscopy (AFM) the formation of 6P nano-needles (composed of lying molecules) following 6 discrete orientations defined by the Gr lattice [1, 2]. Through in-situ measurements during growth of 6P, we directly probe the charge transfer as the interfacial dipoles are formed. The amount of charge transferred per adsorbed molecule is only about one thousandth of an electron transferred per molecule, indicating very weak interaction.

For 6P growth on ultrathin, exfoliated hBN – which is a 2D insulator – again needle-like structures with preferential growth directions $\pm 5^\circ$ off the zigzag direction of the substrate are observed [3]. This finding could be explained in conjunction with density functional theory (DFT) calculations revealing the 6P adsorption site by the formation of a (-629) contact plane of bulk 6P. For the growth of the polar, acene-like molecule dihydrotetraazaheptacene (DHTA7) on Gr and hBN also crystalline needles are found. In this case, they are oriented close to the armchair direction of the substrates with a 9° deviation which originates from the dipolar interaction of the molecules as demonstrated by DFT calculations. Light-assisted electrostatic force microscopy based charging and charge spreading experiments have been used to investigate the influence of light on the conductivity of DHTA7 needles and needle networks. It was found that both red and green visible laser light allows for charge spreading over large distances (several tens of micrometers). On the other hand, in the dark DHTA7 needles appear as not conductive and injected charges remain trapped within narrow segments ($\sim 1 \mu\text{m}$) of the needles for an extended period of time (several hours) even in ambient conditions.

Work has been performed in collaboration with M. Kratzer, A. Matković, B. Genser (Leoben), J. Vujin, B. Vasić, R. Gajić (Belgrade), Z. Chen, O. Siri, C. Becker (Marseille), D. Lüftner, and P. Puschnig (Graz).

REFERENCES

- [1] M. Kratzer, S. Klima, C. Teichert, B. Vasić, A. Matković, U. Ravelić, R. Gajić, J. Vac. Sci. Technol. B **31**, 04D114 (2013).
- [2] M. Kratzer, C. Teichert, Nanotechnology **27**, 292001 (2016).
- [3] A. Matković, J. Genser, D. Lüftner, M. Kratzer, R. Gajić, P. Puschnig, C. Teichert, Sci. Rep. **6**, 38519 (2016).

Precision measurements for compact vapor-cell atomic clocks

C. Affolderbach, M. Gharavipour, F. Gruet, W. Moreno, M. Pellaton, and G. Mileti

¹*Laboratoire Temps – Fréquence (LTF), Institut de Physique*

Université de Neuchâtel, Neuchâtel, Switzerland

e-mail: christoph.affolderbach@unine.ch

Compact atomic clocks (≤ 3 liters volume) based on alkali vapor cells are key components in a variety of applications such as synchronization in telecommunication networks or as highly stable on-board clocks in global navigation satellite systems such as GPS, GLONASS, GALILEO and others. The introduction of laser optical pumping in alkali vapor cells [1] and pulsed Ramsey interrogation schemes [2] have enabled important improvements in clock performance for various applications [3].

In a first part of this presentation, we will present our studies towards a highly compact realization of a high-performance Rb vapor cell atomic clock, based on the pulsed Ramsey interaction scheme. We present our realizations of a compact (< 2.5 liters volume) frequency-stabilized laser head with pulsed optical output and a highly compact microwave cavity resonator (45 cm^3 volume), and discuss their key performances in view of the clock application. Compared to our previous studies on continuous-wave (CW) Rb clocks [1], the pulsed scheme allows for a strong reduction of the light-shift effects that are among the main sources of instability in this type of atomic clocks. Based on detailed measurements of the light shift in both the CW and Ramsey scheme we discuss on the origin of the residual light shift in the Ramsey scheme and strategies for its further reduction.

In a second part we will discuss variants of the pulsed optical-microwave Rabi and Ramsey interrogation schemes and show how they can be used for measuring important parameters of the atomic sample and its environment in the clock system, such as the spatial distribution of the microwave [4] or static [5] magnetic fields across the vapor cell. An optically-detected variant of classical spin echo technique [6] is presented for measuring intrinsic relaxation times in the vapor cell.

We thank our former colleagues T. Bandi and S. Kang of UniNE-LTF, as well as A. Skrivervik, A. Ivanov, C. Stefanucci (all EPFL-LEMA), P. Treutlein, A. Horsley, G.-X. Du (Basel University), B. M. Jelenković, I. S. Radojičić, A. J. Krmpot (University of Belgrade), and the colleagues of the EMRP-IND55 MCllocks project consortium for fruitful collaborations.

REFERENCES

- [1] T. Bandi, C. Affolderbach, C. Stefanucci, F. Merli, A. K. Skrivervik, G. Mileti, *IEEE Trans. UFFC* 61, 1769 (2014).
- [2] S. Micalizio, C. E. Calosso, A. Godone, and F. Levi, *Metrologia* 49, 425 (2012).
- [3] S. Micalizio, F. Levi, A. Godone, C. E. Calosso, B. François, S. Guérandel, D. Holleville, E. De Clercq, L. De Sarlo, P. Yun, J. M. Danet, M. Langlois, R. Boudot, M A. Hafiz, E. Sahin, C. Affolderbach, S. Kang, F. Gruet, M. Gharavipour, G. Mileti, B. Desruelle, *proc. joint IFCS and EFTF meeting, Denver CO, USA, April 12-16, 2015*. pp. 456-461.
- [4] A. Horsley, G.-X. Du, M. Pellaton, C. Affolderbach, G. Mileti, P. Treutlein, *Physical Review A*, 88, 063407 (2013).
- [5] C. Affolderbach, G.-X. Du, T. Bandi, A. Horsley, P. Treutlein, G. Mileti, *IEEE Trans. Instrum. Meas.* 64, 3629 (2015).
- [6] E. L. Hahn: *Spin Echoes*, *Phys. Rev.* **80**, 580 (1950).

Time-resolved studies of femtosecond laser surface ablation of dielectrics and semiconductors (in air)

D. van Oosten

Debye Institute for NanoMaterials Science, Utrecht University,

Utrecht, The Netherlands

e-mail:D.vanOosten@uu.nl

In my talk I will discuss our most recent results on the surface ablation dynamics of dielectrics and semiconductors (silica and silicon, but also water) upon tightly focused ($\sim 2 \mu\text{m}$) single femtosecond laser pulse excitation. In experiments, we study the ablation process using a time-resolved imaging arrangement. We record transient reflectivity images during surface ablation for delays that extend from tens of femtoseconds to tens of nanoseconds.

To understand the process theoretically, we combine a finite difference time domain (2D-FDTD) model, coupled to multiple rate equations (MRE) to describe the excitation and heating of electrons in the material, taking into account the influence the resulting electron plasma has on the propagation of light. We simulate both the propagation of the pump and the probe at different time delays using this method. We find excellent agreement between the theoretically and experimentally obtained transient reflectivities, thus validating our numerical approach.

Using the simulation, we can then estimate the laser energy deposited in the material in the form of ionisation and heating, and thereby understand the initial conditions of the ablation process (~ 1 ps). Finally, by studying the dynamics of the expanding vapour plume and a shock-wave in the surrounding air, we can determine the energy used in actual removal of material and therefore (to our knowledge) for the first time quantify the efficiency of the femtosecond laser ablation process.

Dark Line, Lump and X-solitary Waves in Optical Media

F. Baronio and S. Wabnitz

*Istituto Nazionale di Ottica CNR and Dipartimento di Ingegneria dell'Informazione,
Università di Brescia, Italy
e-mail: fabio.baronio@unibs.it*

The propagation of high-intensity, ultra-narrow and ultra-short light pulses in quadratic and cubic nonlinear media is a complex multidimensional phenomenon which leads to substantial spatiotemporal pulse rearrangement. The spatiotemporal dynamics is influenced by the interaction of various physical effects, in particular diffraction, material dispersion and nonlinear response. This problem has attracted strong interest over the past decades, leading to the generation and the manipulation of high-intensity femtosecond and attosecond pulses [1]. During the last decades, extensive research activities concerning the self-focusing behavior of intense ultra-short pulses have shown that the spatial and temporal degrees of freedom have to be considered together. When the effects of diffraction, dispersion and nonlinearity become comparable, the most fascinating result of space-time coupling is the possibility to form light bullets or spatiotemporal solitons [2-5]. In this talk, we show our recent contributions to the field of nondiffractive and nondispersive spatiotemporal solitons in Kerr media [6,7]. At first, we show the existence and properties of dark line solitary waves of the (2+1)D nonlinear Schrodinger equation (NLSE), which governs the propagation in self-focusing with normal dispersion. Dark lines represent holes of light on a continuous wave background. We show nontrivial web patterns generated under interactions of line solitons, which give birth to dark X solitary waves. Then we show the existence and interactions of a family of spatiotemporal dark lump solitary wave of the (2+1)D nonlinear Schrodinger equation (NLSE), which governs the propagation in self-defocusing with anomalous dispersion. Dark lumps represent multidimensional holes of light on a continuous wave background.

The analytical dark solitary solutions are derived by exploiting the connection between the (2+1)D NLSE and the (2+1)D Kadomtsev-Petviashvili (KP) equation [8], a well-known equation of hydrodynamics. The latter constitutes the natural extension of the well-known (1+1)D Korteweg-de Vries (KdV) equation and it is widely employed in plasma physics and hydrodynamics [9] in its two different forms, the so-called KP-I type and KP-II type, depending on the sign of the transverse perturbation to the KdV equation. Finally, we discuss the important issue of the stability of the predicted dark line, X and lump solitary waves.

This finding opens a novel path for the excitation and control of optical solitary waves, of hydrodynamic nature.

Acknowledgments: the present research has received funding from the European Union's Horizon 2020 research and innovation programme under the Marie Skłodowska-Curie grant agreement No 691051.

REFERENCES

- [1] R. Boyd, *Nonlinear Optics*, 3rd ed. Academic Press, London (2008).
- [2] Y. Silberberg, *Opt. Lett.* 15, 1282 (1990).
- [3] X. Liu, L. J. Qian, and F.W. Wise, *Phys. Rev. Lett.* 82, 4631 (1999).
- [4] F. Baronio, C. De Angelis, P.H. Pioger, V. Couderc, and A. Barthelemy, *Opt. Lett.* 29, 986 (2004).
- [5] C. Conti, S. Trillo, P. Di Trapani, G. Valiulis, A. Piskarskas, O. Jedrkiewicz, and J. Trull, *Phys. Rev. Lett.* 90, 170406 (2003).
- [6] F. Baronio, S. Wabnitz, and Y. Kodama, *Phys. Rev. Lett.* 116, 173901 (2016).
- [7] F. Baronio, S. Chen, M. Onorato, S. Trillo, S. Wabnitz, and Y. Kodama, *Opt. Lett.* 41, 5571 (2016).
- [8] B.B. Kadomtsev and V.I. Petviashvili, *Sov. Phys. - Dokl.* 15, 539 (1970).
- [9] Y. Kodama, *J. Phys. A: Math. Theor.* 43, 434004 (2010).

Spontaneous parametric down-conversion in periodically structured media

Frank Setzpfandt

*Institute of Applied Physics, Abbe Center of Photonics, Friedrich-Schiller-Universität Jena
Jena, Germany*

e-mail: f.setzpfandt@uni-jena.de

Photon pairs, optical quantum states consisting of exactly two photons, are an important resource for quantum optics. Shaping their properties, e.g. their spectra, propagation directions, and entanglement, is a key for harnessing the fascinating potential of quantum optics.

In integrated optics, the spatial degree of freedom is defined by the discrete waveguide modes or paths the photons are propagating in. Controlling it is mandatory to use the advantages of integrated optics for quantum technology. In the last years, several integrated optical chips combining photon-pair generation by spontaneous nonlinear processes and photon routing by means of waveguide optics have been developed [1].

One approach to control the path degree of freedom of photon pairs is to combine pair generation and spatial control into one integrated component. In the last years we could show for photon pair generation by spontaneous parametric down-conversion (SPDC) [2] that particularly integrated periodic structures are an effective tool to achieve such spatial control.

In SPDC, a short wavelength pump photon is spontaneously decaying into signal and idler photons of longer wavelength. This process is controlled by the phase mismatch between the interacting waves. Using nonlinear waveguide arrays, periodic arrangements of parallel coupled waveguides, where the pump beam was confined in just one waveguide whereas signal and idler could couple between waveguides, we demonstrated that by changing the phase mismatch, the generated photon pairs could be tuned from showing highly non-classical spatial correlations to resembling a purely classical wave [3]. This control results from a complex interplay between nonlinear pair generation by SPDC and linear propagation of signal and idler ruled by the periodic diffraction relation of the waveguide array. In a simpler system of just two waveguides, both of which were pumped, this ability of spatial control enabled simultaneous control of entanglement and spatial distribution of the generated photon pairs by classical parameters of the pump [4]. Using the spatial characteristics of the waveguide modes, it is furthermore possible to generate the two photons of a pair in different waveguides [5], adding additional means of controlling their spatial distribution.

Instead of using integrated optical systems with transverse periodicity, also single waveguides with a periodicity along the propagation direction, e.g. photonic crystal waveguides, can be used to control photon pair propagation. Here, the periodic structure provides additional wavevectors, which allow to achieve phasematching of pump, signal, and idler waves propagating in different directions along the waveguide [6]. We could show that in photonic crystal waveguides made from lithium niobate, this can be used to create path-entangled Bell-states using just a single waveguide [6].

The described possibilities for controlling photon pairs in integrated optical structures using periodicity help to realize the potential of quantum optics on optical chips.

REFERENCES

- [1] A. S. Solntsev and A. A. Sukhorukov, *Reviews in Physics* 2, 19 (2017).
- [2] D. C. Burnham and D. L. Weinberg, *Phys. Rev. Lett.* 25, 84 (1970).
- [3] A. S. Solntsev, F. Setzpfandt et al., *Phys. Rev. X* 4, 031007 (2014).
- [4] F. Setzpfandt, et al., *Laser & Photonics Review* 10, 131 (2016).
- [5] F. Setzpfandt, A. S. Solntsev, and A. A. Sukhorukov, *Optics Letters* 41, 5604 (2016).
- [6] S. Saravi, T. Pertsch, and F. Setzpfandt, *Phys. Rev. Lett.* 118, 183603 (2017).

Confocal synaptology – a simple method for the assessment of synaptic re-arrangements in neurodegenerative disorders and upon nervous system injury

Igor Jakovcevski

Experimental Neurophysiology, German Center for Neurodegenerative Diseases, Bonn, Germany; Institute for Molecular and Behavioral Neuroscience, University of Cologne, Center for Molecular Medicine Cologne, Germany

e-mail: igor@enp.org

The nervous system is a unique exception from the definition which states that cell is a structural and functional unit of tissue systems and organs. Functional unit of the nervous system is a synapse, contact between two nerve cells. As such, synapses are the focus of investigations of nervous system organization and function, as well as readouts for the progression of various nervous system disorders. In the past decade development of antibodies specific to presynaptic terminals has enabled us to assess, at the optical, laser scanning microscopy level, these sub-cellular structures, and provided a simple method for quantification of various synapses. Indeed, excitatory (glutamatergic) and inhibitory synapses can be visualized using antibodies against the respective vesicular transporters, and choline-acetyl transferase visualizes cholinergic synapses throughout the central nervous system. I will present results of several studies which used this method to evaluate this structural equivalent of functional outcome upon spinal cord and femoral nerve injuries, as well as in mouse models of neurodegeneration due to genetic defects, including the model of Alzheimer's disease. The results implicate disease- and brain region-specific changes in specific types of synapses, which correlate well with the degree of functional deficit caused by the disease process. Additionally, results are reproducible between various studies and experimental paradigms, supporting the reliability of the method. To conclude, this quantitative approach enables fast and reliable estimation of the degree of the progression of neurodegenerative changes and can be used as a parameter of recovery.

Single Photons: Hong-Ou-Mandel Experiments and Beyond

Mohammad Reza¹, Jörg Wrachtrup^{1,2}, and Iija Gerhardt^{1,2}

¹*Institute of Physics, University of Stuttgart and Institute for Quantum Science and Technology, IQST, Pfaffenwaldring 57, D-70569 Stuttgart, Germany*

²*Max Planck Institute for Solid State Research, Heisenbergstrasse 1, D-70569 Stuttgart, Germany*
e-mail: i.gerhardt@fkf.mpg.de

30 years ago a pioneering experiment of two photon coalescence was performed by Hong, Ou and Mandel [1,2]. It showed for the first time that two overlapping photons, which enter into two different ports of a 50:50 beam-splitter, have a vanishing probability to be both transmitted and both reflected on the beam-splitter.

Theoretical proposals how to use these photons for all kind of quantum information processing were developed and the powerful proposal of Knill, Laflamme and Milburn ('KLM') [3] proves that a variety of protocols can be implemented solely with linear optical elements. Such schemes were experimentally realized quickly after. In the past 10 years, more and more single photon sources were researched, with stunning properties and different quality features – all aiming for quantum information processing, and to a good extend based on the KLM proposal.

Here we present a single molecule based single photon source. Beside its high flux (>1 Mio counts per second; detected clicks) and narrow-band nature (<20MHz) it features more interesting properties: The photons are spectrally aligned with the atomic sodium D-line transitions [4]. Therefore, an efficient filtering scheme, based on Faraday rotation in a hot atomic sodium vapor has been developed. It features a GHz wide transmission band with above 80% transmission, and a suppression of more than 4 orders of magnitude [5]. The filter allows to suppress residual background fluorescence to a minimum and enables almost pure single photons in an experiment.

The experiments on the single photon nature and the Hong-Ou-Mandel coalescence are straight forward – but in the case when the photons arrive at the beam-splitter with orthogonal polarization [6], even more interesting properties of the resulting photon state occur: All options of transmission and reflection are now independent of each other, and a coincidence detection allows to measure photonic entanglement. The Hong-Ou-Mandel dip can also be regained, when the path information of the incoming photons is erased at the detectors – this forms a delayed “choice” quantum eraser [7,8], since depending on how the measured data is processed, the Hong-Ou-Mandel interference does or does not occur in the same measured data-set.

Our measurements are accompanied by the description of the one-arm correlation, which is a Hanbury Brown and Twiss-type measurement in one of the output arms of the Hong-Ou-Mandel interferometer. The measurement reveal the perfect Fourier-limited performance of our sodium resonant single photon source [9].

REFERENCES

- [1] Hong, C. K., Ou, Z. Y. & Mandel, L., *Phys. Rev. Lett.* **59** 2044-2046 (1987).
- [2] Rarity, J. G. & Tapster, P. R., *J. Opt. Soc. Am. B* **6** 1221-1226 (1989).
- [3] Knill, E., Laflamme, R. & Milburn, G. J., *Nature* **409** 46-52 (2001).
- [4] Siyushev, P., Stein, G., Wrachtrup, J. & Gerhardt, I. *Nature* **509** 66-70 (2014).
- [5] Kiefer, W., Reza, M., Wrachtrup, J. & Gerhardt, I. *Applied Physics B: Lasers and Optics* **122** 1-12 (2016).
- [6] Shih, Y. H. & Alley, C. O. *Phys. Rev. Lett.* **61** 2921-2924 (1988).
- [7] Kwiat, P. G., Steinberg, A. M. & Chiao, R. Y. *Phys. Rev. A* **45** 7729-7739 (1992).
- [8] Kim, Y.-H., Yu, R., Kulik, S. P., Shih, Y. & Scully, M. O. *Phys. Rev. Lett.* **84** 1-5 (2000).
- [9] Kim, J.-H., Richardson, C. J. K., Leavitt, R. P. & Waks, E. *Nano Letters* **16** 7061-7066 (2016).

Probing Ultrafast Magnetization Dynamics with Resonant X-ray Scattering Techniques

J. Lüning

University Pierre et Marie Curie, Paris, France

e-mail: jan.luning@upmc.fr

Since the discovery of the ultrafast demagnetization phenomenon by E. Beaurepaire and colleagues in 1996 [1], the field of femtomagnetism has developed to an active research area. Initial experiments relied mostly on all-optical pump-probe techniques, which raised concerns about optical artifacts affecting the measurement. Since these limitations can be overcome by X-ray based techniques, the advent of sources providing femtosecond short X-ray pulses was awaited for by the interested community. In addition to accessing the complete electronic structure, X-ray techniques offer additional advantages. First of all, this is their shorter wavelength, which matches naturally the nanometer length scales expected to be of relevance in ultrafast magnetization dynamics. Furthermore, X-ray techniques provide via the accessible core electron absorption resonances element sensitivity and offer a wide variety of magnetic dichroism effects exploitable as contrast mechanism, for example, in scattering experiments. This allows probing of the magnetization dynamics of individual components of complex, heterogeneous materials on the nanometer length scale. These expectations were indeed fulfilled already by the first experiments realized at the femtosecond pulsed tunable X-ray sources emerging since the mid 2000's, i.e., the BESSY femtoslicing facility (e.g., Ref. [2]) and HHG sources (e.g., Ref. [3]). With the recent advent of X-ray free electron lasers (XFELs) emitting in the XUV and soft X-ray photon energy range, unprecedented experimental capabilities became available.

In this talk I will review how we [3-7] have exploited femtosecond pulsed X-ray sources to study ultrafast magnetization dynamics. Employing resonant magnetic small angle X-ray scattering as probe technique, we have combined femtosecond temporal with nanometer spatial resolution [8]. This has enabled us to obtain experimental evidence for the occurrence of spin transport by the excited, polarized valence electrons [3,4], a phenomenon modeled theoretically in 2010 [9]. To follow these dynamics in real space, we have employed time resolved X-ray Fourier Transform holography [10] to obtain images with combined femtosecond time and nanometer spatial resolution [6]. I will conclude with the presentation of the first results obtained with our novel X-ray pulse streaking technique, which allows us to follow the initial magnetization dynamics with a single intense femtosecond short XFEL pulse [7]. This technique, which is applicable also to a wide variety of other phenomena, is in particular suited to reveal non-reproducible dynamics in ultrafast phenomena.

REFERENCES

- [1] E. Beaurepaire et al., *Phys. Rev. Lett.* **76**, 4250 (1996).
- [2] C. Stamm et al., *Nature Materials* **6**, 740 (2007).
- [3] B. Vodungbo et al., *Nature Comm* **3**, 999 (2012).
- [4] B. Pfau et al., *Nature Comm* **3**, 1100 (2012);
- [5] T. Wang et al., *Phys. Rev. Lett.* **108**, 267403 (2012);
- [6] C. von Korff Schmising et al., *Phys. Rev. Lett.* **112**, 217203 (2014).
- [7] M. Buzzi et al., *Scientific Reports* (2017).
- [8] B. Vodungbo et al., *Euro Phys Lett* **94**, 54003 (2011).
- [9] M. Battiato et al., *Phys. Rev. Lett.* **105**, 027203 (2010).
- [10] S. Eisebitt et al., *Nature* **432**, 885 (2004).

Lipid wrapping as a molecular initiating event in nanotoxicology through fluorescence microspectroscopy and super-resolution microscopy

I. Urbančič^{1,2}, M. Garvas¹, B. Kokot¹, H. Majaron¹, P. Umek^{1,3}, M. Škarabot¹, F. Schneider², S. Galiani², Z. Arsov¹, T. Koklič^{1,3}, A. Mertelj¹, I. Muševič^{1,4}, C. Eggeling², J. Štrancar^{1,3}

¹ "Jozef Stefan" Institute, Ljubljana, Slovenia

² Weatherall Institute of Molecular Medicine, University of Oxford, UK

³ Center of excellence NAMASTE, Ljubljana, Slovenia

⁴ Faculty of Mathematics and Physics, University of Ljubljana, Ljubljana, Slovenia

e-mail: janez.strancar@ijs.si

Our bodies are being increasingly exposed to a myriad of nanoparticles (NP). Being uptaken either by ingestion or inhalation, NP acquire a shell of biomolecules, usually designated as NP corona. According to vast majority of references, corona is considered to be mainly constituted from proteins captured during NPs' initial contact with biological system. From physical perspective, this should be a rather rare since NPs will most probably be uptaken via inhalation, where they inevitably interact with the lipid-rich alveolar surfactant layers. Until recently, interaction between NPs and lipids have been more or less ignored, but during the last years this became increasingly important topic in nanotoxicology. To address this I will show a number of biophysical experiments proving that with well-defined surface properties of metal-oxide nanoparticles and at certain dose such NPs can trigger different molecular events from simple-adhesion to a full-lipid wrapping which can lead to more dramatic NP-induced membrane destabilization. Fluorescence microspectroscopy, superresolution and non-linear microscopy as well as (cross-)correlation spectroscopy data will be shown together with transmission electron microscopy and electron paramagnetic resonance spectroscopy results.

Bright solitons in ultracold atoms

L. Salasnich

*Dipartimento di Fisica e Astronomia “Galileo Galilei”
Universita di Padova,
via Marzolo 8, 35131 Pddova, Italy
e-mail:luca.salasnich@unipd.it*

We review relevant old and recent experimental [1,2,3] and theoretical [4,5] results on the dynamics of bright solitons in Bose-Einstein condensates made of alkali-metal atoms and under external optical confinement.

REFERENCES

- [1] K.E. Strecker, G.B. Partridge, A. Truscott, and R.G. Hulet, *Nature* 417, 150 (2002).
- [2] L. Khaykovich, F. Schreck, G. Ferrari, T. Bourdel, J. Cubizolles, L.D. Carr, Y. Castin, and C. Salomon, *Science* 296, 1290 (2002).
- [3] J.H.V. Nguyen, De Luo, and R.G. Hulet, arXiv:1703.04662.
- [4] L. Salasnich, A. Parola, and L. Reatto, *Phys. Rev. Lett.* 91, 080405 (2003).
- [5] Y.V. Kartashov, B.A. Malomed, and L. Torner, *Rev. Mod. Phys.* 83, 247 (2011).

Applications of 3D laser lithography

M. Zamfirescu¹, B. Calin¹, F. Jipa¹ and Irina Paun¹

¹*Center for Advanced Laser Technologies (CETAL)*

National Institute for Laser, Plasma and Radiation Physics (INFLPR)

Atomistilor 409, Magurele 077125, Romania

e-mail: marian.zamfirescu@inflpr.ro

The laser material processing is a versatile technique that allows for fabrication of various structures with resolutions down to submicrometer [1]. Different laser-matter interaction effect could be involved for laser structuring such as: laser ablation, laser melting and resolidification, glass densification in bulk transparent materials, photopolymerisation. The highest resolution is obtained in 3D by femtosecond laser pulses focused in photoresist materials. The material structuring is based on nonlinear absorption effect produced by ultrashort laser pulses in photopolymers transparent to the laser radiation.

A review of applications of 3D laser processing of photopolymers is presented. At Center for Advanced Laser Technologies (CETAL) infrastructure, complex geometries are produced for applications such as microfluidics, micro-targets for laser interactions in ultra-intense regime, micro-optics, photonic crystals, etc. [2,3].

REFERENCES

- [1] F. Jipa, A. Dinescu, M. Filipescu, I. Anghel, M. Zamfirescu, and R. Dabu, *Opt. Express* 22, 3356-3361 (2014).
- [2] M. Mihailescu, I.A. Paun, M. Zamfirescu, C.R. Luculescu, A.M. Acasandrei, M. Dinescu, *J Mat. Science* 9, 4262-4273 (2016).
- [3] I.A. Paun, M. Zamfirescu, C.R. Luculescu, A.M. Acasandrei, C.C. Mustaciosu, M. Mihailescu, M. Dinescu, *App. Surf. Science* 392, 321-331 (2017).

Optical properties of 2D colloidal semiconductor quantum wells and hybrid structures

Mikhail Artemyev

Research Institute for Physical Chemical Problems of the Belarusian State University

Minsk, Belarus

e-mail: m_artemyev@yahoo.com

Colloidal $A^{II}B^{VI}$ nanoplatelets (NPLs) are the new class of quantum-sized semiconductor nanostructures with strong quantum confinement in the thickness direction. $A^{II}B^{VI}$ are useful model objects for studying basic optical properties of 2D semiconductor nanocrystals that depend on their lateral size, thickness, structure and spatial arrangement [1]. During the synthesis the thickness of atomically-flat NPLs can be precisely controlled in 2-5 monolayers range resulting in spectrally narrow excitonic optical transitions both in absorption and photoluminescence spectra. Large lateral sizes of NPLs lead to the realization of the GOST (Giant Oscillator Strength) effect which causes an order of magnitude larger two-photon absorption and photoluminescence excitation coefficients for CdSe NPLs if compared to other types of colloidal $A^{II}B^{VI}$ nanocrystals (0D quantum dots and 1D nanorods) [2]. GOST effect also allows observation of the excited state emission from p-states of CdSe NPLs well below ground state saturation [3]. Sharp excitonic absorption bands in CdSe NPLs combined with the weak lateral quantum confinement result in the large electro-optical Quantum Confined Stark effect that is much stronger than in the corresponding 1D or 0D CdSe nanocrystals [4].

Colloidal chemistry allows synthesize not only core CdSe, but more complex CdSe/CdS and CdSe/ZnS core-(epitaxial) shell NPLs with stable and bright photoluminescence for practical applications. By changing epitaxial overgrowth of CdSe core NPLs from 2D to 1D regime CdSe-CdS, CdSe-CdTe and CdTe-CdSe heteronoplatelets with core-wings structure can be obtained [5]. CdSe-CdS hetero-NPLs possess type-I band alignment and show the photon antenna effect, while CdSe-CdTe and inverted CdTe-CdSe epitaxial core-wings hetero-NPLs possess type-II band alignment with efficient electron and hole separation between core and the wings. Such spatial charge separation results in the indirect radiative exciton recombination with surprisingly high (50%) photoluminescence quantum yield and large Stokes shift.

By controlling the surface chemistry of CdSe NPLs the self-assembly of CdSe NPLs can be achieved into stacks of controlled length with regularly arranged NPLs [6]. Single or multiple layers of laterally oriented NPLs can be deposited onto flat substrates and implemented into waveguides or other hybrid structures that enable examination of orientation-dependent optical properties of NPLs and achieve collective optical effects (FRET, lasing).

REFERENCES

- [1] A.W. Achtstein, A. Schliwa, A. Prudnikau, M. Hardzei, M. Artemyev, C. Thomsen, and U. Woggon, *Nano Lett.* 12, 3151 (2012).
- [2] R. Scott, A.W. Achtstein, A. Prudnikau, A. Antanovich, S. Christodoulou, I. Moreels, M. Artemyev, and U. Woggon, *Nano Lett.* 15, 4985 (2015).
- [3] A.W. Achtstein, R. Scott, S. Kickhöfel, S.T. Jagsch, S. Christodoulou, G.H.V. Bertrand, A. Prudnikau, A. Antanovich, M. Artemyev, I. Moreels, A. Schliwa, and U. Woggon, *Phys. Rev. Lett.* 116, 116802 (2016).
- [4] A.W. Achtstein, A. Prudnikau, M.V. Ermolenko, L.I. Gurinovich, S.V. Gaponenko, U. Woggon, A.V. Baranov, M.Y. Leonov, I.D. Rukhlenko, A.V. Fedorov, and M. Artemyev, *ACS Nano* 8, 7678 (2014).
- [5] A. V. Antanovich, A. V. Prudnikau, D. Melnikau, Y. P. Rakovich, A. Chuvilin, U. Woggon, A. W. Achtstein and M. V. Artemyev, *Nanoscale* 7, 8084 (2015).
- [6] Artsiom Antanovich, Anatol Prudnikau, Anna Matsukovich, Alexander W Achtstein, Mikhail Artemyev. *J. Phys. Chem. C* 120, 5764 (2016).

Advancements in high efficiency semiconductor lasers for high power applications

Paul O. Leisher

*Lawrence Livermore National Laboratory
Livermore, California, United States of America
e-mail:leisher1@llnl.gov*

High power, high efficiency semiconductor diode lasers are used as the primary pump source in virtually all new solid state and fiber laser systems. In many cases, the output power scalability of the full system is limited by the pump diode performance (power, spatial brightness, and/or spectral brightness). Over the past decade, research and development in the commercial sector has resulted in significant improvements increase in each of these areas. Both diode laser power and spatial brightness are thermally-limited, and addressing each requires addressing the waste heat flux in the device. Improved power conversion efficiency at the operating point provides a straightforward path to reducing the waste heat flux, yet diode lasers are not much more efficient today than they were ten years ago. Newer advanced epitaxial design techniques, however, have enabled longer cavity lengths while maintaining high efficiency. This approach reduces the total heat flux which enables greater power extraction at equivalent junction temperature and reduces the magnitude of the thermal lens responsible for brightness loss. Improvements in spectral brightness have been made by wavelength locking through the use of external gratings. This work reviews the principal technical challenges and recent advancements in the development of high power, high efficiency semiconductor lasers for pumping and direct use applications.

Stimulated Brillouin Scattering in Silicon Photonics

P.T. Rakich¹

¹*Yale University, Department of Applied Physics
New Haven CT, USA
e-mail: peter.rakich@yale.edu*

Both Kerr and Raman nonlinearities are radically enhanced by tight optical-mode confinement in nanoscale silicon waveguides [1]. Counterintuitively, Brillouin nonlinearities—which arise from the coupling between photons and acoustic phonons—are exceedingly weak within these highly nonlinear silicon waveguides [2]. In conventional silicon waveguides, material response and poor acoustic confinement effectively stifle Brillouin nonlinearities. However, new optomechanical waveguides—that control both light and sound—have recently transformed Brillouin interactions into the strongest and most tailorable nonlinearities in silicon [3]–[5].

In this paper, we explore the new device physics that enables dramatic enhancement of Brillouin nonlinearities, and we demonstrate a range of highly engineerable new stimulated Brillouin interactions in silicon waveguides by controlling both light and sound within a growing ecosystem of Brillouin-active optomechanical waveguides. In particular, we describe the recent realization of high performance Brillouin amplifiers in silicon using forward intra-modal Brillouin interactions [6]. We show how the unusual properties of forward-Brillouin interactions can be used to create microwave-photon filtering technologies that have no analogue in all-optical signal processing [7].

Building on these concepts, we introduce a new type of multi-mode optomechanical waveguide that creates phonon-mediated coupling between optical modes with distinct spatial profiles. This process, termed stimulated inter-modal scattering, produces unusual new nonlinear dynamics[8]. From a technology perspective, this process is intriguing because the incident and scattered fields propagate in distinct spatial modes, permitting unique forms of mode-multiplexing and dynamical mode conversion. We show that this interaction opens the door to a range of Brillouin processes that enable everything from slow-light [9], to Brillouin-induced transparency [10], to new laser technologies in silicon [11].

REFERENCES

- [1] H. Rong, A. Liu, R. Nicolaescu, M. Paniccia, O. Cohen, and D. Hak, *Applied Physics Letters*, 12, 2196 (2004).
- [2] P. T. Rakich, C. Reinke, R. Camacho, P. Davids, and Z. Wang, *Physical Review X*, 2, (2012).
- [3] H. Shin et al., *Nat Commun* 4, 1944 (2013).
- [4] R. Van Laer, B. Kuyken, D. Van Thourhout, and R. Baets, *Nat Photon* 3, 199 (2015).
- [5] E. A. Kittlaus, H. Shin, and P. T. Rakich, *Nat Photon*, 7, 463, (2016).
- [6] E. A. Kittlaus, N. T. Otterstrom, and P. T. Rakich, *Nature Communications* 8, 15819 (2017).
- [7] H. Shin, J. A. Cox, R. Jarecki, A. Starbuck, Z. Wang, and P. T. Rakich, *Nat Commun* 6, 6427 (2015).
- [8] M. S. Kang, A. Brenn, and P. St.J. Russell, *Phys. Rev. Lett.*, 15, 153901, (2010).
- [9] Y. Okawachi et al., *Phys. Rev. Lett.*, 94, 153902, (2005).
- [10] J. Kim, M. C. Kuzyk, K. Han, H. Wang, and G. Bahl, *Nat Phys* 3, 275 (2015).
- [11] N. T. Otterstrom, R. O. Behunin, E. A. Kittlaus, Z. Wang, and P. T. Rakich, arXiv:1705.05813, (2017).

Signal Propagation Time through Hollow-Core Fibres and its Low Sensitivity to Temperature

R. Slavík¹, E. Numkam Fokoua¹, M. N. Petrovich¹, N. V. Wheeler¹, T. Bradley¹, F. Poletti¹, and D.J. Richardson¹

¹*Optoelectronics Research Centre, University of Southampton, Southampton SO17 1BJ, United Kingdom
e-mail:r.slavik@soton.ac.uk*

Optical fibres enable the propagation of optical signals over large distances. Although the intensity (power) of a propagating signal is relatively insensitive to fluctuations in the ambient temperature, its phase ϕ and propagation time τ through the fibre are not. A standard single-mode telecom fibre suffers from a propagation time temperature sensitivity of 39 ps/km/K (at 1550 nm wavelength) [1]. This can pose significant challenges in many diverse application areas of optical fibres in physics and engineering. Primary examples lie in applications in which very precise timing signals need to be disseminated for synchronization purposes in large experimental infrastructures such as synchrotrons, linear particle accelerators, large telescope arrays, and in phase arrayed antennae. A value of 39 ps/km/K equates to a phase temperature sensitivity of about 48 rad/m/K. This can adversely affect many applications relying on fibre interferometers (e.g. fibre optic sensors [2], quantum-optics [3], interferometric measurement techniques, and so on), in which maintaining stable interference would require temperature stabilization at the *mK* level. Similarly, a few key optical metrology applications require the dissemination of optical signals at a precise frequency, for example to compare distant ultra-precise clocks (e.g., national standard clocks) with a precision (fractional stability) at/below the 10^{-18} level [4]. Such a level of precision is easily compromised by thermally-induced changes in optical path length (temperature drift) with time that unavoidably result in a Doppler frequency shift [4].

Here, we review our recent results [5,6] in which we showed that Hollow-Core Fibres (HCF) offer significantly reduced thermal sensitivity relative to solid-core fibres in terms of propagation time/phase. We further discuss the design and demonstration of an optical fibre in which the propagation time is fully insensitive to temperature variations.

The extremely low levels of thermal sensitivity of propagation delay through an optical fibre we have achieved will bring significant improvements in the generation and transfer of signals with precise frequency and timing, allowing the levels of stability only now achievable in specialized metrology laboratories to be realized in the external world. We expect that the ability to provide stable latency will allow new approaches in well-established fields, e.g., enabling time-synchronous data transfer in optical communications, allowing, e.g., for lower latency and simplification of data processing, and helping to open up emerging new fields such as relativistic geodesy.

Acknowledgements: EPSRC (EP/K003038/1, EP/P030181/1, EP/I061196X, EP/I01196X/1). Royal Society and Wolfson Foundation.

REFERENCES

- [1] A.H. Hartog, A.J. Conduit, and D.N. Payne, *Optical and Quantum Electron.* **11**, 265-273 (1979).
- [2] V. Dangui, H.K. Kim, M.J.F. Digonnet, and G.S. Kino, *Opt. Express* **13**, 6669-6684 (2005).
- [3] J. Minář, H. Reidmatten, Ch. Simon, H. Zbinden, and N. Gisin, *Phys. Rev. A* **77**, 052325 (2008).
- [4] K. Predehl et al., *Science* **336**, 441-444 (2012).
- [5] R. Slavík, G. Marra, E. Numkam Fokoua, N. Baddela, N.V. Wheeler, M. Petrovich, F. Poletti, and D.J. Richardson, *Sci. Rep.* **5**, 15447 (2015).
- [6] E. Numkam Fokoua, M.N. Petrovich, T. Bradley, F. Poletti, D.J. Richardson, and R. Slavík, *Optica* **4**, 659-668 (2017).

Hot Rydberg atoms and more

R. Löw

*5th Institute of physics, University of Stuttgart
Stuttgart, Germany*

e-mail:r.loew@physik.uni-stuttgart.de

The exceptional large polarizability of highly excited Rydberg states can be exploited in manifold ways in spectroscopy, quantum optics and many body quantum physics. Most experiments on interacting Rydberg atoms in the last decade have been carried out with ultracold gases. But when it comes to real world applications it is desirable to use thermal vapours instead of ultra-cold gases. With the help of specialized vapour cells, hollow core fibres, integrated photonics and novel detection methods it is also possible to observe many interesting Rydberg induced phenomena at room temperature. I will give an overview on our coherent spectroscopy methods, the importance of Rydberg-Rydberg interactions [1], aggregation dynamics [2], optical bistabilities [3], electro-optical effects and much more. In the end I will give an outlook on how these hot Rydberg gases can be converted into potential applications for quantum optics and quantum enhanced sensing.

REFERENCES

- [1] T. Baluktian, et. al., Phys. Rev. Lett. 110, 123001 (2013).
- [2] A. Urvoy, et. al., Phys. Rev. Lett. 114, 203002 (2015).
- [3] D. Weller, et. al., Phys. Rev. A 94, 063820 (2016).

Synchrotron light based spectro-microscopies: Illumination of cellular disorders in neuro-degenerative diseases

Tanja Dučić

Synchrotron light source CELLS – ALBA, Carretera BP 1413, Barcelona, Spain

e-mail:tducic@cells.es

Molecular neuroscience is in need of new techniques that would broaden the set of tools available for elucidation and investigation of known and to be discovered disease features [1]. Here, three examples of X-ray imaging aspects of neuro-diseases will be presented: *i*) the 3D-insight into sub-cellular changes in cortical astrocytes isolated from a transgenic rat model for Amyotrophic lateral sclerosis, by using soft X-ray full field tomography, combined with the Fourier transformed infra-red (FTIR) spectro-microscopy, *ii*) X-ray fluorescence imaging and spectroscopy on primary midbrain neurons relevant for Parkinson's disease [2], and *iii*) an example of synergistic usage of different X-ray imaging methods on glioblastoma cells (type of brain and spine tumor) [3].

X-ray cryo-microscopy is a rather novel microscopic approach in life science in general, complementary to other conventional microscopies. It can provide information on the organization of cellular and subcellular features in whole intact and unstained cells, at resolution intermediate between that of visible light- and electron microscopy (around 30-40 nm) [1]. The single cell intrinsic sample thickness does not limit X-ray microscopy, and thus it can collect data without cell sectioning, or chemical fixation, which in classical microscopy introduces artifacts in cellular elemental and structural compartmentalization. In addition, the correlation of information with visible light- and FTIR microscopy has become an important source of information in study of biological events at different levels. Combining complementary imaging techniques, including different X-ray microscopies, will allow us to generate deeper insight into structural and molecular modifications on the cellular/organelles level.

This approach allows us to draw conclusions about the pathophysiological role of trace metals and other chemical elements in different neurological diseases and nervous system cancer. The final goal is to unify the efforts in different X-ray microscopy imaging modalities to understand cellular disorders in all types of nervous system related diseases.

REFERENCES

- [1] T. Salditt and T. Dučić, book chapter in *Super-Resolution Microscopy Techniques in the Neurosciences Series*, 257–290 (2014).
- [2] T. Dučić, E. Carboni, B. Lai, et al, *ACS Chem. Neurosci.*6, 1769–1779 (2015).
- [3] T. Dučić, T. Paunesku, S. Chen, et al, *Analyst* 142, 356-365(2017).

Backward-wave optical parametric interactions in structured nonlinear media

V. Pasiskevicius, C. Canalias, A. Zukauskas

Department of Applied Physics, Royal Institute of Technology (KTH), Stockholm, Sweden
e-mail: vp@laserphysics.kth.se

Rapid progress in structuring technologies of second-order nonlinear materials (the so called quasi-phase-matched or QPM materials) since the beginning in the middle of 1990's has brought essential changes in the way optical frequency converters are being designed and used. Combination of high nonlinearities and of a freedom to design the phases in three-wave-mixing (TWM) interactions is unique in and is extremely useful in all applications of nonlinear optics. The range of materials where structuring of the second-order nonlinearity has been demonstrated is steadily increasing - by now including not only ferroelectric crystals but also III-V semiconductors and glasses - each of them offering their distinct benefits. In addition, the QPM materials allow realizing TWM processes which would be impossible in usual birefringence phase-matched $\chi^{(2)}$ media. Here we present recent breakthroughs in the structuring of ferroelectric crystals from KTiOPO_4 isomorph family with periodicities on sub-micrometer scale [1]. Such structures enabled for the first time to realize novel types of nonlinear optical devices, namely, backward-wave optical parametric oscillators (BWPO) with rather unique spectral properties.

BWPO relies on counter-propagating TWM interaction where the pump photon is split in the nonlinear crystal into mutually counter-propagating signal and idler photons. When the pump reaches a well-defined threshold value, the counter-propagating TWM establishes distributed nonlinear feedback and oscillation starts. The distributed feedback obviates the need for cavity mirrors and therefore makes the device inherently single-mode. The theoretical concept of the BWPO has been proposed in 1966 by S. E. Harris [2], however, in the same paper, he cautioned that it would be impossible to realize such device in near and mid-infrared using standard, birefringence phase matched nonlinear materials. The reason is that the momentum mismatch is very large in counter-propagating interactions and simply natural birefringence in the known nonlinear materials is not sufficient to compensate it. This can be done by employing QPM materials, which however need to be structured on a sub-micrometer scale. It took more than 40 years to achieve the required structuring precision and demonstrate experimentally the first BWPO [3]. The spectral properties of the parametric waves generated in BWPO are radically different from those observed in a usual optical parametric oscillator with co-propagating TWM. First the parametric wave co-propagating with the pump inherits the phase profile of the pump making the BWPO close to ideal frequency translator [4]. Second, the counter-propagating parametric wave is by necessity narrowband and for proper condition would automatically represent transform-limited signals without any additional spectral filtering or manipulation. This is a highly useful property for many sensing and LIDAR applications, considering that the wavelength of the backward-propagating wave, typically in mid-infrared, can be designed at will by properly structuring material and finely tuned by crystal temperature and/or the interaction geometry. It should be mentioned that the efficiency of BWPO in current state-of-the-art QPM crystals is very high, readily exceeding 50%, owing to effective suppression of the back-conversion effects, which typically limit the efficiency and spectral quality of usual optical parametric oscillators.

REFERENCES

- [1] A. Zukauskas, G. Strömquist, V. Pasiskevicius, F. Laurell, M. Fokine, and C. Canalias, *Opt. Mater. Express*, **1**, 1319 (2011).
- [2] S. E. Harris, *Appl. Phys. Lett.* **9**, 114–116 (1966).
- [3] C. Canalias and V. Pasiskevicius, *Nat. Photonics*, **1**, (2007).
- [4] G. Strömquist, V. Pasiskevicius, C. Canalias, and C. Montes, *Phys. Rev. A* **84**, 23825 (2011).

Research opportunities within Laserlab-Europe and ELI

A. Borzsonyi^{1,2}

¹*ELI-ALPS, ELI-Hu Nonprofit Kft, Szeged, Hungary*

²*Department of Optics and Quantum Electronics, University of Szeged, Szeged, Hungary*

e-mail: Adam.Borzsonyi@eli-alps.hu and badam@titan.physx.u-szeged.hu

Lasers and photonics, one of five key enabling technologies identified by the European Union, are not only essential for the scientific future but also for the socio-economic security of any country. Laser technology is a key innovation driver for highly varied applications and products in many areas of modern society, thereby substantially contributing to economic growth. Laserlab-Europe [1] aims to strengthen Europe's leading position and competitiveness in this key area. The Consortium now brings together 33 leading organisations in laser-based inter-disciplinary research from 16 countries. Together with associate partners, Laserlab covers the majority of European member states. 22 facilities offer access to their labs for research teams from Europe and beyond.

Laserlab-Europe aims to promote the use of advanced lasers and laser-based technologies for research and innovation on a European scale. One of the main objectives is to serve a cross-disciplinary user community, from academia as well as from industry, by providing transnational access to a comprehensive set of advanced laser research facilities, including two free-electron laser facilities, in a highly co-ordinated fashion. Access is provided free of charge, including travel and accommodation, however, the selection is based on the scientific excellence of the proposal, reviewed by an external and independent Selection Panel. Priority is given to new users. A typical access project has a duration of 2 to 4 weeks. Applicants are encouraged to contact any of the facilities directly to obtain additional information and assistance in preparing a proposal.

Similarly to Laserlab-Europe, excellent research opportunities are going to be provided by the new emerging user facilities of the Extreme Light Infrastructure (ELI, [2]). The major research equipments of the European distributed research facility are based on short pulse laser sources operating in the 100 W average power regime. The peak power and the repetition rate range from 1 TW at 100 kHz up to multiple PW at few Hz. The systems are designed for stable and reliable operation, yet to deliver pulses with unique parameters, especially with unmatched fluxes and extreme bandwidths. This exceptional performance will give ways to a set of secondary sources with incomparable characteristics, including light sources ranging from the THz to the X-ray spectral ranges, and particle sources.

REFERENCES

[1] <https://www.laserlab-europe.eu>

[2] <https://eli-laser.eu>

Progress reports

Development and application of an electronic sensing system by using polymer optical fibre with sensitive zone

D. Stupar¹, J. Bajić² and M. Živanov²

¹*Frobas doo, Novi Sad, Serbia*

²*Faculty of Technical Sciences, University of Novi Sad,
Novi Sad, Serbia*

e-mail:stupar986@gmail.com

Polymer optical fibre technology ensures design of high performance, low-cost sensing systems capable to provide attractive performances in comparison to conventional sensing systems. Most notable application of polymer optical fibre in sensing applications is automotive industry [1]. Application of polymer optical fibres can be found in research papers in various fields [2-5].

In this paper an electronic sensing system is developed to ensure high quality measurements with fibre-optic sensors based on intensity modulation. The system consists of fibre optic sensor and three pairs of optical sources and photodetectors capable for easy mounting the sensing optical fibres. Also, the developed system enables usage of an external optical source or photodetector. The system also has the possibility of wireless and remote measurement. As sensing element in the described sensing system, PMMA Step Index (SI) optical fibre with sensitive zone is used. A method for fabrication of the fiber-optic sensor with sensitive zone is also presented. The developed sensing system is characterized with a very good repeatability, and very good electronic sensing system stability.

The implemented electronic system is tested for structural health monitoring, actually for crack detection in civil engineering structures [6]. Sensing system for structural health monitoring is characterized by a good linearity. Also, the same system is applied for human joint movement monitoring [7]. The sensor is characterized by linear response and the sensitivity of 20 mV/°. The implemented sensing system consists of communication electronic device which is used to enable wireless communication with the computer by using a ZigBee module. Client and server applications are implemented in order to distribute the results obtained by measurement and to provide remote measurements. Compared with previously developed fiber-optic sensing systems for human joint movements monitoring, the proposed fiber-optic sensing systems are characterized with a very simple and low-cost design, as well as the possibility to distinguish positive and negative bending.

REFERENCES

- [1] Ziemann, O., Krauser, J., Zamzow, P.E., Daum, W.: POF Handbook, 2nd ed. Springer, Berlin (2008).
- [2] Peters, K.: Polymer optical fiber sensors-a review. *Smart Mater Struct* 20(1), 1-17 (2011).
- [3] Moraleda, A.T., Garcia, C.V., Zaballa, J.Z., Arrue, J.: A temperature sensor based on a polymer optical fiber macro-bend. *Sensors-Basel* 13(10), 13076-13089 (2013).
- [4] Kuang, K.S.C., Cantwell, W.J., Scully, P.J.: An evaluation of a novel plastic optical fibre sensor for axial strain and bend measurements. *Measurement Science and Technology* 13(10), 1523-1534 (2002).
- [5] Kuang, K.S.C., Akmaluddin, Cantwell, W.J., Thomas, C.: Crack detection and vertical deflection monitoring in concrete beams, using plastic optical fibre sensors. *Measurement Science and Technology* 14(2), 205-216 (2003).
- [6] Stupar, D.Z., Bajić, J.S., Dakić, B.M., Slankamenac, M.P., Živanov, M.B.: The possibility of using a plastic optical fibre as sensing element in civil structural health monitoring. *Physica Scripta* 2013(T157), 1-4 (2013).
- [7] Stupar, D.Z., Bajic, J.S., Manojlovic, L.M., Slankamenac, M.P., Joza, A.V., Zivanov, M.B.: Wearable low-cost system for human joint movements monitoring based on fiber-optic curvature sensor. *Ieee Sens J* 12(12), 3424-3431 (2012).

Frequency comb cooling of rubidium atoms

N. Šantić, I. Krešić, A. Cipriš, T. Ban and D. Aumiler
Institute of Physics, Bijenička 54, 10 000, Zagreb, Croatia
e-mail: ikresic@ifs.hr

Techniques for laser cooling of neutral atomic vapours have been developed extensively in the period of the last three decades. Cooling and trapping of molecular vapours has, on the other hand, proven a more difficult task, due to their complex energy level structure, with the first successful experiments appearing only recently [1].

The frequency comb, because of its broad spectrum consisting of equidistant narrow lines, is a promising candidate for cooling of molecules and atoms with complicated level structures. Since each narrow line drives a single optical transition, the technique has the potential to simplify setups with multiple continuous-wave (cw) lasers.

We demonstrate frequency comb cooling of ^{87}Rb atoms. A cloud of $N = 10^8$ atoms, prepared in a cw retro-reflected configuration, is released from a magneto-optical trap and made to interact for $t = 3$ ms with a pair of red detuned frequency comb beams counter-propagating along a single axis. The narrowing of the cloud dimension along the cooling axis indicates the existence of an optical molasses, and temperature measurements performed with a time-of-flight technique confirm a sub-Doppler cooling down to $T \approx 100$ μK . Demonstration of sub-Doppler cooling by a comb line with an average power of $P \approx 1$ μW highlights the potential of this technique.

In addition to these experimental results, we also present schemes to simultaneously cool multiple atomic species and simple molecules [2].

REFERENCES

- [1] E. S. Shuman, J. F. Barry and D. DeMille, *Nature*, **467**, 820–823 (2010); J. F. Barry, D. J. McCarron, E. B. Norrgard, M. H. Steinecker, D. DeMille, *Nature*, **512**, 286–289 (2014).
- [2] D. Aumiler and T. Ban, *Phys. Rev. A*, **85**, 063412 (2012).

Low-cost optical sensors for absolute rotary position measurement

Jovan S. Bajić¹, Dragan Z. Stupar¹, Ana Joža¹, Branislav Batinić¹, Nikola Laković¹, Miloš B. Živanov¹

¹*University of Novi Sad, Faculty of Technical Sciences,
Department of Power, Electronic and Telecommunication Engineering,
Novi Sad, Serbia,
e-mail:bajic@uns.ac.rs*

Rotary position sensors represent one of the most important types of sensors in many industrial applications making them an important topic in research and development. In great number of systems, machines or processes, there is a need for monitoring the position of some rotating part. Mechanisms for converting angular into linear displacement further expand need for these types of sensors. In addition, sensors for position and displacement measurement (both angular and linear) are often part of a larger, complex sensors (such as velocity, acceleration, force or pressure sensors).

Many interesting solutions for rotary position measurement have been proposed over the years. This type of sensor can be implemented using various effects and phenomena such as the Hall effect, magneto resistors, magneto transistors, law of electromagnetic induction, phenomenon of eddy currents, capacitance change or modulation of the optical signal. Selection of the rotary position sensor for a particular application is usually a trade-off between demands set for a given application and the functionality and limitations of available types of sensors.

Comparison of the performance and characteristics of different types of sensors for rotary position measurement is shown in many scientific and technical papers [1-8]. Several general conclusions can be carried out reviewing existing solution for rotary position measurement. Compact and reliable industrial sensors are very expensive. Low-cost sensors also have low and/or limited resolution and accuracy. High-resolution sensors proposed and published in recent research papers often require complex measurement setups or complex manufacturing processes, making them expensive solutions. Also, a common problem of many proposed solutions is the transfer characteristic which is susceptible to the noise influences (either due to mechanical vibrations or electromagnetic radiation). Therefore, development of a robust, simple structured, low-cost sensor with high resolution and high accuracy is very important for satisfying market needs.

This work represents an extension of our previous work [9]. In this work, a novel, simple and low-cost absolute rotary position sensors based on RGB to cylindrical coordinate color space transformation are presented. Two possible implementations using single color sensor and multiple optical reflection sensors will be discussed. Measurement results acquired by the implemented sensor prototype using optical reflection sensors showed excellent performance parameters. Measurement resolution was better than 0.05° , while measurement accuracy was around 0.2% of full scale measurement range (360°).

REFERENCES

- [1] A. Ellin, G. Dolsak, *Sensor Review*, 28, 150–158 (2008).
- [2] *The Advantages of Capacitive vs Optical Encoders*, CUI, Inc., (2014).
- [3] J. Tulk, *Innovative Encoders For Demanding Applications*, Fraba, Inc., (2009).
- [4] M. Dimmler, C. Dayer, *Optical Encoders for Small Drives*, *IEEE/ASME Transaction on Mechatronics*, 1, 278–283 (1996).
- [5] V. Hilgsmann, P. Riendeau, *Proceedings of IEEE Sensors*, 2004, 1137–1142 (2004).
- [6] T. Fabian, G. Brasseur, *IEEE Transactions on Instrumentation and Measurement*, 47, 280–284 (1998).
- [7] *Absolute Encoder Design: Magnetic or Optical ?*, iC-Haus GmbH, (2012).
- [8] D. Kreit, *Inductive Versus Capacitive Position Sensors*, Zettlex UK Ltd., (2011).
- [9] J.S. Bajić, D.Z. Stupar, B.M. Dakić, M.B. Živanov, L.F. Nagy, *Sensors and Actuators, A: Physical*. 213, 27–34 (2014).

Mid-infrared fibre laser sources and their application for vibrational spectroscopy

Maria Chernysheva

Aston Institute of Ohotonic Technologies, Aston University, Birmingham, UK

e-mail:m.chernysheva@aston.ac.uk

Since the 2000s, Mid-infrared light sources and sensors have become an object of extensive research and industrial interest as rapidly growing industrial sectors (markets estimated to reach £7 and £1 billion by 2019). Their application is spanning across greenhouse gases and pollutants monitoring, optical frequency standards for spectroscopy, global positioning systems (GPS) and optical clocks, free space and fibre optical communications, LIDAR systems and novel diagnostic techniques.

One of the general approaches to reach the Mid-infrared wavelength band is the supercontinuum generation, i.e. broadening of ultrafast laser spectrum in the highly nonlinear optical fibres. The recent works show the possibility to cover over 3 octaves in the Mid-infrared [1], or deep-UV region[2]. As the most straightforward approach, the record-broadband supercontinuum sources are based on high-power, yet, complex optical parametrical oscillators (OPO) [1].

More sophisticated Mid-IR laser sources, coming on the heels of OPO, are Mid-IR fibre lasers. The direct Mid-IR fibre laser pulsed generation was enabled at 2.75 and 2.85 μm in Erbium and Holmium-doped fluoride glass fibre lasers [3,4], correspondingly. Nowadays, the continuous development of fluoride glass and ZBLAN fibres production technology have enabled the generation of 207 fs pulses with a peak power of 3.5 kW at 2.8 μm [5].

In 2002, M.C. Downer presented pioneering work on gas-filled fibres and announced “a new era in the nonlinear optics of gases”. Since then a wide range of nonlinear effects in gas-filled fibres has been demonstrated, including supercontinuum generation [6]. Application of acetylene-filled hollow-core fibres as a gain medium enabled to achieve continuous wave and pulsed generation in the spectral band of 3.1–3.2 μm [7].

The vibrational spectroscopy is based on molecular resonant absorption in broad Mid-IR range. The technique measures vibrational energy levels, which are associated with the chemical bonds in the sample. The energy levels are determined by the masses of atoms in each molecule, the shape of the molecular potential energy surfaces, and the associated interaction between electronic and nuclear vibrational motion. Therefore, the spectrum of vibration energies of each sample is unique, like a fingerprint. This enables application of vibrational spectroscopy for sample identification, composition characterization and chemical reaction monitoring. Current gold standards in molecular vibrational absorption measurement are based on three principal methods: Raman, infrared and inelastic neutron scattering spectroscopies [8]. The introduction of Fourier transform infrared (FTIR) spectrometer reaching 20 μm band along with the application of rapidly growing computational tools have pushed forward research on vibrations of polyatomic molecules, including bio-tissues. However, such factors as low resolution and complexity of data analysis have quickly overshadowed the initial excitement in FTIR vibrational spectroscopy.

In the report, I will review the current progress in Mid-IR fibre lasers and potential of their application for vibration spectroscopy to replace expensive and large-scale FTIR by compact fibre laser technology.

REFERENCES

- [1] C. R. Petersen et al. *Nature Photonics* 8(11) 830-834 (2014).
- [2] X. Jiang et al. *Nature Photonics* 9, 133-139 (2015).
- [3] T. Hu et al. *Optics Letters* 39, 2133-2136 (2014).
- [4] A. Haboucha et al. *Optics Letters* 39, 3294-3297 (2014).
- [5] S. Duval et al. *Optica* 2, 623-626 (2015).
- [6] D. Churin, et al. *Optical Materials Express* 3, 1358-1364 (2013).
- [7] M.R.A. Hassan, et al. *Optica* 3(3) 218- 221 (2016).
- [8] D.N. Sathyanarayana “Vibrational spectroscopy: theory and applications,” *New Age International*, (2015).

Photoacoustic response of a transmission photoacoustic configuration for two-layer samples with thermal memory

M.N. Popovic¹, M. Nestic¹, D. Markushev², M. Zivanov³, S. Galovic¹

¹*Vinca Institute of Nuclear Sciences, Belgrade, Serbia*

²*Institute of Physics, Belgrade, Serbia*

³*Faculty of Technical Sciences, University of Novi Sad, Serbia*

e-mail:maricap@vin.bg.ac.rs

Over the last thirty years, multilayered systems have increasingly drawn attention due to their growing appearance in both natural and artificial structures. A number of measurements require the adsorption of an electrically conductible, anti-reflection and/or optically absorbing layer, which induces the necessity for theoretical modelling of the system as two-layered structure, when characterized or imaged by these methods. In this paper, the models of photoacoustic (PA) response are derived for transmission PA setup configurations of two-layered optically transparent samples with thermal memory. These models are considered a generalization of the models used so far, in two directions: first, the impact of finite heat propagation velocity through both layers is included; second, the existence of volume absorption in both layers is taken into account. These studies are important for the fundamental investigations of heat transfer mechanisms in soft matter, as well as for numerous applied researches, such as self-heating problems of very large scaling integration (VLSI) circuits, engineering of physical properties of the multi-layer structures etc.

REFERENCES

- [1] J. Medina, Y. G. Gurevich, G. N. Logovinov, P. Rodriguez and G. Gonzalez de la Cruz, *Molecular Physics* 100, 3133-3138 (2002).
- [2] A. M. Mansanares, H. Vargas, F. Galembeck, J. Buijs, D. Bicanic, *J. Appl. Phys.* 70, 7046-7050 (1991).
- [3] D.D. Markushev, J. Ordonez-Miranda, M.D. Rabasovic, S. Galovic, D.M. Todorovic, S.E. Bialkowski, *J. Appl. Phys.* 117, 245309 (2015).
- [4] J.L. Pichardo-Molina, J.J. Alvarado-Gil, *J. Appl. Phys.* 95, 6450-6456 (2004).
- [5] L. Olenka, A.N. Medina, M. L. Baesso, A.C. Bento, *Braz J Phys* 32, 2B (2002).
- [6] S. Galović, D. Kostoski, *J. Appl. Phys.* 93, 3063-3071 (2003).
- [7] S. Galović, Z.Šoškić, M. Popović, D. Čevizović and Z. Stojanović, *J. Appl. Phys.* 116, 024901 (2014).

Electronic Properties of Interfaces between Domains in Organic Semiconductors

M. Mladenovic^{1,2} and N. Vukmirovic²

¹*Institute of Chemical Sciences and Engineering,
École polytechnique fédérale de Lausanne,
Lausanne, Switzerland*

²*Institute of Physics Belgrade,
Belgrade, Serbia*

e-mail: marko.mladenovic@epfl.ch

The aim of this thesis is to provide a link between atomic and electronic structure of different types of interfaces between domains in organic semiconductors. In polycrystalline small-molecule organic semiconductors interfaces are formed between single crystalline domains. We found that grain boundaries in polycrystalline naphthalene introduce trap states within the band gap of the material [1,2]. Trap states are localized on closely spaced pairs of molecules from opposite sides of the boundary. Realistic conjugated polymers, such as poly(3-hexylthiophene) (P3HT), contain mixed crystalline and amorphous domains. We found that HOMO state of the interface between crystalline and amorphous domain in P3HT belongs to crystalline domains [3]. States that belong to both domains and trap states were not found. Effects of thermal disorder are important in realistic conjugated polymers. Our results show that disorder in backbone chains of P3HT has strong effect on the electronic structure and leads to the localization of the wave functions of the highest states in the valence band, similar to the ones that occur in amorphous polymers [2,4]. At the interfaces between two materials in organic electronic devices, effects of spontaneous polarization in one or both of them on electronic properties can be pronounced. We show that ordered P3HT exhibits spontaneous polarization along the backbone direction, which is caused by the lack of inversion symmetry due to head-to-tail side chains arrangement [5]. We additionally show that spontaneous polarization in ordered P3HT keeps significant values even at room temperature when the effects of thermal disorder are important.

REFERENCES

- [1] M. Mladenovic, N. Vukmirovic, I. E. Stankovic, *J. Phys. Chem C.* 117, 15741 (2013).
- [2] M. Mladenovic, N. Vukmirovic, *Adv. Funct. Mater.* 25, 1915 (2015).
- [3] M. Mladenovic, N. Vukmirovic, *Phys. Chem. Chem. Phys.* 16, 25950 (2014).
- [4] M. Mladenovic, N. Vukmirovic, *J. Phys. Chem C.* 119, 23329 (2015).
- [5] M. Mladenovic, N. Vukmirovic, *J. Phys. Chem C.* 120, 18895 (2016).

Plasmonics for infrared detectors

Marko M. Obradov

*Center of Microelectronic Technologies, Institute of Chemistry, Technology and Metallurgy,
University of Belgrade, Serbia*

e-mail: marko.obradov@nanosys.ihtm.bg.ac.rs

Plasmonics studies properties of metamaterials which support surface plasmon polariton (SPP) resonance. SPP are collective oscillations of free carrier plasma coupled with electromagnetic waves propagating at an interface between conductor and dielectric. One of the more notable characteristic of plasmonic metamaterials is localization of electromagnetic radiation on subwavelength scale [1]. As such plasmonic metamaterials offer a novel approach to photodetector enhancement as light localization within photodetector active area directly translates into increased density of optical states. Since plasmon frequency of most natural conductors (metals) is in the ultraviolet or visible part of the spectrum plasmonic light localization yielded excellent results in enhancement of solar cells[2]. To apply plasmonic approach at longer wavelengths it is necessary to develop a suitable method of redshifting the plasmonic resonant response as well as means of suppressing increased material losses at longer wavelengths.

Two approaches have been developed to bring plasmonic enhancement of semiconductor detectors from visible to medium and long wavelength infrared parts of the spectrum. The first approach is based on the use of submicrometer spherical (spheroidal) conductive particles deposited on detector surface [3]. Use of transparent conductive oxides (TCO) instead of metals for the particles reduces the material losses and redshifts the resonant response [4]. Immersing the particles in a dielectric material allows for practically arbitrary positioning of resonant response but limits the efficiency of the structure due to reflective surface between free space and dielectric material. To counter this antireflective layer with gradient index of refraction is positioned on top of the dielectric layer. Changing particle geometry by changing the size of different spheroid axes allows the spectral positioning and magnitude of the plasmonic resonance to be tuned separately [5].

The second approach is based on using metallic extraordinary optical transmission (EOT) arrays deposited on photodetector surface, here redshifting is achieved by tuning the geometrical properties of the structure [6]. By superpositioning two 2D arrays of apertures on the single EOT array additional modes of transparency are achieved as well as suppression of the material losses due to the reduced content of metal [7]. Furthermore in this case optical vortices are formed in the photodetector active area with a possibility to tune the spectral and spatial positioning of the vortices.

Plasmonic localization allows for reduction of IR detector active area volume (thickness) which translates into reduced generation-recombination (g-r) noise without sacrificing detector sensitivity. This means that it is possible to suppress g-r noise by a purely passive method [3]. Increase in detector performance can be used as is or potentially sacrificed to achieve plasmonically enhanced IR detectors at room temperature with their characteristics similar to those of conventional devices cooled with liquid nitrogen.

REFERENCES

- [1] J. B. Pendry, D. Schurig, D. R. Smith, *Science*, 312, 5781 (2006).
- [2] S. V. Boriskina, H. Ghasemi, G. Chen, *Mat. Today*, 16, 10 (2013).
- [3] M. Obradov, Z. Jakšić, D. Vasiljević-Radović, *J. of Opt.*, 16, 12 (2014).
- [4] P. West, S. Ishii, G. Naik, N. Emani, V. Shalaev, A. Boltasseva, *Laser & Photon. Rev.*, 1 (2010).
- [5] M. Obradov, D. Tanasković, O. Jakšić, D. Vasiljević-Radović, *Opt. Quant. Electron.*, 48, 4, (2016).
- [6] J. B. Pendry, L. Martín-Moreno, F. J. Garcia-Vidal, *Science*, 305, 5685, (2004).
- [7] D. Tanasković, Z. Jakšić, M. Obradov, O. Jakšić, *J. of Nanomat.*, 2015, 22, (2015).

Instabilities in nonlinear systems

N. Tarasov¹, A. M. Perego¹ and S. K. Turitsyn¹
¹*Aston Institute of Photonic Technologies, Aston University,
Birmingham, B4 7ET, United Kingdom
e-mail:n.tarasov1@aston.ac.uk*

Instabilities play an important role in a variety of physical and biological processes. From galaxies to zebra stripes, instabilities in nonlinear systems are responsible for the formation of patterns and structures. Discovering the new instabilities and harnessing their power is not only important for our understanding of the universe, but for practical applications too, ranging from creation of ultrashort optical pulses to improving stability of laser systems.

In this work, we review the recent progress in the field of instabilities, with the greater emphasis on the fibre based systems. One of the recent advancements in the field is the demonstration of competing Turing and Faraday instabilities in a fibre cavity with inhomogeneous dispersion profile [1]. In this work to observe the competing instabilities a train of square pulses was launched into the passive cavity at the rate finely tuned to the free spectral range of the cavity. By abruptly increasing the pump power in the system, a transition from Turing to Faraday instability is observed, which is evident from the frequency shift of the spectral sidebands.

Another recent work showed how dissipation induced instabilities in nonlinear optics can occur for a CW pump field propagating through a nonlinear medium (e.g. an optical fibre or a χ_2 crystal) due to unbalanced losses for signal and idler waves. Counterintuitively, dissipation plays a destabilizing role for the CW field leading to exponential amplification of spectral sidebands in the spectral region where losses have been applied. Such dissipation-induced instabilities, occurring without satisfying any phase-matching conditions may provide interesting solutions for the design of a new class of fibre optics parametric amplifiers with tunable gain spectrum, pulsed light sources and optical parametric oscillators.

Further, we report on our recent work on passive mode-locking of a Raman fibre laser by the recently predicted new type of parametric instability – the dissipative Faraday instability [2, 3], where spatially periodic zig-zag modulation of spectrally dependant losses can lead to pattern formation in temporal domain. The high harmonic mode-locking is achieved in a very simple experimental configuration with the laser cavity formed of optical fibre and two chirped fibre Bragg gratings, and no additional mode-locking elements. The results not only open the possibilities for novel designs of mode-locked lasers, but extend beyond fibre optics to other fields of physics and engineering.

REFERENCES

- [1] F. Copie, M. Conforti, A. Kudlinski, S. Trillo, and A. Mussot, *Opt. Letters*, 42, 435 (2017).
- [2] A. M. Perego, N. Tarasov, D.V. Churkin, S. K. Turitsyn, and K. Staliunas, *Phys. Rev. Lett.*, 116, 028701 (2016).
- [3] N. Tarasov, A. M. Perego, D. V. Churkin, K. Staliunas, and S. K. Turitsyn, *Nat. Commun.* 7, 12441 (2016).

Surface enhanced Raman spectroscopy of thiocyanine coated silver nanoparticle clusters

U. Ralević¹, G. Isić¹, B. Laban², D. Vasić Aničijević³, V. Vodnik³, U. Bogdanović³, V. Vasić³, V. M. Lazović¹ and R. Gajić¹

¹*Institute of Physics Belgrade, University of Belgrade,
Belgrade, Serbia*

²*Faculty of Natural Sciences and Mathematics, University of Priština,
Kosovska Mitrovica, Serbia*

³*Vinča Institute of Nuclear Sciences, University of Belgrade,
Belgrade, Serbia*

e-mail:uros@ipb.ac.rs, isicg@ipb.ac.rs

Metallic nanoparticles are known for their remarkable ability to confine and enhance the electromagnetic fields incident upon them. These nanoobjects have thus been successfully utilized as a platform for enhancing the intensity of light scattered from analyte molecules residing in their close vicinity. A perfect example is surface enhanced Raman spectroscopy (SERS) in which the confined, strong electromagnetic fields transfer the electromagnetic energy to the analyte thereby increasing the magnitude of the analyte phonon-modulated dipole moment and consequently its Raman scattering efficiency [1]. The SERS enhancement factors depend on various factors such as the topology of the metallic nanoobjects, and can be as high as 10^{11} [1]. Large enhancement factors render SERS a very versatile technique which can be used for detection of extremely small amounts of analyte adsorbed on the surface of metallic nanoobjects [2] as well as for studies on a single molecule level [3].

Here we investigate silver nanoparticle clusters deposited on an insulating substrate as a platform for SERS, using confocal Raman microspectroscopy and a finite element based numerical analysis. The analysis of SERS enhancement based on rigorous numerical simulations of Maxwell equations for the case of plane wave scattering on random silver nanoparticle clusters, shows that the highest field enhancement factors are reached at collective nanoparticle plasmon resonances and become redshifted in elongated clusters with an increasing number of particles. From an inspection of electromagnetic field distribution on nanoparticle surfaces, a conclusion is reached that at least 90% of the total enhancement originates from nanogaps between adjacent nanoparticles, implying that the SERS experiments are sensitive only to adsorbates located in these gaps. The latter conclusion is used to aid the experimental SERS study of the thiocyanine (TC) dye adsorption on the surface of silver nanoparticle clusters. By analyzing the SERS spectra of TC dye coated nanoparticle clusters, we find that the adsorption of this particular dye is strongly influenced by the capping anions which are initially conformed on the surface of the nanoparticles.

REFERENCES

- [1] M. Kerker, D.-S. Wang, H. Chew, Surface enhanced Raman scattering (SERS) by molecules adsorbed at spherical particles, *Appl. Opt.* 19 3373 (1980).
- [2] Y. Kitahama, Y. Tanaka, T. Itoh, M. Ishikawa, Y. Ozaki, Identification of thiocyanine J-aggregates adsorbed on single silver nanoaggregates by surface-enhanced Raman scattering and emission spectroscopy, *Bull. Chem. Soc. Jpn.* 82 1126 (2009).
- [3] A. B. Zrimsek, N. L. Wong, R. P. Van Duyne, Single Molecule Surface-Enhanced Raman Spectroscopy: A Critical Analysis of the Biantalyte versus Isotopologue Proof, *J. Phys. Chem. C* 120 5133 (2016).

Contributed papers

1. Quantum optics and ultracold systems
2. Nonlinear optics
3. Optical materials
4. Biophotonics
5. Devices and components
6. Optical communications
7. Laser spectroscopy and metrology
8. Ultrafast optical phenomena
9. Laser - material interaction
10. Optical metamaterials and plasmonics
11. Other topics in photonics

Ultralow propagation of optical pulses in hot potassium vapor

B. Zlatković¹, A. J. Krmpot¹, D. Arsenović¹, I. S. Radojičić¹, M. M. Ćurčić¹, Z. Nikitović¹, and B. M. Jelenković¹

¹*Institute of Physics,
Belgrade, Serbia
e-mail:bojan@ipb.ac.rs*

Parametric non-degenerate four wave mixing (4WM) is a nonlinear process in which two pump photons mix in order to create photons with different frequencies. This process is realized via double lambda scheme by stimulating a four-stage cyclical transition resulting in the emission of amplified probe and conjugate photons. Parametric non-degenerate four wave mixing is a promising tool for producing continuous squeezed light [1] and slowed optical pulses [2]. Recent demonstration of this phenomenon in hot potassium vapor [3] has motivated our investigation of slowed optical pulses in the same medium.

In our experiment double lambda scheme is realized on D1 line of potassium isotope ³⁹K. We have studied the influence of the vapor cell temperature i.e. density of potassium atoms, one photon detuning and two photon detuning and the length of the optical pulse on the slowing of optical pulses in 4WM medium.

The laser frequency is locked at various one photon detunings (700 MHz to 1600 MHz) from the $4S_{1/2}F_g=1 - > 4P_{1/2}$ transition. The probe is detuned 460 MHz (ground state hyperfine splitting) with respect to the pump beam and scanned around the Raman resonance. The vacuum potassium vapor cell is heated up to 150°C. The pump and probe beam intersect at small angle (3 mrad) set by the phase matching condition. Gaussian shaped probe pulses of length of 80ns were created by electrooptic modulator. and the delay, fractional delay and distortion of probe and conjugate pulses was measured.

We have observed probe delays up to 160 ns and fractional delays up to 2 and slightly less for conjugate. These delays were followed by up to 1.8 times of broadening of probe and conjugate pulses (with respect to width of entering probe pulse). These results motivate further work on this subject that will, as we believe, lead to improvements in slowing of optical pulses.

REFERENCES

- [1] V. Boyer, A. M. Marino, R. C. Pooser, P. D. Lett, *Science* 321, 544–547 (2008).
- [2] C. F. McCormick, V. Boyer, E. Arimondo, P. D. Lett, *PRL* 99, 143601 (2007).
- [3] B. Zlatkovic, A. J. Krmpot, N. Sibalić, M. Radonjic, B. M. Jelenkovic, *Laser Phys. Lett.* 13, 015205 (2016).

Parallel solvers for dipolar Gross-Pitaevskii equation

V. Lončar¹, D. Vudragović¹, S. K. Adhikari², and A. Balaž¹

¹*Scientific Computing Laboratory, Center for the Study of Complex Systems,
Institute of Physics Belgrade, University of Belgrade, Serbia*

²*Instituto de Física Teórica, UNESP – Universidade Estadual Paulista, São Paulo, Brazil*
e-mail:vladimir.loncar@ipb.ac.rs

We present serial and parallel semi-implicit split-step Crank-Nicolson algorithms for solving the dipolar Gross-Pitaevskii equation [1, 2], used for study of ultracold Bose systems with the dipole-dipole interaction. Six parallel algorithms will be presented: C implementation parallelized with OpenMP targeting single shared memory system [3], CUDA implementation targeting single Nvidia GPU [4], hybrid C/CUDA implementation combining the two previous approaches, and their parallelizations to distributed memory systems using MPI [5]. We first give an overview of the split-step Crank-Nicolson method and describe how the dipolar term is computed using FFT, which forms the basis of all presented algorithms. We then move on to describing the concepts used in each of the parallel implementations, and finally present a performance evaluation of each algorithm. In our tests OpenMP implementation demonstrates a speedup of 12 on a 16-core workstation, CUDA version has a speedup of up to 13, hybrid version has a speedup of up to 16, while the MPI parallelization yields a further speedup of 16 for the OpenMP/MPI version, speedup of 10 for the CUDA/MPI version, and speedup of 6 for the hybrid version.

REFERENCES

- [1] P. Muruganandam, et. al., *Comput. Phys. Commun.* 180, 1888 (2009).
- [2] R. Kishor Kumar, et. al., *Comput. Phys. Commun.* 195, 117 (2015).
- [3] D. Vudragović, et. al., *Comput. Phys. Commun.* 183, 2021 (2012).
- [4] V. Lončar, et. al., *Comput. Phys. Commun.* 200, 406 (2016).
- [5] V. Lončar, et. al., *Comput. Phys. Commun.* 209, 190 (2016).

Effect of conduction band Non-parabolicity on the intersubband transitions in ZnO/Mg_xZn_{1-x}O Quantum Well Heterostructures

Y. Chrafi¹, L. Moudou¹, K. Rahmani², I. Zorkani³

¹*LDD Faculty of Sciences and Technologies, Beni Mellal-Morocco*

²*LIRST Faculty of Polydisciplinary, Beni Mellal-Morocco*

³*LPS, Faculty of Sciences Dhar Mehraz, Fès-Morocco*

e-mail: younescharafih@gmail.com

In this paper, we have calculated the electronic states and the intersubband transition energy in ZnO/Mg_xZn_{1-x}O quantum well structures (QW), with 20% of Magnesium in both the parabolic and the non-parabolic cases. Our calculations are performed in the context of the approximation of the envelope function formalism and using the finite difference method.

The results show that the intersubband transition energy increases rapidly with well width until $L_w=5\text{nm}$ and becomes almost constant (specially transitions E_{13} et E_{23}). The non-parabolicity effect is neglect.

Wavelength λ_{23} decreases with well width until $L_w=5\text{nm}$ and becomes constant. The non-parabolicity effect is more pronounced for small QW ($L_w \leq 5\text{nm}$) and less marked in narrow and large QW. A good agreement is obtained with the existing literature values [1-2].

In addition, we are studied the coefficient of transmission, and The Absorption coefficient for 4(nm)/2(nm)/4(nm) geometry. We notice that when the height of barrier increases the coefficient of transmission decreases. It will be necessary to provide more energy to the electron so that it can cross the barrier. We also notice the variations related to a phenomenon of reflexion quantum. In addition, when the QW size decreases, the intensity of the absorption peak shows a marked increase. The physical reasons for these relationships were analyzed in depth.

REFERENCES

- [1] H. Akabli, A. Almaggoussi, A. Abounadi, A. Rajira, K. Berland, and T. G. Andersson, Superlattices and Microstructures 52, 70 (2012).
- [2] S.H. Park, D. Ahn, AIP Advances 6, 15014 (2016).

Deformation of the Fermi Surface

Vladimir Veljić¹, Antun Balaž¹ and Axel Pelster²

¹*Scientific Computing Laboratory, Center for the Study of Complex Systems,
Institute of Physics Belgrade, University of Belgrade, Serbia*

²*Physics Department and Research Center OPTIMAS, Technical,
University of Kaiserslautern, Germany*

e-mail: vveljic@ipb.ac.rs

In the presence of isotropic interactions, the Fermi surface of an ultracold Fermi gas is spherical. Introducing anisotropic and long-range dipole-dipole interaction (DDI) to the system deforms the Fermi surface to an ellipsoid, as was experimentally observed in a degenerate dipolar Fermi gas of erbium atoms [1]. The deformation is caused by the interplay between the strong magnetic DDI and the Pauli exclusion principle. It was also observed that the atomic cloud follows the rotation of the dipoles when the direction of the external magnetic field is changed, keeping the major axis always parallel to the direction of the maximum attraction of the DDI. Here we present a generalization of the previous Hartree-Fock mean-field theory [2, 3], where the magnetic field was assumed to be parallel to one of the harmonic trap axes. We now extend our calculations for an arbitrary orientation of the magnetic field. In order to obtain the ground state and analyze the resulting deformation of the Fermi surface, we minimize the total energy of the system, which enables us to determine its Thomas-Fermi radii and momenta. These analytical and numerical calculations are in agreement with observations from the Innsbruck experiment [1] and are relevant for understanding similar ongoing experiments with ultracold fermionic dipolar atoms.

REFERENCES

- [1] K. Aikawa, et al., *Science* **345**, 1484 (2014).
- [2] F. Wächtler, A. R. P. Lima, and A. Pelster, eprint arXiv:1311.5100 (2013).
- [3] V. Veljić, A. Balaž, and A. Pelster, *Phys. Rev. A* **95**, 053635 (2017).

Transport dynamics in optical lattices with flux

A. Hudomal¹, I. Vasić¹, H. Buljan², W. Hofstetter³, and A. Balaž¹

¹*Scientific Computing Laboratory, Center for the Study of Complex Systems,
Institute of Physics Belgrade, University of Belgrade, Serbia*

²*Department of Physics, University of Zagreb, Croatia*

³*Institut für Theoretische Physik, Johann Wolfgang Goethe-Universität,
Frankfurt am Main, Germany*

e-mail:ana.hudomal@ipb.ac.rs

Recent cold atom experiments have realized artificial gauge fields in periodically modulated optical lattices [1,2]. We study the dynamics of atomic clouds in such systems by performing numerical simulations using the full time-dependent Hamiltonian and compare results with the semiclassical approximation. Under constant external force, atoms in optical lattices with flux exhibit an anomalous velocity in the transverse direction. We investigate in detail how this transverse drift is related to the Berry curvature and Chern number, taking into account realistic experimental conditions.

REFERENCES

- [1] G. Jotzu, M. Messer, R. Desbuquois, M. Lebrat, T. Uehlinger, D. Greif, T. Esslinger, *Nature* **515**, 237 (2014).
- [2] M. Aidelsburger, M. Lohse, C. Schweizer, M. Atala, J. T. Barreiro, S. Nascimbène, N. R. Cooper, I. Bloch, N. Goldman, *Nat. Phys.* **11**, 162 (2015).

Quantum phase gate based on quantum Zeno dynamics

H. V. Do¹, C. Lovecchio¹, S. Gherardini¹, M. Müller¹, F. Caruso^{1,2} and F. S. Cataliotti^{1,2}

¹*LENS, Dipartimento di Fisica e Astronomia - Università degli Studi di Firenze, via Nello Carrara 1,
50019 Sesto Fiorentino, Italy*

²*Istituto Nazionale di Ottica INO-CNR, Largo Enrico Fermi 4, 50125 Firenze
e-mail:do@lens.unifi.it*

Quantum Zeno dynamics (QZD) were recently demonstrated with Bose-Einstein condensates (BEC) [1] and with Rydberg atoms [2]. In our experiment we work with internal degrees of freedom of a BEC of ^{87}Rb atoms created on an Atom Chip. In the presence of a constant magnetic bias field, we drive the dynamics between magnetic sub levels on the same hyperfine ground states using a radio-frequency (RF) field. We exploited QZD with a Raman coupling between different hyperfine levels to constrain atoms to evolve in two Hilbert subspaces.

We choose the 4 logical input states of a 2-qbit gate among the two subspaces; with D-CRAB optimization [3] we design a control RF pulse to perform a phase gating operation. We make use of a recently developed state reconstruction technique [4] to perform input and output state tomography in order to characterize the gate operation.

Given that in the same system we can make use of Raman and microwave transitions between the different hyperfine manifolds in order to perform single q-bit operations, our use of QZD allows the demonstration of a complete set of logical gates within a single rubidium atom.

REFERENCES

- [1] F. Schafer et al., *Nature Commun.* **5**, 3194 (2014).
- [2] A. Signoles et al., *Nature Physics* **10**, 715–719 (2014).
- [3] N. Rach et al., *Phys. Rev. A* **92**, 062343 (2015).
- [4] C. Lovecchio et al., *New J. Phys.* **17**, 093024 (2015).

Open-Dissipative Gross-Pitaevski Approach to Photon BEC Dynamics

Enrico Stein, Axel Pelster

Department of Physics and Research Center Optimas,

University of Kaiserslautern

Kaiserslautern, Germany

e-mail: estein@rhrk.uni-kl.de, axel.pelster@physik.uni-kl.de

Already in 2010, a Bose-Einstein condensate of photons has been created [1]. To this end, a dye-filled microcavity is pumped by a laser. The used dye plays in this experimental setup a crucial role in the condensation process. On the one hand, the specific absorption and emission spectrum provides the thermalization of the photon gas at room temperature, whereas on the other hand it introduces an effective photon-photon interaction via changing the dye refractive index. The dominant interaction effect turns out to be thermal lensing due to a temperature-related shift of refractive index [2].

We show, that these effects can be described consistently by using an open-dissipative Gross-Pitaevski approach as it is widely used in the community of exciton-polariton condensates [3]. In our context this means to set up a pair of coupled mean-field equations, one for the coherent condensate wave function and one for the diffusion of temperature in the dye solution. With this approach at hand, we determine at first the steady state of the resulting photonic Bose-Einstein condensate, from which we deduce a value of the photon-photon interaction reproducing the experimental value [2]. Furthermore, we perform a linear stability analysis of the BEC steady state, yielding both the Bogoliubov spectrum and its damping.

REFERENCES

[1] J. Klaers, J. Schmitt, F. Vewinger and M. Weitz, *Nature* **468**, 545 (2010).

[2] J. Klaers, J. Schmitt, T. Damm, F. Vewinger and M. Weitz, *Appl. Phys. B* **105**, 17 (2011).

[3] M. Wouters and I. Carusotto, *Phys. Rev. Lett.* **99**, 140402 (2007).

Excitation spectra of a Bose-Einstein condensate with an angular spin-orbit coupling

I. Vasić and A. Balaž

*Scientific Computing Laboratory, Center for the Study of Complex Systems,
Institute of Physics Belgrade, University of Belgrade, Pregrevica 118, 11080 Belgrade, Serbia
e-mail:ivana.vasic@ipb.ac.rs*

A theoretical model of a Bose-Einstein condensate with an angular spin-orbit coupling has recently been proposed [1,2] and it has been established that a half-skyrmion represents the ground state in a certain regime of spin-orbit coupling and interaction. We investigate low-lying excitations of this phase by using the Bogoliubov method and numerical simulations of the time-dependent Gross-Pitaevskii equation [3]. We find that a sudden shift of the trap bottom results in a complex two-dimensional motion of the system's center of mass. This response is markedly different from the response of a competing phase, and comprises two dominant frequencies. Moreover, the breathing mode frequency of the half-skyrmion is set by both the spin-orbit coupling and the interaction strength, while in the competing state it takes a universal value. Effects of interactions are especially pronounced at the transition between the two phases.

REFERENCES

- [1] M. DeMarco and H. Pu, Phys. Rev. A 91, 033630 (2015).
- [2] Y.-X. Hu, C. Miniatura, and B. Grémaud, Phys. Rev. A 92, 033615 (2015).
- [3] I. Vasić and A. Balaž, Phys. Rev. A 94, 033627 (2016).

A distinguishable single excited-impurity in a Bose-Einstein condensate

Javed Akram^{1,2}

¹*Department of Physics, COMSATS, Institute of Information Technology
Islamabad, Pakistan*

²*Institute für Theoretische Physik, Freie Universität Berlin, Arnimallee
14, 14195 Berlin*

e-mail:javedakram@daad-alumni.de

We investigate the properties of a distinguishable single excited state impurity pinned in the center of a trapped Bose-Einstein condensate (BEC) in a one-dimensional harmonic trapping potential by changing the bare mass of the impurity and its interspecies interaction strength with the BEC. We model our system by using two coupled differential equations for the condensate and the single excited-impurity wave function, which we solve numerically. For equilibrium, we obtain that an excited-impurity induces two bumps or dips on the condensate for the attractive- or repulsive-interspecies coupling strengths, respectively. Afterwards, we show that the excited-impurity induced imprint upon the condensate wave function remains present during a time-of-flight (TOF) expansion after having switched off the harmonic confinement. We also investigate shock-waves or gray quad-solitons by switching off the interspecies coupling strength in the presence of harmonic trapping potential. During this process, we found out that the generation of gray bi-soliton or gray quad-solitons depends on the bare mass of the excited-impurity in a harmonic trap.

Photonic simulation of open quantum systems with various exchange statistics

Milan Radonjić^{1,2} and Philip Walther¹

¹*Faculty of Physics, University of Vienna,
Vienna, Austria*

²*Institute of Physics Belgrade,
Belgrade, Serbia*

e-mail: milan.radonjic@univie.ac.at, milan.radonjic@ipb.ac.rs

Photonic quantum technology has reached a point where it is almost viable to use photonic setups to simulate the behavior of other quantum systems. Realistic quantum systems are inevitably influenced by the external environment – they are open. When the environment introduces pronounced memory effects, one speaks of non-Markovianity. The need to understand and the possibility of exploiting this phenomenon as a potential resource for quantum information tasks has spurred an increasing interest in generating and manipulating non-Markovian quantum dynamics using various experimental platforms, including photonic setups.

The essentially distinct dynamical behavior of quantum entities obeying different exchange statistics (e.g., bosonic, fermionic or anyonic) has to leave a marked signature on non-Markovianity. We will describe the project that ultimately aims to emphasize and to explore theoretically the versatility of photonic setups for simulating and studying the interplay between various exchange statistics and quantum non-Markovianity, with the ultimate goal of identifying and experimentally validating the benefits for quantum information applications.

Electromagnetically induced transparency in degenerate 3-level ladder-type system

Lj. Stevanović, N. Filipović and V. Pavlović
*Department of Physics, Faculty of Sciences and Mathematics,
 University of Niš, Serbia
 e-mail: ljstevanovic@junis.ni.ac.rs*

Electromagnetically induced transparency (EIT) is the physical phenomenon that allows light to be transmitted through a medium without any losses, despite the medium being originally opaque [1,2]. Simultaneously, EIT causes the decrease of the group velocity of light, which has been realized in practice by various experiments [3]. By taking advantage of these peculiar properties, it is now possible to apply this effect in various scientific and technical fields such as quantum optics, quantum computing, optical spectroscopy and magnetometry [4].

This paper is dedicated to the study of the EIT effect in the 3-level atomic system in the ladder configuration, with the middle level being 3-fold degenerate. Here, the levels are labeled as $|1\rangle$, $|2\rangle$, $|3\rangle$, $|4\rangle$ and $|5\rangle$, with $|1\rangle$ being the ground state, $|2\rangle$, $|4\rangle$ and $|5\rangle$ the degenerate sublevels of the middle level, and $|3\rangle$ the highest energy level. This system interacts with the probe and the control laser field, polarized in such manner that the probe field induces transition $|1\rangle \rightarrow |2\rangle$, and the control field excites transition $|2\rangle \rightarrow |3\rangle$. Furthermore, the observed system undergoes the spontaneous emission in such way that level $|3\rangle$ decays to $|2\rangle$, $|4\rangle$ and $|5\rangle$, and $|2\rangle$, $|4\rangle$ and $|5\rangle$ decay to $|1\rangle$. Therefore, the subject of this work is the 3-level ladder-type open system, which differs from the system studied in [5] by the fact that here the middle level is degenerate.

Master equations for this system are then derived and solved in the stationary regime. Real and imaginary parts of the density matrix element ρ_{21} , defining the susceptibility of the atom with respect to the probe field, are both plotted as the function of the probe field detuning. The influence of the change of the control Rabi frequency and spontaneous emission coefficients on the shape of the transparency window is also investigated. Moreover, the 3-level ladder-type closed system is studied as well, with the aim to examine how the degeneracy of the middle level affects the appearance of the EIT effect. Finally, the analysis of the problem in the dressed-state basis is given.

The results found show that, for the low values of the control Rabi frequency, the two-photon absorption in the open system occurs, contrary to the transparency window observed in the closed system. In order to obtain the EIT effect in the open system, the higher values of the control Rabi frequency are required. In addition, increasing the spontaneous emission coefficients causes the decrease of the height of the absorption peaks, together with the increase of the full width at half maximum of the peaks. It is also shown that the increase of the spontaneous emission coefficient from level $|3\rangle$ to $|2\rangle$ increases the height of the bottom of the transparency window, while decays from $|2\rangle$ to $|1\rangle$ have almost no effect on this quantity. All these results are in the agreement with the theoretical predictions given by the dressed-state analysis.

REFERENCES

- [1] K.-J. Boller, A. Imamoglu, S. E. Harris, *J. Phys. Rev. Lett.* 66, 2593 (1991).
- [2] M. Fleischhauer, A. Imamoglu, J. P. Marangos, *Rev. Mod. Phys.* 77, 633 (2005).
- [3] S. E. Harris, J. E. Field, A. Kasapi, *Phys. Rev. A* 46, R29 (1992).
- [4] M. D. Lukin, *Rev. Mod. Phys.* 75, 457 (2003).
- [5] H. S. Moon, H.-R. Noh, *Opt. Express* 21, 7447 (2013).

Husimi function for time-frequency analysis in optical, microwave and plasmonics applications

Milena D Davidović¹, Miloš D Davidović², Ljubica D Davidović³, Vladimir A Andreev⁴, Dragomir M Davidović²

¹ Faculty of Civil Engineering, University of Belgrade, Serbia

² Vinca Institute, University of Belgrade, Serbia

³ Institute of Physics, University of Belgrade, Serbia

⁴ P N Lebedev Physical Institute, Moscow, Russia

e-mail: milena@grf.bg.ac.rs

Many real-world signals, occurring in everyday engineering practice are non-stationary, and as a result, their frequency components may change gradually or abruptly over time. Such signals are typically analyzed using Fourier transform, however, this type of analysis is often not sufficient to reveal the true nature of localized (in time) frequency content. This is where time-frequency analysis (TFA) can be of great help. Several approaches of TFA exist, and in this paper we use Husimi function (Gaussian smoothed Wigner function) for this purpose [1,2,3].

Both the Wigner and Husimi functions are the phase space quasidistributions in quantum mechanics [4,5]. In quantum mechanics, Husimi function of a quantum mechanical state arises when simultaneous measurement of quantum conjugated observables - coordinate and momentum, is performed. Similarly, in signal analysis, conjugated variables are time and frequency. If the measurement has the highest physically possible accuracy (as dictated by the Heisenberg uncertainty relations), then the product of standard deviations of conjugated observables equals $\hbar/2$ and Gaussian smoothed Wigner function for in such a way chosen parameters is known as a Husimi function (HF) [2,5].

In this paper, characteristic signals which describe behavior of several devices used in optics, microwave engineering and plasmonics were obtained via 3D electromagnetic numerical simulations. These signals, and their time and frequency evolution, were then analyzed using specifically tailored HF.

REFERENCES

- [1] E. Wigner, Phys. Rev. 40, 749, (1932).
- [2] K. Husimi, Prog. Phys. Math. Soc. Jpn. 22, 264, (1940).
- [3] Chun, Y. J., Lee, H. W., Annals of Physics, 307(2), 438 (2003).
- [4] Davidović, M. D., Davidović, M. D., Vojisavljevic, V. Acta Phys. Pol. A 116, 4, 675 (2009).
- [5] Davidović, D. M., Lalović, D., Phys. A 182, 643 (1992).

Quasi-stable rotating solitons supported by a single spiral waveguide

Aleksandra I. Strinić^{1,2}, Milan S. Petrović^{2,3}, Najdan B. Aleksić^{1,2} and Milivoj R. Belić²

¹*Institute of Physics, University of Belgrade, P.O.Box 68, 11080 Belgrade, Serbia*

²*Texas A&M University at Qatar, P.O.Box 23874, Doha, Qatar*

³*Institute of Physics, P.O.Box 57, 11001 Belgrade, Serbia*

e-mail: strinic@ipb.ac.rs

We investigate numerically light propagation in a single spiral waveguide formed in a nonlinear photorefractive medium for the spatial frequency of the waveguide rotation above frequencies which correspond to the stable rotary motion. The general procedure for finding exact fundamental solitonic solutions in the spiraling guiding structures, based on the modified Petviashvili's iteration method, gives only the solutions with low accuracy in this regime. Such solitons, supported by the spiral waveguide, perform quasi-stable rotational oscillatory motion, with inevitable soliton decay. We find that, for each set of physical parameters, there exists a beam power with practically negligible wave radiation.

Routing of optical beams by asymmetric defects in (non)linear waveguide arrays

M. Stojanović Krsić¹, S. Jovanović², A. Mančić³ and M. Stepić⁴

¹Faculty of Technology, University of Niš, Leskovac, Serbia

²Faculty of Natural Sciences and Mathematics, University of Priština, Kosovska Mitorovica, Serbia

³Faculty of Natural Sciences and Mathematics, University of Niš, Niš, Serbia

⁴Vinča Institute of Nuclear Sciences, Belgrade, Serbia

e-mail: mstepic@vin.bg.ac.rs

Uniform one-dimensional (1D) nonlinear waveguide array, consisting of parallel, evanescently coupled waveguides represent a special case of 1D photonic crystal [1]. Matured fabrication procedures enable production of arrays whose intrinsic parameters (such as shape and dimensions of the waveguides, coupling strength between them, nonlinear response,...) may be easily changed. The possibility to manipulate light propagation through photonic crystals in a fully controllable fashion, have promise in the field of all-optical communications and photonic devices. However, unavoidable material imperfections, together with slight deviation during fabrication and misusage lead to existence of random defects in the system, which considerably hamper the control of the light flow. These imperfections enable the existence of different types of stable, localized defect modes (breathers and solitons [2]) which may be useful in routing, blocking and filtering of light. Interestingly, various defects may be intentionally inserted in uniform waveguide arrays, enabling studies of defect modes and their influence on light dynamics [3-5]. Interface of two semi-infinite waveguide arrays represent a type of structural (geometric) defect which also can host different localized modes [6, 7]. Recently, the influence of two nonlinear defects on light propagation through linear waveguide array [8] and the steering of discrete breathers in a linear lattice with two nonlinear defects [9] have been explored. Finally, light trapping, reflection and transmission near defect modes in composite linear photonic lattices have been investigated [10].

Here, we studied numerically (by split-step Fourier method) light beam propagation through either uniform or composite 1D (non)linear waveguide arrays having two asymmetric defects, a situation which can be fairly well modeled by the paraxial time-independent Helmholtz equation. Embedded asymmetric defects are either linear or nonlinear. Effects of different positions and widths of asymmetric defects on the light beam propagation have been examined and compared with a case of embedded symmetric defects. Various types of modes localized at these defects and in their vicinity have been found. We also have explored influence of asymmetric defects on tilted beam propagation and identify regimes of trapping, total reflection and transmission of light. Presented results provide an insight into the light beam dynamics in the presence of asymmetrical linear and nonlinear defects and might be useful in several all-optical applications such as filtering and steering of light beams through the optical medium.

REFERENCES

- [1] J. D. Joannopoulos, S. G. Johnson, J. N. Winn, R. D. Meade, "Photonic crystals: molding the flow of light", Princeton University Press, Princeton, New Jersey, Second edition (2008).
- [2] S. Flach, A. V. Gorbach, Phys. Rep. 467, 1 (2008).
- [3] U. Peschel, R. Morandotti, J. S. Aitchison, H. S. Eisenberg, Y. Silberberg, Appl. Phys. Lett. 75, 1348 (1999).
- [4] F. Fedele, J. K. Yang, Z. G. Chen, Opt. Lett. 30, 1506 (2005).
- [5] L. Morales-Molina, R. A. Vicencio, Opt. Lett. 31, 966 (2006).
- [6] S. Darmanyan, A. Kobaykov, F. Lederer, JETP 93, 429 (2001).
- [7] A. Kanshu, C. E. Rüter, D. Kip, P. P. Beličev, I. Ilić, M. Stepić, V. M. Shandarov, Opt. Express 19, 1158 (2011).
- [8] V. A. Brazhnyi, B. A. Malomed, Opt. Comm. 324, 277 (2014).
- [9] X. -D. Bai, B. A. Malomed, F. -G. Deng, Phys. Rev. E 94, 032216 (2016).
- [10] M. Stojanović Krsić, A. Mančić, S. Jovanović, M. Stepić, Opt. Comm. 394, 6 (2017).

Four wave mixing in potassium vapor with off-resonant double lambda system

D. Arsenović, M. M. Ćurčić, B. Zlatković, A. J. Krmpot, I. S. Radojičić, T. Khalifa and B. M. Jelenković
Institute of Physics,
Belgrade, Serbia
e-mail: marijac@ipb.ac.rs

Nowadays, four-wave mixing (FWM) in alkali vapors is a hot topic, essential for exploring new states of light [1] and for quantum information [2]. We studied theoretically and experimentally non-degenerate four-wave mixing (FWM) in potassium vapor. The effect was generated by employing co-propagating pump and probe beams, and using the interaction scheme known as double-lambda scheme. Results obtained by the theoretical model were compared to experimental results obtained using the setup described in [3].

Theoretical model is based on the semi-classical treatment of the FWM processes. We start with solving numerically Bloch equations for density matrix elements of all populations and coherences, relevant for our double-lambda scheme. The coherences are further utilized for calculation of atomic polarization, which is used in the propagation equations for amplitudes of electrical fields of pump, probe and conjugate beams. This kind of approach, with fully numerical calculations and without perturbation theories and approximations, makes our model one of the most detailed among other models of FWM processes.

We have calculated and measured gains of the probe and the conjugate, defined as the ratio of probe and conjugate intensities at the exit from the K vapor cell, and the intensity of the probe beam at the entrance in the cell. Theoretical and experimental profiles of gains for a wide range of relevant parameters were compared and analyzed. Dependences on angle between pump and probe, two photon Raman detuning, one photon detuning from the D1 line, atomic densities and probe power are included in our results. Parameters were chosen for exceptionally high gains of probe and conjugate beams.

Qualitative agreement of experimental results with theoretical predictions was observed. FWM in alkali atoms is a complex process where dependence of efficiency of FWM on one parameter is related to values of other parameters. Strong dependence of the gain profile vs angle on the pump power and atom densities were observed. For a one-photon detuning from D1 transition of the order of 1 GHz, and the vapor density of $\sim 5 \cdot 10^{12} \text{ cm}^{-3}$, system acts as a strong phase insensitive amplifier. Gains vs two photon Raman detuning are narrow resonances with the width of the order of 10 MHz, depending on the angle between pump and probe and on one-photon detuning. Resonances are shifted from the zero two photon detuning by a different value, from 0 to -10 MHz, depending on the one photon detuning from D1 line and to a smaller extend on the angle. For the low probe power gain value up to 500 was obtained.

REFERENCES

- [1] C. F. McCormick *et al.*, Phys Rev A 78, 043816 (2008).
- [2] C. Shu *et al.*, Nat Comm. 7, 12783(2016).
- [3] B. Zlatkovic *et al.*, Las Phys Lett 13, 015205 (2015).

Towards the fully developed statistical approach of vector rogue waves

A. Mančić¹, A. Maluckov², F. Baronio³, Lj. Hadzievski², S. Wabnitz³

¹Faculty of Sciences and Mathematics, University of Niš, Serbia

²Vinca Institute of Nuclear Sciences, Belgrade, Serbia

³INO-CNR and DII, University of Brescia, Brescia, Italy

e-mail:anam@pmf.ni.ac.rs

The emergence, dynamics and prediction of rogue waves (RW) have been in the focus of interest in diverse fields of science (oceanography, physics of fluids, optics, ultra cold matter, sociology, bio-sciences) in the last decade [1].

Recently, we have started a study aimed to go deeply into the genesis and dynamics of multiparametric vector RW solutions in the context of the Manakov model by adopting statistical methods [2]. Particularity of vector RWs (semirational localized modes) is that they can feature both exponential and rational dependence on coordinates. These solutions can be reduced to the vector Peregrine solitons and bright- and dark-rogue wave composites for special parameter values [3,4].

Here, we present recent results of the preparatory phase of our study in which we try to find proper RW classifiers, like the significant wave height is in the context of scalar models in oceanography and optics [1]. Therefore, we firstly considered the 2D – vector generalization of the significant height vector as a classifier. It is defined as a vector quantity whose two components are related to the maximum absolute deviation of the amplitude of corresponding RW components from the initial finite background field level. We consider as extreme ones those events characterized by the significant height vector whose components, either one or both, are above the threshold value. Particular, on-going effort is made in determining proper threshold values.

The general vector form of the nonlinear Schrödinger equation, which can be written as:

$$i \frac{\partial u^{(1)}(x,t)}{\partial t} + \frac{\partial^2 u^{(1)}(x,t)}{\partial x^2} - \left(\gamma_{11} |u^{(1)}(x,t)|^2 + \gamma_{12} |u^{(2)}(x,t)|^2 \right) u^{(1)}(x,t) \\ = 0i \frac{\partial u^{(2)}(x,t)}{\partial t} + \frac{\partial^2 u^{(2)}(x,t)}{\partial x^2} - \left(\gamma_{21} |u^{(1)}(x,t)|^2 + \gamma_{22} |u^{(2)}(x,t)|^2 \right) u^{(2)}(x,t) = 0$$

and it was analyzed numerically by adopting the pseudo-spectral methods. The $u^{(1)}(x,t)$ and $u^{(2)}(x,t)$ represent the wave envelopes, γ_{ij} ($i, j=1,2$) are inter ($i \neq j$) and intra ($i = j$) nonlinear terms, t is the evolution variable, and x is a second independent variable. These equations reduce to Manakov system in the limit $\gamma_{ij}=g$, $i, j=1,2$. The meaning of variables depends on the context (fluid dynamics, plasma physics, nonlinear optics, etc). It has been shown analytically and numerically that different type of RWs can be observed in the presented model, depending on the system parameters [5]. This enables us to directly check our results with respect to various types of RWs. Statistical measures based on the height and amplitude distributions, their moments, return time statistics, etc, are numerically calculated.

The study presented here is only a small fragment of our attempt to establish a full statistical analysis of the vector RWs.

REFERENCES

- [1] M. Onorato, S. Residori, U. Bortolozzo, A. Montina, and F. T. Arecchi, Phys. Report 528, 47 (2013).
- [2] S. Toenger, T. Godin, C. Billet, F. Dias, M. Erkintalo, G. Gentry, and J. M. Dudley, Scientific Reports, 5, 10380 (2015).
- [3] F. Baronio, A. Degasperis, M. Conforti, and S. Wabnitz, Phys. Rev. Lett. 109, 044102 (2012).
- [4] F. Baronio, S. Chen, Ph. Grelu, S. Wabnitz, and M. Conforti, Phys. Rev. A 91, 033804 (2015).
- [5] Yu.V. Bludov, V.V. Konotop, and N. Akhmediev, Eur. Phys. J. Special Topics 185, 169 (2010).

Signatures of non-quenched disorder in the wave pattern's spreading in flat band geometries

G. Gligorić¹, A. Maluckov¹

¹*P* Group, Vinca Institute of Nuclear Sciences,
Belgrade, Serbia*

e-mail:goran79@vin.bg.ac.rs

Symmetry and topology properties of periodic networks are closely related with the appearance and dynamics of wave patterns propagating through them. In this context, the particular attention of scientific community has been focused on to the flat-band (FB) systems, which provide conditions for completely dispersionless propagation of highly localized modes - compactons [1]. These modes, which owe their existence to the phenomena of destructive interference, particularly responded to the presence of quenched disorder and qualitatively changed the properties of Anderson localization [2]. Also, one of the intriguing problems is related with the effect of the non-quenched disorder on the wave dynamics in different periodic networks. So far, the studies of the wave spreading properties in the presence of varying disordered potential were focused on the lattices with simple geometries (simple one and two-dimensional periodic lattices) [3,4]. Here, we will focus on the FB networks with non-quenched disorder in order to better understand the interplay between different aspects of wave dynamics caused by disorder and system's topological and geometrical properties.

REFERENCES

- [1] O. Derzhko, J. Richter, M. Maksymenko, *Int. J. Mod. Phys. B* 29, 1530007 (2015).
- [2] D. Leykam, S. Flach, O. Bahat-Treidel, A. S. Desyatnikov, *Phys. Rev. B* 88, 224203 (2013).
- [3] L. Levi, Y. Krivolapov, S. Fishman, M. Segev, *Nat. Phys.* 8, 912 (2012).
- [4] C. D'Errico *et al*, *New J. of Phys.* 15, 045007 (2013).

Molecules in a bicircular strong laser field

D. Habibović¹, A. Čerkić¹, M. Busuladžić^{2,1}, A. Gazibegović-Busuladžić¹, S. Odžak¹, E. Hasović¹, and D. B. Milošević^{1,3,4}

¹Faculty of Science, University of Sarajevo, Zmaja od Bosne 35, 71 000 Sarajevo, Bosnia and Herzegovina

²Faculty of Medicine, University of Sarajevo, Čekaluša 90, 71 000 Sarajevo, Bosnia and Herzegovina

³Max-Born Institut, Max-Born Strasse 2a, 12489 Berlin, Germany

⁴Academy of Sciences and Arts of Bosnia and Herzegovina, Bistrik 7, 71000 Sarajevo, Bosnia and Herzegovina

e-mail: dhfizika1@gmail.com

Nonlinear laser-induced molecular processes have attracted much attention in the last few years. Specially, the strong-laser-field scientific community has focused attention on the behavior of atoms and molecules in the so-called bicircular laser field [1,2,3]. Bicircular field is a two-color laser field having coplanar circularly polarized counter-rotating components of frequencies $r\omega$ and $s\omega$, with r and s integers [4].

We investigate high-order above-threshold ionization or (H)ATI of homonuclear diatomic molecules and high-order harmonic generation (HHG) of polar molecules by the bicircular field using the improved molecular strong-field approximation [5,6,7]. In this paper we are able to identify two rotational and two reflection symmetries which are satisfied in ATI of homonuclear diatomic molecules. Both rotational symmetries are valid for the direct as well as for the rescattered HATI electrons [5]. In the case of molecular high-order harmonic generation (HHG), we show that for BF_3 molecule, there is a strong asymmetry in the emission of high harmonics with opposite helicities. This asymmetry depends on molecular orientation [6]. Selection rules for HHG by a bicircular field are also analyzed in detail [7]. Also, it was shown that it is possible to introduce spin into attoscience with spin-polarized electrons produced by a bicircular laser field [8].

Support by the Federal Ministry of Education and Science, Bosnia and Herzegovina, is gratefully acknowledged. This work was also supported in part by the Deutsche Forschungsgemeinschaft (DFG) within the Priority Programme Quantum Dynamics in Tailored Intense Fields (QUTIF).

REFERENCES

- [1] O. Kfir *et al.*, Nat. Photon. **9**, 99 (2015).
- [2] T. Fan *et al.*, Proc. Natl. Acad. Sci. USA **112**, 14206 (2015).
- [3] D. M. Reich and L. B. Madsen, Phys. Rev. Lett. **117**, 133902 (2016).
- [4] D. B. Milošević and W. Becker, Phys. Rev. A **62**, 011403(R) (2000).
- [5] M. Busuladžić, A. Gazibegović-Busuladžić, and D. B. Milošević, Phys. Rev. A **95**, 033411 (2017).
- [6] S. Odžak, E. Hasović, and D. B. Milošević, Phys. Rev. A **94**, 033419 (2016).
- [7] D. B. Milošević, J. Phys. B **48**, 171001 (2015).
- [8] D. B. Milošević, Phys. Rev. A **93**, 051402(R) (2016).

Enhanced second harmonic generation in lithium niobate photonic crystal cavities

Reinhard Geiss¹, Séverine Diziain², Michael Steinert¹ and Thomas Pertsch¹

¹*Institute of Applied Physics, Abbe Center of Photonics, Friedrich-Schiller-Universität Jena, Max-Wien-Platz 1, 07743 Jena, Germany*

²*Institute for Experimental Physics II, University of Leipzig, 04103 Leipzig, Germany, e-mail: reinhard.geiss@uni-jena.de*

Lithium niobate (LN) is a ferroelectric crystal which is commonly used in nonlinear and integrated optics because of its strong second order nonlinearity and its large transparency range. Nonetheless, the conversion efficiency of nonlinear processes is typically very weak. Additional enhancement mechanisms must therefore be implemented. In this contribution, enhanced second harmonic generation in a self-suspended LN photonic crystal cavity is presented.

To interact efficiently with the PhC structure, the light needs to be confined to the plane of the PhC. This is realized by patterning of the PhC lattice of holes in a thin self-suspended LN membrane forming a planar waveguide. A suitable substrate for these structures is lithium niobate on insulator (LNOI) which consists of a few hundred nanometer thin LN layer and a several micrometer thick silica layer on a LN wafer. The fabrication starts with planar dry etching of the top z-cut LN layer down to the designed membrane thickness of ~370 nm[1]. The following micro structuring is done by focused ion beam (FIB) milling of the holes through the full membrane thickness. Subsequently, the silica layer is selectively removed by wet etching through the holes until the PhC area is completely underetched. The PhC resonator is a L3 cavity that consists of a line of three missing holes in the ΓK direction of an hexagonal lattice of holes with radii of 150 nm and a lattice period of 530 nm. The holes at both line defect extremities are shifted away from the defect and their radii are shrunk to achieve a higher Q factor than the unmodified cavity [2]. A total of sixteen holes with enlarged radii have been placed around the defect with twice the period. These holes modify the field distribution of the fundamental cavity mode to radiate vertically rather than at grazing angles [3][4][5]. This modification allows to efficiently exciting the fundamental TE-polarized mode from the far-field at normal incidence during the following experimental study of the linear and nonlinear optical properties of this cavity with a modified confocal microscope. The resulting linear spectrum shows a resonance at 1356.0 nm corresponding to a cavity mode with a Q factor of 678, which is approximately confirmed by 3D-FDTD simulations: 1362.8 nm and a Q factor of 1550[6]. The simultaneously measured second harmonic spectrum shows an enhancement with a Q factor of 640 at 678 nm, corresponding to twice the linear resonance frequency. The generated second harmonic furthermore shows the expected quadratic dependence on the incident fundamental harmonic power.

These findings prove that the second harmonic enhancement is due to the strong field confinement inside the cavity mode. Photonic crystal (PhC) cavities in LN allow for the confinement of light to a very small volume which makes them efficient building blocks for photonic integrated circuits with high integration density for applications in nonlinear optics.

REFERENCES

- [1] R. Geiss, S. Diziain, M. Steinert, F. Schrepel, E.-B. Kley, A. Tünnermann, and T. Pertsch, *Phys. Status Solidi Appl. Mater. Sci.*, vol. 2425, no. 10, pp. 2421–2425(2014).
- [2] Y. Akahane, T. Asano, B.-S. S. Song, and S. Noda, *Nature*, vol. 425, no. 6961(2003).
- [3] S. L. Portalupi, M. Galli, C. Reardon, T. F. Krauss, L. O’Faolain, L. C. Andreani, and D. Gerace, *Opt. Express*, vol. 18, no. 15, pp. 16064–73(2010).
- [4] S. Diziain, R. Geiss, M. Zilk, F. Schrepel, E.-B. Kley, A. Tünnermann, and T. Pertsch, *Appl. Phys. Lett.*, vol. 103, no. 25, p. 251101(2013).
- [5] S. Diziain, R. Geiss, M. Zilk, F. Schrepel, E.-B. Kley, A. Tünnermann, and T. Pertsch, *Appl. Phys. Lett.*, vol. 103, no. 5, p. 51117(2013).
- [6] S. Diziain, R. Geiss, M. Steinert, C. Schmidt, W.-K. Chang, S. Fasold, D. Füßel, Y.-H. Chen, and T. Pertsch, *Opt. Mater. Express*, vol. 5, no. 9, p. 2081(2015).

Solitons generated by self-organization in bismuth germanium oxide single crystals during the interaction with laser beam

V. Skarka^{1,2,3}, M. Lekić¹, A. Kovačević¹, B. Zarkov⁴, and N. Z. Romčević¹

¹*Institute of Physics, University of Belgrade, Pregrevica 118, 11080 Belgrade, Serbia*

²*Science Program, Texas A&M University at Qatar, P.O. Box 23874, Doha, Qatar*

³*Laboratoire de Photonique d'Angers, EA 4464, University of Angers, 2 Boulevard Lavoisier 49045 Angers Cedex 01, France*

⁴*Directorate of Measures and Precious Metals, Mike Alasa 14, 11000 Belgrade, Serbia*
e-mail:vladimir.skarka@univ-angers.fr

The self-organization is based on the balance of antagonistic effects, with nonlinearity-induced self-contraction arresting diffraction and/or dispersion in order to generate stable localized nonlinear optical structures called solitons [1]. Spatial Kerr solitons correspond to the compensation of diffraction by a cubic Kerr nonlinearity. However, in two- and three-dimensional systems, the laser beam or pulse undergo a catastrophic collapse unless a saturating nonlinearity is also present, as it was established using synergy of variational method and numerical simulations [2-5]. Such Kerr solitons are hard to obtain experimentally especially in solid state systems. The generation of 2D optical solitons has been recently demonstrated only in liquid carbon disulfide [6].

We present here the experimental, theoretical, and numerical investigations of Kerr solitons generated by self-organization in black and yellow high quality bismuth germanium oxide (BGO) single crystals. A laser beam of increasing power induces competing cubic and quintic nonlinearities. The numerical evolution of 2D complex cubic-quintic nonlinear Schrödinger equation with measured values of nonlinearities shows the compensation of diffraction by competing cubic and quintic nonlinearities of opposite sign, i.e., the self-generation of stable solitons. Experiments as well as numerical simulations show higher nonlinearity in the black BGO than in the more transparent yellow one. Experimentally obtained solitons are in good agreement with numerical results.

REFERENCES

- [1] Y. S. Kivshar and G. P. Agrawal, *Optical Solitons: From Fibers to Photonic Crystals* (Academic, 2003).
- [2] V. Skarka, N. B. Aleksić, *Phys. Rev. Lett.* 96, 013903 (2006).
- [3] V. Skarka, N. B. Aleksić, H. Leblond, B. A. Malomed, and D. Mihalache, *Phys. Rev. Lett.* 105, 213901 (2010).
- [4] V. Skarka, N. B. Aleksić, M. Lekić, B. N. Aleksić, B. A. Malomed, D. Mihalache, and H. Leblond, *Phys. Rev. A* 90 (2), 023845 (2014).
- [5] V. Skarka, N. B. Aleksić, W. Krolikowski, D. N. Christodoulides, S. Rakotoarimalala, B. N. Aleksić, M. Belić, *Opt. Express* 25, 284183 (2017).
- [6] E. L. Falcao-Filho, C. B. de Araújo, G. Boudebs, H. Leblond, and V. Skarka, *Phys. Rev. Lett.* 110, 013901 (2013).

Broad-band femtosecond pulses, λ^3 type diffraction and X-waves. Evolution and management

V. Slavchev¹, A. Dakova^{2,3}, D. Dakova², K. Kovachev³ and L. Kovachev³

¹Faculty of Pharmacy, Medical University - Plovdiv, Bul. Vasil Aprilov 15-A, 4002 Plovdiv, Bulgaria

²Faculty of Physics, University of Plovdiv "Paisii Hilendarski", 24 Tsar Asen Str., 4000 Plovdiv, Bulgaria ³Institute of Electronics, Bulgarian Academy of Sciences, 72 Tzarigradsko shossee, 1784 Sofia, Bulgaria

e-mail:valerislavchev@yahoo.com

The experimental [1] and theoretical [2, 3] investigation of the diffraction of attosecond pulses describe one unexpected parabolic deformation of their intensity profile at few diffraction lengths. This deformation was called from the authors in [1] " λ^3 diffraction". In [2, 3] it was shown that this phenomenon can be solved analytically in the frame of linear non-paraxial evolution equation of the amplitude of the electrical field. Investigating the evolution of phase-modulated femtosecond pulses (20-30 fs), authors in [4] demonstrated that broad-band ($\Delta k_z \approx k_0$) pulses also diffract in λ^3 regime. Shortly, Fresnel's law does not work for broad-band laser pulses and their diffraction is similar to attosecond ones.

On the other hand, by using diffraction grating or other optical dispersion elements the spectrum of the femtosecond pulse can be not only extended, but also the sign of the chirp parameter can be changed. In the present work, it is studied more precisely the influence of this sign of the chirp parameter on the linear and nonlinear evolution of phase-modulated femtosecond pulses.

For negative chirp in linear regime of propagation, the diffraction is also of λ^3 type, but with the parabolic deformation of the intensity profile inverted with respect to the axis Oz . Thus, by properly used chirp parameters this process can be managed. In nonlinear regime of propagation, depending on the sign of chirp parameter, it is observed different types of nonlinear X-waves.

REFERENCES

- [1] N. Naumova, J. Nees, I. Sokolov, B. Hou and G. Mourou, Relativistic Generation of Isolated Attosecond Pulses in λ^3 focal volume, Phys. Rev. Lett. 92 (6), 063902 (2004).
- [2] L. Kovachev and K. Kovachev, Diffraction of Femtosecond Pulses: Nonparaxial Regime, J. Opt. Soc. Am. A 25 (9), 2232-2243 (2008); Erratum, J. Opt. Soc. Am. A 25 (12), 3097-3098 (2008).
- [3] Lubomir M. Kovachev and Daniela A. Georgieva, A class of localized solutions of the linear and nonlinear wave equations, Journal of Geometry and Symmetry of Physics, 27, 67-82 (2012).
- [4] A. M. Dakova, L. M. Kovachev, K. L. Kovachev, D. Y. Dakova, Fraunhofer type diffraction of phase-modulated broad-band femtosecond pulses, Journal of Physics: Conference Series 594, 012023, doi:10.1088/1742-6596/594/1/012023 (2015).

Sum frequency conversion of compact Q-switched cryogenic slab RF discharge CO laser radiation in nonlinear ZnGeP₂ crystal

A. Ionin¹, I. Kinyaevskiy¹, Yu. Klimachev¹, Yu. Kochetkov^{1,2}, A. Kozlov¹, L.V.Seleznev¹,
D. Sinitsyn¹, D. Zemtsov^{1,2}

¹*P.N. Lebedev Physical Institute of the Russian Academy of Sciences, Moscow, Russia*

²*National Research Nuclear University MEPhI, Moscow, Russia*

e-mail: umk@lebedev.ru

For the first time, collinear frequency conversion in a nonlinear crystal ZnGeP₂ was realized using a compact Q-switched cryogenic slab RF discharge CO laser. All previous studies of sum-frequency generation (SFG) of a multi-line CO laser radiation in nonlinear crystals were made with low- pressure DC discharge CO lasers operating in Q-switch mode (see for example [1]). However, slab RF discharge lasers are more compact and have some advantages over DC discharge lasers such as a possibility to provide pulse-periodic pumping, relatively low voltage, higher efficiency, a feasibility of igniting a large active volume at gas pressure of several tens of Torr without external ionizing sources. One of such CO lasers operating under cryogenic cooling was recently launched in Q-switch mode by a rotating mirror [2]. The laser design and its operation in Q-switch mode is described in detail in [2, 3].

The laser active volume in our experiments was 400x16x5 mm. Gas mixture CO:O₂:He = 1:0.3:10 at gas pressure of 37 Torr was used. RF power pulse duration T equaled 350 μs, and its peak power was 800 W. Pulse repetition frequency was 100 Hz, the delay time between beginning of RF power pulse and Q-switching time was 500 μs. The laser pulse duration was 0.7 μs (FWHM). We obtained high laser peak power (~3 kW), large number of spectral lines (~90) and wide spectral range of lasing (4.95÷6.6 μm). In the experiments laser radiation was focused onto a ZnGeP₂ crystal using CaF₂ lenses with the focal lengths F=300 and 200 mm.

Dependences of external conversion efficiency (ECE) on distance between the front face of the crystal and the focusing lens, and dependences of ECE on the laser radiation incidence angle with the crystal were measured. The maximum value of ECE for F=300 mm was ~0.44%, and taking into account the Fresnel reflection from the crystal faces, corresponded to internal conversion efficiency of ~0.83%. For F=200 mm ECE was 4.4%, which corresponded to internal conversion efficiency of ~8.2%. This value does exceed one obtained in [1].

The experimental SFG spectrum obtained at the maximum conversion efficiency contained ~200 spectral lines in the range from 2.5 to 3.2 μm. It should be noted that the maximum peak power of SFG spectrum corresponded to a wavelength near 2.8 μm that corresponded to pump wavelength of 5.6 μm, whereas the CO laser spectrum had the strongest lines near 5.1 μm (phase-matching angle is ~48° in ZnGeP₂ crystal). Such a difference is associated with the specificity of CO laser multiline radiation conversion, which is not critical for the phase-matching angle [1]. Wavelength 5.1 μm falls on the declining part of the phase-matching angle dependence upon a wavelength. Multiline conversion efficiency in this case is lower than that for the case when phase-matching angle corresponds to the minimum of phase-matching angle versus a pump wavelength (~46° at wavelength 5.8 μm). Therefore, this conversion is most effective at a phase-matching angle lying in the range 46-48° depending on pump radiation spectrum and focusing condition [4]. In our case most effective multiline SFG corresponded to the phase-matching angle of ~47°.

This research was supported by the Russian Science Foundation, Grant #16-19-10619.

REFERENCES

- [1] Yu. Andreev, A. Ionin, I. Kinyaevskiy, et al. Quantum Electronics 43, 139 (2013).
- [2] A. Ionin, Yu. Kochetkov, A. Kozlov, et al. Laser Phys. Lett. 14, 055001 (2017).
- [3] A. Ionin, A. Kozlov, O. Rulev, et al. Appl. Phys. B: Lasers and Optics, 122, 183 (2016).
- [4] A. Ionin, I. Kinyaevskiy, Yu. Klimachev, et al. Laser Phys. Lett. 14, 065401 (2017).

Realizing a periodic photonic lattices by synthesized Mathieu-Gauss beams

J. M. Vasiljević¹, Alessandro Zannotti², D. V. Timotijević^{1,3}, Cornelia Denz², D. M. Jović Savić¹

¹*Institute of Physics, University of Belgrade, P.O. Box 68, 11001 Belgrade, Serbia*

²*Institute of Applied Physics and Center for Nonlinear Science (CeNoS), Westfälische Wilhelms-Universität Münster, 48149 Münster, Germany*

³*Science Program, Texas A&M University at Qatar, P.O. Box 23874 Doha, Qatar*
e-mail: jadranka@ipb.ac.rs

Over the years, non-diffracting wave configurations have drawn considerable attention, particularly in the areas of optics, atom physics, biophysics, as well as optical tweezing [1], and nonlinear optics [2, 3]. The interest in such optical waves is due to the fact that, their transverse intensity distributions propagate unchanged for hundreds of diffraction lengths. The potential of non-diffracting structures is of significant importance for advances in discrete and nonlinear modern photonics [4, 5]. One prominent class of non-diffracting waves is given by Mathieu beams, which appear as translationally invariant solution of the Helmholtz equation in elliptic cylindrical coordinates.

Synthesizing two or more non-diffracting Mathieu-Gauss (MG) beams, we demonstrate a powerful new approach for the creation of two-dimensional (2D) aperiodic photonic lattices, in a single writing process in parallel. Depending on the beam configurations of coherently superimposed MG beams, their mutual distances, angles of rotation or phase relations we are able to realize transverse invariant propagating intensity distributions capable to optically induce corresponding refractive index lattices in photosensitive media. Our approach features the fabrication of versatile aperiodic lattices with controllable properties as well as quasi one-dimensional structures. Our results and methods enable further investigations of light propagating in such aperiodic photonic lattices, and could find applications in modern optical information processing.

REFERENCES

- [1] V. Garcés-Chávez, D. McGloin, H. Melville, W. Sibbett, and K. Dholakia, *Nature* 419, 145 (2002).
- [2] J.W. Fleischer, M. Segev, N. K. Efremidis, and D. N. Christodoulides, *Nature* 422, 147 (2003).
- [3] H. Martin, E. D. Eugeniya, and Z. Chen, *Phys. Rev. Lett.* 92, 123902 (2004).
- [4] F. Diebel, B. M. Bokić, M. Boguslawski, A. Piper, D. V. Timotijević, D. M. Jović, and C. Denz, *Phys. Rev. A* 90, 033802 (2014).
- [5] F. Diebel, B. M. Bokić, D. V. Timotijević, D. M. Jović Savić, and C. Denz, *Opt. Express* 23, 24351 (2015).

Measurement of powerful ultrashort UV pulse parameters

A.A. Ionin¹, D.V. Mokrousova^{1,2}, D.A. Piterimov^{1,2}, L.V. Seleznev¹, A.V. Shutov¹, E.S. Sunchugasheva¹,
N.N. Ustinovskii¹, V.D. Zvorykin¹

¹*P.N. Lebedev Physical Institute of Russian Academy of Sciences, Moscow, Russia*

²*Moscow Institute of Physics and Technology, Moscow Region, Russia,*

e-mail: daria.mokrousova@yandex.ru

Ultrashort UV pulses with high critical power have a lot of applications, such as triggering and guiding of high-voltage electric discharges and lightning protection [1], formation of the waveguides for microwave radiation [2], environmental monitoring [3]. The most common way to obtain powerful ultrashort UV pulse is to amplify seed UV ultrashort pulse in a gas laser amplifier. During amplification a pulse passes through the windows of gas chambers, and due to the dispersion in pass-through optics it undergoes temporal elongation and phase modulation. Thus, the parameters of amplified pulse differ from seed emission's ones. Interaction pulse parameters are very important for the interpretation of experimental results and the comparison with numerical simulations. Hence the aim of the present work was the determination of amplified pulse duration, critical power for self-focusing and transversal distribution measurement. We used obtained data for processing the results of experimental investigation of regularized filamentation of sub-TW sub-ps UV pulse with central wavelength of 248 nm. This pulses were generated on hybrid Ti:sapphire- KrF laser facility [4]. Usually the duration of ultrashort pulses is measured with autocorrelators based on second harmonic generation phenomenon. Unfortunately, second harmonic of far UV pulses (such as 248 nm) is difficult to deal with, that is why we used single-shot autocorrelator on the gas mixture of Xe, F₂(in He) and Ar suggested in [5]. Obtained pulse duration was approximately 900 fs. To detect wide-aperture UV pulse transversal energy density distribution we used an optical glass as a screen which luminescence was collected to the CCD camera by the objective lens. Thus we were able to have qualitative vision of transversal distribution, but to measure such characteristics as typical size of "hot spots" in a beam, we needed to calibrate luminescence of the screen. For this purpose we experimentally found the dependence of energy density from glass luminescence that is a calibration function. While investigating multiple filamentation the critical power for self-focusing is essential to be known. Critical power can decrease with stretching of a pulse (and beam phase modulation in pass-through optics), so we measured it directly. Energy of UV light quantum is about 5 eV, and focused laser beam can ionize air in the waist even if it's peak power is less then critical one. However, in this case formed plasma channel is symmetrical relatively to focal plane. When laser power exceeds critical power the channel becomes asymmetrical. Thus measuring plasma distribution along the channel with different laser pulse energies, we were able to determine the energy which corresponds to critical power for self-focusing. We applied these methods in the experiment on regularization of UV beam filamentation via amplitude mask. The array of approximately hundred of filaments was observed. We calibrated luminescence distribution that leads to enhancement of contrast between intensive filament and weak energy reservoir. From calibrated energy density distributions we calculated filament radius, energy in one hole of the mask and compared it with critical power. This work was supported by RFBR (grants 15-32-20966 and 17-02-00722).

REFERENCES

- [1] X.M. Zhao, J.-C. Diels, C.Y. Wang, J. M. Elizondo, IEEE Quant. Electron., 31 (3), 599 (1995).
- [2] R.R. Musin, M.N. Shneider, A.M. Zheltikov, R.B. Miles, Appl.Opt. 46, 5593 (2007).
- [3] A.A. Ionin et al., Opt. Atmosfery i Okeana 29 (03), 200 (2016).
- [4] V.D. Zvorykin, S.A. Goncharov, A.A. Ionin et al., Quant. Electron. 47 (4), 319 (2017).
- [5] N. Sarukura, M. Watanabe, A. Endoh, S. Watanabe, Opt. Lett. 13(11), 996 (1988).

Polarization properties of vector solitons in optical fibers

A. Dakova^{1,2}, L. Kovachev², D. Dakova¹, D. Georgieva³ and V. Slavchev⁴

¹*Faculty of Physics, University of Plovdiv "Paisii Hilendarski", 24 Tsar Asen Str., 4000 Plovdiv, Bulgaria*

²*Institute of Electronics, Bulgarian Academy of Sciences, 72 Tzarigradsko shossee, 1784 Sofia, Bulgaria*

³*Faculty of Applied Mathematics and Computer Science, Technical University of Sofia, 8 Kliment Ohridski Blvd., 1000 Sofia, Bulgaria*

⁴*Faculty of Pharmacy, Medical University - Plovdiv, Bul. Vasil Aprilov 15-A, 4002 Plovdiv, Bulgaria*
e-mail: anelia.dakova@gmail.com

It is well-known that single-mode optical fibers support two polarization modes (A_x and A_y). As result of that, natural basis for investigating the evolution of optical pulses in such kind of waveguides are vector two coupled nonlinear equations describing nonlinear interaction between laser pulses of the two polarization states. These equations admit soliton solutions in negative dispersion region and their interaction, due to cross phase modulation, was studied by authors in [1,2]. Soon after that in [3] was shown that the critical power for observation of a linearly polarized fundamental soliton is 2/3 times smaller than that needed for formation of circularly polarized soliton. The investigation of optical pulses with polarization different from circular and linear (elliptical) was done in approximation when the amplitude of one of the waves is much smaller than the other. It was observed a rotation of the minor and major axes of the ellipse. Generally, the problem with arbitrary elliptical polarization with same amplitudes and initial phase difference between the components in the frames of has not been studied in detail in the literature. On the other hand, in [4] was reported on the experimental and numerical evidence of energy exchange between the components of vector solitons due to processes of degenerated four wave mixing.

In present work is being reviewed the periodic exchange of energy between components of the elliptically polarized vector solitons. Its amplitude and phase essentially depend on the rate of polarization ellipticity of the initial pulses. In quasi-CW regime, when time derivatives can be set to zero, the system of equations is analytically solved. The obtained solutions, in the form of Jacobi elliptic functions, describe the intensities of the components of vector solitons.

REFERENCES

- [1] C. R. Menyuk, IEEE J. Quantum Electron. QE-25, 174 (1987).
- [2] C. R. Menyuk, Opt. Lett. 12, 614 (1987); J. Opt. Soc. Am. B 5, 392 (1988).
- [3] Y. Silberberg, Y. Barad, Rotating vector solitary waves in isotropic fibers, Optics Letters Vol. 20, Issue 3, pp. 246-248 (1995).
- [4] H. Zhang, D. Y. Tang, L. M. Zhao, N. Xiang, Coherent energy exchange between components of a vector soliton in fiber lasers, Optics Express Vol. 16, Issue 17, pp. 12618-12623 (2008).

Optical-Terahertz Solitons

A.N. Bugay¹ and S.V. Sazonov²

¹*Joint Institute for Nuclear Research, Dubna, Russia*

²*National Research Centre «Kurchatov Institute», Moscow, Russia*

e-mail:bugay_aleksandr@mail.ru

Multidimensional spatiotemporal optical solitons (light bullets) [1] are nondiffracting and nondispersing wavepackets localized both in time and space. Most concerns in this field are related to the problem of pulse stability in various nonlinear optical media [2].

In present report we consider specific kind of parametric solitons related to difference frequency generation. It was predicted [3] that optical rectification (OR) phenomena provides a mechanism of two-component soliton formation for strong enough pump light pulses and extensive nonlinear media with negligible absorption. In result a coupled state of envelope optical pulse and a unipolar terahertz pulse is expected. The phase matching condition for such interaction is the equality of optical group velocity to terahertz phase velocity. Such soliton phenomena is well known in plasmas (Zakharov-Benney resonance) and in molecular systems (Davydov solitons), but is still poorly recognized in nonlinear optics.

Here we have formulated a generalized theoretical model for OR including both the response of anisotropic nonresonant bulk medium and the impact of two-level resonant impurities, which could be dispersed or layered inside a base nonlinear medium. Previously, we demonstrated [4] that resonant interaction can be used to fit the phase matching condition due to nonlinear slowing down of light pulse propagating in the self-induced transparency (SIT) regime. Also, nonsymmetric resonant impurities, such as the artificial low-dimension structures (quantum dots, wells, wires) and polar molecules, have been shown to be very promising material for highly efficient frequency conversion and generation of solitons [5-8]. In our study we considered real GaAs-based low-dimension structures, for which SIT was observed [9].

Study of light bullets was conducted by analytic variational methods and by numerical simulations. Both resonant and nonresonant modes of interaction with impurities were analyzed. In the case of resonance SIT pulse experiences transverse filamentation and divides on several filaments, which further form an array of light bullets coupled with unipolar terahertz pulses. The stability of these bullets is provided by the resonant optical component, which is in agreement with related research on SIT solitons [10]. Terahertz component is localized much stronger in space and time than optical one. In nonresonant case such solitons also can exist with the exception of several restrictions regarding their stability. The group velocity dispersion must be negative and the intensity of terahertz counterpart must exceed a threshold value. The influence of artificial impurities helps to meet those requirements. Unlike the resonance case, the stability is determined by the terahertz component.

REFERENCES

- [1] Y. Silberberg, *Opt. Lett.* 15, 1282 (1990).
- [2] B.A. Malomed, D. Mihalache, F. Wise, L. Torner, *J. Opt. B: Quant. Semicl.* 7, R53 (2005).
- [3] A.N. Bugay, S.V. Sazonov, *Phys. Rev. E* 74, 066608 (2006).
- [4] A.N. Bugay, S.V. Sazonov, *Phys. Lett. A* 374, 1093 (2010).
- [5] M. Kocinac, Z. Iconic, V. Milanovic, *Optics Commun.* 140, 89 (1997).
- [6] M. Agrotis, N.M. Ercolani, S.A. Glasgow, J.V. Moloney, *Physica D.* 134, 138 (2000).
- [7] X. Song, W. Yang, Z. Zeng, R. Li, Z. Hu, *Phys. Rev. A* 82, 053821 (2010).
- [8] S.V. Sazonov, *Opt. Commun.* 380, 480 (2016).
- [9] O. Karni, A. Capua, G. Eisenstein et al. *Opt. Expr.* 21, 26786 (2013).
- [10] M. Blaauboer, B. A. Malomed, G. Kurizki, *Phys. Rev. Lett.* 84, 1906 (2000).

Vortices and topological structures in photorefractive materials

M. Čubrović¹ and M. Petrović²

¹*Scientific Computing Lab, Center for the Study of Complex Systems, Institute of Physics,
Belgrade, Serbia*

²*Institute of Physics, Belgrade, Serbia*
e-mail:mcubrovic@gmail.com

We consider the collective behavior and stability of topologically nontrivial patterns in laser beams propagating through a photorefractive crystal by analytical and numerical means. The photorefractive medium leads to the self-focusing of the beam, giving rise to complex stationary patterns for some choices of initial conditions. When two beams with winding phase (vortices) propagate from the opposite ends of the crystal, their interaction mimics the planar Heisenberg antiferromagnets and can be described by a phase diagram obtained from renormalization group analysis. Different phases are visually recognizable and can be identified in numerical simulations. If the crystal has defects (holes), the long-range order is lost but individual vortices can still be stable in a pattern akin to a spin glass.

We then consider a deeper question: can such topological configurations behave as optical solitons, i.e. propagate through each other without interacting? With the counterpropagating vortex system considered above, this is obviously not the case as they interact and show collective behavior. The question is considered in the framework of the Lax pair formalism and the answer seems to be non-universal, depending strongly on the details of the propagation geometry and the properties of the crystal. The construction of such solutions remains attractive if elusive, because of the robustness of optical solitons to perturbations which are inevitable in experiment.

Exact traveling and solitary wave solutions to the generalized Gross-Pitaevskii equation with cylindrical potential

Nikola Z. Petrović¹

¹*Institute of Physics, University of Belgrade, Belgrade, Serbia*
e-mail: nzpetr@ipb.ac.rs

Ever since solitons have been experimentally realized in Bose-Einstein condensates [1] there has been a great interest in finding exact solutions to the Gross-Pitaevskii equation which describes such systems [2]. Of particular interest due to practical concerns is to trap the Bose-Einstein condensate in a cylindrical potential, i.e. a potential which confines the condensate in the radial direction, but not the axial direction. Such potentials would allow the formation of 1D solitons which are expected to be stable [1].

In our previous work [3,4] we used the Jacobi Elliptic Function (JEF) expansion technique to find solutions to the (3+1)-D Gross-Pitaevskii equation with distributed coefficients and in a spherical potential. We obtained stable solutions under the regime of dispersion management, i.e. sinusoidally varying the diffraction coefficient and the nonlinearity coefficient [4,5]. In our paper we modify the methods presented in [3,4] to obtain solutions for the cylindrical case, for which the three transverse dimensions are no longer symmetric. The solutions end up combining the features of the solutions for the spherical potential and the solutions of the ordinary Nonlinear Schrödinger equation described in [6]. We also examine the case of the planar potential where confinement happens in only one transverse dimension.

REFERENCES

- [1] S. Burger et. al. , Phys. Rev. Lett. 83, 5198 (1999).
- [2] F. Dalfovo et. al., Rev. Mod. Phys. 71, 463 (1999).
- [3] N. Z. Petrović, M. Belić and W.-P. Zhong, Phys. Rev. E 81, 016610 (2010).
- [4] N. Z. Petrović, N. Aleksić, A. Al Bastami and M. Belić, Phys. Rev. E 83, 036609 (2011).
- [5] N. Z. Petrović, N. Aleksić and M. Belić, Optics Express 23, 10616 (2015).
- [6] M. Belić, N. Z. Petrović, et. al., Phys. Rev. Lett. 101, 123904 (2008).

Nonlinear Fourier analysis of a mode-locked laser

M. Kamalian, A. M. Perego, J. Prilepsky and S. K. Turitsyn

Aston Institute of Photonic Technologies

Birmingham, UK

e-mail: kamalian@aston.ac.uk

Nonlinear Fourier transform (NFT), also known as the inverse scattering transform in mathematical literature [1], is the method that can be used to identify and single out coherent (solitonic) and incoherent (dispersive radiation) components of a pulse. NFT has been implemented in fibre optics to overcome the nonlinear distortions due to its capability to effectively linearise the nonlinear Schrödinger equation (NLSE) [2]. The latter is often used as a master model describing the light propagation down single-mode fibres [2]. NFT can also be effectively utilised to study the properties of the electric field evolution both in passive fibres [3] and in fibre lasers [4]: due to its explicitly decomposing our signal into solitonic and dispersive parts, the NFT is an ideal tool to identify the contribution of coherent structures and their dynamics. The necessary condition for the use of NFT is that the nonlinear system under study needs to be integrable, meaning associated to a set of ordinary linear differential equation with invariant spectral parameter.

Mode-locked lasers can be generally described through the nonlinear dynamical models that usually involve the so-called cubic/quintic complex Ginzburg-Landau equation (CQGLE) [5]. However, this equation does not exactly match the requirements for the application of the NFT formalism, i.e. integrability; this requirement actually means that the system under investigation should be very close to the pure cubic NLSE. Although a rigorous reduction of the CQGLE to an integrable NLSE model is an open question, the existence of solitons in such lasers as solutions of the CQGLE encouraged us to implement the NFT in order to analyse the peculiarities of pulses dynamics, similar to the ideas of [3]. In this regard, we have used NFT merely as a monitoring tool providing a representation of the signal in the NFT domain. We have identified different coherent structures considering the features of the NFT spectrum transformation associated with the electric field evolution.

First we performed the numerical simulations of a mode-locked laser where the formation of pulses is induced by the nonlinear polarization rotation that acts as an effective saturable absorber. After that we calculated the nonlinear spectrum of the field cross-sections to analyse the behaviour of the electric field analysing, specifically, the dynamics and interactions of coherent structures. This dynamics can be retrieved by studying the evolution to specific discrete eigenvalues (complex analogues of frequencies) emerging from the NFT pulse decomposition.

We have shown that emergence and disappearance of coherent structures can indeed be predicted by looking at the evolution of NFT spectrum. The NFT, hence, can be reckoned as a promising tool for understanding and controlling laser dynamics.

REFERENCES

- [1] V. E. Zakharov and A. B. Shabat, *Sov. Phys. JETP*. 34 (1972).
- [2] S. K. Turitsyn, J. E. Prilepsky, S. T. Le, S. Wahls, L. L. Frumin, M. Kamalian, and S. A. Derevyanko, *Optica* 4(3), 307--322 (2017).
- [3] S. Randoux, P. Suret, and G. El, *Sci. Rep.* 6, 29238 (2016).
- [4] S. Sugavanam, M. Kamalian, J. Peng, J. E. Prilepsky, and S. K. Turitsyn, *CLEO/Europe-EQEC* (2017).
- [5] A. Komarov, H. Leblond, and F. Sanchez, *Phys. Rev. E* 72, 025604 (2005).

Nonlinear light scattering and nonlinear absorption in photorefractive LiNbO₃ crystals studied by Z-scan technique

S.M. Kostritskii¹, M. Aillerie², E. Kokanyan³, O.G. Sevostyanov⁴

¹*RPC Optolink, Sosnovaya al. 6A, STMP bd.5, Zelenograd, 124489, Moscow, Russia*

²*LMOPS, University of Lorraine and Supélec, 2, rue E. Belin, 57070 Metz, France*

³*Institute for Physical Research, National Academy of Sciences of Armenia, 378410 Ashtarak*

⁴*Phys. Dept., Kemerovo State University, 650043, Kemerovo, Russia*

e-mail: skostritskii@optolink.ru

Characterization of nonlinear optical materials is a key step in order to choose the most adequate material for a given nonlinear optical process. The value of index of nonlinear refraction (NLR) n_2 and nonlinear absorption (NLA) β is interesting for high-intensity applications. In the case of some often used nonlinear optical materials, like LiNbO₃ (LN), photorefraction (PR) is also present as a nonlinear effect, providing a significant extra contribution to NLR and nonlinear scattering (NLS) [1].

It has been established that the wide-angle polarization-isotropic photoinduced light scattering (PILS) gives the significant contribution to transmission modulation observed by the open-aperture Z-scan technique in photorefractive LiNbO₃ crystals. This kind of nonlinear scattering, i.e. PILS, was studied in undoped and zirconium-doped LiNbO₃ crystals ([Zr] is ranged from 0.5 to 2.5 mol%). Open-aperture Z-scan studies of these crystals show that nonlinear scattering (NLS) is dominating over NLA caused by the two-photon absorption in Zr-doped crystals at [Zr] \geq 0.88 mol% even at low light intensities, while in undoped crystals the NLS gives a marked transmission attenuation only at moderate and high light intensities (> 20 W/cm²).

A modified Z-scan experimental setup is used to separate contributions of NLA and NLS in the Z-position dependent attenuation of transmittance. Both the NLA and NLS coefficients are estimated by theoretical fit of the open-aperture Z-scan curves. The relation between the NLS coefficient and gain factor Γ [2], which is describing the efficiency of the direct coupling between the pump and scattered waves, has been derived by us together with initial (seed) scattering ratio m_0 . The actual value of the gain factor have been found to be nonmonotonously dependent on Zr concentrations with maximum values, $\Gamma = 20.7$ cm⁻¹, at $0.88 \leq [\text{Zr}] \leq 1.0$ mol%.

According to recent finding [1,3], such a strong NLS should lead to good limiting characteristics. The study of optical limiting characteristics was made with the set-up used for Z-scan measurement, but at fixed crystal position. Thus, optical limiting threshold in the moderately and strongly Zr-doped ([Zr] \geq 0.88 mol%) crystals is in 10÷32 times (depending on [Zr]) lower than in undoped LiNbO₃. According to these results, the appropriate Zr-doping could be regarded as a good advice to improve the congruent lithium niobate for some specific photorefractive applications, e.g. optical limiting [3].

REFERENCES

- [1] F.Z. Henari, K. Cazzini, F.E. Akkari, W.J. Blau, *Appl. Phys. Lett.* 78, 1373 (1995).
- [2] M. Goukov, M. Imlau, Th. Woike, *Phys. Rev. B* 77, 235110 (2008).
- [3] G. Cook, J.P. Duignan, D.C. Jones, *Optics Commun.* 19, 393 (2001).

Gain analysis for fiber optical parametric amplifier in presence of attenuation and dispersion fluctuations

M. S. Kovacevic¹, Lj. Kuzmanovic¹, and A. Djordjevich

¹*Faculty of Science, University of Kragujevac, Serbia*

²*Department of Mechanical and Biomedical Engineering, City University of Hong Kong, Hong Kong, China*
e-mail: kovac@kg.ac.rs

In this work, the gain of the fiber optical parametric amplifier (FOPA) has been investigated. The analysis is based on the four-wave mixing using numerical simulations. It is assumed that the pump and signal waves undergo attenuation with random perturbations of the zero-dispersion wavelength (ZDWL). Also the impact of fiber attenuation is included for both dual-pump and single-pump FOPA with special attention on the wavelength dependence of attenuation. In order to study the impact of random fluctuation of ZDWL on gain, the fiber is segmented with random fluctuation of ZDWL that is assumed to follow Gaussian distributions. The fiber attenuation results in reduction of signal gain and the fluctuations of ZDWL lead to variation of gain spectrum.

REFERENCES

- [1] M. E. Marhic, N. Kagi, T.K. Chiang, and L.G. Kazovsky, *Opt. Express* **21**, 573 (1996).
- [2] M. E. Marhic, P. Anderkson, P. Petropoulos, S. Radic, C. Peucheret, and M. Jayayerifar, *Laser Photonics Rev.* **9**, 50 (2015).
- [3] K. K. Y. Wong, M. E. Marhic, K. Uesaka, and L. G. Kazovsky, *IEEE Photon. Tech. L.* **15**, 911 (2002).
- [4] J. Hansryd, P. A. Anderkson, M. Westlund, L. Li, and P.-O. Hedekvist, *IEEE J. Sel. Top. Quant. Electronics* **8**, 506 (2002).
- [5] M. A. Foster, A. C. Turner, J. E. Sharping, B. S. Schmidt, M. Lipson, and A. L. Gaeta, *Nature*, **9**, 960 (2006).
- [6] J. D. Harvey, S. G. Murdoch, S. Coen, R., Leonhardt, D. Mechin, and K. K L. Wong, *Opt. Quant. Electron* **39**, 1103 (2007).
- [7] M. Farahmand, and M. de Sterke, *Opt. Express* **12**, 136 (2004).
- [8] F. Yaman, Q. Lin, S. Radic, and G. P. Agrawal, *IEEE Photonic Tech. L.* **16**, 1292 (2004).
- [9] G. P. Agrawal, *Nonlinear Fiber Optics*, 3rd ed. San Diego, CA: Academic, (2001).

Analytical and dynamical generation of higher-order solitons and breathers of the extended nonlinear Schrödinger equation on different backgrounds

S. N. Nikolić^{1,2}, Najdan B. Aleksić^{1,2}, Omar A. Ashour^{1,3}, Milivoj R. Belić¹, Siu A. Chin³

¹Science program, Texas A&M University at Qatar, P.O. Box 23874 Doha, Qatar

²Institute of Physics Belgrade, University of Belgrade, Belgrade, Serbia

³Department of Physics and Astronomy, Texas A&M University, College Station, TX 77843, USA

e-mail: stankon@ipb.ac.rs

We investigate the analytical and dynamical generation of higher-order solitons and breathers of the extended nonlinear Schrödinger equation (NLSE) on different backgrounds. We included the operators up to the fifth-order dispersion, called Hirota, Lakshmanan-Porsezian-Daniel (LPD), and quintic operator [1,2].

The Darboux transformation (DT) is used to construct proper initial conditions for dynamical generation of high-intensity solitons and breathers of different order on a uniform background [3,4]. We provide expressions for the Lax pair generating functions and the procedure for calculating higher-order solutions when Jacobi elliptic functions are the background seed solutions of extended NLSE. It is shown that the peak height of each soliton or breather in the nonlinear Darboux superposition adds linearly, to form the intensity maximum of the final solution. We also show that breather-to-soliton conversion can be used to produce solitons of higher amplitude and that the periodicity of Akhmediev breathers can be utilized for dynamical generation of rogue waves.

The dynamical evolution of higher-order solitons and breathers is important in the situations when the existence of such solutions is questionable in the presence of modulation instability. Namely, the DT might provide analytical higher-order solutions that might not exist, owing to modulation instability, which usually exists in these solutions.

REFERENCES

- [1] A. Ankiewicz, D. J. Kedziora, A. Chowdury, U. Bandelow, N. Akhmediev, *Phys. Rev. E* **93**, 012206 (2016).
- [2] D. J. Kedziora, A. Ankiewicz, A. Chowdury, N. Akhmediev, *Chaos* **25**, 103114 (2015).
- [3] S. A. Chin, O. A. Ashour, S. N. Nikolić, M. R. Belić, *Physics Letters A* **380**, 3625 (2016).
- [4] S. N. Nikolić, N. B. Aleksić, O. A. Ashour, M. R. Belić, S. A. Chin, *Nonlinear Dynamics*, DOI: 10.1007/s11071-017-3540-z (2017).

Enhancing conductivity of self-assembled transparent graphene films with UV/Ozone Treatment

T. Tomasević-Ilić¹, Đ. Jovanović¹, J. Pešić¹, A. Matković^{1,2}, M. Spasenović¹, R. Gajić¹

¹*Graphene Laboratory (GLAB) of the Center for Solid State Physics and New Materials, Institute of Physics, University of Belgrade, Pregrevica 118, 11080 Belgrade, Serbia*

²*Present address: Institute of Physics, Montanuniversität Leoben, Franz Josef Straße 18, 8700 Leoben, Austria
e-mail:ttijana@ipb.ac.rs*

We demonstrate enhanced electrical conductivity of self-assembled transparent large area graphene films by UV/ozone treatment. Graphene as a material with high optical transparency and conductivity is an excellent choice for transparent electrodes in various optoelectronic devices [1]. Langmuir-Blodgett (LB) and Langmuir-Shaefer (LS) assembly are methods for simple, large-scale and cost-effective production of thin graphene films [2]. However, uncontrollable monolayer assembly into thin films and large defect density often leads to reduced LB and LS film conductivity. There is much effort to decrease sheet resistance of these films with annealing, chemical doping and functionalization [3, 4]. Here, we examine the effects of exposure to ultraviolet radiation and ozone (UVO) on LB/LS self-assembled graphene thin films by UV/VIS spectrophotometry, resistance measurements and Raman spectroscopy. We observe that the intensity of the D peak in Raman spectra of our graphene films decreases after UVO exposure, indicating a lower defect density. Also, sheet resistance decreased by an order of magnitude without loss in film transparency. We conclude that in contrast to the degrading effects it has on mechanically exfoliated and CVD-grown single layer graphene [5, 6], UVO treatment on LB/LS self-assembled graphene thin films leads to local defect patching which enhances the film conductivity while retaining the high optical transparency. We propose that our approach is suitable for various materials with a multitude of active edges and a large area of reactive surface making the solution-processed thin films usable in practical optoelectronics applications.

This work is supported by the Serbian MPNTR through Projects OI 171005 and by Qatar National Research Foundation through Projects NPRP 7-665-1-125. We thank the EU and Republic of Serbia for financing through the Science-Industry Collaboration Program administered by the Innovation Fund.

REFERENCES

- [1] F. Bonaccorso et al., *Nat. Photonics* 4, 611 (2010).
- [2] Li X. et al., *Nat. Nanotechnol.* 3, 538 (2008).
- [3] T. Tomasevic et al., *Opt. Quant. Electron.* 48, 319 (2016).
- [4] A. Matkovic et al., *2D Mater.* 3 015002 (2016).
- [5] E. X. Zang et al., *Appl. Phys. Lett.* 101, 121601 (2012).
- [6] S. Zhao et al., *Nanotechnol.* 23, 355703 (2012).

One-step synthesis of NIR-responsive NaYF₄:Yb,Er@Chitosane nanoparticles for biomedical application

I. Dinic¹, A. Djukic-Vukovic², L. Mojovic², M.G. Nikolic³, M.D. Rabasovic³,
A.J. Krmpot³, O. Milosevic¹ and L. Mancic¹

¹*Institute of Technical Sciences of SASA, Belgrade, Serbia*

²*Department of Biochemical Engineering and Biotechnology*

Faculty of Technology and Metallurgy, University of Belgrade, Serbia

³*Photonic Center, Institute of Physics Belgrade, University of Belgrade, Zemun, Belgrade, Serbia*

e-mail: lidija.mancic@itn.sanu.ac.rs

There is a great technological interest in synthesis of lanthanide doped upconverting nanoparticles with specific morphological characteristics and efficient luminescence response suitable for biomedical use [1]. A conventional approach for generation of such particles comprises decomposition of organometallic compounds in an oxygen-free environment and additional ligand exchange [2,3]. The biocompatible and water soluble NaYF₄:Yb,Er@Chitosane particles used in this study were synthesized through facile one-pot hydrothermal synthesis and were characterized using X-ray powder diffraction (XRPD), Fourier-transform infrared (FTIR) spectroscopy, field emission scanning and transmission electron microscopy (FESEM and TEM) and photoluminescence measurement (PL). Due to the presence of the amino groups at their surface these particles exhibit excellent hydrophilic properties and low cytotoxicity against human gingival fibroblasts (HGF), which was proven by MTT assay. Furthermore, upon 980 nm laser irradiation the as-prepared particles were successfully used for *in-vitro* visualization of the primary cell cultures of head and neck squamous carcinoma cells (HNSCC). In a NaYF₄:Yb,Er phase upconversion is enabled by the sequential absorption of two or more near-infrared photons by Yb³⁺ and subsequent energy transfer to the long-lived metastable electron states of Er³⁺ which produces luminescence emission at visible spectra after relaxation.

REFERENCES

[1] C. Chen, C. Li, Z. Shi, Adv.Sci.1600029 (2016).

[2] H.X. Mai, Y.W. Zhang, R. Si, Z.G. Yan, L.S. Sun, L.P. You, C.H. Yan, J. Am. Chem. Soc., 128, 6426 (2006).

[3] Y. Wei, F.Q. Lu, X.R. Zhang, D.P. Chen, Chem. Mater., 18, 5733 (2006).

Defect detection in aluminum using pulse thermography for a sample width periodic structure

V. Damnjanović¹, Lj. Tomic², G. Dikić³, B. Milanović⁴ and S. Petričević⁵

¹*Faculty of Mining and Geology, University of Belgrade, Serbia*

²*Military Technical Institute, Belgrade, Serbia*

^{3,4}*Military Academy, Belgrade, Serbia*

⁵*School of Electrical Engineering, University of Belgrade, Serbia*

e-mail:ljubisa.tomic@gmail.com

This paper presents experimental results of aluminum test plate using infrared video thermography in pulsed defectoscopy, by comparing noise reduction with conventional and Wiener filtering method [1,2]. Extraction of a meaningful signal from pulse thermography is subject to both intrinsic limitations imposed by thermal diffusion, and extrinsic factors including camera sensitivity, noise, input energy and reflected background radiation. Presented here are given comparative results of temperature contrast filtering on test plate surface: basic harmonic, mean value and Wiener filter of infrared pixels along the central line.

A special sample was prepared for the experiment, where on one side of an aluminum plate equally spaced grooves were produced, making a periodic defect structure with certain space frequency and certain depth [3]. The other side of the plate was illuminated by short light pulses and the temperature distribution on the same side was analyzed by pulse infrared thermography. Temperature distribution on the plate surface was also periodic, showing maximal above the grooves, i. e. defects, and minimal where there were no defects.

Experimental results were obtained by a standard thermal imaging camera. Infrared camera FLIR SC620 generates a thermal image of observed test samples, converts it to a visible image and transmits that image to the display unit. The time history of the surface temperature after the absorption of a short light pulse is used to obtain information about the subsurface structure and the thermo-physical properties of the material.

REFERENCES

- [1] L. Tomic, A. Kovacevic, V. Damnjanovic, P. Osmokrovic, *Measurement*. 46, 2263 (2013).
- [2] G. Dikic, L. Tomic, V. Damnjanovic, B. Milanovic, *Surface Review and Lett*. 22, 1550032 (2015).
- [3] L. Tomic, J. Elazar, *NDT&E International*. 60, 132 (2013).

Rare-earth enabled silicon light emitting diodes for the near-infrared

M. A. Lourenço^{1,2} and K. P. Homewood^{1,2}

¹*Materials Research Institute and School of Physics and Astronomy, Queen Mary University of London, Mile End Road, E1 4NS London, United Kingdom*

²*Advanced Technology Institute, Faculty of Engineering and Physical Sciences, University of Surrey, Guildford, Surrey GU2 7XH, United Kingdom*
e-mail: m.lourenco@qmul.ac.uk

Enabling light emission in silicon has potential applications, including in the 1.5 μm region for optical communications. The 2 μm region is also of considerable interest because of medical applications, and also gas sensing and free space optics. Silicon is not an efficient light emitting material and several approaches have been attempted to overcome this problem, including the incorporation of rare earth (RE) elements into Si substrates. Here we report and compare the luminescence in the near-IR of a wide range of REs (Ce, Pr, Nd, Sm, Eu, Gd, Tb, Dy, Ho, Er, Tm and Yb) doped silicon light emitting devices. The REs are introduced using ion implantation into standard n-type silicon wafers pre-implanted with boron to form both the p-n junction and an engineered dislocation loop array. The dislocation engineering approach [1], based on the controlled introduction of dislocation loops into the silicon lattice, is needed to reduce or suppress the thermal quenching and to obtain efficient luminescence.

We see sharp emissions, corresponding to the REs internal transitions, in samples doped with Dy, Ho, Er and Tm. Considering the extensive spectral range of rare earth internal transitions, ranging from the UV to the IR, this technology opens up many applications for silicon as an emissive material. In particular, room temperature light emission at 1.5 μm and in the 2.0 μm eye-safe spectral region have been obtained from dislocation engineered structures co-doped with Er and Tm, respectively.

The REs Eu, Yb and Ce have their lowest energy internal transitions above the silicon bandgap and therefore emission due to these REs should not occur in silicon. Remarkably, we see the first and surprising occurrence of red shifted Eu, Yb and Ce emission in silicon and demonstrated IR LEDs operating under conventional forward bias. This has been attributed to the direct intercession of the silicon providing a primary state replacing the usual intrinsic excited Eu^{3+} , Yb^{3+} and Ce^{3+} states, $^5\text{D}_0$, $^7\text{F}_{5/2}$, and the $5d^1$ levels respectively. This assumption is corroborated by crystal field analysis [2], which shows that the observed emission lines originate from the implanted REs. The direct involvement of the bulk band states and the absence of the normal “third party” energy transfer lead to much greater effective optical emission, as evidenced here by up to a 900 fold enhancement of EL intensity at the key 1.3 to 1.5 μm optical communication wavelength compared to classical RE devices. These results alter previous thinking on the behaviour of REs with semiconductors.

REFERENCES

- [1] Wai Lek Ng, M. A. Lourenço, R. M. Gwilliam, S. Ledain, G. Shao, K. P. Homewood, *Nature* 410, 192 (2001).
- [2] M. A. Lourenço, M. A. Hughes, K. T. Lai, I. M. Sofi, W. Ludurczak, L. Wong, R. M. Gwilliam, K. P. Homewood, *Adv. Funct. Mater.* 26, 1986 (2016).

Band edge modified rare-earth doped silicon for efficient mid-infrared photodetectors

K. P. Homewood^{1,2} and M. A. Lourenço^{1,2}

¹*Materials Research Institute and School of Physics and Astronomy, Queen Mary University of London, Mile End Road, E1 4NS London, United Kingdom*

²*Advanced Technology Institute, Faculty of Engineering and Physical Sciences, University of Surrey, Guildford, Surrey GU2 7XH, United Kingdom*
e-mail: k.p.homewood@qmul.ac.uk

We describe a new phenomenon - band edge modification (BEM) of rare earth (RE) transitions in materials [1]. BEM refutes previous assumptions on the interaction of REs with semiconductors and other hosts. The application here is in the commercially most important semiconductor – silicon. This new technology extends silicon photodetection to the mid-IR.

Silicon detectors and cameras currently completely dominate the ultra violet, visible and very near-IR regions - however they do not work well beyond 1.1 μm . We have used ion implantation to introduce europium, ytterbium and cerium into silicon photodiodes; also formed by ion implantation. We show that BEM enables efficient silicon detectivity to be extended from 1.1 μm , at the silicon band gap, out to the important mid-IR region.

Intrinsic RE transitions are internal to the RE manifolds and so not able to contribute directly to carrier conduction by charge transfer to the energy bands of the host. Consequently, this makes them of little use for optical detectors. In contrast, band edge modified RE levels interact directly here with the silicon bands giving extended photovoltaic detection in otherwise conventional silicon photodiodes. The wavelengths detected using Eu, Yb and Ce range from the near-IR at 1.1 μm , the band gap of silicon, out to the mid-IR.

The responsivities and detectivities of these new silicon detectors offer a real challenge to existing detector materials and devices in the 2 to 6 μm range - currently dominated by more challenging, and expensive materials such as mercury cadmium telluride, indium antimonide and the arsenides. Replacing these materials with silicon would offer enormous benefits in cost, reliability and also integration with the silicon microelectronics for detection and imaging. An additional benefit is using much less toxic materials and production processes – a major concern with current technologies.

Low leakage currents achievable in silicon based photodiodes mean that further development of this new mid-infrared silicon (MIRSIL™) technology could lead to thermoelectrically cooled or even room temperature detectors. Current commercial detectors in this area have to be cooled to liquid nitrogen temperatures (77 K) to achieve the performance needed for most applications. Higher operating temperature (HOT) detectors are an industry aim and, particularly if implemented in silicon, would be a major breakthrough.

REFERENCES

[1] M. A. Lourenço, M. A. Hughes, K. T. Lai, I. M. Sofi, W. Ludurczak, L. Wong, R. M. Gwilliam, K. P. Homewood, *Adv. Funct. Mater.* 26, 1986 (2016).

Selection of optical polymers in lens design

N. Sultanova¹, S. Kasarova¹, I. Nikolov² and R. Kasarov¹

¹*Department of Mathematics and Physics,
University "Prof. Dr. Assen Zlatarov" - Burgas, Bulgaria*

²*Department of Optics and Spectroscopy,
Sofia University "St. Kliment Ohridski", Bulgaria
e-mail:sultanova@btu.bg; kasarova_st@yahoo.com*

Selection of polymers in lens design is based on knowledge of their optical and material properties. They have already successfully replaced glasses not only in consumer but in high quality optics. In addition to sufficient clarity and transparency, polymers provide more degrees of freedom in optical design and production. Injection moulding technologies offer a low-cost alternative to glass with some additional advantages as reduced weight, high impact resistance, greater range of configuration possibilities and ability to integrate proper optical and mechanical features.

Different measuring techniques were applied to obtain precise refractometric data of various types of polymer materials at 22 wavelengths between 406 and 1320 nm. Bulk polymer samples as well as thin films have been studied [1, 2]. We have investigated optical and some material properties of principal polymers as polymethyl methacrylate, polystyrene and polycarbonate, copolymers styrene acrylonitrile and methyl methacrylate styrene, many trade-marks as CTE-Richardson, Zeonex, Optorez, NAS 21 Novacor, Bayer, and some development materials, produced by the USA Eastman Chemical Company. Dispersion analysis in the visible and in the near infrared spectrum has been accomplished. Important characteristics in lens design as principal and partial dispersions, Abbe numbers, relative partial and first order dispersions, reflection coefficients of polymer surfaces have been estimated.

A drawback of polymer materials is their much higher temperature sensitivity in comparison to glasses. Variation of refractive index and dispersion with temperature is evaluated on base of measured refractive data and the determined thermo-optical coefficients in the range 10 ÷ 50 °C [3]. Thermal linear and volume expansion coefficients, thermal "glass" and thermo-optical constants of studied plastics have been derived to evaluate alteration of optical and material constructive parameters and the temperature induced aberrations of polymer components. Reducing of thermal effects is possible in hybrid glass-plastic optical systems and proper choice of the housing materials.

Selection of appropriate optical polymers in lens design is illustrated on base of examples of all-plastic and hybrid glass-plastic objectives. Computing of geometrical and wave aberrations is accomplished to ensure image quality of the designed optical systems.

REFERENCES

- [1] N. Sultanova, C. Ivanov, I. Nikolov, *Opt. Quant. Electron.* 35, 21-34 (2003).
- [2] N. Sultanova, S. Kasarova, I. Nikolov, *J. Phys. Conf. Ser.* 356, 0120409 (2012).
- [3] S. Kasarova N. Sultanova, I. Nikolov, *J. Phys. Conf. Ser.* 253 (1), 012028 (2010).

Photoluminescence spectroscopy of CdSe nanoparticles embeded in transparent glass

M. Gilić¹, R. Kostić¹, D. Stojanović¹, M. Romčević¹, B. Hadžić¹, Z. Lazarević¹, J. Trajić¹,
J. Ristić-Đurović¹, N. Romčević¹

¹*Institute of Physics, University of Belgrade, Serbia*
e-mail: rkostic@ipb.ac.rs

In this paper we present photoluminescence measurements of CdSe nanoparticles embeded in transparent glass. Sample is prepared using an original technique, which combines both heat treatment, below glass crystalization temperature, and ultraviolet laser irradiation at 244 nm. Photoluminescence spectra were excited by several lines of Ar-laser line (514.5 nm, 501.7 nm, 496.5 nm, 488 nm) measured using a Jobin Yvon model U-1000 monochromator, with a conventional photocounting system.

Photoluminescence spectra displayed one main emission band at 2.14 eV. We identify this bands energy as basic interband transition in CdSe nanoparticle. We calculated energy of basic ($1s_h-1s_e$) transition in spherical CdSe quantum dot (QD), within infinite potential barrier, in effective-mass approximation (EMA). Parameters of CdSe, electron and hole effective masses, energy gap and dielectric permittivity are transferred from literature [1]. On the basis of this model, average radius of synthesized CdSe QDs is about 3 nm.

REFERENCES

[1] M. Sahin, S. Nizamoglu, A. E. Kavruk, H. V. Demir, J. Appl. Phys. 106, 043704 (2009).

Improved thermal and mechanical properties of tot'hema–gelatin eco-friendly films

B. Muric, D. Pantelic, D. Vasiljevic and B. Jelenkovic
Institute of Physics,
Belgrade, Serbia
e-mail: muric@ipb.ac.rs

Today, biodegradable films have known as significant eco-friendly food packaging materials to reduce of plastic wastes [1]. Biodegradable films were mainly made from some biopolymers such as polysaccharides [2], and proteins [3]. Among them, gelatin [4] considered to be the most ideal candidate.

The thermal and mechanical properties of tot'hema-gelatin films were investigated to determine their suitability as eco-friendly films. The influence of different tot'hema concentrations on the physicochemical properties of gelatin films, and consequently on mechanical, and thermal properties was analyzed. A series of tot'hema-gelatin films were made by the gravity settling method. Results showed that prepared films were plasticized by tot'hema adding, and their mechanical properties (tensile strength, elastic modulus, elongation at break) were significantly improved. With the increase of tot'hema content, thickness and tensile strength (TS) of gelatin films increased, and the elongation at break (EB) decreased. Gelatin films containing 30% tot'hema had limit values of the thickness. In addition, thermal properties characterized by differential scanning calorimetry (DSC) showed that the thermal stability of films was better. In the thermograms of gelatin modified films, four endothermic peak can be observed. Briefly, the films prepared from gelatin and tot'hema showed great potential for packaging applications.

REFERENCES

- [1] A. Etxabide, I. Leceta, S. Cabezudo, P. Guerrero, K. de la Caba, *ACS Sustainable Chem. Eng.* 4, 4626 (2016).
- [2] C. Li, J. Luo, Z. Qin, H. Chen, Q. Gao, J. Li, *RSC Adv.* 5, 56518 (2015).
- [3] X. Liu, R. Song, W. Zhang, C. Qi, S. Zhang, J. Li, *Sci Rep.* 7, 44289 (2017).
- [4] X. Wu, Y. Liu, W. Wang, Y. Han, A. Liu, *J Food Process Eng.* 40, e12469 (2017).

Ab-initio calculations of electronic and vibrational properties of Sr and Yb-intercalated graphene

A. Šolajić¹, J. Pešić¹ and R. Gajić¹

¹*Institute of Physics, Center for Solid State and New Materials, Belgrade, Serbia*
e-mail: solajic@ipb.ac.rs

In the last couple of years, 2D materials have gained a leading role in material science and have been attracting a great attention due to their unique physical and chemical properties. Intercalation is one of the powerful tools for making 2D materials even more exciting by providing an additional doping and tunable properties.

Graphene, a two-dimensional honeycomb lattice of carbon atoms, possess various fascinating physical, structural and electronic properties, which make it an excellent candidate for applications in electronics and photonics. Structures based on intercalated graphite have been extensively studied, showing many new properties and exotic physics [1,2]. This inspired many to investigate a single or few-layer intercalated graphene.

Intercalated graphene has many extraordinary properties that are not present in pristine graphene [3-6]. It is also different compared to bulk intercalated graphite materials and has great spectra of characteristics induced by various intercalants, usually alkali or alkaline earth metals. This opens new possibilities for further research and a wide range of applications. Although some of those structures have even been realised experimentally [7,8], there are many more to come, with a great potential for both theoretical and experimental investigations. Based on the first principle calculations, such as Density Functional Theory (DFT) and Density Functional Perturbation Theory (DFPT), it is possible to calculate various electronic and optical properties as well as to simulate some of the most used spectroscopic techniques (like IR and Raman spectroscopy). Those methods enable a comparison with existing experimental data, as well as for getting directions for a new research and experiments.

In this paper, we present the results of a DFT study on electronic and vibrational properties of the graphene intercalated with Sr and Yb, taking into account that their corresponding bulk compounds have been mostly investigated so far. The calculations were performed in Quantum Espresso software package [9].

This work is supported by the Serbian MPNTR through Project OI 171005 and by Qatar National Research Foundation through Projects NPRP 7-665-1-12.

REFERENCES

- [1] T. E. Weller, M. Ellerby, S. S. Saxena, R. P. Smith, and N. T. Skipper, *Nat. Phys.* 1, 39 (2005).
- [2] Csányi, G., Littlewood, P. B., Nevidomskyy, A. H., Pickard, C. J., Simons, B. D. *Nat. Phys.* 1, 42–45 (2005).
- [3] Pešić J., Gajić R., Hingerl K. and Belić M., *EPL* 108 67005 (2014).
- [4] J. Chapman, Y. Su, C. A. Howard, D. Kundys, A. N. Grigorenko, F. Guinea, A. K. Geim, I. V. Grigorieva & R. R. Nair, *Scientific Reports* 6, 23254 (2016).
- [5] G. Profeta, M. Calandra, F. Mauri, *Nat. Phys.*, 8, 131 (2012).
- [6] Pešić J., Damljanović V., Gajić R., Hingerl K. and Belić M., *EPL*, 112 6 67006 (2015).
- [7] Kanetani K, Sugawara K, Sato T, Shimizu R, Iwaya K, Hitosugi T, Takahashi T, *PNAS* 109, 19610–19613 (2012).
- [8] Ludbrook, B.M. et al., *PNAS* 112, 11795–11799 (2015).
- [9] P. Giannozzi, et al *J.Phys.:Condens.Matter*, 21, 395502 (2009).

Influence of x-ray irradiation on the dielectric properties of YbF₃-doped (Ba/Ca)F₂ crystals

M. Stef¹ and I. Nicoara¹

¹West University of Timisoara, Faculty of Physics
Timisoara, Romania

e-mail: marius.stef@e-uvt.ro

MeF₂ crystals (Me = Ca, Ba and Sr) find applications as a transmitting window over a wide wavelength range, as a fast scintillator involving emission at 195 nm and 220 nm and doped with rare-earth (RE) ions as laser material. The trivalent RE-ions usually occupy a cation substitutional position in MeF₂ lattice and charge compensation is required in order to maintain the electrical neutrality of the system. The extra positive charge is compensated by an interstitial fluorine ion. This indeed leads to a complex site structure including so-called isolated centers, pairs (or dimers) of adjacent rare-earth ions, clusters, etc., depending on the nature of the substituted cation, of the RE dopant and of the dopant concentration. In order to understand the optical properties of the crystals it is important to know the type of the charge compensating defects that are formed. On the other hand the RE ions can be stabilized in the divalent state in MeF₂ lattice, besides the trivalent state, with which can coexist. It is known that certain fraction of Yb³⁺ ions can be reduced to divalent state by various methods or directly in the as-grown crystals using high deoxidization growth conditions.

Local compensation by pairing of Yb³⁺ ions with interstitial F⁻ ions create electric dipoles whose relaxation are observed as dielectric relaxation. Temperature and frequency dependence of the complex dielectric constant (the dielectric spectrum) gives information about the impurity-defect aggregates [1, 2].

The optical absorption (OA) spectra of MeF₂ crystals reveal various color centers after x-ray irradiation. The obtained color centers depend on the crystal quality, on the impurity in the crystals, and on the photons energy. The color of the irradiated crystals is due to their absorption bands in the visible spectral region.

The goal of this work is to study the dielectric spectra of the YbF₃-doped (Ba/Ca)F₂ crystals in order to obtain information about the influence of x-ray irradiation on the impurity-defect formation in these crystals.

Various concentrations YbF₃ -doped (Ba/Ca) F₂ crystals have been grown using the conventional Bridgman method. Transparent colorless crystals of about 10 mm in diameter over 5-6 cm long were obtained in graphite crucible in vacuum (~ 10⁻¹ Pa) using a shaped graphite furnace [3], the pulling rate was 4mm/h. The optical absorption spectra reveal the existence of both Yb²⁺ and Yb³⁺ ions.

The dielectric measurements were performed using a RLC Meter ZM 2355, over the temperature range 150–300 K, at nine audio-frequencies 1–100 kHz. The real part of the dielectric constant, ϵ_1 , has been calculated from the measured capacitance. The ϵ_2 has been then calculated from $D = \epsilon_2 / \epsilon_1$ ($D = \tan \delta$ is the dielectric loss). The relaxation parameters (the activation energy for dipole reorientation and relaxation time constant) have been calculated in order to characterize the observed relaxations. We assign the observed relaxation to trigonal type (C_{3v}) centers in BaF₂ host and C_{4v} centers in CaF₂. The number of the dipoles, N_D , that contribute to the dielectric relaxation have been determined from the dielectric spectra; the correlation between N_D and the optical spectra has been also discussed. A comparison of dielectric spectra of CaF₂:YbF₃ and BaF₂:YbF₃ crystals is also given.

REFERENCES

- [1] J. Fontanella and D. J. Treacy, J. Chem. Phys. 72, 2235 (1980).
- [2] I. Nicoara, M. Stef, Eur. Phys. J. B 85, 180 (2012).
- [3] D. Nicoara, I. Nicoara, Mater. Sci. Eng. A 102, L1 (1988).

Bifurcation in reflection spectra of holographic pullulan diffraction grating

S. Savić-Šević, D. Pantelić, V. Damljanović and B. Jelenković

Institute of Physics, University of Belgrade, Pregrevica 118, 11080 Zemun, Belgrade, Serbia
e-mail:savic@ipb.ac.rs

Reflection volume hologram gratings, fabricated using a single-beam method, usually have only one Bragg peak in the spectrum. Z. Wang et al. [1] noted the appearance of multiple peaks in the spectrum of volume diffraction grating recorded in dichromated gelatin, phenomenon that looks like bifurcation within the Bragg plateau. We also observed bifurcation phenomenon in the spectrum of diffraction gratings recorded in dichromated pullulan (DCP), which is a polysaccharide doped with chromium. Compared to dichromated gelatin, the DCP material is simpler to prepare and process, it is insensitive to humidity, thus retaining high resolution and diffraction efficiency [2]. The typical number of appeared peaks in the spectrum is two, three, or four. It was found that a multi-peak phenomenon is accompanied by wider band gap.

In order to understand multi-peak structure of band gaps, experimental results were compared with theoretically predicted results. The theoretical model investigates effects of several important parameters: absorption of radiation within the photosensitive layer, non-uniform thickness of the layer, refractive index modulation and non-uniform spatial period of the grating. Numerical reflection spectra of volume Bragg gratings have been calculated by the method of characteristic matrix [3]. Our model suggests that multi peak structures are produced by uneven modulation of Bragg layers inside the volume hologram. The results of calculation are in agreement with experimental results.

REFERENCES

- [1] Z. Wang, D. Liu, J. Zhou, *Opt. Lett.* 31, 3270 (2006).
- [2] S. Savić-Šević, D. Pantelić, *Applied optics* 46, 287 (2007).
- [3] M. Born, E. Wolf, *Principles of Optics*, Pergamon (1980).

Discrete and Selective Absorption in Crystalline Molecular Nanofilms

M. Vojnović¹, A.J. Šetrajić – Tomić¹, S.M. Vučenović², J.P. Šetrajić³

¹University of Novi Sad, Faculty of Medicine; Novi Sad, Vojvodina – Serbia

²University of Banja Luka, Faculty of Sciences, Department of Physics; Banja Luka, Republic of Srpska – B&H

³University of Novi Sad, Faculty of Sciences, Department of Physics; Novi Sad, Vojvodina – Serbia

e-mail: setrajcic.a@gmail.com

Recent research in nano-optical engineering and in nanomedicine as well, seek for methods of construction various type of nano-markers, nano-carriers and ways to deliver drugs in exactly determined regions of body [1,2]. In this process it is important to find methods of recognition certain type of molecules. It is obvious that optical recognition would be the easiest and most effective way to do it.

Our research presents a model of molecular ultrathin crystalline film and inside it generated exciton system and corresponding methodology of analysis of their optical characteristics. Properties of these spatially very restricted structures are very sensitive to their surrounding surfaces. Using the two-time Green's functions, adapted for crystalline structures with break symmetry [3,4], and graphical-numerical software, we have calculated energy spectra and possible exciton states [5].

We have showed that the appearance and the presence of localized states in the surfaces and in the boundary layers of the film depend on the thickness of the film and the film surrounding, presented through the perturbation parameters on surfaces.

Optical properties in these structures demonstrate discrete and very selective resonant absorption spectra, depending on their perturbation on their surfaces.

REFERENCES

- [1] Y. Pathak, D. Thassu: Drug Delivery Nanoparticles – Formulation and Characterization, Informa, New York (2009).
- [2] K. Wood, P. Hammond, D. Schmidt, S. Wrightman and B. Andaya: Thin Film Delivers Drugs, Biophotonics, Cambridge, Mass., Feb. 12, 2008; <http://www.photonics.com>.
- [3] J.P. Šetrajić, D.I. Ilić, B. Markoski, A.J. Šetrajić, S.M. Vučenović, D.Lj. Mirjanić, B. Škipina and S.S. Pelemiš, Physica Scripta T 135, 014043: 1-4 (2009).
- [4] V.D. Sajfert, J.P. Šetrajić, S.K. Jaćimovski and D. Popov, Quantum Matter 3/4, 307 (2014).
- [5] J.P.Šetrajić: Exact Microtheoretical Approach to Calculation of Optical Properties of Ultralow Dimensional Crystals, ArXiv, eprint arXiv:1004.2387 (04/2010); Opto-Electron.Rev. – accepted (2017).

Optical properties of atomic layer deposition prepared Al-doped ZnO for photonic applications

N. Bozhinov¹, V. Marinova¹ and D. Z. Dimitrov^{1,2}

¹*Institute of Optical Materials and Technologies, BAS, Sofia, Bulgaria*

²*Institute of Solid State Physics, BAS, Sofia, Bulgaria*

e- mail: bozhinov31@abv.bg

Transparent Conductive Oxide (TCO) films play an important role in optoelectronic devices such as thin film solar cells and light emitting diodes (LEDs). Among various materials under development for TCO applications, Al-doped ZnO (AZO) film is a particularly attractive material because of its excellent properties, such as higher thermal stability, good resistance against damage by hydrogen plasma and low cost of fabrication, compared to indium tin oxide. The Al doping of ZnO is substitutional as Al³⁺ ions replace Zn²⁺ ions in ZnO lattice. Each ionized Al atom contributes one extra valence electron as amobile charge carrier, so Al doping improves the electrical conductivity of the material considerably. While doping ZnO with a suitable amount of Al can increase its material properties notably, excessive doping could adversely affect carrier mobility due to ionised impurity scattering [1]. Therefore, on prime importance is to determine the optimal doping concentration of AZO. Films of Aluminum-doped Zinc Oxide are observed to be transparent and electrically conductive. They have high transmission in the visible region as well as transmission to IR wavelengths up to ~12 μm .

Atomic Layer Deposition (ALD) is a self-limiting deposition method that is characterized by alternating exposure of the growing film to chemical precursors, resulting in the sequential deposition of mono layers over the exposed sample surface. The self-limiting nature of the vapor-solid reactions ensures pinhole free coatings with a precise thickness controlled at the atomic scale and a superb conformality onto large scale substrates with complex topologies [2].

Thin films of Al-doped ZnO are prepared by ALD on Si and quartz glass substrates at temperature of 200 °C. The influence of Al content on the structure, optical, and electrical properties of AZO films is investigated. The optical properties and sheet resistance of the films with different Aluminum doping are measured and calculated. Refractive index (n), extinction coefficient (k), absorption coefficient α and thickness (d) of the films are determined simultaneously from transmittance and reflectance measurements at normal light incidence of films deposited simultaneously on two types of substrates – transparent (optical glass or fused silica) and opaque (Si-wafer). It is found that n and k decrease with wavelength. Using both the data for refractive index and Bruggemann effective medium approximation the volume fractions of Al₂O₃ and ZnO are calculated by optical means. Optical band gap is determined using the obtained values of the absorption coefficient α and Tauc plots. It is observed that the full range of sheet resistance, from 50 Ω/sq to M Ω/sq , can be obtained with AZO by varying film thickness and deposition parameters. The obtained parameters are an indication that AZO is appropriate low cost replacement transparent conducting oxide (TCO) of Indium Tin Oxide (ITO) for all photonics applications.

Finally, applications of AZO layers as transparent conductive electrodes in Liquid Crystal display devices are demonstrated.

Acknowledgement: The financial support by the Bulgarian Science Fund under the project FNI-DH-08/9 is gratefully acknowledged.

REFERENCES

- [1] T. Minami, *Semicond. Sci. Technol.*, 20, S35 (2005).
- [2] R. W. Johnson, A. Hultqvist, S. F. Bent, *Materials Today*, 17, 236 (2014).

An example of two-dimensional crystal structure with semi-Dirac electronic dispersion

V. Damljanović¹ and R. Gajić²

¹*Institute of Physics Belgrade, University of Belgrade, Pregrevica 118, 11080 Belgrade, Serbia*

²*Graphene Laboratory (GLAB) of Center for Solid State Physics and New Materials, Institute of Physics, University of Belgrade, Pregrevica 118, Belgrade, 11080, Serbia*

e-mail: damlja@ipb.ac.rs

In nanophysics, notion “semi-Dirac dispersion” denotes an electronic dispersion which is Dirac-like along certain direction in two-dimensional Brillouin zone (BZ) and quadratic along the orthogonal direction. Semi-Dirac materials are in the focus of research lately due to their intriguing physical properties. These include anisotropic Klein tunneling, characteristic response to magnetic field and peculiar photoresponse to circularly polarized light. To help search for new materials with the semi-Dirac cones, we have recently formulated a set of group-theoretical conditions that allow such dispersion and have provided the list of symmetry groups satisfying them [1]. In present contribution we have considered a tight-binding model on a structure that belongs to diperiodic (layer) group $p11b$ (Dg5). This group belongs to our list [1] and should host the semi-Dirac cones in the vicinity of A and B points in the BZ. We have calculated electronic dispersion in the vicinity of these points. Obtained dispersion is of a semi-Dirac type thus confirming our theory. Here we also discuss other possible candidates for two-dimensional semi-Dirac materials by search Materials project database with particular attention to layered structures published in [2].

REFERENCES

- [1] V. Damljanović, R. Gajić, *J. Phys.: Condens. Matter* 29, 185503 (2017).
- [2] G. Cheon et al., *Nano Letters* 17, 1915 (2017).

Ab-initio study of optical properties of MoS₂ and WS₂ compared to spectroscopic results of liquid phase exfoliated nanoflakes

Jelena Pešić¹, Jasna Vujin¹, Tijana Tomašević-Ilić¹, Marko Spasenović¹, Radoš Gajić¹

¹Graphene Laboratory (GLAB) of the Center for Solid State Physics and New Materials,
Institute of Physics, University of Belgrade,
Pregrevica 118, Belgrade, 11080, Serbia
e-mail: yelena@ipb.ac.rs

MoS₂ and WS₂ are part of the family of transition metal dichalcogenide crystals (TMDC). TMDCs have emerged as a new class of semiconductors that display distinctive properties at a thickness of one and few layers [1-3]. They have also attracted much interest for applications in optoelectronics as detectors, photovoltaic devices and light emitters [4-8].

Spectroscopic techniques are among the most important methods for research in the field of nanoscience and nanotechnologies. Parallel with the development of experimental methods, computational science becomes a very valuable tool in pursuit for new low-dimensional materials and their characterization. Employing high-end modeling codes, it is possible to simulate from first principles more than a few spectroscopic techniques. Using approaches based on density functional theory (DFT), including density functional perturbation theory, time-dependent DFT and many-body perturbation theory, implemented in the Quantum Espresso software package [9], we study optical properties of low-dimensional materials, MoS₂ and WS₂.

We calculate the dielectric function within the framework of the random-phase approximation (RPA) [10] based on DFT ground-state calculations, starting from eigenvectors and eigenvalues all calculated with Quantum Espresso. The final goal of our theoretical work is a comparison to corresponding experimental data. We compare our computational results with optical measurements on MoS₂ and WS₂ nanoflakes. MoS₂ and WS₂ were exfoliated by ultrasonic treatment in low-boiling point organic solvent [11-15] and characterized using UV/VIS spectrophotometry. We use our results for analysis of optical properties of liquid phase exfoliated MoS₂ and WS₂ nanoflakes, as a proven method for analysis of basic optical properties of 2D materials [11].

This work is supported by the Serbian MPNTR through Project OI 171005 and by Qatar National Research Foundation through Projects NPRP 7-665-1-12

REFERENCES

- [1] S. Z. Butler, et al., ACS Nano 7, 2898 (2013).
- [2] Q. H. Wang, et al., Nat Nano 7, 699 (2012).
- [3] X. Xu et al., Nat Phys 10, 343 (2014).
- [4] A. Pospischil, M. M. Furchi, and T. Mueller, Nat Nano 9, 257 (2014).
- [5] B. W. H. Baugher, et al., Nat Nano 9, 262 (2014).
- [6] L. Britnell, et al., Science 340, 1311 (2013).
- [7] F. H. L. Koppens, et al., Nat Nano 9, 780 (2014).
- [8] J. Ross, Nat Nanotechnol. 4, 268 (2014).
- [9] P. Giannozzi et al., J. Phys.:Condens. Matter 21 395502 (2009) <http://www.quantum-espresso.org>
- [10] Brener, N.E., Phys. Rev. B 12, 1487, (1975).
- [11] A. Matković et al., 2D Mater. 3(1), 015002 (2016).
- [12] T. Tomašević-Ilić, et al. Opt Quant Electron 48: 319, (2016).
- [13] T. Tomašević-Ilić et al., submitted (2017).
- [14] R. Panajotović et al. Book of Abstracts, SPIG 2016, 182-185, (2016).
- [15] J. Vujin et al. Book of Abstracts RAD 2016, (2016).
- [16] J. Pešić et al. , Opt Quant Electron, 48:368 (2016).

Nanostructured films based on Au nanocrystals of different morphology for SERS

T.H. Beinyk¹, N.A. Matveevskaya¹, S.V. Dukarov²

¹ SSI "Institute for Single Crystals" Institute for Single Crystals of NAS of Ukraine, 60 Nauky Ave, 61001, Kharkiv, Ukraine.

² V.N. Karazin Kharkiv National University, 4 Svobody Sq., Kharkiv, 61022, Ukraine.
e-mail: beynik@isc.kharkov.ua

Recently the development of new multifunctional materials based on gold nanocrystals (Au NCs) has been of great interest due to their unique properties. Film structures based on Au NCs are widely used in optoelectronics, medicine, catalysis, and surface enhanced Raman spectroscopy (SERS) for determining the trace amounts of substances. Films based on nonspherical Au NCs are promising candidates for using in SERS due to the possibility of adjusting the plasmon resonance to a certain frequency. Due to the nonspherical morphology of Au NCs, which are elements of the film structure, namely the presence of sharp ends, on which there is a significant electric field strength increasing caused by the excitation of delocalized valence electrons (surface plasmons) of Au NCs by the electromagnetic wave, films based on nonspherical Au NCs can be used as SERS-substrates for registration of intermolecular interactions of individual molecules. In this connection preparation of stable film materials based on Au NCs with precisely controlled NC size and morphology is an important task.

The aim of the work was to develop methods for producing nanostructured films based on Au NCs of different morphology and size for creating effective SERS-substrates, study their properties, establish the relationship between Au NC morphology and their properties.

One of the effective methods of film producing is template synthesis, which allows controlling the filling density of the substrate by Au NCs and provides a high uniformity of their sizes. Stable monolayer film structures based on Au nanospheres, nanoellipses and nanostars with an average NC size in the range of 20-80 nm and 20% size dispersion were obtained.

Characterization of the obtaining films (structure, composition, size, optical properties) was carried out by high resolution scanning and transmission electron microscopy, X-ray photoelectron spectroscopy and optical spectroscopy.

It was shown that the Au NC morphology significantly influences on the optical properties of the produced film structures. The surface plasmon resonance (SPR) maximum of monolayer structures based on Au nanospheres (the average NC size is 50 nm) is observed in the region of 540 nm. In the case of monolayer structures based on Au nanoellipses (the average transverse NC size is 22 nm, longitudinal – 30 nm), the transverse SPR is in the region of 535 nm, longitudinal SPR is in the region of 650 nm, for the Au nanostar based films (the average NC size is 70 nm) the SPR peak is in the region of 620 nm.

It was shown that nanostructured films based on Au nanostars are the most promising SERS-substrates: the enhancement factor of Rhodamine 6G Raman signal using films based on nanostars reaches 10^6 , dye concentration is 10^{-5} M.

Self-polarization effects in spherical core-shell quantum dot

D. Stojanović, R. Kostić

Institute of Physics, University of Belgrade, Serbia

e-mail:dusanka@ipb.ac.rs

Single electron in spherical shell in infinite potential barrier is investigated. Schrödinger equation in effective mass approximation (EMA) for this spherical heterosystem is solved to get eigenenergies and corresponding wave functions. In case of infinite potential barrier the ground state energy depends only on the shell width. Self-polarization potential is obtained by solving Poisson equation in three concentric spherical regions: core, shell and surrounding medium. Shell self-polarization energy depends on geometry (core and shell radius) and the dielectric mismatch at the QD boundaries. Self-polarization energy is used as perturbation. One electron ground state energy results are presented in this paper.

CdSe is placed in the shell. Surrounding medium is dielectric of smaller permittivity (vacuum or water), that is the most realistic case. The dielectric permittivity core influences to energy of ground state is analyzed.

The self-polarization changes of ground state energy for different compositions, i.e. core and shell radius, are presented. For smaller core radius and the same shell thickness (which imply the same unperturbed ground state energy) bigger is the energy correction, i.e. perturbed energy state, for one value of the core dielectric permittivity. Increase of core dielectric permittivity produces decrease of energy correction.

Sb- based phase- change materials

D. Z. Dimitrov^{1,2}

¹*Institute of Solid State Physics, Bulgarian Academy of Sciences, Sofia, Bulgaria*

²*Institute of Optical Materials and Technologies, Academy of Sciences, Sofia, Bulgaria*

e-mail: dzdimitrov@issp.bas.bg

The most important issues in the development of materials for nonvolatile Phase-change Random Access Memories (PCEAM) are the speed of reversible transformation between amorphous and crystalline states, the sensitivity of the phase change material especially in point of view of the reset current and the stability of both amorphous and crystalline phase [1]. Doped Sb – based phase change materials possess growth dominated crystallization, the crystallization speed being increased with scalability. Pure antimony films show explosive crystallization at room temperature. Alloying with other elements can increase the amorphous stability. Especially the addition of Ge or Ga to the Sb film enhances the amorphous state stability, as a result of large activation energy for crystallization, and leads to large increase in the crystallization temperature. Sb – based materials combine high crystallization rates with excellent amorphous phase stability. These materials possess higher crystallization speed and improved amorphous state stability in comparison to GST materials [2]. The recrystallization time (crystallization of an amorphous volume in crystalline background) is for example as follows: Ge₁₅Sb₈₅ – 15 ns, In₁₅Sb₈₅ – 6 ns and Ga₁₅Sb₈₅ – 31 ns. The basic concept of the GeSb based phase-change materials engineering is starting with the GeSb alloy or InSb alloy near to the eutectic composition as main component and addition of various third components doping in low percentage. High – crystallization speed combined with higher glass-transition (crystallization) temperature and lower melting temperatures are expected with these phase-change materials. The key challenge in the research of Sb based materials for PCRAM application are the possibility to obtain a threshold (electronic) switching behavior and the magnitude (contrast) of the resistance changes between amorphous and crystalline states of the Sb-based alloys. Sb based materials as thin films were prepared by co-sputtering from two or three targets. Alloy targets with compositions Ge₁₅Sb₈₅, In₂₀Sb₈₀ as well as single element targets as Sn and Zn were used. Some of the experiments are performed on mixed dielectric material/ Sb-based alloy samples. ZnS-SiO₂ is used as dielectric material or nitrogen alternatively was introduced into the phase-change alloy compositions by reactive sputtering in mixed Ar/N₂ atmosphere. Electrical resistance is measured in thin film samples deposited onto SiN coated Si coupons. Resistance experiments are performed at heating rates of 5, 10, 20 and 40 °C/min in Ar gas. These measurements further are used for crystallization activation energies observation by following the crystallization temperatures change during heating with different heating rates. Activation energies (E_a) of 5.71eV and 5.07eV for GeInSbZn and GeInSbSn respectively are calculated from the data. DSC/DTA and XRD/XPS measurements are performed as well. It is found that GeInSb and GeSb based materials possess improved crystallization speed and amorphous state stability in comparison to GST materials. Single phase crystallization is observed in ternary GeInSb and quaternary GeInSb alloys with appropriate Zn and Sn doping. The limit of the doping concentration of Zn and Sn to the GeInSb for single phase crystallization is found to be ≤ 7 at.% of Zn and up to 18 at.% of Sn. Two order of magnitude change in electrical resistance is measured during the phase transformation in these alloys. Melting temperature below 500 °C and crystallization temperatures around 200 °C are characteristic for these alloys furthermore making them attractive for the practical application implementation.

Acknowledgement: The financial supports by the Bulgarian Science Fund under the project FNI-T-02/26 is gratefully acknowledged.

REFERENCES

- [1] S. Raoux, *Annu. Rev. Mater. Res.*, 39, 25–48 (2009).
- [2] M. Wuttig, S. Raoux, *Z. Anorg. Allg. Chem.*, 638(15), 2455–2465 (2012).

Electronic and optical properties of square HgTe quantum dots

D. B. Topalović^{1,2}, V. V. Arsoski¹, N. A. Čukarić¹, M. Ž. Tadić¹ and F. M. Peeters³

¹*School of Electrical Engineering, University of Belgrade, Serbia*

²*Vinča Institute of Nuclear Sciences, University of Belgrade, Serbia*

³*Department of Physics, University of Antwerp, Groenenborgerlaan 171, B-2020 Antwerp, Belgium*

e-mail:dusan.topalovic@vin.bg.ac.rs

After decades of applications for photovoltaic devices, HgTe has recently gained popularity due to its unique topological properties. As a matter of fact, HgTe quantum wells host the gapless edge states, which are protected by time reversal symmetry. Those states were predicted by comprehensive theory [1], which was then confirmed by experiment [2]. In addition to HgTe quantum wells, HgTe quantum dots have been recently explored. Quantum confined states in HgTe colloidal quantum dots [3] were demonstrated to allow for fine tuning of the energy spectra from close to near infrared region [4-6].

We investigate the electronic and optical properties of square shaped HgTe quantum dots. The electronic structure is calculated by means of the nearest neighbour tight binding (TB) method in a $sp^3d^5s^*$ basis where spin-orbit coupling is included [7]. A large number of hopping parameters is taken into account with the aim to accurately describe *inverted band structure*. The exciton states are modelled as the first-order corrections of the single particle spectra due to the Coulomb and exchange interactions [8]. The dipole moment is determined by including only the intraorbital terms, which was previously demonstrated to be a reasonable approximation for graphene, silicene, and phosphorene quantum dots [9,10]. And the appearance of trivial edge states is avoided by removing the dangling bonds from the quantum dot.

The result of this study is that the peculiar edge states exist in square HgTe quantum dots. Furthermore, influence of in-plane electric field and perpendicular magnetic field on the optical absorption spectra is investigated. The edge and bulk states are found to behave differently in external fields, and those differences are explored and analyzed in detail.

REFERENCES

- [1] B. A. Bernevig, T. L. Hughes, S. C. Zhang, *Sci.* 314, 5806 (2006).
- [2] M. König, S. Wiedmann, C. Brüne, A. Roth, H. Buhmann, L. W. Molenkamp, X. L. Qi, S. C. Zhang, *Sci.* 318, 5851 (2007).
- [3] G. Allan and C. Delerue, *Phys. Rev. B.* 86, 165437 (2012).
- [4] A. Rogach, A. Eychmüller, S. Hickey, and S. Kershaw, *Small* 3, 536 (2007).
- [5] T. Rauch, M. Boberl, S. F. Tedde, J. Furst, M. V. Kovalenko, G. Hesser, U. Lemmer, W. Heiss, and O. Hayden, *Nat. Photonics* 3, 332 (2009).
- [6] S. Keuleyan, E. Lhuillier, and P. Guyot-Sionnest, *J. Am. Chem. Soc.* 133, 16422 (2011).
- [7] J. C. Slater and G. F. Koster, *Phys. Rev.* 94, 6 (1954).
- [8] S. Lee, J. Kim, L. Jönsson, J. W. Wilkins, G. W. Bryant, G. Klimeck, *Phys. Rev. B* 66, 235307 (2002).
- [9] L. L. Li, D. Moldovan, W. Xu, and F. M. Peeters, *Nanotechnology* 28, 085702 (2017).
- [10] H. Abdelsalam, M. H. Talaat, I. Lukyanchuk, M. E. Portnoi, and V. A. Saroka, *J. Appl. Phys.* 120, 014304 (2016).

Polarization holographic gratings with high diffraction efficiency recorded in azopolymer PAZO

L. Nedelchev^{1,2}, D. Ivanov², N. Berberova¹ and D. Nazarova¹

¹*Institute of Optical Materials and Technology, Sofia, Bulgaria*

²*University of Telecommunications and Post, Sofia, Bulgaria*

e-mail:lian@iomt.bas.bg

Azopolymers are one of the most efficient materials able to record the polarization state of light. As a result, they have numerous applications in the field of polarization holography, such as data storage and diffractive optical elements with unique properties [1-3]. An essential parameter for each diffractive element, in particular a diffraction grating, is its diffraction efficiency η i.e. the ratio between the intensity of the diffracted light and the intensity of light incident to the grating.

In order to optimize the recording conditions and obtain high-efficient polarization holographic gratings, in the present work we study the dependence of the diffraction efficiency on the recording angle and thickness of a series of azopolymer layers.

Thin film samples with thicknesses 470, 850 and 2400 nm are prepared by spin-coating of a water soluble azopolymer PAZO (poly[1-[4-(3-carboxy-4-hydroxyphenylazo)benzenesulfonamido]-1,2-ethanediyl, sodium salt] [4]. An interference pattern is recorded in these samples, formed by two plain waves with left and right circular polarization (LCP and RCP) from a He-Cd gas laser ($\lambda_{\text{rec}} = 442$ nm). The diffraction efficiency of the gratings is probed in real time during the recording with a right hand circularly polarized (RCP) probe laser with wavelength $\lambda_{\text{probe}} = 635$ nm. Three recording angles are used – $2\theta = 10^\circ$, 20° and 30° , where 2θ is the angle between the two recording beams.

The kinetics of diffraction efficiency $\eta(t)$ in the +1 diffraction order are presented and compared, depending on the film thickness and recording angle. Our experimental results indicate that highest diffraction efficiency (more than 40%) is obtained for the sample with thickness 2400 nm and for recording angle $2\theta = 10^\circ$. As the holographic recording in azopolymers is usually accompanied by formation of surface relief gratings [5,6], the surface topography of the recorded samples is also investigated by atomic force microscopy and the AFM scans are presented.

Acknowledgements: Lian Nedelchev and Dimana Nazarova are grateful for the financial support provided by Bulgarian Science Fund under the project ДН 08/10. Deyan Ivanov and Nataliya Berberova acknowledge the financial support of the Bulgarian Science Fund under the project ДМ 08/1.

REFERENCES

- [1] L. Nikolova, P. S. Ramanujam, *Polarization Holography*, Cambridge University Press (2009).
- [2] L. Nedelchev, T. Todorov, L. Nikolova, Tz. Petrova, N. Tomova, V. Dragostinova, Proc. SPIE 4397, 338 (2001).
- [3] G. Martinez-Ponce, T. Petrova, N. Tomova, V. Dragostinova, T. Todorov, L. Nikolova, Opt. Lett. 29, 1001 (2004).
- [4] L. Nedelchev, D. Nazarova, G. Mateev, N. Berberova, Proc. of SPIE 9447, 94471I-1 (2015).
- [5] P. Rochon, E. Batalla, A. Natansohn, Appl. Phys. Lett. 66, 136 (1995).
- [6] D. Kim, S. Tripathy, L. Li, J. Kumar, Appl. Phys. Lett. 66, 1166 (1995).

Optical and microstructural characterization of NiO:K

P. Petkova¹, A. Boukhachem², P. Vasilev¹ and V. Altonyan¹

¹*Shumen University "Konstantin Preslavsky",
Shumen, Bulgaria*

²*Unité de physique des dispositifs à semi-conducteurs,
Faculté des sciences de Tunis,
Université de Tunis
e-mail:Petya232@abv.bg*

In this work, we have investigated the Faraday rotation and Verdet constant of potassium doped nickel oxide thin films [1]. The effective mass of nickel electrons presented as a function of frequency for all investigated thin films. The frequencies of longitudinal and transverse phonons are also determined. The damping ratio is calculated in the spectral region 330 – 610 nm. The concentration and the drift velocity of free charge carriers are presented as a function of wave length. The effective mass of NiO:K (1%) has the largest values in the spectral region between 320 nm and 460 nm. This conclusion can be useful when these thin films are applied as light-emitting diodes.

For all potassium doped thin films the damping ratio has large values. This result is very important for their application as solar cells.

REFERENCES

[1] A. Loukil, A. Boukhachem, M. Ben Amor, M. Ghamnia, K. Raouadi, *Ceramics International* 42, 8274 (2016).

Luminescence thermometry using $\text{Gd}_2\text{Zr}_2\text{O}_7:\text{Eu}^{3+}$

M.G. Nikolic¹, M.S. Rabasovic¹, J. Krizan², S. Savic-Sevic¹, M.D. Rabasovic¹, B.P. Marinkovic¹, A. Vlastic¹
and D. Sevic¹

¹ *Institute of Physics, Belgrade, Serbia*

² *AMI d.o.o., Ptuj, Slovenia*

e-mail: sevic@ipb.ac.rs

Thermographic phosphors are materials that are synthesized in such a way that their structural stability regarding various parameters including the temperature, pressure, magnetic field, electromagnetic radiation could be obtained. They typically consist of a ceramic host and rare-earth dopant. These materials are widely used in many applications [1-9]. The temperature dependency of their luminescence is used for temperature sensing.

In this study we investigate temperature dependence of luminescence spectra of nanopowder samples of $\text{Gd}_2\text{Zr}_2\text{O}_7:\text{Eu}^{3+}$. Europium doped $\text{Gd}_2\text{Zr}_2\text{O}_7$ nanopowders were prepared by Solution Combustion Synthesis (SCS) method [10]. The structural characteristics of obtained material were confirmed by SEM images and XRD analysis [10]. The identification and time resolved analysis of fast decayed (from $^3\text{D}_1$ state) and slow decayed (from $^5\text{D}_0$ state) europium lines in this host were performed using TR-LIF (Time resolved Laser induced Fluorescence) spectroscopy experimental setup. The setup consist of tunable OPO (Optical Parametric Oscillator) laser and streak camera, explained in more detail in [11].

The photoluminescence spectra used for analysis of $\text{Gd}_2\text{Zr}_2\text{O}_7:\text{Eu}^{3+}$ nano phosphor optical emission temperature dependence were acquired using continuous laser diode excitation at 405 nm and Ocean Optics spectrometer USB2000. We plotted the temperature sensing calibration curves based on various combinations of ratio of intensities of two europium optical emission lines. It seems that any combination of one slow decayed and one fast decayed line could be an optimal choice for temperature measurements. Finally, we concluded that the intensity ratio of spectral lines at 613 nm and 539 nm seems to be a good choice for temperature measurements. Our results show that the synthesized material can be efficiently used as thermographic phosphor up to 700 K.

REFERENCES

- [1] M. Aldén, A. Omrane, M. Richter, G. Särner, 37, 422 (2011).
- [2] S. W. Allison., G. T. Gillies, Rev. Sci. Instrum, 68, 2615 (1997).
- [3] L.P. Goss, A.A. Smith, M.E. Post, Rev Sci. Instrum, 60, 370 (1989).
- [4] J.P. Feist, A.L. Heyes, K.L. Choy, B. Su, Proceedings of IEEE; 6.1 (1999).
- [5] A.L. Heyes, Journal of Luminescence, 129, 2004 (2009).
- [6] M.M. Gentleman, D.R. Clarke, Surface & Coatings Technology, 93, 188 (2004).
- [7] A. H. Khalid, K. Kontis, Sensors, 8, 5673 (2008).
- [8] M R. Cates, S. W. Allison, S. L. Jaiswal, D. L. Beshears, Oak Ridge National Laboratory, Report ORNL/TM-2002/71
- [9] J.I. Eldridge, T.P. Jenkins, S.W. Allison, D. E. Wolfe, E. H. Jordan, Development of YAG:Dy Thermographic Phosphor Coatings for Turbine Engine Applications, 58h International Instrumentation Symposium San Diego, CA, June 5-8, (2012).
- [10] M.S. Rabasovic, D. Sevic, J. Krizan, M. Terzic, J. Mozina, B.P. Marinkovic, S. Savic-Sevic, M. Mitric, M.D. Rabasovic, N. Romcevic, Journal of Alloys and Compounds, 622, 292 (2015).
- [11] M.S. Rabasovic, D. Sevic, M. Terzic, and B.P. Marinkovic, Nucl. Inst. Meth. B.279, 16(2012).

Using infrared radiation for the measurement of arterial blood flow waveform

B. Stojadinović¹, Z. Nestorović¹, D. Žikić¹

¹*Institute of Biophysics, Faculty of Medicine,
University of Belgrade, Serbia
stojadinovic.bojana@gmail.com*

Analyzing the blood flow waveform can be obtained very useful information for medical diagnostics. The blood flow waveform can be measured using the optical properties of blood. Red blood cells contain hemoglobin which transports the oxygen to the cells. Absorption spectra for oxyhemoglobin and deoxyhemoglobin are differ. The oxyhemoglobin has significantly lower absorption of the 660 nm wavelength than deoxyhemoglobin, while at 940 nm its absorption is slightly higher.

Using absorption spectra of oxyhemoglobin we development of optical sensor for non-invasive measurements of arterial blood flow waveform. The sensor is based on a physical principle of reflective photoplethysmography (PPG) [1,2]. As the light source we used serially connected infrared diodes (wavelength 890 nm) whereas NPN silicon phototransistors were used as light detectors. The electronic components were molded into square package and poured with silicone. Such preparation produced an elastic superficies that allowed excellent attachment of the sensor on the skin's surface. Moreover, a serial connection of infrared diodes and phototransistors completely eliminated signal artifacts caused by minor muscle contractions. The sensor can be used to measure the blood flow waveform for the arteries that are located close to the skin surface, such as the carotid, radial and femoral artery.

The presented sensor design is suitable for clinical measurement of arterial blood flow where further analysis of the waveform is required. This is especially important for the blood flow analysis in patients with different forms of arrhythmia, in patients with epilepsy, in patients suffering from different forms of a sleep disorder where severe disorders in the arterial blood flow could be present causing consequentially thrombosis. Our new sensor design may also find application in analysis of heart rate adaptation during and after physical activity and for different medical treatment monitoring.

REFERENCES

- [1] D. Žikić, *Journal of Medical Engineering & Technology* 32, 23-29 (2008).
- [2] D. Zikich & D. Zikic, *Arterial Blood Flow Sensor. IFMBE Proceedings* 22, 1158–1162 (2008).

Study on relationship between amyloid- β peptides and metal ions *via* two-photon excitation fluorescence microscopy

S. Jovanic¹, N. Loncarevic², M. Rabasovic¹, A. Krmpot¹, M. Jovic², S. Kanazir², and B. Jelenkovic¹

¹*Photonic centre, Institute of Physics,
Belgrade, Serbia*

²*Institute for Biological Research "SinišaStanković",
University of Belgrade, Serbia
e-mail:sjovanic@ipb.ac.rs*

We developed home-built nonlinear laser scanning microscopy [1] which was used for the investigation of amyloid β (A β) peptide aggregation process in the presence of metal ions. A β cascade aggregation process is one of the most studied hypothesis about causes of Alzheimer's disease (AD). AD is a progressive brain disorder that is the most prevalent cause of dementia in the elderly population and the third leading cause of death in developed countries. Factors that are believed to affect A β fibrillization *in vivo* include metal ions such as Cu(II) and Zn(II)[2].

Main technique in this research is most well known variation of nonlinear microscopy, two-photon excitation fluorescence microscopy (TPEF). Samples are originated from blood serums 4th to 12th months old AD mouse model system. Autofluorescence signal was obtained for the determination of A β level by TPEF microscopy. Absolute concentration of Cu(II) and Zn(II) ions was measured by mass spectrometry. From this data we will be able to determine correlation level between A β level and metal ions concentration. Another approach to study relationship between A β development into mature fibrils and metal ions concentration was on *ex vivo* AD mouse brain slices. During defined time stages of A β development each brain slice was treated with Cu(II) and Zn(II) ions and imaged *via* TPEF microscopy.

Accurate results on blood serums have potential to include this AD biomarker in standard diagnostic procedures. In general, our findings can be of the importance for novel treatments with metal ions in AD.

Acknowledgments: This work is supported by bilateral project 451-03-01038/2015-09/1 between Ministry of Education, Science and Technological Development -MESTD of Republic of Serbia and German Academic Exchange Service-DAAD, MESTD of Republic of Serbia projects OI 173056, OI 171038 and III45016 and the Fogarty International Research Award, NIH (R03AG046216).

REFERENCE

- [1] M. D. Rabasovic' et al., J. Biomed. Opt. 20(1), 016010 (2015).
[2] D. J Selkoe and J. Hardy, EMBO Mol. Med. 8(6), 595-608 (2016).

Two-photon excited hemoglobin fluorescence for *ex vivo* microscopy analysis of erythrocytes at single cell level

I. T. Drvenica¹, A. Stančić¹, S. Jovanić², V. Lj. Ilić¹, M. D. Rabasović², D. V. Pantelić², B. M. Jelenković², B.M. Bugarski³, A. J. Krmpot²

¹*Institute for Medical Research, University of Belgrade, Dr Subotića 4, 11 129 Belgrade, Serbia*

²*Institute of Physics Belgrade, University of Belgrade, Pregrevica 118, 11 080 Belgrade, Serbia*

³*Department of Chemical Engineering, Faculty of Technology and Metallurgy, University of Belgrade, Karnegijeva 4, 11 000 Belgrade, Serbia*

e-mail:ivana.drvenica@imi.bg.ac.rs

Fluorescence of hemoglobin, the main intracellular component of erythrocytes, upon excitation by ultra-short pulses in red and near infrared region [1-3], allows two-photon excited fluorescence (TPEF) microscopy to be used as a tool for label-free imaging of these cells, even *in vivo* [4]. Despite wide applicability of erythrocytes in diagnostic tests, and distribution of hemoglobin as a marker of their functional status under physiological or pathological conditions [5], data on spatial distribution of hemoglobin at the single cell level are scarce.

Based on findings reported by Zheng and co-workers [1], we have utilized TPEF microscopy to map the spatial distribution of hemoglobin in porcine erythrocytes *ex vivo*. Porcine erythrocytes were used as extremely susceptible cells to stress and thus represent a good model system to study influence of different factors (heat, humidity, malnutrition, infections...) on erythrocyte morphology and hemoglobin distribution. The custom made experimental set up for NLSM utilized the train of the femtosecond pulses from Ti:Sapphire laser (Coherent, Mira 900-F) at 730 nm. The repetition rate was 76MHz, and pulse duration was 160fs.

The results demonstrate that the resolution of the TPEF microscopy is good enough for the analysis of erythrocytes at single cell level. Two different morphological types of porcine erythrocytes, normocytes and echinocytes, collected during mild autumn and extremely hot summer, respectively, were clearly differed by TPEF microscopy. Besides, erythrocytes having intermediate morphology i.e. having some characteristics of both abovementioned morphological extremes were also found. The distribution of hemoglobin in erythrocytes noticeably followed the cells' shape, where erythrocytes with altered morphology demonstrated significant accumulation of hemoglobin in cells' protrusions. During TPEF microscopy experiments fluorescence emission from the exposed cells increased, but longer exposure led to irreversible change of erythrocytes, as already shown in literature [3]. Since functional status of erythrocytes *in vivo* (both in physiological or pathological states) and *ex vivo* (e.g. transfusion bag) [3] is accompanied with change of morphology and consequently altered distribution and functionality of hemoglobin, result of this study even though obtained on animal cell model, confirmed strong potential of TPEF microscopy for such application in biomedical research. However, *in vivo* tests by TPEF microscopy merit further experimental optimization.

This work is supported by bilateral project 451-03-01038/2015-09/1 between Ministry of Education, Science and Technological Development -MESTD of Republic of Serbia and German Academic Exchange Service-DAAD and by projects III45016, III 46010 and OI 171038 of MESTD of Republic of Serbia.

REFERENCES

- [1] W. Zheng, D. Li, Y. Zeng, Y. Luo, J. Y. Qu, Biomed. Opt. Express. 2, 71 (2010).
- [2] G. O. Clay, C. B. Chaffer, D. Kleinfeld, J. ChemPhys. 126, 025102 (2007).
- [3] I. Saytashev, R. Glenn, G.M. Murashova, S.Osseiran, D. Spence, C. L. Evans, M. Dantus, Biomed. Opt. Express. 7, 3449 (2016).
- [4] D. Li, W. Zheng, W. Zhang, S. K. Teh, Y. Zeng, Y. Luo, J. Y. Qu, Opt. Lett. 36, 2638 (2011).
- [5] V. V. Revin, et al. BioMed. Res. Int. 973973 (2015).

Feasibility study of TPEF, SHG & CFM for soft tissue neoplasia analysis

Ts. Genova¹, E. Borisova¹, G. Stanciu², D. Tranca², O. Semyachkina-Glushkovskaya³, D. Gorin³, I. Terziev⁴

¹*Institute of Electronics, Bulgarian Academy of Sciences, 72, Tsarigradsko Chaussee Blvd., 1784 Sofia, Bulgaria*

²*Center for Microscopy – Microanalysis and Information Processing, University “Politehnica” Bucharest, Bucharest, Romania*

³*Saratov State University, 83, Astrahanskaya str., 410012, Saratov, Russian Federation*

⁴*Queen Jovanna-ISUL University Hospital, 8, Bialo More str., 1527 Sofia, Bulgaria*

e-mail:ts.genova@gmail.com

Standard cancer diagnostics, based on examination of tissue biopsy samples, include multiple steps of time consuming preparation of tissue slides that includes formalin fixation, paraffin embedding, sectioning and staining (most frequently with hematoxylin and eosin (H&E)). Every step of this procedure alters the natural characteristics of the tissue that could be diagnostically valuable and multiplies the risk of formation of artifacts in the samples, which could lead to mistakes in the diagnosis. [1]

The application of nonlinear microscopy techniques, such as two-photon excitation fluorescence (TPEF) and second harmonic generation microscopy (SHG) and confocal fluorescence microscopy (CFM), has proven to be useful for observation of peculiarities and patterns in ex vivo tissue samples for differentiation between neoplasia and healthy tissue.[2,3] Implementation of these microscopy techniques in cancer research and pathology would benefit from investigation of different protocols for processing of the samples and how they affect the quality of the images and their diagnostic value.

This study is dedicated to the comparison of images from hematoxylin and eosin (H&E) stained, unstained paraffin embedded, as well deparaffinized and rehydrated biopsy tissue sections with two-photon excitation fluorescence, second harmonic generation and confocal fluorescence microscopy.

Routinely processed and stained with H&E samples are characterized mainly by the fluorescence of the eosin itself that deposits in structural proteins. The images obtained from unstained paraffin embedded sections are diagnostically unusable to the paraffin interfering with the signal from the tissue samples. Hence deparaffinization of the samples was carried on, also rehydration was performed for further restoration of the tissue sections to a physiological state [4]. For mounting of the rehydrated tissue samples Apathy's mounting media was used, since it is aqueous based, suitable for longer storage, has a refractive index close to the one of the used coverslips, but most importantly was deemed non fluorescent and applicable for fluorescent microscopy. However, high level of the noise in the acquired images was observed that we considered to arise exactly from the mounting media. The images obtained by unstained samples, where the signal originates solely from endogenous sources, were comparable with the ones obtained by H&E stained sections.

The results could be beneficial for translational cancer studies, obtaining additional information from paraffin-embedded archived samples for retrospective studies or to gain more knowledge from and for rare samples.

REFERENCES

- [1] P. Bindhu, R. Krishnapillai, P. Thomas, and P. Jayanthi, *J Oral Maxillofac Pathol* 17(3), (2013).
- [2] G. Thomas, J. van Voskuilen, H. Gerritsen, H. Sterenborg, J. Photochem. Photobiol. B: Biology (141),(2014).
- [3] P. Thong, M. Olivo, S. Tandjung, M. Movania, *IEEE J. Quantum Electron* 18, (2012).
- [4] M. Monaghan, S. Kroll, S. Brucker. *Tissue Engineering: Part C* 22(6), pp. 517-523(2016).
- [5] S. Ravikumar, R. Surekha, R. Thavarajah, *Journal of Dr. NTR University of Health Sciences* 3, (2014).

***Phycomyces blakesleeanus* hypha cell wall surgery by Ti:Sapphire laser**

T.Pajic¹, K.Stevanovic², N. Todorovic³, A. Krmpot⁴, M. Rabasovic⁴, V. Lazovic⁴, D. Pantelic⁴, B. Jelenkovic⁴
and M. Zivic²

¹University of Belgrade, Serbia

²University of Belgrade - Faculty of Biology, Serbia

³Institute for Biological Research, University of Belgrade, Serbia

⁴Institute of Physics, University of Belgrade, Serbia

e-mail: tanjapajic4@gmail.com

The ion channels on the membrane of filamentous fungi remain uninvestigated to this day due to their inaccessibility to patch-clamp pipette, brought about by sturdy cell wall. Small number of described channels is from very specific types of cells (wall less mutants or sporangiophore aerial cell membrane). The enzymatic approaches of cell wall removal, albeit successful on plant cells, failed when applied to fungi. In order to obtain clean “patchable” membrane from any type of filamentous fungal cell we undertook a task of finding the conditions for cut of the small part of the hyphal wall by laser surgery on the model filamentous fungus organism, *Phycomyces blakesleeanus*. The successful wall surgery should result in exposure of large enough portion of cell membrane with a minimal damage to the protoplast. Therefore, we performed series of experiments with cell plasmolysis in hypoosmotic media and subsequent deplasmolysis, to determine the conditions for reliable retraction of cytoplasm that could be reversed. Next, hyphae, grown on glass coverslips coated with collagen, were plasmolysed and mounted on the stage of the homemade nonlinear laser scanning microscope for imaging and cell surgery [1]. The Ti:Sapphire laser (Coherent, Mira 900-F) has been used as a light source in the microscope. It has operated at 730nm. This wavelength enables two photon excitation of auto-fluorescence in cytoplasm, as well as dye (Calcofluor white), visualizing fungi wall. We have used Carl Zeiss, EC Plan-NEOFLUAR, 40×1.3 oil immersion objective for focusing of the laser beam and collection of fluorescence. A visible interference filter (415nm - 685 nm) in front of detector has been used to remove scattered laser light. The successful cutting of cell wall could be achieved within the range of laser intensities and cutting speeds (dwell times). Throughout the experiment, fungi were kept in azide or Brefeldin A in order to block the process of depositing the new wall material. Afterwards, hyphae were slowly deplasmolysed to induce exit of a portion of the protoplast through the laser-cut hole in the cell wall. However, in some instances, the part of the protoplast bulged through the hole immediately after cell surgery, while the cell was still in hypertonic solution. In other instances, the cytoplasm remained away from the cut hyphal apex even through series of slow incrementing hypotonic solutions. Finally, when laser cutting was applied on the side of the cell only, as to cut a small hole, the successful exit of a portion of protoplast through the hole during deplasmolysis could be reliably achieved.

REFERENCES

[1] Mihailo D. Rabasović, et al, *J Biomed Opt* 20 016010 (2015).

Peculiarities of cw laser beam imaging of contrasting small-depth inclusions in highly-scattering media

T. Dreischuh, L. Gurdev, O. Vankov, E. Toncheva, L. Avramov, D. Stoyanov
Institute of Electronics, Bulgarian Academy of Sciences
72 Tsarigradsko Chaussee, Sofia 1784, Bulgaria
e-mail: tanjad@ie.bas.bg

A single-sided optical (cw-laser irradiation-based) detection of characteristic inhomogeneities (inclusions, e.g., ill places in tissues) in highly-scattering homogeneous host media (e.g. healthy tissues) is performed by evaluating the difference between the backscattered-light intensity distributions over the entrance/exit plane of the medium in the presence and absence of inclusions. According to the conventional wisdom, the information-carrying signal obtained in such a way should be positive and stronger at a higher turbidity of the inclusion compared to the host medium; and vice versa, in the opposite case. This is so indeed when the inhomogeneity of interest is located at a relatively large depth (e.g., over 1 cm in front of the sensing laser beam) in the host medium. An inverse effect is observable, however, at smaller depths of the inclusions. Then, the “positive inclusions” may produce “negative signals”, and vice versa. Thus, the main purpose of the present work is to clarify, explain and illustrate theoretically and experimentally this inverse effect and estimate its potential for applications.

The analysis of the effect is based on results obtained by us theoretically and proved experimentally concerning the features of the intensity distribution of laser light backscattered from liquid tissue-like phantoms of different turbidity. The tissue-mimicking phantoms employed in the experiments were Intralipid (IL)–20% dilutions of different concentrations in distilled water. The inhomogeneities, infused into test tubes perpendicular to the laser beam, were made of the same material as the host medium, but having different IL concentration. The optical receivers, whose aperture size is considerably smaller than the test tube diameter and the width of the intensity distribution measured, were scanned normally to the laser beam and at some distance (~ several millimeters) away from its axis.

According to the theoretical expectations, the experimental results show that the inverse effect is present at small depths of the inhomogeneities when they are not entirely enveloped by the scattering-widened laser beam. In addition, the IL concentration in both the host medium and the ingredient should exceed 0.7%. In the opposite case, or when one of the concentrations is below 0.7% and the other one is over this value, the inverse effects arisen have more complicated appearance. At larger depths, where the inclusion is entirely enveloped by the laser light beam, the inverse effect does not appear.

The results obtained in the work would allow one to develop approaches for determining the depth, size and contrast of characteristic inhomogeneities in turbid media. This, in turn, would help solving the so-called (lesion) specificity problem in the optical diagnostics and tomography. The knowledge acquired would also assist in achieving a more profound understanding of the process of formation of the backward light fluxes in laser sensing of vast-scale highly scattering objects in the atmosphere and space.

Acknowledgements: This work has been supported by the Bulgarian National Science Fund under the project DFNI-B02/9/2014 “Development of biophotonics methods as a basis of oncology theranostics”.

Compact lasers for innovative non-invasive biomedical research and diagnostics

Karina S. Litvinova¹, Sergei G. Sokolovski², Edik U. Rafailov²

¹*Aston Medical Research Institute, Aston Medical School, Birmingham, UK,*

²*Optoelectronics and Biomedical Photonics Group, Aston Institute of Photonic Technologies, Aston University, Birmingham, UK*

e-mail:k.litvinova@aston.ac.uk

For over half a century, laser technology has undergone a technological revolution. These technologies, particularly semiconductor lasers, are employed in a myriad of fields. Optical medical diagnostics, one of the emerging areas of laser application, are on the forefront of application around the world. Optical methods of non- or minimally invasive bio-tissue investigation offer significant advantages over alternative methods, including rapid real-time measurement, non-invasiveness and high resolution (guaranteeing the safety of a patient) [1,2]. These advantages demonstrate the growing success of such techniques.

We will outline the recent status of laser technology applied in the biomedical field, focusing on the various available approaches. We will further consider the advancement and integration of several complimentary biophotonic techniques into single multimodal devices, the potential impact of such devices and their future applications [3]. Based on our own studies, we will also cover the simultaneous collection of physiological data with the aid a multifunctional diagnostics system, concentrating on the optimisation of the new technology towards a clinical application [4-11]. Such data is invaluable for developing algorithms capable of delivering consistent, reliable and meaningful diagnostic information, which can ultimately be employed for the early diagnosis of disease conditions in individuals from around the world.

REFERENCES

- [1] Tuan Vo-Dinh. Biomedical Photonics Handbook, Second Edition: Biomedical Diagnostics. 889 Pages (2014).
- [2] Boas D, Pitris C, Ramanujam N, editors. Handbook of Biomedical Optics. Boca Raton: CRC Press (2011).
- [3] Rogatkin D a., Sokolovski SG, Fedorova K a., Stewart N a., Sidorov V V., Rafailov EU. Proc. SPIE. 7890:78901H (2011).
- [4] Dunaev A V, Sidorov V V, Stewart NA, Sokolovski SG, Rafailov EU. Proc. SPIE. 857205 (2013).
- [5] Makovik I.N., Andrey V. Dunaev A.V., Victor V. Dremin V.V., Krupatkin A.I., Sidorov V.V., Khakhicheva L.S., Muradyan V.F., Pilipenko O.V., Rafailov I.E. and Litvinova K.S. JIOHS. 11(1) (2017).
- [6] Dremin V.V., Sidorov V.V., Krupatkin A.I., Galstyan G.R., Novikova I.N., Zherebtsova A.I., Zherebtsov E.A., Dunaev A.V., Abdulvapova Z.N., Litvinova K.S., Rafailov I.E., Sokolovski S.G., Rafailov E.U. Proc. SPIE. 9698, 969810 (2017).
- [7] Litvinova K.S., Ahmad S., Wang K., Rafailov I.E., Sokolovski S.G., Rafailov E.U., Ahmed A. Proc. SPIE. 9689, 96893H (2016).
- [8] Rafailov E.U., Litvinova K.S., Sokolovski S.G. Proc. SPIE 9550, 95500G (2015).
- [9] Litvinova KS, Ahmad S, Wang K, Rafailov IE, Sokolovski SG, Zhang L et al. Proc. SPIE. 96893H–8 (2016).
- [10] Rafailov IE, Dremin VV., Litvinova KS, Dunaev AV., Sokolovski SG, Rafailov EU. J Biomed Opt. 21: 025006 (2016).

Study of acute complications of diabetes mellitus type II by Raman spectroscopy

M.Miletic^{1,2}, S.Askrabic¹, D. Popovic³, M.Djordjevic³, I. Mrdovic³ and Z. Dohcevic-Mitrovic¹

¹*Institute of Physics, University of Belgrade
Belgrade, Serbia*

²*Faculty of Biology, University of Belgrade
Belgrade, Serbia*

³*Emergency Centre, Clinical Centre of Serbia,
Belgrade, Serbia*

e-mail:sonask@ipb.ac.rs

Among major acute complications of diabetes are ketoacidosis and hyperglycemic hyperosmolar state. Diabetic ketoacidosis (DKA) appears due to the insulin deficiency, which causes hyperglycemia and increased lipolysis, and, as a result, increased level of ketone bodies in blood and urine. This reduces pH value of blood, leading to metabolic acidosis. Hyperglycemic hyperosmolar state (HHS) is characterized by extremely high serum glucose level and hyperosmolality without significant ketone bodies production. However, some overlapping between the characteristics of DKA and HHS may exist. Precise diagnosis, as well as clinical and biochemical hour-by-hour monitoring, is crucial for the adequate treatment of these severe and life-threatening conditions.

Raman spectroscopy, a non-invasive method which is based on the effect of inelastic light scattering and can be used for molecular fingerprinting of various biomaterials [1], was applied in order to try to discern between DKA and HHS conditions in a label-free and time efficient manner. Raman spectra of blood serum and plasma of patients diagnosed with diabetes type 2 with/without acute complications of ketoacidosis and HHS were obtained. Spectra were acquired in the range 350-3700 cm^{-1} using excitation line of 532 nm and afterwards background corrected with polynomial function of 5th order. Dominant features of the majority of spectra are positioned at 1003 cm^{-1} , 1155 cm^{-1} , 1515 cm^{-1} and belong to phenylalanine and beta carotene (resonantly enhanced) vibrations. Amide (protein) and lipid related bands were registered in the intervals (1200 -1380) cm^{-1} and (1450-1700) cm^{-1} .

Potential of Raman spectroscopy for differentiation between the two acute complications of diabetes is analyzed by use of principal component analysis (PCA). PCA was performed using different spectral intervals in order to classify spectra of serum and plasma from different patients according to the inter-spectra variations in these intervals. Most pronounced differences between the spectra of serum of patients with ketoacidosis compared to the spectra of serum of HHS patients were expressed in the high-wavenumber region containing C-H and O-H vibrations.

REFERENCES

[1] C. G. Atkins, K. Buckley, M. W. Blades and R.F.B. Turner, *Applied Spectroscopy* 71, 767 (2017).

Synchrotron based X-ray microscopy for the verification of trace metals and SOD1 protein aggregates in intact astrocytes from arat model of amyotrophic lateral sclerosis

S. Stamenković¹, B. Lai², P. Andjus¹ and T. Dučić³

¹Center for laser microscopy, Faculty of Biology,
University of Belgrade, Serbia

²Advanced Photon Source, Argonne National Laboratory, Argonne, USA

³CELLS – ALBA, Carrer de la Llum 2-26, 08290 Cerdanyola del Vallès, Barcelona, Spain
e-mail:stefan.stamenkovic@bio.bg.ac.rs

Amyotrophic lateral sclerosis (ALS) is a fatal neurodegenerative disorder targeting lower and upper motor neurons of the central nervous system. Although a number of pathological processes have been described in ALS, the exact mechanisms leading to the selective motor neuron vulnerability are still not known. However, the interplay between motor neurons and astrocytes is considered crucial in the outcome of the disease. Mutations causing a toxic gain of function in the Cu,Zn superoxide dismutase (SOD1) are abundant in familial cases of ALS. The expression of mutant SOD1 has also a substantial impact on astrocytes, contributing through non-cell autonomous mechanisms to motor neuron pathology and disease spread.

Our study was set to answer the following questions in the pathophysiology of ALS by working with the hSOD1 G93A rat model and by using the hard X-ray fluorescence microscopy as well as the soft X-ray tomography:

- i) In which stage could we identify “hotspots” of trace metals and protein aggregates accumulated at the subcellular level by using cryo-preserved cell cultures of astrocytes?
- ii) Which is the structural organization and cellular localization of SOD1 protein aggregates in the ALS model astrocytes?
- iii) What is the ultra-structural organization of mitochondria in the ALS model in comparison to non-transgenic astrocytes?

Here we combined two different synchrotron light based microcopies: the soft X-ray microscopy and tomography in carbon absorption contrast in the so-called “water window” energy range in order to examine structural changes in astrocytes, to investigate intracellular protein aggregates and their relations with changes in mitochondrial ultra-structure, and hard X-ray fluorescence at 10keV in order to study the cellular distribution of trace metals, which play a pivotal role in ALS as well as in other neurodegenerative proteinopathies [1].

For the X-ray microcopies we used the whole intact astrocytes, close to their natural state, without any staining or chemical embedding or mechanical (cutting) change, *i.e.* cryo-preserved cells by vitrification [2]. The soft X-ray microscope helped to elucidate protein aggregates *in situ*, as well as the mitochondrial ultra-structural changes. We present here the data on structural changes at the sub-cellular level, where we localized the centres of intracellular protein aggregation in astrocytes, combined with detailed trace metals maps in intact astrocytes.

It is very important to understand the initial process of the formation of these biomolecular disease markers and the development of their structure-function relationship. This may finally offer therapeutic time windows and solutions for overcoming mutant SOD1 cytotoxicity as well as proteinopathies with aggregations in general.

REFERENCES

- [1] T. Dučić, S. Stamenković, B. Lai, P. Andjus. Multimodal synchrotron radiation microscopy of intact astrocytes from the G93A rat model of amyotrophic lateral sclerosis. *Manuscript* (2017).
- [2] T. Salditt and T. Dučić, book chapter in *Super-Resolution Microscopy Techniques in the Neurosciences* Springer, 257–290 (2014).

Light controllable TiO₂-Ru nanocomposite system encapsulated in small unilamellar vesicles for anti-cancer photodynamic therapy

M. Matijević¹, M. Nešić¹, I. Popović¹, M. Stepić¹, M. Radoičić¹, Z. Šaponjić¹ and M. Petković¹

¹*Vinča Institute of Nuclear Sciences, Belgrade, Serbia*

e-mail: milica.m@vin.bg.ac.rs

Approximately 13 million of new cancer cases are diagnosed every year, and the mortality rate is projected to rise, with an estimation of 13.1 million deaths in 2030 [1]. The conventional cancer treatments such as chemotherapy, radiotherapy and surgery suffer from serious drawbacks that hamper patients' healing and recovery: radiation therapy is limited by the cumulative radiation dose, chemotherapy is frequently associated with systemic side-effects, while rather high recurrence rate is associated with surgical resection of tumors.

Photodynamic therapy, which implies combined use of a photosensitising medicament and low-intensity light to cause selective damage to the target tissue, is an alternative tumor-ablative, function-sparing and cost-effective oncologic approach [2]. Usually, medicaments are delivered to diseased tissues by different types of nanoparticle (NP) carriers. The light-induced medicament activation is based on the intrinsic optical properties of a medicament carrier and a medicament itself. In most cases, a NP-based medicament carrier or a medicament itself acts as photosensitizers [PSs], by triggering the free radical reactions in cells leading eventually to the cell death. The most PSs are characterized by high lipophilicity, and due to that, different encapsulation strategies have been explored to protect the hydrophobic PS from the aqueous environment.

We used TiO₂ NPs for medicament carriers because of their availability, non-toxicity, stability and possibility of surface modification. On the other hand, Ru(II)(dcbpy)₂Cl₂ complex, that belongs to the second generation of metallodrugs, can be easily attached to the TiO₂ surface via carboxyl groups [3], while central metal ion remains free for the interaction with biomolecules. Additionally, this system has genotoxic effect on melanoma cells [4].

The aim of the present study was to modify the nanocomposite system (NCS) based on the Ru complex and TiO₂ NPs in order to increase the cellular uptake and its efficiency against tumor cell lines. We have stabilized a colloidal dispersion of TiO₂ NPs on pH 7 by surface modification, whereas NCS was formed as described in our previous work [4]. NCS was encapsulated in the small unilamellar vesicles made mainly of phosphatidylcholine and phosphatidylethanol-amine [5]. Binding of Ru-complex to the surface of the TiO₂ NPs was confirmed by Fourier transform infrared spectroscopy. The influence of light of various wavelengths and intensity on the complex release kinetics from encapsulated and non-encapsulated NCS was investigated, and both these systems had shown exceptional light-controllable complex-release ability.

REFERENCES

- [1] J. Ferlay et al., International Agency for Research on Cancer 127, 2893 (2008).
- [2] T. J. Dougherty et al., J. Natl. Cancer Res. 90, 889 (1998).
- [3] T. Savić et al., Nanoscale 4, 1612 (2012).
- [4] M. Nešić et al., Opt. Quant. Electron. 48, 119 (2016).
- [5] M. Immordino, F. Dosio, L. Cattel, Int. J. of Nanomedicine 1, 297 (2006).

Application of multiparametric cardiac measurement system in ejection fraction calculation

Marjan Miletić¹, Marija D. Ivanović¹, Lana Popović Maneski², Boško Bojović¹

¹*Vinca Institute of Nuclear Sciences, Belgrade, Serbia*

²*Institute of Technical Sciences of the Serbian Academy of Sciences and Arts, Belgrade, Serbia*

e-mail:marjanmil@yahoo.com

Ejection fraction (EF) is the most used parameter for characterisation of Heart Failure (HF) condition. EF is commonly calculated using echocardiography, which is an expensive non-invasive method and not used in primary healthcare. Systolic time intervals (STI) represent a non-invasive and inexpensive method for determination of EF [1, 2].

Heart failure (HF) is the single most expensive diagnosis in medicine. 2–3% of adult population in developed countries have HF diagnosis. It is not detectable by ECG test and it is commonly detected in a late stage, when the process is irreversible [2-5].

In this paper, a multiparametric cardiac measurement system for determination of STI is presented. Measurement system consists of sensors for simultaneous acquisition of electrocardiographic (ECG), phonocardiographic (PCG), photoplethysmographic (PPG) and cardiovascular (CV) pulsation signals. CV pulsation signals are measured by long period grating (LPG) fiber-optic sensors [6].

Two non-invasive methods for measuring systolic time intervals (STI) were applied on a set of 6 healthy volunteers, based on ECG, PCG and CV pulsation signals. CV pulsation signals were measured on carotid artery with PPG and LPG sensors.

In the first method, EF was calculated from the obtained STI signals, using CV carotid pulsations measured with the PPG sensor, giving EF values in the range from 0.60 to 0.68, with maximal standard deviation of 0.05. In the second method, EF was obtained using CV carotid pulsations measured with LPG sensor, giving EF values in the range from 0.60 to 0.66, with maximal standard deviation 0.06. Calculated values of EF with both methods were in the 0.55 to 0.75 range which corresponds to normal EF range in healthy individuals.

REFERENCES

- [1] M. D. Ivanović, “An optical Fiber-Grating device for measuring cardiovascular and respiratory pulsations”, Ph.D. dissertation, University of Belgrade, Belgrade, Serbia, (2014).
- [2] L. N. Katz, H. S. Feil, I. Auricular fibrillation. *Arch Intern Med*, vol. 32, p. 672, (1923).
- Peacock WF et al. *Congest Heart Fail.* (2003).
- [3] Stewart S, et al. *Eur J Heart Fail.* (2001).
- [4] Lloyd-Jones D, et al. *Circulation.* (2010).
- [5] Mosterd A, et al. *Heart* (2007).
- [6] M. D. Petrović, A. Daničić, V. Atanasoski, S. Radosavljević, V. Prodanović, N. Miljković, J. Petrović, D. Petrović, B. Bojović, Lj. Hadžievski, T. Allsop, G. Lloyd and D. J. Webb, *Phys. Scr. T*, vol. T157, pp. 014022 (1-4) (2013).

Nonlinear microscopy as a novel method for studying insect morphology

D. Pavlović¹, D. Pantelić¹, A. Krmpot¹, M. Rabasović¹, V. Lazović¹, M. Vrbica², S. Ćurčić²

¹*Institute of Physics, University of Belgrade, Serbia*

²*Institute of Zoology, University of Belgrade – Faculty of Biology, Serbia*

e-mail: danica.pavlovic@ipb.ac.rs

Insects are the most numerous group of animals on the Earth, with more than a million described species and the total number of species estimated to be six to ten millions [1]. Insect taxonomists face difficult tasks of describing, classifying and identifying vast numbers of entirely new or little-known species. Most common classification of insects is based on morphological characteristics of adults. The mouthparts, wing venation, surface cuticular structure or even internal organs, such as different glands and reproductive organs could have each a high taxonomic value. These structures can be seen in most cases only under high-resolution microscope.

Fluorescence of chitin, as the most abundant component of insect integument, makes nonlinear microscopy (NLM) useful imaging technique in entomology. This is a novel technique [2, 3], with several advantages compared to classical or confocal microscopy. Namely, there is no need for staining or tissue clearing, penetration depth is large and photo-damage reduced [3]. Here we present a part of our morphological study of several insect species, inhabiting Serbia. Detailed images of the mouthparts, head, abdominal segments and genitalia were recorded by NLM using two-photon excited fluorescence (TPEF). All important taxonomic characters, such as number and position of certain setae, sub-micron structure of cuticle, shape of copulatory organs can be analyzed, performed measurements calculated quantitatively and further used in morphometrics, thus helping in taxa identification and taxonomy.

REFERENCES

- [1] P. W. Price et al., Cambridge University Press. (2011).
- [2] C. H. Chien et al., *Journal of Biomedical Optics*, 16(1), (2011).
- [3] M. Rabasović et al., *Journal of Biomedical Optics*, 20(1), (2015).

Confocal image analysis of immunohistochemistry of connexin isoforms during the second trimester of gestation of the human fetal brain development

Dušica Kočović¹, Mandakini B. Singh³, Jasmina Tadić², Svetlana Vrzić-Petronijević², Pavle R. Andjus¹ and Srdjan D. Antic³

¹*Faculty of Biology, University of Belgrade, Studentski Trg 3, Belgrade, Serbia*

²*Clinical Center of Serbia, Faculty of Medicine, University of Belgrade, Višegradska 26. 11 000 Belgrade, Serbia*

³*Department of Neuroscience, University of Connecticut Health Center, Farmington, CT 06030, USA
e-mail:dusica.kocovic@bio.bg.ac.rs*

Little is known about cellular, molecular and physiological properties which underlie early neural electrical activity in the human fetal brain during in utero development. It was suggested that connexins, a family of transmembrane proteins forming gap junctions (which allow exchange of molecules between two cells) or hemichannels (which allow passage of ionic currents and molecules between extracellular and intracellular space), play an important role in the generation of electrical activity in the developing human fetal cortex [1]. The main goals of our study was to determine, by means of immunofluorescence and confocal microscopy, the connexin isoforms that are present in the human fetal cortex during the second trimester of gestation and to develop the best method for quantitative analysis of their distribution in different human cell types. To detect connexin molecules, we performed immunohistochemistry on cryotome microsections harvested from postmortem human fetal brain tissue samples. We used polyclonal antibodies against: 1) neuronal marker NeuN; 2) connexin isoforms Cx26, Cx36, Cx45; and the cell nucleus marker ToPro. Image acquisition was obtained on a confocal laser scanning microscope LSM 510 in multitrack configuration, with two objective lenses Plan-Apochromat 63X oil and Plan-Neofluar 20X; An Argon laser (spectral lines 457 nm, 488 nm and 514 nm) was used with secondary antibody Alexa Fluor 488 with emission max at 617 nm and ToPro with emission max at 660 nm, in addition, a dichroic mirror 488/543/633, with band pass filter 505-530 and two long pass filters 585 and 650 nm were used. The analysis of obtained images was done using the ImageJ program [2]. Our approach consisted of detecting and counting neuronal and non-neuronal (putative neuron progenitors and glial) cells that express different connexin isoforms. The overall number of cells positive for the nuclear stain (ToPro), were tested for the expression of signal for NeuN and a graphic mask was created from cells that also show connexin stainings in their membranes. This mask, formed by ROI manager in ImageJ program, was used to characterize connexin-expressing neurons in different gestational weeks and different cortical zones (e.g. cortical plate, subplate and subventricular zone). Preliminary results showed that in the second trimester of gestation, neurons are the main cell population that contains connexins in their membrane. Thus, we concluded that connexin isoforms Cx26, Cx36 and Cx45 were significantly expressed during the second trimester of gestation in the postmitotic neurons of the human fetal cortex.

REFERENCES

- [1] A.R. Moore, W.L. Zhou, C.L. Sirois, G.S. Belinsky, N. Zecevic and S.D. Antic, PNAS 16;111(37): E3919 – E3928 (2014).
[2] E.C. Jensen, Anat rec: 296: 378-381 (2013).

Combined photoacoustic and optical microscopy for the detailed description of ciliary body anatomy

George J. Tserevelakis¹, Stella Avtzi¹, Miltiadis K. Tsilimbaris², and Giannis Zacharakis¹

¹*Foundation for Research and Technology Hellas, Institute of Electronic Structure and Laser, N. Plastira 100, Heraklion, Crete, Greece, GR-70013*

²*University of Crete, School of Medicine, Laboratory of Vision and Optics, Voutes Campus, Heraklion, Crete, Greece, GR-71003*

e-mail: tserevel@iesl.forth.gr

The ciliary body constitutes an ocular structure of high importance for both ophthalmologists and vision scientists due to its significant role in the secretion of aqueous humor in the anterior chamber by the epithelium cells, as well as, the accommodation of the eye through the dynamic change of the crystalline lens optical power [1]. During the previous decades, several studies have attempted to delineate the anatomy and the physiological function of the ciliary body using scanning electron microscopy (SEM) [2], to acquire high resolution superficial observations of *ex vivo* specimens. On the contrary, the application of optical based microscopy techniques for similar investigations has only been reported in a small number of cases, and with the presence of several limitations including the extremely small field of view and the lack of imaging contrast specificity. In this work, we present the application of a prototype hybrid microscope incorporating photoacoustic and optical imaging modalities [3], [4] for the detailed three-dimensional imaging of the whole ciliary body in rabbit eyes.

The system is developed around a modified inverted optical microscope serving as a platform for the hybrid imaging apparatus. For the photoacoustic signal excitation, the microscope employs a variable repetition rate diode pumped ns laser (energy per pulse: 29.4 μ J, pulse width: 10 ns, selected repetition rate: 6.8 kHz) emitting infrared radiation at 1064 nm and 532nm after frequency doubling. Regarding fluorescence excitation, a continuous wave (CW) diode laser (power: 4.5 mW) emitting at 450 nm is employed, whereas a flip mount mirror switches between the two modalities. The sample is sequentially raster scanned using a sub- μ m precision set of motorized stages and the generated photoacoustic and fluorescence signals are detected by employing a piezoelectric ultrasonic transducer (transmission mode) and a high sensitivity photomultiplier tube (reflection mode) respectively.

It was observed that the acquired photoacoustic and glutaraldehyde induced autofluorescence images were spatially complementary, each of them offering unique anatomical information regarding the examined specimens such as the pars plana and pars plicata ciliary body portions, the iris, as well as, the attached zonule fiber strands.

We anticipate that this novel and powerful diagnostic approach will have the potential to be used in biomedical research involving ocular accommodation, ageing effects (e.g. presbyopia), or several ciliary body abnormalities, shedding more light, in this manner, on the physiological function and pathology of the human eye.

REFERENCES

- [1] E.R. Tamm, E. Lütjen-Drecoll, *Microsc. Res. Tech.*, **33** (5), pp. 390-439 (1996).
- [2] J.W. Rohen, *Invest. Ophthalmol. Vis. Sci.*, **18** (2), pp. 133-144 (1979).
- [3] G.J. Tserevelakis, D. Soliman, M. Omar, V. Ntziachristos, *Optics Letters*, **39**, 1819-1822 (2014).
- [4] G.J. Tserevelakis, M. Tsagkaraki, G. Zacharakis, *J. Microsc.*, **263** (3), pp. 300-306 (2016).

Analysis of human healthy dentin microstructure by using two photon excitation fluorescence microscopy and second harmonic generation

Tijana Lainović¹, Mihailo Rabasović², Larisa Blažić^{1,3}, Dejan Pantelić²,
Aleksandar Krmpot², Vladimir Lazović², Branislav Jelenković²

¹Faculty of Medicine, School of Dentistry, University of Novi Sad, Novi Sad, Serbia

²Institute of Physics, University of Belgrade, Belgrade, Serbia

³Clinic of Dentistry of Vojvodina, Novi Sad, Serbia

e-mail: tijana.lainovic@gmail.com

Human dentin is an organized hard, mineralized tissue of a tooth, composed of 70 wt% calcified tissue (hydroxyapatite), 20 wt% the organic phase (mostly composed of collagen type 1 and the other fibrils, glycosaminoglycans and proteoglycans), and 10 wt% water [1]. Dentin has a specific tubular structure containing tubules, peritubular and intertubular parts, biologically arranged to meet the specific mechanical, nutritional, sensory and reparative needs of a tooth [2].

The aim of this study was to analyze the microstructure of human dentin with the advanced microscopy tools, in order to get better insight into the architecture of healthy dentin.

The healthy premolar teeth were extracted for the orthodontic reasons, and collected in accordance with the ethical requirements for ex-vivo investigations, which was approved by the Ethical Committee of the Clinic of Dentistry of Vojvodina. The teeth were cleaned, and kept in 0.5 % Chloramine solution until the examination. The slices of teeth were prepared using a hard tissues microtome. The images of dentinal microstructures were obtained by the homemade nonlinear microscopy setup [3]. Ti-sapphire laser, adjusted at 730 nm wavelength, was used as an excitation source for two-photon excitation fluorescence (TPEF), while 840 nm excitation was used for the second harmonic generation (SHG).

The dentinal tubular, peritubular and intertubular structures were clearly presented. Natural human dentin enables the label-free and fixation-free visualization of its architectural content by the TPEF microscopy, owing to its intrinsic autofluorescence. The SHG can be detected due to the presence of collagen type I in dentin, which is a triple helical molecule, assembled in organized, non-centrosymmetric directional fibrils [4]. Images of healthy dentin could serve as a reference point for comparison and investigation of internal structural changes in dentin, affected by caries or non-caries lesions, or changed after the use of various restorative materials and procedures.

Acknowledgments. Research was supported by the Ministry of Education, Science and Technological Development of the Republic of Serbia (Projects. III 46010, ON 171038 and TR 035020)

REFERENCES

- [1] M. Goldberg, A.B. Kulkarni, M. Young, A. Boskey, *Front. Biosci. (Elite Ed)*. 3, 711 (2011).
- [2] S.R. Stock, A.C. Deymier-Black, A. Veis, A. Telsler, E. Lux, Z. Cai, *Acta Biomater.* 10, 3969 (2014).
- [3] K. Bukara, S. Jovanić, I.T. Drvenica, A. Stančić, V. Ilić, M.D. Rabasović, D. Pantelić, B. Jelenković, B. Bugarski, A.J. Krmpot, *J Biomed Opt* 22, 026003 (2017).
- [4] R. Elbaum, E. Tal, A.I. Perets, D. Oron, D. Ziskind, Y. Silberberg, H.D. Wagner, *J. Dent.* 35, 150 (2007).

Second harmonic generation imaging of collagen fibers in the uninvolved human rectal mucosa 10 cm and 20 cm away from the malignant tumor

Sanja Despotović¹, Ivana Lalić¹, Novica Milićević¹, Živana Milićević¹, Mihailo Rabasović², Dejan Pantelić², Svetlana Jovanić² and Aleksandar Krmpot²

¹*Institute of Histology and embryology, Medical faculty, University of Belgrade, Serbia*

²*Institute of Physics Belgrade, University of Belgrade, Serbia*

e-mail: sanjadesp@med.bg.ac.rs

The aim of our study was to investigate the organization of collagen fibers utilizing second harmonic generation (SHG) microscopy in the lamina propria of the rectal mucosa in the remote surrounding of the malignant tumor. We demonstrated the structural alterations (reduced cellularity, alterations of Liberkuhn crypts and tissue edema) of the lamina propria of the mucosa 10 cm and 20 cm away from the rectal adenocarcinoma. Our study also provided indications that the collagen fibers in the rectal lamina propria could be affected [1].

Tissue samples were endoscopically collected from 30 patients with adenocarcinoma located in the sigmoid colon. The biopsies were taken 10 cm and 20 cm away from the malignant tumor in the caudal direction. The samples of rectal mucosa collected at the same institution from 30 healthy persons with a family history of intestinal malignancy, were used as control.

Masson trichrome staining on formalin-fixed, paraffin-embedded tissue was used to visualize collagen fibers. Also, to exclude the possibility that the observed changes could be due to methodology used (fixation or staining), an original labframe nonlinear laser scanning microscope (NLM) [2] was used for SHG imaging of collagen distribution on fixation- and label-free colon tissue samples. The incoming infrared femtosecond pulses from the tunable mode-locked Ti:Sapphire laser (Coherent, Mira 900) were directed onto the sample by a dichroic mirror through the Zeiss EC Plan- Neofluar40x/1.3 NA oil immersion objective. The laser wavelength was 840nm, and the SHG was selected by narrow bandpass filter at 420 nm (Thorlabs FB420-10, FWHM 10nm). The average laser power on the sample was 30 mW with pulse duration of 160fs and repetition rate of 76MHz which produced 2.5 kW of peak power.

On Masson trichrome stained tissue, the collagen fibers in the lamina propria of healthy persons were massive, intimately appositioned and orderly organized. At the distance 10 cm away from the tumor the collagen fibers were feeble and loosely arranged. The enlarged spaces were notable between the collagen fibers, indicating the presence of tissue edema. Similar alterations of collagen fibers, but less prominent, were observed 20 cm away from the tumor.

SHG images on fresh, label-free tissue completely confirmed the aforementioned findings. The profound remodeling of collagen fibers is even more clearly noticeable on 3D reconstruction model obtained from SHG images. In the lamina propria 10 cm away from the tumor collagen fibers became fragile, increasingly disordered and the crypts architecture appeared disturbed.

We documented the profound alterations of collagen fibers in the rectal lamina propria 10 cm and 20 cm away from the malignant tumor.

Acknowledgment: This work is supported by bilateral project 451-03-01038/2015-09/1 between Ministry of Education, Science and Technological Development -MESTD of Republic of Serbia and German Academic Exchange Service-DAAD and by projects 175005, III45016 and OI 171038 of MESTD of Republic of Serbia.

REFERENCES

- [1] Despotović SZ, Milićević NM et al. *Histol Histopathol* **29**, 229-234(2014).
 [2] Rabasovic MD, Pantelić DV et al. *J Biomed Opt* **20**, 016010(2015).

Voltage-Sensitive Dye Imaging of Membrane Potential Transients in Thin Dendritic Branches of Cortical Pyramidal Neurons

Jesse A. White, Mandakini B. Singh and Srdjan D. Antic
*Stem Cell Institute, Institute for Systems Genomics,
University of Connecticut Health,
263 Farmington Avenue,
Farmington, CT 06030, USA
e-mail: antic@uchc.edu*

Thin dendritic branches of cortical pyramidal neurons receive and process information from other neurons in the form of electrical signals. The integration of electrical signals from a large number of synapses onto a single neuron is a complex process, underlying information processing in the mammalian brain, sensory perception, cognition and motor output. In order to understand information processing in individual cortical neurons, it is necessary to understand dendritic membrane properties and rules of dendritic integration (summation of synaptic inputs). The gap in the understanding of these mechanisms and processes is caused by technical limitations related to studying the physiology of thin dendrites by physiological recordings. Thin dendrites, such as basal, oblique and apical tuft branches of cortical pyramidal cell, do not tolerate standard microelectrode recordings. To overcome this problem here we utilize optical imaging of voltage transients occurring in distal dendrites. Layer 5 pyramidal cells in brain slices were patched (whole-cell) injected with voltage-sensitive dye JPW-3028, and the dye was allowed to diffuse into the dendritic tree for at least 60 min. Fluorescent images of dendritic contours were then projected onto the fast CCD camera and sampled at 1,000 – 2,000 frames per second. Brief pulses of depolarizing current were injected into the cell body to evoke action potentials. Backpropagating action potentials were recorded optically in basal dendrites. Synaptic stimulations were used to evoke excitatory postsynaptic potentials (EPSP) and dendritic NMDA spikes, while recording optically at the site of input, in basal dendrites. Our goal is to characterize both voltage waveforms underlying local dendritic voltage transients (bAPs, EPSPs and NMDA spikes) and correlate them with the somatic voltage transients recorded via standard patch microelectrode. We plan to deduct dendritic membrane properties and the overall functional organization of the basilar dendritic tree by comparing the aforementioned voltage waveforms in subsequent sweeps; each sweep under different stimulation paradigm or in the presence of drugs that block specific membrane channels.

Supported by NIH Grant U01-MH109091.

Designing Multi-Functional Plasmonic Nanoparticles for Cancer Theranostics

E. D. Onal¹ and K. Guven¹

¹*Koc University Department of Physics,
Istanbul, Turkey
e-mail: eonal@ku.edu.tr*

Plasmonic nanoparticles (NPs) have been actively studied as a minimally invasive approach for treating cancer. The use of gold NPs in cancer diagnosis and therapy takes a new turn with the recent synergistic approaches which combine multiple therapeutic (e.g. chemotherapy, immunotherapy, photothermal and photodynamic therapy) and imaging techniques (NP-assisted optical/thermal imaging) on the same nanoparticle platform [1]. Unlike a standalone functionality which requires the maximization of a particular parameter (for instance the optical absorption of the NP for conventional photothermal therapy – PTT [2]) this new approach necessitates a weighted optimization of NP properties (e.g. absorption & scattering cross sections, induced local electric fields) towards multiple tasks, while taking the in-vivo constraints into account. The most prominent constraint imposed by the biological environment is the light penetration problem into the human body. Transmitting light deep into the tissue to activate plasmonic NPs is achieved by utilizing specific wavelength bands where human body is most transparent. These wavelength bands (biological transparency windows) are located in near-infrared (NIR) region of the spectrum. So far, NP-assisted cancer treatments are demonstrated in NIR-I (700–950 nm) and NIR-II (1000–1350 nm). Recently, new transparency windows at longer wavelengths are discovered: NIR-III (1600–1870 nm) and NIR-IV (2100–2300 nm). These transparency windows provide significantly better light penetration, and thus have great potential for prospective cancer diagnosis and therapeutics [3].

The biological environment also imposes a constraint on the size and shape of NPs for their internalization into the cancer cells. The relation between the NP size and the cellular uptake is still vague, and varies significantly with the cell type and the NP shape. The internalization of gold NPs smaller than 100 nm (resonant in NIR-I and –II) is documented by a number of studies [4]. However, there is need for further experimental evidence to support cellular uptake of the gold NPs (300–500 nm) utilized in NIR-III and -IV. We proposed self-assembling NPs as an alternative solution to bypass the size limitation. These nanostructures are based on elements smaller than 100 nm which can first be transferred individually through the cell membrane and then assembled into a chain. The self-assembly of NPs via DNA or protein assistance is well documented and was recently demonstrated in intracellular scale [5]. These nanoparticles are lithographically fabricatable; and also easily adaptable to low-cost chemical growth methods for mass production.

The present work is motivated with this background to explore new venues in NP-assisted cancer theranostics with a focus on 3 issues: (i) the potential advantages of NIR-III and -IV in multi-modal cancer therapeutics compared to the currently used NIR-I and –II, (ii) the performance of self-assembling NPs compared to their monolithic counterparts, (iii) the complexities of designing multi-functional NPs in comparison to stand-alone strategies. We conclude by projecting these outcomes into the search for an optimum NP design; and suggest a versatile approach for designing both monolithic and self-assembling multi-functional NPs that carry therapeutic and diagnostic modalities.

REFERENCES

- [1] Y. Wang, Y. Xie, J. Li, et al. *ACS Nano* 11, 2 (2017).
- [2] E. D. Onal, K. Guven, *J. Phys. Chem. C* 121, 1 (2017).
- [3] L. Shi, L. A. Sordillo, A. Rodríguez-Contreras, et al. *J. Biophotonics* 9, 38 (2016).
- [4] L. M. Maestro, E. Camarillo, J. A. Sánchez-Gil, et al. *RSC Adv.* 4, 54122 (2014).
- [5] R. Ahijado-Guzmán, G. González-Rubio, J. G. Izquierdo, et al. *ACS Omega* 1, 388 (2016).

Method of preparing biomedical samples for cancer detection by infrared spectroscopy

J. L. Ristić-Djurović¹, S. T. Ćirković¹, N. Paunović¹, J. T. Juloski², S. R. De Luka³, V. M. Ćuk², M. Romčević¹,
A. M. Trbović³ and N. Romčević¹

¹*Institute of Physics, University of Belgrade, Belgrade, Serbia*

²*University Medical Center “Zvezdara”, Clinic for Surgery “Nikola Spasić”, Belgrade, Serbia*

³*Institute of Pathological Physiology, School of Medicine, University of Belgrade, Belgrade, Serbia*
e-mail: jasna@ipb.ac.rs

Most conventional cancer detection methods are based on the histopathology or tumor markers [1]. In the histopathology, stained tissue samples are visually inspected for various morphological changes under the microscope. Despite the software aids developed for picture analysis the method still remains heavily dependent on subjective, empirical expertise of specialists whose judgments were used to establish threshold levels of variables used in cancer detection. The immunohistochemistry as the most common of cancer marker methods uses the presence or over-expression of certain marker molecules to detect cancerous tissues. The drawback of this method is its limitation to those molecules, i.e., cancer markers it is designed for. In the last two decades, the vibrational spectroscopy applied to tissues emerged as a “molecular pathology” method for cancer detection [2]. The method provides spectral signature of all cellular components present in a sample; therefore, it probes the entire genome, proteome and metabolome of cells and tissues [3]. Consequently, it is sensitive to any changes in the biomolecular compositions and as such offers information that cannot be obtained by any of the conventional methods for cancer detection.

The biomedical samples for spectroscopic analysis are usually prepared by cutting several micrometer thin layers from a formalin-fixed paraffin-embedded tissue or from a frozen tissue [1, 2]. The cuts are then mounted on a suitable substrate, for example zinc selenide, calcium fluoride, barium fluoride. Additionally the samples may undergo deparaffinization or drying. Our samples were prepared in three steps. First, after surgical resection, the tissue specimens were opened, abundantly rinsed with sterile saline solution, dried on a sterile cloth, placed in a liquid nitrogen tank, and transported to the Pathophysiology laboratory of the School of Medicine where all sample tubes were transferred to a -80°C freezer where they were kept until further processing. In the second phase of sample preparation procedure the tissues were chopped at room temperature and homogenized. Homogenates were placed on a microscope slide and then dried in a sterilizator at 60°C for 1 h to remove bulk water. After drying, the samples were scratched from the slide and transferred to eppendorf tubes. In the final sample preparation stage the obtained tissue and dried KBr powder were mixed in the standard as well as in the three times larger ratio and the mixtures were pressed into tablets. Optionally, after 24 h the tablets were grounded and pressed again into tablets. The infrared spectra of the samples obtained using four different preparation procedures were compared. It was shown that larger tissue content as well as additional grounding improves infrared spectra quality.

REFERENCES

- [1] M. Diem, A. Mazur, K. Lenau, J. Schubert, B. Bird, M. Miljković C. Krafft, J. Popp, J. Biophotonics 6, 855 (2013).
- [2] G. Bellisola, C. Sorio, Am. J. Cancer Res. 2, 1 (2012).
- [3] G. Clemens, J. R. Hands, K. M. Dorling, M. J. Baker, Analyst 139, 4411 (2014).

Fetal Actometer Based on Optical Fibre Gratings

V. Atanasoski¹, M. Ivanovic², N. Stojanovic³, Lj. Hadzievski² and J. Petrovic²

¹University of Belgrade, Serbia

²Vinca Institute of Nuclear Sciences, University of Belgrade, Serbia

³Deutsches Elektronen-Synchrotron (DESY), Hamburg, Germany

e-mail: jovanap@vin.bg.ac.rs

Monitoring of fetal activity has been used to check wellbeing of fetus both clinically and in homecare. Clinically, fetal movements are monitored by an ultrasound transducer [1], simultaneously with the fetal heart rate and the uterine contractions measured by a tococardiograph (CTG) [2]. The absence of correlation between the fetal activity and the changes in its heart rate signals potential problems, the heaviest being the stillbirth [3]. In homecare, fetal movement is monitored by pregnant women directly, detection fully relying on mother's perception. It has been shown that mother's perception agrees with the fetal movement registered by an ultrasound actometer in 79% of cases in 34-40 weeks gestation period and in 72% of cases in 31-34 weeks gestation period [4]. The partial reliability of such a measurement indicates that a more accurate, objective and convenient monitoring method is needed in homecare. To further take a load off mother, who is supposed to perform measurements several times a day, the new sensor should be wearable and the readout of fetal movements automatic.

We propose a fetal actometer based on optical fibre grating sensors that can satisfy the above requirements. Long-period gratings are sensitive to changes in pressure, tension and curvature, hence to external changes of mother's abdomen caused by fetal movement. Detection was performed by monochromatic lateral filtering technique that relies on the transmitted power measurement at a specified wavelength [5]. An additional reference sensor was used to register mother's perception. To extract the useful information and produce a user-friendly output, an algorithm for counting fetal movements and their demarcation in the signal was developed. Traces of the maternal heart beat and breathing as well as fetal hiccups were eliminated by spectral filtering. The signal processing software is sensor independent and can be used with other actographs.

Results of the study performed on healthy women in the third trimester of pregnancy show 75% agreement between the number of movements registered by the LPG sensors and mothers. A systematic difference between the signals came from the movements that the sensors registered but mothers did not perceive. The number of false positives, however, can be established only in comparison with the ultrasound detection. The good agreement with the maternal perception and the absence of cross-talk with the fetal heart rate measurement, along with the sensors' light weight, robustness and wearability, indicates their potential for use in hospitals and homecare and encourages further clinical studies.

REFERENCES

- [1] K. Maeda, J. Obstet. Gynaecol. 42(1), 5 (2016).
- [2] E. Z. Zimmer, M. Y. Divon and A. Vadasz, Eur. J. Obstet. Gynecol. Reprod. Biol. 25, 89 (1987).
- [3] J. F. Pearson and J. B. Weaver, Brit. Med. J. 1 (6021), 1305 (1976).
- [4] A. C. De Witt and J. G. Nijhuis, Ultrasound Obstet. Gynecol. 22, 152 (2003).
- [5] M. Petrovic et al., Biomed. Opt. Express 5, 1136 (2014).

Time resolved luminescence spectra of greater celandine (*Chelidonium majus* L.)

M. S. Rabasovic, D. Sevic, M. D. Rabasovic, M. G. Nikolic and B. P. Marinkovic
Institute of Physics, Belgrade, Serbia
e-mail:majap@ipb.ac.rs

The greater celandine (*Chelidonium majus* L.) is a medicinal plant of the poppy family. It grows mainly in Europe and Asia. This herb is a rich source of biologically active substances used for the treatment of various diseases. It has been demonstrated that both alkaloid extracts and purified alkaloids from that plant exhibit distinct anti-inflammatory, spasmolytic, anti-microbial, and anti-tumour activities [1–4]. The most important alkaloid components of this plant are protopine, chelidonine, coptisine, sanguinarine, allocryptopine, chelerythrine. Identification and quantitative analysis of these individual alkaloids is important in developing and utilizing resources of greater celandine. Moreover, this analysis provides better insight into the mechanism of the biological action of specific alkaloids.

In this study we analyze optical characteristics of greater celandine solution extracts. The samples of *Chelidonium majus* L. were collected from courtyard of our institute. Solutions were extracted with ethanol from plant samples and their time resolved optical characteristics were analyzed using our TR-LIF (Time resolved Laser induced Fluorescence) spectroscopy experimental setup. The setup consist of tunable OPO (Optical Parametric Oscillator) laser and streak camera. It was used previously for analysis of solution samples of biological interest and it is described in more detail in our earlier publications [5-7].

Results of our analysis reveal two distinct optical emission bands with different excitation characteristics. Time resolved analysis of luminescent spectra show that lifetimes of both bands are in nanosecond domain.

REFERENCES

- [1] M. Kulp, O. Bragina, P. Kogerman, M. Kaljurand, *Journal of Chromatography A*, 5298, 1218 (2011).
- [2] G.-Y. Zuo, F.-Y. Meng, X.-Y. Hao, Y.-L. Zhang, G.-C. Wang, G.-L. Xu, *J. Pharm. Pharm. Sci.* 11, 90 (2008).
- [3] V. Kaminsky, M.D. Lootsik, R. Stoika, *Centr. Eur. J. Biol.* 1, 2 (2006).
- [4] K.-M. Cho, I.-D. Yoo, W.-G. Kim, *Biol. Pharm. Bull.* 29, 2317 (2006).
- [5] B. P. Marinkovic, A. Delneri, M. S. Rabasovic, M. Terzic, M. Franko, and D. Sevic, *J. Serb. Chem. Soc.* 79, 185 (2014).
- [6] M. S. Rabasovic, D. Sevic, M. Terzic, and B. P. Marinkovic, *Phys. Scr.*T149, 014076 (2012).
- [7] M. S. Rabasovic, D. Sevic, M. Terzic, and B. P. Marinkovic, *Nucl. Inst. Meth. B.*279, 16 (2012).

Quantitative characterization of receptor-receptor interactions in live cells using dual-color fluorescence cross-correlation spectroscopy

V. Radoi, A. A. Ghavanini, J. Rüegg, E. Kosek and V. Vukojevic

*Department of Clinical Neuroscience, Center for Molecular Medicine CMM L8:01, Karolinska Institutet
Stockholm, Sweden*

e-mail: vladana.vukojevic@ki.se

Fluorescence Correlation Spectroscopy (FCS) and its dual-color variant Fluorescence Cross-Correlation Spectroscopy (FCCS) are unique analytical methods with single-molecule sensitivity that enable us to quantitatively characterize the concentration, motility and interactions between molecules of interest in solution and in live cells [1-4]. FCS relies on the use of specific arrangement of optical elements in a confocal microscope to generate in the sample a minute observation volume element (OVE) and analyzes the time course of spontaneous fluctuations in fluorescence intensity in this sub-femtoliter-sized OVE to extract information about the average number of molecules and their dynamic behavior. FCCS takes advantage of the cross-correlation between two spectrally distinct signals simultaneously recorded in separate detectors for analyzing molecular interactions between different species.

We have used dual-color FCCS to quantitatively characterize in live PC12 and HEK293 cells interactions between the mu-opioid receptor tagged with the enhanced Green Fluorescent Protein (MOP-eGFP) and the serotonin 5-HT_{1A} receptor tagged with a spectrally distinct variant of the Red Fluorescent Protein (5-HT_{1A}-Tomato) and assess the effect of selected agonists (morphine and serotonin) on these interactions [5].

Our study shows that prolonged (18 h) treatment with 750 nM morphine facilitates MOP hetero-dimerization with 5-HT_{1A}. Combined treatment with equimolar concentrations of MOP and 5-HT_{1A} agonists abolishes hetero-dimerization.

REFERENCES

- [1] E.L. Elson, *Methods Enzymol.* 518, 11 (2013).
- [2] E.L. Elson, *Biophys J.* 101, 2855 (2011).
- [3] V. Vukojević, A. Pramanik, T. Yakovleva, R. Rigler, L. Terenius, G. Bakalkin, *Cell. Mol. Life. Sci.* 62, 535 (2005).
- [4] V. Vukojević, D.K. Papadopoulos, L. Terenius, W.J. Gehring, R. Rigler, *Proc. Natl. Acad. Sci. USA*, 107:4087-4092 (2010).
- [5] V. Radoi, E. Kosek, V. Vukojevic, IASP 16th World Congress on Pain 55, PW0284 (2016).

Effect of Size and Geometry of Quantum Dots on Performance of Time Resolved Fluorescence Spectroscopy; A Monte Carlo Study

Amid Rahi¹, Tahereh Tekieh², and Pezhman Sasanpour¹

¹*Department of Medical Physics & Biomedical Engineering, School of Medicine, Shahid Beheshti Medical University*

Tehran, Iran

²*School of Nanoscience, Institute for Research in Fundamental Sciences (IPM),*

Tehran, Iran

e-mail: pesasanpour@sbmu.ac.ir

As one of the techniques of optical biopsy category, time resolved fluorescence spectroscopy and imaging are from promising methods in detection and diagnosis, specially in discriminating healthy and cancerous tissues [1]. As a non invasive method, this technique earns data form lifetime and intensity of fluorescence signal. Even though intensity based techniques are easily implemented and data extractions are less complicated, according to some uncontrollable ambiguities, the accuracy of the method is uncertain.

Comparing with traditional fluorescent tags, Quantum dot are from powerful potential candidates for substitution in this method considering their brightness, higher signal to noise ratio, higher quantum efficiency, absorption/emission spectrum and life time. Their longer lifetime is more desirable in this technique. Engineering size and composition of quantum dots will be resulted in tunable properties which are required for different application.

We have studied effect of size and distribution of quantum dots in different tissue structures, in performance and efficiency of time resolved fluorescence spectroscopy. The spectrum of different quantum dots are calculated considering their size and composition and are incorporated in our Monte Carlo code for modeling of light transport inside the tissue accordingly [2]. Considering the modeling results, performance of detection between normal and cancerous tissue has been calculated accordingly.

REFERENCES

- [1] D. S. Kittle, F. Vasefi, C. G. Patil, A. Mamelak, K. L. Black, and P. V. Butte, *Scientific Reports* 6 (2016).
- [2] Lihong V. Wang, Hsin-i Wu, *Biomedical Optics: Principles and Imaging*, John Wiley & Sons (2007).

Optimized Design of Intensity Based Plasmonic Fiber Biosensor; Modeling and Experiment

Mitra Abedini¹, Raheleh Mohammadpour², Mohsen Ahmadi¹, and Pezhman Sasanpour¹

¹*Department of Medical Physics & Biomedical Engineering, School of Medicine,
Shahid Beheshti Medical University*

Tehran, Iran

²*Institute for Nanoscience and Nanotechnology (INST), Sharif University of Technology,*

Tehran, Iran

e-mail: pesasanpour@sbmu.ac.ir

An optical fiber based biosensor has been designed and optimized exploiting surface plasmon resonance (SPR). The main application of the sensor is for measurement of urine specific gravity (USG). Since USG indicates the ability of the renal tubules to concentrate or dilute glomerular filtrate, it has been considered as a vital factor for human's health. The number of various molecules, molecular weight and their size in urine effect on USG therefore it estimates solute concentration which is dependent on the refractive index accordingly.

Based on the sensitivity of SPR to the local variation of refractive index, and based on the simplicity of optical fiber compared to prism based method, the structure has been selected accordingly [1]. The advantage of fiber based structures including flexibility, low cost, compact size and make them suitable for in vivo applications. Considering complexity of wavelength based system, the intensity based measurement has been proposed. Even though the intensity based techniques are more uncomplicated, but the sensitivity and accuracy of measurement is of great concern.

In this regard, we have proposed a novel method for intensity based SPR fiber sensors. The method is based on exploiting measurement of absorption using two distinct wavelengths. In order to have the maximum of sensitivity, selectivity and independency, the structure and thickness of the metallic thin film should be optimized. Based on theoretical analysis using transfer matrix method, we have calculated the optimized condition for the sensor operation considering two distinct wavelengths of 650 nm and 780 nm [2]. Based on the results of analysis, the structure has been fabricated and tested accordingly and the experimental results were in accordance with the theoretical analysis.

REFERENCES

- [1] G. Liang, Z. Luo, K. Liu, Y. Wang, J. Dai, and Y. Duan, " Critical Reviews in Analytical Chemistry, vol. 46, pp. 213-223, (2016).
- [2] M. Born and E. Wolf, Principles of optics: electromagnetic theory of propagation, interference and diffraction of light: Elsevier, (2013).

The effect of short-term fish oil supplementation on Alzheimer disease-like pathology in 5xFAD mouse model

Milena Jović, Nataša Lončarević-Vasiljković, Desanka Milanović, Vladimir Avramović, Marjana Brkić, Selma Kanazir

*Institute for Biological Research “Siniša Stanković”,
University of Belgrade, Serbia
e-mail: milena.jovic@ibiss.bg.ac.rs*

Alzheimer's disease (AD) is a neurodegenerative disease characterized by progressive memory loss and dementia. Pathologically, the disease is recognized by the presence of senile plaques (deposition of beta amyloid (A β) peptides), neurofibrillary tangles, and neuronal loss. Clustering of microglial cells at sites of A β deposition in the brain is also an important pathological feature of AD. At present, there is no effective treatment for AD.

To investigate the influence of fish oil (FO) supplementation, like potential treatment, we used transgenic 5xFAD mice which rapidly recapitulate major hallmarks of AD amyloid pathology. Three-month old female 5xFAD mice received FO (100 μ l/animal/day) via oral gavage during 3 weeks period. Histological analysis was used to detect changes in pathological features of AD in parietal cortex in 5xFAD mice. ThioflavinS and AmiloGlo were used to visualize plaques, soluble A β peptide was detected by A β 42 antibody, SMI31 antibody was used for neuritic dystrophy and Iba-1 antibody for microglial cells. Immunostaining was observed by confocal microscopy. Quantification was done by Image J program.

We showed that short-term FO supplementation is capable of inducing significant decreased of number of plaques, total A β levels, and preventing the emergence of neuritic dystrophy in parietal cortex of 5xFAD mice. Also, FO supplementation led to increase in overall microglial number, and enhanced clustering of microglial cells around amyloid plaques. We confirmed and extended previous findings suggesting that FO has a typical pleiotropic effect and we believe that FO in combination with others drugs could be good approach for long-term treatment in AD suppression.

Acknowledgements: This study was supported by the Ministry of Education, Science and Technological Development, Republic of Serbia (grant ON173056) and the Fogarty International Research Award, NIH(R03AG046216).

A New Method for Multi-Bit and Qudit Transfer Based on Commensurate Waveguide Arrays

J. Krsic¹, P. Veerman² and J. Petrovic¹

¹*Vinca Institute of Nuclear Sciences, University of Belgrade, Serbia*

²*Fariborz Maseeh Dept. of Mathematics and Statistics, Portland State University, Portland, OR, USA*

e-mail: jovanap@vin.bg.ac.rs

Faithful parallel transfer of bits of information between computer components is a necessary condition for fast classical and quantum computation. Moreover, it has recently been suggested that the stability of quantum computation may be increased by using qudits and their representations as multiple qubits [1]. Transfer of an n -qudit and n qubits require number of channels that scale linearly and exponentially with n , respectively. This puts strict demands on dense packaging and scalability of interconnects. However, the transfer through densely packed optical interconnects is impeded by cross-talk between them. Proposed solutions to this problem entail high index-contrast waveguides [2], wavelength multiplexing [3], multimode waveguides [4] and supermodes [5].

We propose a new method and the hardware for the parallel transfer of bits, qubits and qudit states. The method is based on the full state revivals in linearly coupled commensurate waveguide arrays (WGAs). Commensurability of eigenvalues enforces periodicity of light dynamics and hence, full phase and amplitude revivals of the initial state. An n -element array can faithfully transfer an n -bit classical state and a quantum state encoded in an n -dimensional basis. The latter enables transfer of $\log_2 n$ qubits and an n -qudit. However, while the arrays with $n < 4$ waveguides are always commensurate, the eigenvalues of longer arrays are commensurate only for certain ratios of their coupling coefficients. The key challenge in engineering of commensurate arrays is to find these ratios by solving the non-trivial inverse eigenvalue problem. Such problems are analytically solvable in a small number of cases and are, in general, of polynomial complexity. Analytical solutions have been reported for mirror-symmetric arrays composed of 4 or 5 optical waveguides [6]. Here, we present analytical solutions for arrays with up to 9 waveguides and use them to design commensurate WGAs that are accessible to modern fabrication techniques, such as direct laser writing [7].

REFERENCES

- [1] E. O. Kiktenko et al., *Phys. Lett. A* 379, 1409–1413 (2015).
- [2] R. Chen, *Appl. Phys. Lett.* 61 (IQ), 9 (1992).
- [3] K. Kintaka et al., *Journal of Lightwave Technology* 28(9), 1398 (2010).
- [4] Y. Yadin and M. Orenstein, *J. Lightwave Technol.* 24, 380 (2006).
- [5] S. Ö. Arik and J. M. Kahn, *IEEE Photon. Technol. Lett.* 25 (21), 2054 (2013).
- [6] J. Petrovic, *Opt. Lett.* 40, 139 (2015).
- [7] A. Szameit and S. Nolte, *J. Phys. B: At. Mol. Opt. Phys.* 43, 163001 (2008).

Digital holography of graphene oxide paper acoustic membranes

J. Mitrić¹, D. Abramović², D. Todorović^{3,4}, N. Demoli², M. Spasenović¹

¹*Graphene Laboratory (GLAB) of the Center for Solid State Physics and New Materials,
Institute of Physics, University of Belgrade,
Pregrevica 118, Belgrade, 11080, Serbia*

²*Institute of Physics, Bijenička c. 46, PO Box 304, 10001 Zagreb, Croatia*

³*School of Electrical Engineering, University of Belgrade, Bulevar kralja Aleksandra 73, 11120 Belgrade, Serbia*

⁴*Dirigent Acoustics Ltd, Mažuranićeva 29/9, 11050 Belgrade, Serbia*

e-mail: jmitric@ipb.ac.rs

Foil – like materials became almost unavoidable in industrial technology. Their applications are numerous, starting from protective and adhesive layers, chemical filters to electronic or optoelectronic components. Graphene oxide paper, as one of the most recent foil – like materials is made by assembly of individual graphene – oxide sheets. Its properties are superior compared to other materials when it comes to strength, stiffness and its macroscopic flexibility [1] which make it potentially a good candidate as a new material for vibrating membranes which are primary elements of every condenser microphone, loudspeaker and many other acoustic devices.

Here we report vibrating acoustic membranes made of graphene oxide paper. We use digital holography in a quasi – Fourier configuration and time averaging to study the modal structures of the membranes [2, 3]. For comparison, we performed the same holographic measurements on membranes made of Mylar, aluminum, parafilm and different kinds of filter paper. We have found resonance frequencies and shapes of the vibrating modes for every tested material. We also calculated fundamental frequencies for every given material. Graphene oxide paper shows the richest modal behavior of all tested materials with multiple interesting and complex modes at frequencies between 20 Hz and 5 kHz.

This work is supported by the Serbian MPNTR through Projects OI 171005. We thank the EU and Republic of Serbia for financing through the Science – Industry Collaboration Program administered by the Innovation Fund.

REFERENCES

- [1] D. A. Dikin, et al., Nature 448, 457 (2007).
- [2] N. Demoli and I. Demoli, Optics Express 13, 4812 (2005).
- [3] P. Picart, et al., Optics Letters 28, 1900 (2003).

Polarized Intensity Reduction of Red-Sea Glint Reflection

R. Avrahamy¹, B. Milgrom², S. Hava¹

¹*Department of Electrical and Computer Engineering,
Ben Gurion University, Beer-Sheva, Israel*

²*School of Electrical Engineering,
The Jerusalem College of Technology, Israel
e-mail:roiav@post.bgu.ac.il*

Reflection from waves in the sea will appear as glints that can affect observation in marine environment. The variations in the sea water reflection glints occur faster than the eye can distinguish and are optical phenomena that cause light source to appear sparkled. Position and timing of these glints are determined by many variables.

Considering observation and detection systems at maritime environment, glints may inflict significant saturation in some areas of photography. Saturation impose great difficulties for the observers, producing blinding glares and increasing fatigue. In addition, glints give rise to marine target detection challenges. At times, certain objects can "hide behind" these glints making it very difficult to sense.

The aim of the study was reduction of glints in the Red-Sea using an approach based on the degree and angle of polarization. We have studied the quantitative relationship between the flashes and the background at maritime environment.

Experiments using a dedicated setup, carried out an analysis in a qualitative and quantitative manner, using image processing and comparing with theory. A survey with observers was performed to examine effectiveness of the solution.

REFERENCES

- [1] S. Kay, J. Hedley and S. Lavender, *Remote Sensing*, vol. 1, no. 4, pp. 697- 730, (2009).
- [2] X. He, Y. Bai, Q. Zhu and F. Gong, *Journal of Quantitative Spectroscopy and Radiative Transfer*, vol. 111, no. 10, pp. 1426-1448, (2010).
- [3] D. Lynch, D. Dearborn and J. Lock, *Appl. Opt.*, vol. 50, no. 28, p. F39, (2011).

Self-pulsing in monolithic and external cavity mid-IR QCLs

N. Vukovic¹, J. Radovanovic¹, V. Milanovic¹ and D.L. Boiko²

¹*School of Electrical Engineering,
University of Belgrade, Serbia*

²*Centre Suisse d'Electronique et de Microtechnique,
Neuchâtel, Switzerland*

e-mail: nikolavukovic89@gmail.com

Passive mode-locking or Q-switching regimes are difficult to realize in Mid-IR QCLs because their gain recovery times are much faster than the cavity roundtrip times. As a result, the gain does not provide a “memory effect” that can sustain low-frequency periodic regimes. Experimental observations [1] have shown that some QCLs operating at low excess above lasing threshold exhibit features of multimode Risken-Nummedal-Graham-Haken (RNGH) instability [2,3]. This instability is related to excitation of coherent Rabi oscillations in the gain medium and therefore QCL might exhibit self-pulsations (SP). In our recent theoretical works [4-6] we attribute significant lowering of the RNGH instability threshold in Fabry-Pérot cavity QCLs to the interaction of standing cavity modes on induced gratings of population inversion and coherences. The difficulties for practical use of RNGH SP in free-standing QCLs originate from the quasiperiodic chaotic behavior of the pulse train when the coherence length is smaller than the length of the sample or from a very high oscillation frequency when the sample length is on a 100 μm scale [5].

In this communication we propose to use external-cavity (EC) QCLs in order to obtain regular RNGH self-pulsations with a reduced repetition frequency. Firstly, the propagation time in the EC (the pulse delay time) serves to provide a memory effect and thus improves coherence time of the QCL pulse train. Secondly, the EC reduces the pulse repetition rate. In our model system the front facet of the QCL chip facing the EC reflector is anti-reflection (AR) coated, which is very different from a QCL subjected to the optical feedback [7]. Using a semiclassical travelling wave rate equation model [8] adapted for the case of short (100 μm long) QCL chips [4-6] we demonstrate possibility of (i) bi-stable operation, (ii) lowering of the pulse repetition rate in ~ 1 mm long EC and (iii) suppression of SP in ~ 1 cm long EC.

REFERENCES

- [1] A. Gordon et al., Phys. Rev. A 77 (5), 053804 (2008).
- [2] H. Risken and K. Nummedal, J. Appl. Phys. 39, p 4663, (1968).
- [3] R. Graham and H. Haken, Z. Phys. 213, 420, (1968).
- [4] N. Vukovic et al., Opt. Express 24, 26911-26929 (2016).
- [5] N. Vukovic et al., to be published in IEEE J. Sel. Top. Quantum Electron. 23, no. 6, November/December 2017.
- [6] N. Vukovic et al., Opt. Quant. Electron. 48:254 (2016).
- [7] L. L. Columbo and M. Brambilla, Opt. Express 22, 10105 (2014).
- [8] D. L. Boiko, P. P. Vasil'ev, Opt. Express 20, 9501-9515 (2012).

Eigenmode and frequency domain analysis of the third-order microring filters

M. Radmilović-Radjenović and B. Radjenović
Institute of Physics Belgrade, University of Belgrade,
Belgrade, Serbia
e-mail: marija@ipb.ac.rs

Optical microresonators represent a subject of tremendous significance in modern photonics. The interest in micro cavities able to confine a light field has been growing rapidly in many domains of modern optics, from classical to quantum phenomena, from the linear to the nonlinear regime, from technologies and materials to applications in a variety of different fields [1]. The silicon on insulator (SOI) technology is currently the technology of choice for fabricating microring resonators by using the commercially available SOI wafers. These wafers consist of three layers: The Si-substrate, followed by a silica (SiO_2) buffer layer (usually about $1\mu\text{m}$ thick) and a crystalline Si-layer on top. An important feature of the SOI technology is the high refractive index (n) contrast of the different materials silicon ($n_{\text{Si}} = 3.476$), silica ($n_{\text{SiO}_2} = 1.444$), and air ($n_{\text{air}} = 1$). This high index contrast allows designing small, wavelength-scale nanophotonic structures. SOI photonic structures can be fabricated with complementary metal oxide semiconductor (CMOS) standard processes. CMOS technology is a mature technology that is suited for inexpensive mass-fabrication and that allows high integration capabilities, and high reproducibility. Also, it opens the perspective of combining microelectronic and photonic elements in a single silicon chip.

When several resonators are coupled, the frequency and time domain behavior, as well as the design flexibility, are further enriched comparing to a single cavity, leading to complex and flexible systems that open unmatched opportunities in both the investigation of physical phenomena and their applications. Systems consisting of a few coupled resonators, say $1 < N < 5$, have been proposed for optical filtering and modulation. Microring resonators can operate as either a four-port (add/drop filter) or a two-port (all-pass filter) device. The most common configuration has two bus waveguides and four ports, that is ideally suited for the telecommunication wavelength-filtering applications [2].

In this paper we compare results of the eigenmode analysis of the four-port system consisting of three serially coupled microring and two side access waveguides (third-order add/drop filter) with the transfer functions (S-parameters) calculated in wide spectral range covering telecommunication C band. It is well known that when single microring is coupled to access waveguides or another rings, the resonance frequency will deviate from its original isolated resonator value. This effect, known as coupling-induced resonance frequency shift (CIFS), causes resonance frequency mismatches between individual resonators and thus significantly impacts eigen spectra, as well as transfer characteristics, of the coupled-resonator systems. Both type of calculations are performed using 2D finite elements (FEM) method. The computational domain is closed using standard perfectly matched layer (PML) method. The obtained results show excellent agreement between the two approaches, and they extend results of our previous paper [3], where finite length microring resonator arrays without access waveguides are analysed.

REFERENCES

- [1] W. Bogaerts, P. De Heyn, T. Van Vaerenbergh, K. De Vos, S. Selvaraja, T. Claes, P. Dumon, P. Bienstman, D. Van Thourhout, and R. Baets, *Laser Photonics Rev.* 6, 47 (2012).
- [2] H. C. Liu and A. Yariv, *Optics express* 19, 18, 17653 (2011).
- [3] B. Radjenović, M. Radmilović-Radjenović, and P. Beličev, *Optical and Quantum Electronics* 49, 149 (2017).

Analysis of the transmission and tunneling time characteristics in light propagation through anisotropic media

N. Opacak, J. Radovanovic and V. Milanovic

School of Electrical Engineering,

University of Belgrade, Serbia

e-mail:opacaknn@gmail.com

We consider a planar electromagnetic wave (light beam) encountering a dielectric structure consisting out of two barriers (two separated dielectric slabs). The medium that surrounds the barriers, and through which the wave travels, is assumed to be linear, however, the barrier slabs are made out of an anisotropic material, i.e. a material whose permittivity is represented with a tensor and has a value which depends on the spatial direction of interest [1]. Furthermore, we will consider the slab medium to possess a non-vanishing imaginary part in general case. We will base the barrier medium parameters on realistic and commonly used semiconductor materials e.g. InGaAs [2]. Analytical expressions for the transmission, reflection and absorption probabilities for the analyzed structure will be obtained, and an investigation of their values as a function of the parameter of the material and wavelength of the incident wave will be conducted. Additionally, terms for the relevant tunneling times (group delay, dwell time and self-interference time) will be acquired with similar analysis carried out as in the case of transmission parameters.

REFERENCES

[1] V. Podolskiy, E. Narimanov, Phys. Rev. B 71, 201101(R) (2005).

[2] I. Ilić, P. Beličev, V. Milanović, J. Radovanović, Lj. Hadžievski, J. Electromagnetic Wave Appl. 26, 2323 (2012).

3D finite element eigenmode analysis of coupling mode induced resonance frequency shift in coupled microring resonators

B. Radjenović¹, M. Radmilović-Radjenović¹ and P. Beličev²

¹*Institute of Physics Belgrade, University of Belgrade, Belgrade, Serbia*

²*Vinca Institute of Nuclear Sciences, University of Belgrade, Belgrade, Serbia*

e-mail:bradjeno@ipb.ac.rs

Microring resonators are a rapidly-developing area of research in photonic devices with a wide range of applications including signal processing, filters, sensors, lasers, modulators, switches, memory and slow-light elements [1]. Generally speaking, microring resonators represent frequency selective elements that can perform a variety of functions such as add-drop filtering, switching, and modulating in wavelength-division systems. In coupled-resonator structures, one of the most critical issues is the precise control of the resonance frequency, which depends on both the resonator and cladding material and the resonator geometric parameters (radius, width, height). Also, it has been shown that when single microring is coupled to access waveguides or another rings, the resonance frequency will deviate from its original isolated resonator value. This effect, known as coupling-induced resonance frequency shift (CIFS), which is recently investigated more systematically in [2], causes resonance frequency mismatches between individual resonators and thus significantly impacts the performance of the coupled-resonator systems. By the nature of the problem this effect is most obviously manifested in system eigenspectra, although it is shown [2], [3], that CIFS can be related to the phase responses of the coupling region in the resonator coupling structure.

Several methods are used for calculating the response of a microring resonator such as the prominent FDTD or modeling in terms of semi-analytic coupled-mode theory, usually in two space dimensions (2D) and rarely in 3D. Although 2D calculations are sufficient to explain some concepts and phenomena, the rigorous 3D simulations are necessary to determine the parameters of the devices intended to be used in real WDM systems, especially when the dimensions of the system are comparable with the light wavelength. For many reasons, finite element method (FEM) is the method of choice for accurate and fast simulations of photonic systems. It enables rigorous treatment of full Maxwell's equations in complicated geometries and inhomogeneous domains. Arbitrary high-order methods for faster convergence and the error control through automatic adaptive mesh refinement are available in many commercial and academic FEM packages.

In our previous paper [4] we analysed eigenspectra and CIFS in finite length microring resonator arrays (systems without access waveguides) using 2D FEM method. Here we present a detailed investigation of CIFS effects in coupled microring resonators system configured as the high order serial filter based on eigenspectra analysis using full 3D vectorial FEM method. Such calculations are computationally much more demanding, and require careful devising of adaptive mesh refinement strategy, in order to make it feasible, even on the most powerful workstation.

REFERENCES

- [1] W. Bogaerts, P. De Heyn, T. Van Vaerenbergh, K. DeVos, S. Selvaraja, T. Claes, P. Dumon, P. Bienstman, D. Van Thourhout, and R. Baets, *Laser Photonics Revue* 6, 47 (2012).
- [2] M. Popović, C. Manolatu, and M. Watts, *Optics Express* 14, 3, 1208 (2006).
- [3] Q. Li, M. Soltani, A. Atabaki, S. Yegnanarayanan, and A. Adibi, *Optics Express* 17, 26, 23474 (2006).
- [4] B. Radjenović, M. Radmilović-Radjenović, and P. Beličev, *Optical and Quantum Electronics* 49, 149 (2017).

Coupled-mode theory approximation of scattering parameters of antisymmetric structures

V. Milosevic¹ and B. Jokanovic¹

¹*Institute of Physics,*

Belgrade, Serbia

e-mail:vojislav.milosevic@etf.rs

Waveguides or transmission lines coupled with various types of localized resonators constitute basic building block of many structures, notably many types of filters and metamaterials. Most of such structures published in the literature are symmetrical, by what we consider that they possess mirror-symmetry in respect to the plane that cuts through the middle of the unit cell. Consequently, their scattering parameters will be symmetrical, i.e. reflection will be equal on both sides. However, it has been demonstrated that, by breaking the symmetry, it is possible to excite additional sharp resonant modes, which may lead to interesting effects such as classical analog of electromagnetically induced transparency (EIT) [1].

In this work we have studied structures which consist of a microstrip transmission line, side coupled with two split-ring resonators (SRRs). The gaps of the SRRs are oriented in such a way that the structure is symmetrical under 180° rotation around the central point. These structures have two resonant modes, which can be used to obtain higher-order filters or classical analog of EIT.

Typical way to model and analyze such structures is using equivalent electrical circuit models, however, they have some drawbacks, e.g. they are inherently low-pass and calculating analytical form of scattering parameters may be very difficult. Instead, coupled-mode theory can be used to derive simple approximate expressions for scattering [2]. We will apply the coupled-mode theory to structures under study and derive constraints, which stem from the specific symmetry of the system. Obtained approximate expressions for transmission and reflection will be fitted, and comparison between fitting results and simulated data will be shown.

REFERENCES

- [1] V. A. Fedotov, M. Rose, S. L. Prosvirnin, N. Papasimakis, and N. I. Zheludev, *Phys. Rev. Lett.* 99, 147 401 (2007).
- [2] W. Suh, Z. Wang, and S. Fan, *IEEE Journal of Quantum Electronics* 40, 10, 1511–1518 (2004).

Fabry-Pérot lasers with Al-containing quantum wells in the COBRA generic photonic integration platform

F. Lemaître^{1,2}, J. Decobert², H. Ambrosius¹, G. Binet², N. Lagay², R. Van Veldhoven¹, F. Pommereau² and K. Williams¹

¹*Eindhoven University of Technology – COBRA Research Institute, Eindhoven, The Netherlands*

²*3-5 Lab, Nokia research center, Palaiseau, France*

e-mail: f.lemaitre@tue.nl

Photonic integration aims at keeping the pace of the ever increasing demand of the telecommunication and sensing sectors. The COBRA generic integration platform developed by the Eindhoven University of Technology proposes the integration of complex circuits on a single chip by combining building blocks together. This way many circuits can be made out of the same technology, satisfying a very broad spectrum of applications [1]. In this scope the use of the selective area growth (SAG), developed at the 3-5 Lab, will enable the integration of novel components in the COBRA platform, such as electro-absorption modulators, while keeping only three epitaxial steps. Unlike the COBRA technology, this technique is used with Aluminum-quaternary (Al-Q) materials for its improved electron confinement and hole density uniformity [2].

For the first time Al-Q materials have been used in the COBRA generic platform in order to pave the way to the integration of the SAG. The butt-joint integration used in the platform makes such a change of material delicate, and requires a careful validation. The measurement of Fabry-Pérot lasers fabricated using this new material allow to investigate the structural quality of the integration.

This work presents the measurement of lasers consisting of a ridge waveguide with a middle active section surrounded by two passive sections with a butt-joint interface between them. The total cavity length is 4.6 mm as it is the standard on the COBRA platform, and the cleaved facets of the chip provide 30% reflectors on each side.

The measurement of the optical power output of one facet versus the injected current showed a threshold current about 25mA and a slope efficiency near threshold of 0.12 W/A, which is close to the usual performances of such devices in the COBRA platform.

The investigation of the electrical characteristic of the device shows a current flow at small bias, which stands for a non-radiative recombination phenomenon. At high bias, the differential resistance slightly drops, and after the chip has been cleaved leaving only an active section, this differential resistance drop disappeared. In this way a leakage path with the presence of the active-passive transition and the passive waveguide has been revealed.

The parasitic effects described in this work are minor disruptions to the laser performances. Although an optimization has to be made, the results showed in this work are promising to obtain good performances using the SAG technique with Al-containing quaternary materials.

REFERENCES

- [1] M. Smit, X. Leijtens, H. Ambrosius and al. *Semiconductor science and technology*, vol. 29(8) 083001 (2014).
- [2] J. Decobert, P. Lagrée, H. Guérault, and C. Kazmierski, 25th IPRM conference, pp.1-2 (2013).

Terahertz narrowband transmission filters based on guided mode resonant metallic gratings

A. Ferraro^{1,2}, D. C. Zografopoulos¹, R. Caputo², and R. Beccherelli¹

¹*Consiglio Nazionale delle Ricerche, Istituto per la Microelettronica e Microsistemi (CNR-IMM),
Via del fosso del cavaliere 100, 00133 Rome, Italy*

²*Department of Physics, University of Calabria, Via Ponte Bucci Cubo 33b, 87036 Rende, Italy
e-mail:dimitrios.zografopoulos@artov.imm.cnr.it*

Guided-mode resonances (GMR) manifest as narrow-linewidth transmission or reflection bands when waves diffracted from a grating couple to propagating modes in an adjacent dielectric substrate [1]. Recently, such structures were proposed for the design of narrowband filters operating at terahertz (THz) frequencies, suitable for applications in telecommunications, radar science, or imaging [2].

Here, we investigate both theoretically and experimentally the properties of GMR in terahertz filters based on metallic frequency-selective surfaces (FSS), which are patterned via photolithography on thin films of the low-loss cyclo-olefin polymer Zeonor. Filters with very high quality factors are designed and their spectral response is studied under different conditions, such as oblique incidence, rotation of the polarization plane, and bent configurations. Contrary to the filtering response of standard free-standing FSS-THz filters, we observe extensive tunability of the GMR frequencies by means of mechanically rotation, as well their suppression by bending the flexible substrate [3, 4].

REFERENCES

- [1] P. Magnusson and S. S. Wang, *Appl. Phys. Lett.*, 61, 1022 (1992).
- [2] S. Song, F. Sun, Q. Chen, and Y. Zhang, *IEEE Trans. THz Sci. Technol.*, 5, 131 (2015).
- [3] A. Ferraro, D. C. Zografopoulos, R. Caputo, and R. Beccherelli, *IEEE J. Sel. Top. Quantum Electron.*, 23, 8501308 (2017).
- [4] A. Ferraro, D. C. Zografopoulos, R. Caputo, and R. Beccherelli, *Appl. Phys. Lett.*, 110, 141107 (2017).

Modeling of aircraft IC signature based on comparative tracking

D. Knežević^{1,2}, P. Matavulj¹ and Z. Nikolić³

¹*School of Electrical Engineering, University of Belgrade, Serbia*

²*Military Technical Institute (VTI), Belgrade, Serbia*

³*Faculty of Physics, University of Belgrade, Serbia*

e-mail: dragankn@gmail.com

IC aircraft signature has been studied for many reasons. Some of them are related to quality monitoring during the technological development, the other one to the possibility of tracking of the aircraft in real time, the third in the formation of the appropriate standard target and so forth. This work is related to the methodology for forming standard target aircraft, taking into account the sizes of some parts and the dimensions of the craft, simplified geometry which corresponds to the spatial frequency rate of the model for the representative type of the craft and the effective temperature difference between the total infrared signature of an aircraft, for a chosen geometry, in relation to the cold background of the sky.

The heated area of the aircraft and its exhaust gases during the flight were thoroughly studied, to form, define and adopt standard target aircraft in MWIR part of the EM spectrum. The geometry of the plane [1-2], the Quench Stop Temperature [2], the signature of hot products of combustion from the nozzles [2-4], the distribution of the airborne radiation during the flight [5-6] as well as special mechanical thrust vectoring research projects [4] were analyzed. The results of simultaneous, comparative tracking (monitoring) of two types of aircrafts were processed.

Evaluation of the parameter values for the standard target model of the aircraft [2] is carried out for the sake of analysis and model forming for spatial and temporal filtering of IR image [7]. Varying these parameters is important for the input vectors data during the forming of algorithm for simultaneous tracking of multiple targets in the air.

REFERENCES

- [1] Eurofighter Typhoon, *Technical Guide*01 (2013).
- [2] D. Knežević, *Analysis of IR devices parameters for detection of air targets*, MSc Thesis, University of Belgrade (2001).
- [3] M. S. Ab-Rahman, M. R. Hassan, *ICEEI Conf.*, NW-14(2009).
- [4] A. Clarke, *The Conceptual Design of Novel Future UAV's Incorporating Advanced Technology Research Components*, PhD Thesis, Cranfield University (2011).
- [5] S. P. Mahulikar, H. R. Sonawane, G. A. Rao, *Prog. in Aero. Science* 43, 218-245(2007).
- [6] K. J. Yi, S. W. Baek, B. Gu, S. N. Lee, M. Y. Kim, W. C. Kim, *ISROMAC-15 Conf.*, TH102(2014).
- [7] D. Knežević, P. Matavulj, Z. Nikolić, *9th Photonics Workshop*3-3, (2016).

Graphene acoustic diaphragms

M. Spasenović¹, J. Mitrić¹, D. Abramović², N. Demoli², D. Grujić¹, D. Pantelić¹, D. Todorović^{3,4}

¹*Institute of Physics, University of Belgrade,*

Pregrevica 118, Belgrade, 11080, Serbia

²*Institute of Physics, Bijenička c. 46, PO Box 304, 10001 Zagreb, Croatia*

³*School of Electrical Engineering, University of Belgrade, Bulevar kralja Aleksandra 73, 11120 Belgrade, Serbia*

⁴*Dirigent Acoustics Ltd, Mažuranićeva 29/9, 11050 Belgrade, Serbia*

e-mail:spasenovic@ipb.ac.rs

Vibrating diaphragms have become an important component of acoustics technology, with nearly all commercial microphones and speakers of the past half a century relying on diaphragm vibration. Although few select materials (such as nickel and boPET) are predominantly used because of their favorable properties such as small mass density and large tensile strength, the rise of new materials with superior properties such as graphene demands an assessment of their potential use in acoustic diaphragms.

Here we evaluate various forms of graphene as an acoustic diaphragm material. We fabricate diaphragms from graphene paper and multilayer (~60 layers) CVD graphene and measure their response to acoustic stimuli either in capacitance mode, which most closely resembles actual use in electrostatic condenser microphones, or with digital holography, which allows for physical studies of diaphragm vibration modes [1]. We find that multilayer graphene diaphragms outperform traditional nickel membranes in terms of responsivity, up to 12 dB at audio frequencies [2]. For large-diameter (25 mm) diaphragms that can be made from graphene paper, we detect a rich array of acoustic vibration modes that point to the diaphragms' potential use in pressure sensing or for detection of weak acoustic signals in quiet environments.

Our findings are supported with numerical COMSOL calculations that also reveal that a thicker multilayer diaphragm made of 300 layers of CVD graphene would in theory sustain tension forces that allow ultrasonic reach. Hence we conclude that graphene diaphragms hold potential for miniature low-cost ultrasonic transducers that compete with current piezoelectric technology.

This work is supported by the Serbian MPNTR through project OI 171005. We thank the EU and the Republic of Serbia for financing through the Science – Industry Collaboration Program administered by the Innovation Fund.

REFERENCES

[1] N. Demoli and I. Demoli, *Optics Express* **13**, 4812 (2005).

[2] D. Todorović et al, *2D Materials* **2**, 045013 (2015).

Hybrid organic/inorganic devices for display applications

V. Marinova¹, Y.C. Su², C. C. Chiou², S. Petrov², Ch. Dikov³, D. Dimitrov^{1,4*} and S. H. Lin²

¹*Institute of Optical Materials and Technologies, BAS, Sofia, Bulgaria*

²*Department of Electrophysics, National Chiao Tung University, HsinChu, Taiwan*

³*Central Laboratory of Solar Energy and Energy Sources, BAS, Sofia, Bulgaria*

⁴*Institute of Solid State Physics, BAS, Sofia, Bulgaria*

e-mail: vmarinova@iomt.bas.bg

Liquid-crystal displays (LCDs) are electronically modulated optical devices that use the light-modulating ability of the liquid crystals to control the phase and intensity of light [1]. Presently they play an essential role in modern display technology and continue to occupy the largest global market. Despite of the worldwide use the requirements concerning the response time, power consumption, viewing angles, contrast ratio and easy production stay beyond challenging for the next generation devices. Another urgent concern is that most of LCDs are developed based on indium tin oxide (ITO)- the most common used conductor in photonics technology today. Regardless of high transmittance, low sheet resistance and environmental stability, ITO requires high temperature processing, has poor mechanical flexibility and is restricted due to the indium scarcity in nature. Moreover, ITO limits the transmittance at near infrared spectral range which is critically important for biomedical diagnostics, remote sensing and near infrared image processing [2].

Recently, new transparent conductive layer attracts enormous attention due to the potential they hold related to very high conductivity, low sheet resistance and excellent transparency in a broad spectral range. For example, graphene is regarded as an excellent candidate to replace ITO because of its outstanding properties as high electronic mobility, exceptionally low absorbance and bendability on the flexible substrates. Several devices using alternative of ITO contacts in solar cells, organic light emitting diodes, field-effect transistors and infrared photodetectors has been reported [3,4].

We demonstrate fabrication of large scale graphene, related 2D materials and oxide/metal/oxide multilayers and their applications as transparent conductors. The quality of the layers, grown by low pressure CVD, ALD or magnetron sputtering methods were characterized by several techniques: AFM, SEM, Raman spectroscopy, optical and electrical measurements. Following, hybrid organic-inorganic structures based on strongly birefringent liquid crystals combined with highly photoconductive inorganic substrates using the above transparent conductive layers are prepared and demonstrated. Their modulation characteristics (driving voltage, phase modulation, response time) are compared and will be discussed.

In addition, novel flexible devices, based on graphene or oxide/metal/oxide as electrodes for displays and image processing will be demonstrated.

The proposed devices can find applications in liquid crystal display technologies, display holography, as phase retarders, optically addressed spatial light modulators, etc.

Acknowledgement: Financial support by Bulgarian Science Fund under the project FNI-T-02/26 is gratefully acknowledged.

REFERENCES

- [1] P. Yeh and C. Gu, Optics of liquid crystal displays, Wiley, New Jersey (2010).
- [2] [https://www.cdp.net/en/research/global-reports/global-supply-chain-report-\(2017\)](https://www.cdp.net/en/research/global-reports/global-supply-chain-report-(2017)).
- [3] Q. Zheng and J. K. Kim, Graphene for Transparent Conductors Synthesis, Properties and Applications, Springer (2015).
- [4] A. Stadler, Materials 5, 661 (2012).

Laser Fabrication of Diffractive Optical Elements for Two-dimensional Airy Beams

Bogdan – Ștefăniță Călin^{1,2}, Liliana Preda¹, Florin Jiipa², Marian Zamfirescu²

¹*Department of Physics,*

University “Politehnica” of Bucharest, Romania

²*CETAL, National Institute for Laser, Plasma and Radiation Physics,*

Bucharest – Măgurele, Romania

e-mail:bogdan.calin@inflpr.ro

Recent studies have been focused on the generation of non-diffractive beams such as the bi-dimensional Airy beam [1], which has direct applications in optical trapping and manipulation [2, 3], and light-sheet microscopy [4]. It is generally obtained using a spatial light modulator (SLM) controlled by a computer. These devices can only work with low intensities of the incident beam and require additional hardware in order to function (various electronic components, power source, data transfer protocol, etc).

A SLM is versatile but it is not integrable in low scale optical systems and is not appropriate for high power lasers. An alternative for these problems are Diffractive Optical Elements (DOE), which represent thin micro-structures used for modifying parameters of an incident wave. Many applications are based on utilizing DOE, among which beam shaping is the most common [5 - 7]. A DOE is a passive optical element with reduced size and weight that can modulate beams with greater intensity compared to a SLM. These aspects increase the functionality of the device as it provides increased flexibility for integration in complex optical systems that are reliable, cheap and easy to manufacture.

In this paper, the fabrication and testing of a DOE capable of generating bi-dimensional Airy beams is presented. Airy beams represent a class of non-diffracting beams that have the intensity profile modulated by an Airy function along the propagation direction [8] or the two orthogonal transverse directions [1]. This device's design is based on the “*Detour-Phase*” method [9] of creating a binary equivalent of the multi-level CGH which contains the information necessary to generate the desired transverse intensity distribution. The fabrication method approached in this case represents laser direct writing (LDW) based on laser ablation of thin films. We tested the obtained device using a laser pointer, in air, at room temperature.

REFERENCES

- [1] G. A. Siviloglou, D. N. Christodoulides, *Opt. Lett.* 32(8), 979 – 81 (2007).
- [2] Ziyu Zhao et al. *J. Opt.*, 18(2), article id. 025607 (2016).
- [3] J. Baumgartl et al., *Nat. Photon.* 2, 675-78 (2008).
- [4] Zhengyi Yang et al., *Biomed. Opt. Express* 5(10), 3434 – 42 (2014).
- [5] L. Ionel, C. P. Cristescu. *Optoelectron. Adv. Mat.* 5(9), 906 – 10 (2011).
- [6] L. Ionel. *Rom. Rep. Phys.* 65(3), 984 – 96 (2013).
- [7] Pedro J Valle et al. *J. Opt.* 16(5), article id. 055706 (2014).
- [8] Wei-Ping Zhong et al., *J. Phys. B: At. Mol. Opt. Phys.* 48(17), article id. 175401 (2015).
- [9] A. W. Lohmann, D. P. Paris, *OSA*, 6(10), 1739 – 48 (1967).

Development of composite wavelength tunable interference wedged structures for laser technology, spectroscopy and optical communications

Marin Nenchev¹, Margarita Deneva¹ and Elena Stoykova²

¹*Technical University –Sofia and Plovdiv Branch,
Quantum and Optoelectronics Scientific Laboratory (QOEL) and Department of Optoelectronics and Laser Engineering,
Plovdiv, Bulgaria*

²*Institute of Optical Materials and Technologies, Bulgarian Academy of Sciences, Sofia, Bulgaria
e-mail:marnenchev@yahoo.com*

Based on our previous experience [1-4], we proposed and developed as theory and experimental verification new compact composite tunable wedged interference structures and described their competitive application area. Each structure consists of multi-dielectric reflecting layers separated by transparent wedged layers (gaps) that are suitably superimposed to form a single sandwich type structure. The theoretical description of these structures is based on analysis of the multiple beams interference field formed at reflection and transmission. By choosing suitably the apex angles for separation layers and their optical thicknesses, selection of a single continuously tunable resonance within narrow-line transmission is obtained along the full length of the structure. The theory and experiment confirmed the expected useful property of such structures to combine wide range (~ 10-50 nm and more) linear tuning by simple translation along the wedge arms plane and selection of a very narrow single line (~ 0.01 nm or less). The transmission is of order of 30-50 %. Such structures allow also for working in the reflection mode [2,3], producing angular dispersion at increased efficiency (~ 50-70 %) and tuning at noted above parameters similarly to a diffraction grating but at substantially higher dispersion. We considered also some technological aspects of practical implementation of such structures. The developed structures, realized by superimposed micrometer thickness layers on glass or sapphire plate represent compact thin plane-list-like elements with dimensions of the order of 1 cm x 4 cm x 0.2 cm are of interest for applications in spectroscopy as a highly-dispersive and compact component for spectrum analysis of large size beams, in optical communications as a wavelength division multiplexing devices, permitting independent tuning of each selected output/input by translation of the structure in its plane, in laser technology for cavity spectral control especially for multi-wavelength operation with independent tuning of each selected narrow line and for continuously tunable single mode operation.

REFERENCES

- [1] E. Stoykova and M. Nenchev, J. Opt. Soc. of America JOSA 27, 58-68 (2010).
- [2] M. Nenchev, E. Stoykova, Appl. Optics, 40 (27), 5402-5411 (2001) and the literature therein
- [3] M. Nenchev, Y.H.Meyer, Appl. Phys. 24, 7-9 (1981).
- [4] M. Deneva, P. Uzunova, M. Nenchev, Opt. Quant.Electron, 39, 193-212 (2007).

Temperature Measurement with Ruby gauge

M. Nikolic¹, A. Vlastic¹ and D. Lukic¹

¹*Institute of Physics,*

University of Belgrade, Belgrade, Serbia

e-mail: lukic@ipb.ac.rs

The ruby R-line luminescence is commonly used as a manometer in diamond-anvil cell experiments [1]. It is also among the earliest of materials for which the fluorescence lifetime properties were proposed for thermometric applications. The actual use of ruby as the sensor element in a fiber optic fluorescence lifetime thermometer was perhaps first reported by Grattan [2]. In this thermometer system, a LED was used as the excitation light source and a silicon PIN diode was used for the detection of the fluorescence signal. Using that system, temperature measurement was achieved over the region from room temperature to 1700 C. We found a lot of papers about ruby R-line luminescence in function of temperature. In those papers, they measured lifetime [3], line shift [4] and wavelength difference [5] of R1 and R2 emission lines but we did not find measurements of the intensity ratio of R1 and R2 ruby fluorescence line to our best knowledge. We would like to devise this technique for development of the compact and low-cost system for measuring temperature in the range 200–800 K. To apply the ruby thermometer method, no additional effort is needed beyond that already incurred in the standard ruby pressure measurement.

The luminescent properties, such as the positions and widths of the luminescence peaks, the intensities of the luminescence lines and decay lifetimes of luminescence, change with temperature. The fluorescence intensity ratio (FIR) method is based on the intensity ratio between two emission lines or areas in the photoluminescent spectrum and estimation of temperature based on the ratio of their intensities. This technique is flexible and successful in measuring temperatures where conventional methods employing pyrometer, thermocouples or thermistors, may prove to be unsuitable. The intensity ratio of the detected emission is used to determine the temperature of a surface. This approach is very precise, simple, non-intrusive with a wide temperature range (from 10 K to 2000 K). Two lines are considered appropriate for intensity ratio method if they both have strong emission intensity in the whole temperature range, and if their intensity ratio gives high temperature resolution. This approach eliminates a number of errors coming from fluctuations of the excitation light source, temperature changes of excitation bands and non-uniform dopant's concentrations. A special case of the FIR measurement technique involves using the fluorescence intensities from two closely spaced, "thermally coupled" energy levels which relative population follows a Boltzmann type population distribution and is dependent on the temperature and the energy gap.

Here we used ideal case, where the intensity of one of the emission lines is independent of temperature; in this way a calibration between the ratios of emissions is indicative of temperature. With the increasing temperature, the upper level becomes more populated and therefore the fluorescence from this level gradually increases at the expense of the lower level population. We measured luminescence in function of temperature. We fitted ratio of R1/R2 with the function of temperature. We can see that we can apply this technique in the temperature range from 300 K to 600 K.

REFERENCES

- [1] G. J. Piermarini, S. Block, J. D. Barnett, and R. A. Forman, *J Appl Phys* 46, 2774-2780 (1975).
- [2] Grattan, K.T.V., Selli, R.K., Palmer, A.W., *Rev Sci Instrum* 59(8):1328-1335 (1988).
- [3] Steven P. Jamison, G.F. Imbusch, *Journal of Luminescence* 75, 143-147, (1997).
- [4] Richard C. Powell, Baldassare DiBartolo, Behzad Birang, Charles S. Naiman, *J Appl Phys* 37, 4973 (1966).
- [5] B. A. Weinstein, *Rev Sci Instrum* 57, 910 (1986).

Insight into different module options for the electro-absorption modulator

M. Trajkovic¹, F. Blache², H. Debregeas², K. Williams¹ and X. Leijtens¹

¹*COBRA Research Institute, Eindhoven University of Technology,*

P. O. Box 513, 5600 MB Eindhoven, Netherlands

²*III-V Lab, Campus de Polytechnique, 1 avenue Augustin Fresnel,*

F-91767 Palaiseau Cedex, France

e-mail: m.trajkovic@tue.nl

Photonic integrated circuits (PICs) have shown to be a promising solution for telecommunication transmitter devices in need of small footprint and low power consumption. The technology of integrating many different functionalities on a single chip allows us to design various circuits [1] [2]. However, in order to have a circuit which can be easily integrated in the whole system, we need to pay attention on how the PIC will perform once the driving electronic circuit comes into play. Different options have been used, such as wire bonding the PIC to the electronic circuit as the most standard way, and flip-chipping the PIC on the electronic circuit [3]. Another way of connecting them would be using a stud bump technique [4]. In this work we will concentrate on the modulator, namely the electro-absorption modulator (EAM), and its performance when connected in a module with the electronic part using the two of the mentioned techniques: wire bond and stud bump.

The electro-absorption modulator in comparison with the Mach-Zehnder modulator offers smaller footprint, lower biasing voltage and therefore lower power consumption. For these reasons, in transmitter circuits with many channels, the EAM is a preferred choice. Starting from measurements of S parameters of the modulator fabricated in III-V Lab, we obtain electrical equivalent model of the EAM. Together with the simulation of transmission lines on the photonic chip, we obtain the performance of the modulator in a setting when implemented with the laser. In order to operate the final circuit we need a drive, which operates at 50 Ohm, therefore the rest of the circuit should be matched to it in order to avoid the signal reflection. This is one of the problems which can occur if the driving signal coming directly to the modulator structure, as the modulator usually has quite lower series resistance. Therefore it is usually terminated with a load structure having 50 Ohms. In order to do this load structure can be placed on chip or off-chip. In the first scenario it can introduce extra heat, which increases power consumption. First we look at the case when the load is placed off-chip. For this purpose we use the aluminum-oxide (alumina) interposer, which can have different resistance and capacitance structures and transmission lines. We investigate three different options for the module (photonic chip and the alumina): driving signal comes to the alumina with the load resistance which is further wire-bonded to the PIC; driving signal comes to the EAM wire-bonded to the alumina with load, placed on top of the PIC; and finally, driving signal comes to the EAM connected via stud-bump to the alumina with load on top of the PIC. Using the transmission lines on both the PIC and the alumina, we are able to optimize the influence of the connecting pads and wire-bonds. This allows us to optimize the whole circuit and the performance of the EAM in the module.

REFERENCES

- [1] M. Smit et al, *Journal Semiconductor Science and Technology*, no. 8, pp. 1-41(2014).
- [2] R. Nagarajan, M. Kato, J. Pleumeekers, P. Evans, S. Corzine, S. Hurtt, A. Dentai, S. Murthy, M. Missey, R. Muthiah, R. A. Salvatore, C. Joyner, R. Schneider, M. Ziari, F. Kish and D. Welch, *IEEE Journal of Selected Topics in Quantum Electronics*, vol. 16, no. 5, pp. 1113-1125, (2010).
- [3] S. Kanazawa et al., *Journal of Lightwave Technology*, vol. 35, no. 3, pp. 418-422(2017).
- [4] W. Reinert, T. Harder, "Performance of the Stud Bump Bonding (SBB) Process in Comparison to Solder Flip Chip Technology", 4th International Conference on Adhesive Joining and Coating Technology in Electronics Manufacturing, (2000).

Optimization of the cleaning properties of fog by means of an optical sensor for control of impurities in fog

O. Ivanov¹, P. Todorov¹, S. Markova¹, Y. Ralev¹, J. L. Pérez-Díaz²

¹*Institute of Solid State Physics Georgi Nadjakov – Bulgarian Academy of Sciences, Sofia, Bulgaria*

²*Escuela Politécnica Superior, Universidad de Alcalá, Alcalá de Henares, Spain*

e-mail:ogi124@yahoo.com

When there is some kind of pollution in a certain area, fog is very often used as a cleaning agent. This work presents the possibility to optimize the cleaning properties of fog. For this purpose, a sensor, which is based on the surface photo-charge effect (SPCE), is used to detect the most efficient interaction between fog and impurities, i.e. which fog droplets can be used to most effectively clean an impurity from air. A specially designed automated system for aerosol generation allows a precise control over the fog parameters and the use of fluids with specific concentrations of chemical compounds to be pulverized. The number and the diameter distribution of droplets is varied by changing the feeding gas pressure to the nozzle. The experimental results showed the parameters of fog, which collects most of the impurity.

Systems for 2-dimensional laser scanning of solid surfaces

O. Ivanov¹, K. Pashev, P. Todorov¹, Y. Ralev¹, J. L. Pérez-Díaz², K. Balashev

¹*Institute of Solid State Physics Georgi Nadjakov – Bulgarian Academy of Sciences, Sofia, Bulgaria*

²*Escuela Politécnica Superior, Universidad de Alcalá, Alcalá de Henares, Spain*

e-mail:ogi124@yahoo.com

In this paper, optical systems for scanning by means of a laser, in combination with analog and digital measuring devices, are presented. The prototypes are made for 2-dimensional scanning of different kinds of surfaces and for detection of different irregularities on them. Their operation is based on the laser induced charge effect. Our systems allow various sizes of different kinds of surfaces to be scanned and the results can be visualized on a computer. The aim of this work is to describe these two types of systems (analog and digital) and to show example results from scanning. These results are obtained in a relation to the development of new types of fog sensors, based on the laser radiation-solid interaction.

Multiparameter QKD authentication protocol design over optical quantum channel

Nemanja Miljković¹, Aleksandar Stojanović², Rubens Viana Ramos², Petar Matavulj¹

¹*School of Electrical Engineering,
University of Belgrade, Serbia*

²*Department DETI, Federal University of Ceara,
Fortaleza, Brazil*

e-mail: mnemanja92.etf@gmail.com

While information and communication security are becoming one of the biggest global security issues, the new methodology named quantum key distribution (QKD), that guarantees security by the laws of fundamental physics, is introduced. Without proper authentication QKD technology is insecure. In this paper more general physical architecture (aimed for the authentication of both BB84 and B92 protocols) is proposed and elaborated. In addition, performances of these protocols are evaluated and discussed. These protocols are using polarization as a degree of freedom to transmit secret data. Polarization, as a basic property of light, must be taken into account in any practical QKD system performance evaluation independently from the choice of the degree of freedom.

In our previous work we proposed physical model for authentication of B92 QKD protocol that is based on analogy with optical chaotic systems. That model provided improved security in comparison to recently proposed models [1]. The proposed scheme guarantees high level provable security, which is currently (along with eavesdropper detection), the main merit of quantum cryptography [2]. Also, in that work each relevant authentication step is explained and functionality of that system (along with provable security) is confirmed via simulation. It is very important to note that the proposed optoelectronics schemes for authentication of B92 protocol are based on purely optical schemes which are previously introduced and verified as highly provably secure [3]. Moreover, these technical schemes can be seen as refinements of physical-optical schemes (that integrates quantum cryptographic and chaotic processes in encryption module of QKD communication system) on which are based. The main improvement lies in increased ability to perform synchronization, via introducing increased number of security parameters, which are possible to control electronically.

Information security is quantitative issue. Mathematically speaking, the main difference between quantum and classical security model is the fact that we need multiple number criteria in order to correctly describe quantum security (in classical case, typically, single number criteria may be enough). That fact indicates the intuitive idea that, by increasing the number of secret parameters of the proposed optoelectronics scheme, provable security level of the complete communication system increases. Comparing to [1], power level has been introduced as additional security parameter. Since the mentioned security parameter is easy to control via introducing simple additional electronic module, increased non-linearity will not affect significantly total functionality of the proposed scheme. The main contribution of this work is the fact that, by achieving high level synchronization among Alice and Bob experimental setups, we can determine (with certain probability) quantum channel behaviour, providing complete QKD authentication security model (which authenticates Alice, classical messages and quantum channel with optical losses) at the same time. Finally, complete solution for QKD authentication provides assistant procedure for the lack of ideal quantum detectors.

REFERENCES:

- [1] N. Miljkovic, A. Stojanovic, P. Matavulj, *Proc. TELFOR conf.* 1 915-918 (2016).
- [2] H. Yuen arXiv:1602.07602v1 [quant-ph] Security of Quantum Key Distribution (2016).
- [3] A. Stojanovic, R. V. Ramos, P. Matavulj, *Opt. Quant. Electron.* 48 (2016), 285:1-7.

Reconfigurable all-optical NAND/NOR logic gate based on dual injection-locked laser diodes

M. Lalović, A. Mićević, M. Krstić, J. Crnjanski, A. Totović and D. Gvozdić

School of Electrical Engineering,

University of Belgrade, Serbia

e-mail: marko.krstic@etf.bg.ac.rs

All-optical signal processing is the cornerstone of future optical packet switched networks, which hold the promise of a highly reconfigurable, bandwidth-efficient, and flexible optical layer. Among all other logic gates, NOR and NAND play a significant role on optical computing, switching, and networking, since these, so called “universal gates”, can be used to construct all other gates and thus can serve as the sole building blocks of the optical signal processors. The key features for these all-optical logic gates, in addition to the operation speed, are their reconfigurability, as well as low energy dissipation. There are several proposed schemes to design all-optical gates which can provide reconfigurable NOR/NAND logic. Some of the proposed methods are based on nonlinear vertical-cavity semiconductor gates with saturable absorption [1], while other approaches exploit Mach–Zehnder interferometers configuration comprising two parallel semiconductor optical amplifiers [2] or cross-waveguide geometries including photonic crystal nonlinear cavity [3]. However, these solutions exhibit relatively high thermal footprint and/or demand significant signal powers.

In order to provide an energy efficient and physically compact solution, we propose reconfigurable NAND/NOR all optical logic gate based on the intermodal dual injection-locked semiconductor laser [4]. So far, the injection-locked laser has been used for realization of individual all-optical NOR [5] and NAND gates [6]. However, in our approach, NAND and NOR gate are integrated in one reconfigurable device. The reconfiguration of the scheme that allows conversion from one gate to the other is achieved simply by adjusting the bias current. The bias current shifts the power level needed for suppression of central mode and thus, depending on the level of the two injection powers, central mode gets suppressed or not. In this way, the bias current variation can provide necessary power differences between the slave laser outputs in different regimes of injection-locking, depending on the desired logic. At this point, our proposed NOR logic operates at very low bias currents (order of 15 mA), while NAND logic operates at somewhat higher values, however still considered to be low bias currents (order of 35 mA). The injection powers necessary to achieve the state of logical zero and logical one are fixed in both operation modes (both NAND and NOR), and have values of -7 and 7 dBm, respectively. The wavelengths of the two input signals which lead to dual injection of the slave laser, can be different, which provides an extra degree of freedom for the proposed device. The range of signal wavelength comprises the region around the gain peak, and can be relatively wide.

At this level, we demonstrate the switching speed of 2 Gb/s for both NOR and NAND mode of operation. The extinction ratio for NAND device is around 15 dB, while NOR gate provides better extinction ratio of about 25 dB. The rise and the fall times of NAND gate are both of the order of 200 ps, while in the case of NOR gate, the obtained values for both times are between 50 ps and 100 ps.

REFERENCES

- [1] C. Porzi, M. Guina, A. Bogoni and L. Poti, *IEEE Sel. Top. Quantum Electron* 14, 927 (2008).
- [2] J-Y Kim, J-M Kang, T-Y Kim, and S-K Han, *J. Lightwave Technol.* 24, 3392 (2006).
- [3] Y. J. Jung, S. Yu, S. Koo, H. Yu, S. Han, N. Park, J. H. Kim, Y. M. Jhon and S. Lee, *Conference on CLEO/PACIFIC RIM* (2009).
- [4] S. Zarić, M. Krstić, J. Crnjanski, *Opt Quant Electron* 48, 295 (2016).
- [5] B. Nakarmi, M. Rakib-Uddin and Y. H. Won, *Opt. Eng.* 50, 075201 (2011).
- [6] B. Nakarmi, X. Zhang, and Y. H. Won, *Opt. Express* 23, 26952 (2015).

Ultrahigh-speed hybrid VCSEL for short-distance optical interconnects

V. Topić¹, G. C. Park¹, S. Tandukar¹, L. Ottaviano¹ and I.-S. Chung¹

¹*Department of Photonics Engineering, Technical University of Denmark*

DK-2800 Kgs. Lyngby, Denmark

e-mail:vlato@fotonik.dtu.dk

Limited capacity and high power consumption of electrical interconnects has motivated rising interest and use of optical interconnects for short-distance communications, such as inside large data centers, both for on- and off-chip interconnects [1]. For a light source in these optical interconnects, the energy consumption per /bit (energy/bit) is required to be up to two or three orders of magnitude smaller than the conventional devices. To meet this requirement, many innovative laser diode structures have been proposed. In this work, we aim to experimentally investigate and demonstrate Si-integrated long-wavelength hybrid vertical-cavity lasers (VCLs) that would fit this application [2].

Hybrid vertical cavity lasers (VCLs) are emerging as a promising light source for silicon (Si) photonics, as they can be designed for in-plane light emission into a Si waveguide as well as they have the potential for small energy consumption and the potential for ultra-high-speed operation [3]. In the hybrid VCL, the bottom mirror is a high contrast grating (HCG) reflector which is formed in the Si layer of a Si-on-insulator (SOI) wafer. A III-V compound semiconductor layer including the gain material, is attached to the SOI by using wafer bonding techniques. The top mirror can be part of the III-V layer or be deposited subsequently after the wafer bonding. The HCG reflector is a key element to achieve the aforementioned properties of hybrid VCLs as it has very small field penetration, which allows for significant reduction of modal volume compared to traditional VCLs based on distributed Bragg reflectors. This leads to high direct modulation speeds.

To form a HCG, Si grating needs to be surrounded by low index material on both sides. For that purpose, a 200-nm-thick SiO₂ layer is deposited on the III-V layer before wafer bonding. This thin low refractive index layer also serves as a dummy cavity. Second mirror is formed by depositing 6 pairs of SiO₂/Si DBR layers. The III-V epitaxy is grown on an InP substrate and contains InGaAsP quantum wells (QW) and a tunnel junction. To transfer the III-V epitaxy to a SOI wafer, adhesive bonding method is used. With this method, good bonding strength and yield can be achieved, while requirements on surface flatness and cleanliness are less strict and lower temperatures are needed compared to other bonding methods. For maintaining optical properties of the cavity and good heat dissipation, the bonding is done by using very thin DVS-BCB (divinylsiloxane-bis-benzocyclobutene) polymer [4]. DVS-BCB is diluted with mesitylene in ratio 1:8 to achieve layer thickness as thin as 35 nm, and spin-coated on a III-V die. After short precuring to evaporate mesitylene, the die is manually contacted at room temperature and loaded into wafer bonding tool. Curing is done at low pressure (10⁻⁶ mbar) at 250°C for one hour while a pressure of 400 kPa is applied to the stack. After bonding, the InP substrate is removed by wet etching and the III-V stack is patterned using dry etching. Electrical ohmic contacts and a top DBR mirror are then fabricated. As the final step, a current aperture is formed. Details of device characterization will be presented in the conference.

REFERENCES

- [1] W. H. Hofmann et al., *IEEE Photon. J.* 4, 652–656 (2012).
- [2] I.-S. Chung and J. Mørk, J., *Appl. Phys. Lett.* 97, 151113 (2010).
- [3] G. C. Park et al., *Sci. Rep.*, 6, 38801 (2016).
- [4] S. Keyvaninia, et al., *Opt Mater Express*, 3(1), 35-46 (2013).

Improving Quality of Service in four-channel WDM Ethernet Passive Optical Network

B. Pajčin^{1,2}, P. Matavulj¹ and M. Radivojević³

¹*School of Electrical Engineering,
University of Belgrade, Serbia*

²*IRITEL A.D. Beograd,
Belgrade, Serbia*

³*School of Computing Science,
University Union, Belgrade, Serbia
e-mail:bojan@iritel.com*

Today, Passive Optical Network (PON) is one of the most promising access technologies for providing broadband services to end-users. PON is a single-channel system with fiber as shared resource, hence better fiber utilization can be achieved with implementation of Wavelength Division Multiplexing (WDM) technology for multi-channel support.

Architecture of four-channel WDM EPON which fulfills guaranteed Quality of Service (QoS) is presented in [1]. Implementation energy saving mechanisms in presented four-channel WDM EPON results with the energy efficient WDM EPON presented in [2]. Also, capabilities of energy savings for this access network are discussed in [2], while by simulations obtained values of Key Performance Indicators (KPIs) are listed in [3]. Required changes in structure of Multi Point Control Protocol (MPCP) messages.

It's noticed that redefining Dynamic Bandwidth Allocation (DBA) algorithm could improve KPIs and as a consequence enable providing better services to end-users. Consequences of improving QoS is decrease of energy saving. In [4] is presented how long ONU can sleep when modified DBA is implemented. From [4], it is evident that we can still achieve significant energy savings with improved QoS. Main change in new DBA algorithm is introducing independent bandwidth allocation for each wavelength, which results in efficient bandwidth management and utilization.

This paper presents a new DBA algorithm and changes in the MPCP protocol necessary for its implementation. Mathematical model for modified DBA algorithm is described. Improvements in terms of packet delay and non-allocated bandwidth for each of the three wavelengths that are used are shown. For the most priority services average packet delay is reduced up to 50%, while the application of a new DBA algorithm now allocates from 10% to 75% less bandwidth for each class of service (each wavelength) when compared to results from [3]. Other QoS parameters, packet delay variation and packet loss, are also discussed.

REFERENCES

- [1] M. Radivojevic, P. Matavulj, *The Emerging WDM EPON*, Academic Mind, Belgrade, SRB (2012).
- [2] B. Pajcin, P. Matavulj, M. Radivojevic, *Opt. Quant. Electron.* 48 (2016), 313:1-7.
- [3] B. Pajcin, P. Matavulj, M. Radivojevic, *Proc. FOAN conf.* 1, 29-34 (2016).
- [4] B. Pajcin, P. Matavulj, M. Radivojevic, *Infoteh-Jahorina* 16, 207-210 (2017).

Quiescent points of self-seeded RSOA-FCL with Rayleigh backscattering feedback

A. Totović, J. Crnjanski, M. Krstić and D. Gvozdić
*School of Electrical Engineering,
University of Belgrade, Serbia
e-mail:angiel1006@etf.rs*

Extending the optical link to user premises is one of the main infrastructural advances in optical networks that is eagerly expected, both by general public, and by industry. In order to do so, solutions that are low-cost, low-power-consuming and colorless need to be developed, such that the end-users would not suffer from additional expenses during the transition period. Today, one of the main issues on this road is the realization of the conceptually simple transmitter, which can support dynamical wavelength allocation and can provide sufficiently high traffic throughput [1]. One such solution, that is attracting attention recently, is fiber cavity laser (FCL) based on self-seeded reflective semiconductor optical amplifier (RSOA) [2, 3].

RSOA-FCL may be viewed as an external cavity laser, where the RSOA plays the role of an active mirror – a concentrated, gain-providing reflector, whereas the fiber is an external cavity and a combined reflector. The distributed feedback is achieved through the mechanism of spontaneous Rayleigh backscattering (SRB), whereas the optional, concentrated feedback is realized through the mirror placed at the remote node (RN) fiber end. The operating wavelength can be chosen by placing the optical band-pass filter (OBPF) between the fiber and RSOA. Majority of the research done so far on RSOA-FCLs, assume that the dominant feedback mechanism comes from the existence of the RN mirror, whereas the OBPF is used to achieve lasing by suppressing the amplified spontaneous (ASE) noise in the part of the spectrum that is not of interest [2]. In our study, we show that neither of the two, RN mirror and OBPF, are essential for the RSOA-FCL operation, which significantly simplifies its implementation.

In our work, we numerically demonstrate the RSOA-FCL operation based on SRB and without the OBPF. By numerical simulation, we find the lasing threshold current. Our analysis shows that no lasing exists as long as the steady-state unsaturated standalone RSOA gain is below the gain threshold, determined by the losses due to coupling, fiber attenuation accounting for SRB, and RN mirror reflectivity. In this regime of operation, weak ASE noise determines the RSOA-FCL output power. When the unsaturated standalone RSOA gain reaches the gain threshold, lasing is established. From this point onward, regardless of increase in bias current, the gain of the embedded RSOA remains fixed and equal to the threshold value. Since the increase in bias current shifts the whole steady-state gain-versus-input-power characteristic of the standalone RSOA, in the lasing regime, the quiescent point of the embedded RSOA shifts towards the saturation region. This, in turn, provides a higher power at the embedded RSOA output, and consequently, at the RSOA-FCL output, recorded at the RN.

We compare the results for RSOA-FCL with and without the RN mirror, and we determine the differences in threshold gain and threshold current. Additionally, we investigate the correlation between the RSOA-FCL parameters and the threshold current value, along with the laser P-I characteristics slope.

REFERENCES

- [1] A. A. M. Saleh, J. M. Simmons, *Proc. IEEE*, 100, 1105, (2012).
- [2] S. A. Gebrewold, L. Marazzi, P. Parolari, R. Brenot, S. P. Ó. Dúill, R. Bonjour, D. Hillerkuss, C. Hafner, J. Leuthold, *IEEE J. Sel. Top. Quant. Electron.*, 20, 503, (2014).
- [3] S. A. Gebrewold, R. Bonjour, S. Barbet, A. Maho, R. Brenot, P. Chanclou, M. Brunero, L. Marazzi, P. Parolari, A. Totović, D. Gvozdić, D. Hillerkuss, C. Hafner, J. Leuthold, *Appl. Sci.*, 5, 1922, (2015).

Estimation of Rayleigh scattering loss in a double clad photonic crystal fiber

M. S. Kovacevic¹, Lj. Kuzmanovic¹, and A. Djordjevich²

¹*Faculty of Science,*

University of Kragujevac, Serbia

²*Department of Mechanical and Biomedical Engineering,*

City University of Hong Kong, China

e-mail: ljubica.kuzmanovic@pmf.kg.ac.rs

In this paper the effects of photonic crystal fiber's structure parameters on Rayleigh scattering were investigated in detail. Rayleigh scattering loss (RSL) has been estimated by Rayleigh scattering coefficient (RSC) and numerically based empirical relations for V parameter and W parameter of double clad photonic crystal fibers (DC PCFs). We demonstrated the dependence of RSL on the two structural parameters -air hole diameter and hole pitch. We have shown that RSL depends on the index profiles because of the different optical power confinement factors in every layer. Using these results, the RSL can be optimized for PCF by adjusting the air hole diameter and the hole pitch.

REFERENCES

- [1] K. Saito, M. M. Yamaguchi, A. J. Ikushima, K. Ohsono, and Y. Kurosawa, *J. Appl. Phys.* **95**, 1733 (2004).
- [2] H. Kanamori, H. Yakota, G. Tanaka, M. Watanabe, Y. Ishiguro, I. Yoshida, T. Kakii, S. Itoh, Y. Asano, and S. Tanaka, *J. Lightwave Technol.* **LT-4**, 1144 (1986).
- [3] K. Tsujikawa, K. Tajima, and M. Ohashi, *J. Lightwave Technol.* **18**, 1528 (2000).
- [4] K. Tsujikawa, M. Ohashi, K. Shiraki, and M. Tateda, *Electron. Lett.* **30**, 351 (1994).
- [5] K. Tsujikawa, M. Ohashi, K. Shiraki, and M. Tateda, *Electron. Lett.* **31**, 1940 (1995).
- [6] K. Tajima, in *Optical Fiber Communication Conference*, Vol. 2 of 1998 OSA Technical Digest Series (Optical Society of America, Washington, D.C., 1998), pp. 305-306.
- [7] M. Ohashi, K. Shiraki, and K. Tajima, *J. Lightwave Technol.* **10**, 539 (1992).
- [8] M. Pournoury, D. S. Moon, T. Nayari, S. H. Kassani, M. H. Do, Y. S. Lee, K. Oh, *Opt. Commun.* **317**, 13 (2014).
- [9] K. Saitoh, and M. Koshiba, *Opt. Express* **13**, 267 (2005).
- [10] A.W. Snyder, *Optical Waveguide Theory* Chapman and Hall, New York, (1983).

Relaxation times of population and coherences in Rb vapor

Ivan S. Radojičić¹, Mohammadreza Gharavipour², Aleksandar J. Krmpot¹, Gaetano Mileti² and Brana M. Jelenković¹

¹*Institute of Physic Belgrade, Pregrevica 118, 11080 Zemun, Belgrade, Serbia*

²*Laboratoire Temps-Fréquence (LTF), Institut de physique, Université de Neuchâtel, Switzerland*
e-mail:ivan.radojicic@ipb.ac.rs

Alkali atomic vapors are widely used in many high-resolution atomic physics experiments, of particular importance is their applications in vapor cell atomic clocks or stable frequency standards [1]. Because resonant frequency of such stable oscillators is determined by the frequency of atomic transition, they provide unmatched accuracy and stability. Precisely, clock frequency is the transition between two Zeeman sublevels, with $m_F = 0$, of the two hyperfine levels of ground state of alkali atom. These two sublevels do not change, to the first order, their energy with magnetic field. In an alkali vapor clock a clock time sequence has three separate regions, optical pumping into one of Zeeman sublevels, atom interrogation by the electric field whose frequency is tuned to the clock transition, and probing of the population of one of the Zeeman sublevel. Using ⁸⁷Rb vapor, contained in glass cell together with two buffer gases (Ar and N₂), we have measured population decay time T1 after optical pumping, and decoherence time T2 after two-photon Raman excitations made coherent superposition of the two $m_F = 0$ sublevels. These measurements proceed other tests of particular vapor cell considered to be used in an atomic clock.

In this work we investigate: 1. Rates of population decay after optical pumping, and 2. Decay rates of coherences induced between magnetic sublevels during the interrogation time. For measuring decay of population or T1 time we applied Franzen scheme [2], or relaxation in a dark method. Decay of polarization of the hyperfine levels was measured from the linewidth of the electromagnetically induced transition (EIT) which is due to coherence between the two ground state sublevels, induced by two-photon in Raman resonance to the common excited state. The linewidth of the EIT is a measure of the coherence relaxation time [3], but since it is increased by the power broadenings, T₂ was determined after extrapolating measured EIT linewidths at different laser power, to zero power.

This work was supported by the Swiss National Science Foundation (Scopes project 152511) and Ministry of Education Science and Technological Development of Republic Serbia (III 45016 and OI 171038).

REFERENCES

- [1] J. Camparo, Phys. Today 60, 33 (2007).
- [2] W. Franzen, Phys. Rev. 115, 850 (1959).
- [3] J. Vanier and C. Mandache, Appl. Phys. B Lasers and Optics 87, 565 (2007).

The new system for transferring units of temperature in the optical pyrometry in DMDM

Violeta Stankovic, Boban Zarkov, Slavica Simic
*Directorate for Measures and Precious Metals,
Belgrade, Serbia*
e-mail: violetastankovic@dmdm.rs

New national optical thermometry standard has recently been repaired and maintained in the system for calibration of optical pyrometers with black-body and gray-body by non-contact method in Directorate for Measures and Precious Metals in Serbia (National home for Units and Measures). New national optical thermometry standard – optical pyrometer as a part of calibration system works in two sub-bands whereby the first sub-band means the temperature from 550 °C to 1000 °C and the other 900 °C to 1650 °C. This standard is used to transfer non-contact temperature, from itself to customer's optical pyrometer. Also, the complete system for transferring unit with optical pyrometer as a standard is checked by standard thermocouples measurement in the same system, simultaneously [1].

The output voltage of optical pyrometer and output of standard thermocouples in millivolts have been collected on different values of temperature by virtual instrumentation based on LabView software package. During the acquisition the temperature and voltaic dependence of optical pyrometer and thermocouples are recorded. The paper describes the working principle of the pyrometer and the calibration system for transferring unit by non-contact method [2].

The system has been used to calibrate customer's optical thermometer with measurement uncertainty level of confidence described in paper.

REFERENCES

- [1] J. Fischer, P. Saunders, M. Sadli, M. Battuello, C. Woung Park, Y. Zundong, H. Yoon, W. Li, E. van der Ham, F. Sakuma, Y. Yamada, M. Ballico, G. Machin, N. Fox, J. Hollandt, M. Matveyev, P. Bloembergen, S. Ug ,Uncertainty Budgets for Calibration of Radiation Thermometers below the Silver point , (April 2008).
- [2] J. V. Nicholas, D.R. White, Traceable Temperatures - An introduction to Temperature Measurement and Calibration, New Zealand (2001).

Evaluation of temporal scales of migration of cosmetic ingredients into the human skin by two-dimensional dynamic speckle analysis

E. Stoykova^{1,2}, B. Blagoeva¹, D. Nazarova¹, L. Nedelchev¹, T. Nikova¹,
Y.M. Kim², H.J. Kang²

¹*Institute of Optical Materials and Technologies, Bulgarian Academy of Sciences, Sofia, Bulgaria*

²*VR/AR Research Center, Korea Electronics Technology Institute, Seoul, South Korea*

e-mail: elena.stoykova@gmail.com

Non-destructive detection of physical or biological activity through statistical processing of speckle patterns on the surface of diffusely reflecting objects is a perspective branch in optical metrology [1,2]. Technological advances in computers and optical sensors made possible pointwise processing of a temporal sequence of correlated speckle images. The output is a two-dimensional (2D) spatial contour map of the estimate of a given statistical parameter chosen to characterize the time scales of ongoing processes which lead to microscopic changes of the tested object surface over time. The map is usually called an activity map as it shows the regions of faster or slower laser intensity fluctuations across the object. The pointwise intensity-based processing can be applied to 3D objects and is characterized with simple acquisition of the raw data [3,4]. Due to these valuable features, dynamic speckle analysis has been applied in a variety of biomedical and food quality assessment tasks [1].

The aim of this work is dynamic speckle analysis of the temporal scales of migration of cosmetic ingredients from the skin surface to the lower skin layers. Evaluation of these scales is important for quality assessment of cosmetic products. The measurement included acquisition of correlated in time speckle patterns from skin sections on the arm or on the wrist of a volunteer. For the purpose, the volunteer hand rested on the vibration-insulated table on some suitable background. We solved two tasks. The first one was to find the best recording conditions for capture of the speckle patterns from the skin surface. More specifically, this included: 1) evaluation of diffusely reflected intensity on the skin surface under coherent illumination at different wavelengths by photon migration technique in order to choose the background surface and the illumination wavelength; 2) evaluation of speckle parameters for the patterns acquired for skin sections with and without cosmetic ingredients; 3) selection of the most suitable pointwise algorithms for information retrieval. The pointwise processing makes possible simultaneous acquisition of the raw data for treated and non-treated skin sections by using a proper mask to cover the skin of the volunteer. The second task was determination of the temporal scales of penetration of cosmetic ingredients into the skin.

REFERENCES

- [1] H. Rabal, R. Braga, *Dynamic laser speckle and applications*, CRC Press, Boca Raton (2009).
- [2] R. Arizaga, N. Cap, H. Rabal, M. Trivi, *Opt. Eng.* 41, 287 (2002).
- [3] A. Saúde, F. de Menezes, P. Freitas, G. Rabelo, R. Braga, *JOSA A* 29, 1648 (2012).
- [4] E. Stoykova, D. Nazarova, N. Berberova, A. Gotchev, *Opt. Express* 23, 25128 (2015).

The Global Network of Optical Magnetometers for Exotic physics searches

T. Scholtes¹, Z. Grujić¹, V. Lebedev¹, and A. Weis¹

¹ *Department of Physics, University of Fribourg, Chemin du Musée 3, CH-1700 Fribourg, Switzerland*
e-mail:theo.scholtes@unifr.ch

According to generally accepted insights of modern cosmology, only 5% of the Universe's energy consists of the 'ordinary' matter that stars, planets and we, ourselves are made of. A substantially larger part is attributed to dark energy and dark matter, a yet unknown form of matter that does neither absorb, nor emit, nor scatter light and is not explained within the Standard model of physics.

The Global Network of Optical Magnetometers (GNOME [1]) is a project searching for dark matter by looking for atomic spin perturbations induced by the Earth's motion through the cosmic background.

The GNOME collaboration network consists of a set of optical magnetometer stations distributed over the globe streaming time-stamped local magnetic field readings to a common server, which processes data for website display [2] and for off-line data analysis. The detection of space-time correlated signals of the individual magnetometer nodes of the network would be a signature of transient dark-matter structure composed of exotic fields predicted by a class of dark-matter theories. A distributed multi-station detector network will not only discriminate real sought-for transient events from local magnetic perturbations (false positives), but will furthermore yield directional and temporal information on possible dark-matter interaction events.

One prominent science case for GNOME are so-called axions, proposed dark-matter candidates that may form spatial domain structures, thus giving rise to axion density gradients which may be detected via their coupling to atomic spins.

Currently, GNOME consists of six operational magnetometer nodes and efforts to extend the network by additional stations are on-going. Very recently the network has started its first long-term data-taking run that is expected to set new constraints on hypothetical axion properties. We will report on the status of the project with an emphasis on the Fribourg(Switzerland)-based GNOME node and discuss preliminary findings from the first coordinated long-term run.

REFERENCES

[1] S. Pustelny et al., *Ann. Phys.* 525, 659 (2013).

[2] <https://budker.uni-mainz.de/GNOME>

Light-shift in pulsed optically pumped Rubidium atomic clock

William Moreno, Matthieu Pellaton, Mohammadreza Gharavipour,
Florian Gruet, Christoph Affolderbach and Gaetano Mileti

*Laboratoire Temps-Fréquence (LTF), Institut de Physique
Université de Neuchâtel, Neuchâtel, Suisse
e-mail: william.moreno@unine.ch*

Compact and high-performance Rubidium (Rb) vapor-cell clocks are based on the hyperfine splitting frequency of the ground state of the ^{87}Rb atom. To extract this frequency, we combine optical and microwave spectroscopy in a vapor cell. The light is used to polarize and interrogate the Rb atoms population in the hyperfine ground-states, through optical pumping. While the microwave generated from a quartz oscillator, is used to extract the hyperfine splitting frequency through Ramsey interferometry [1]. This frequency is finally used to frequency stabilize the quartz oscillator. Nowadays, high performance compact atomic clocks achieve fractional short-term (1-100 s) stabilities of the order of few 10^{-13} (equivalent to or better than the short-term fractional frequency stability of Hydrogen masers). However, the medium to long-term (10^2 - 10^5 s) frequency stabilities below 10^{-14} are still challenging to obtain. Various parameters can generate medium-to-long-term instabilities. We quantify the impact of such perturbation via two quantities: a sensitivity coefficient, or shift coefficient, defined as the variation of the clock frequency with respect to the perturbing physical parameter (e.g. a power variation Δp), $\Delta\nu_{\text{clock}} / \Delta p$, and the amplitude of the fluctuation of the perturbing physical parameter itself at various time scales, $\sigma_p(\tau)$.

In this study, we focus on one of the most significant perturbations to the clock frequency when using a laser as optical source: the AC-Stark shift effect, or more commonly the “Light Shift” (LS) [2]. Both the laser intensity (I_L), and laser frequency (f_L), fluctuations perturb the clock frequency. The sensitivity coefficients are described by the intensity- (resp. frequency-) LS coefficients, defined as $\alpha = \Delta\nu_{\text{clock}} / \Delta I_L$ for a fixed laser frequency, and $\beta = \Delta\nu_{\text{clock}} / \Delta f_L$ for a fixed laser intensity I_L . We evaluate the impact of the laser source instabilities on the medium to long term stability of a pulsed optically pumped (POP) Rb clock. Such interrogation has the particularity to separate in time the light and the microwave interactions, and thus to reduce significantly the LS coefficients. However, a recent study has shown that a residual light-shift of the order of 10^{-14} can still be present [3]. In this previous study, LS coefficients were investigated by varying globally the laser intensities during the whole POP interrogation pulse cycle. In the present study, we present a more detailed picture of the light-shift coefficients coming from each phase of the POP interrogation cycle, separating it into contributions arising separately during the pump phase, the detection phase, or the free evolution phase (Ramsey time). We demonstrate that in addition to the AC Stark shift, another light shift effect limits significantly the performances of our clock. We discuss on the combination of these coefficients, deduced for each phase of the interrogation cycle, into a global coefficient and compare it with previous reported results.

Finally, we will present the impact of the light shift on the clock frequency stability, especially at integration time of $\tau = 10^4$ s. We measured global LS coefficients of $\alpha = 3.2 \cdot 10^{-13} / \%$ and $\beta = -1.6 \cdot 10^{-15} / \text{MHz}$ when the laser is stabilized to the $|5S_{1/2}, F = 2\rangle \leftrightarrow |5S_{1/2}, F = 3\rangle$ transition. The main contribution to the α -coefficient is coming from the detection phase with $\alpha_{\text{detection}} = 3 \cdot 10^{-13} / \%$ while the pump phase contribution is lower with $\alpha_{\text{pump}} = -4 \cdot 10^{-14} / \%$. It results in an estimated clock stability limitation coming from the light-shift of $6 \cdot 10^{-14}$ at integration time of $\tau = 10^4$ s. These estimations are in good agreement with our preliminary measured frequency stability reaching $6 \cdot 10^{-14}$ at $\tau = 10^4$ s of integration time.

REFERENCES

- [1] S. Micalizio, C. E. Calosso, A. Godone and F. Levi, *Metrologia*, 49 (2012).
- [2] C. Cohen-Tannoudji, PHD Thesis, Faculté des sciences de l’université de Paris (1962).
- [3] M. Gharavipour, I.S. Radojicic, F. Gruet, C. Affolderbach, A. J. Krmpot, B. M. Jelenkovic and G. Mileti, European Frequency and Time Forum (EFTF), (2016).

Improving the accuracy of cesium magnetometers

Z. D. Grujić¹, P. A. Koss², J. Piller¹, V. Lebedev¹, Y. Shi³, V. Dolgovskiy¹, T. Scholtes¹, S. Colombo¹ and A. Weis¹

¹Physics Department, University of Fribourg, Switzerland

²Instituut voor Kern- en Stralingsfysica Katholieke Universiteit Leuven, Leuven, Belgium

³Institute of Electronics, Chinese Academy of Sciences, Beijing 100190, China

e-mail: zoran.grujic@unifr.ch

A precise control of the applied $\approx 1 \mu\text{T}$ magnetic field B_0 is required for the ongoing search [1] for a permanent neutron electric dipole moment (nEDM) at the Paul Scherrer Institute (Switzerland). Signature of a possible nEDM is sought in terms of a change of the spin precession frequency of ultracold neutrons (UCN) induced by a static electric field applied either parallel or anti-parallel to the applied magnetic field. Ramsey's method of time - ~ 100 s - separated $\pi/2$ -pulses is used to measure the neutron precession frequency. As a contribution to the experiment our group delivered an array of 16 scalar Cs magnetometers mounted both above the high-voltage electrode and below the ground electrode used to apply the electric field to the neutrons. These magnetometers monitor temporal and spatial changes of the B_0 field. Despite their high sensitivity ($\approx 10 \text{ fT}/\text{Hz}^{1/2}$), when operated in the M_x -mode, our magnetometers have an accuracy in the upper pT range due to unavoidable phase setting errors in the deployed phase-feedback method.

Our recent investigation of a Cs magnetometer based on *free spin precession (FSP)*, in which spin orientation (vector polarization) is produced by amplitude-modulated circularly-polarized light [2] showed that – despite satisfactory sensitivity and improved accuracy with respect to the M_x magnetometer – the FSP magnetometer suffers from an (as yet not explained) systematic heading error limiting its accuracy.

Here we present the principle of operation of a magnetometer based on *free alignment precession (FAP)*. Atomic alignment (tensor polarization) is produced by linearly-polarized amplitude-modulated light. After pumping, the FAP signal is detected in a readout phase by the same light beam, set to a constant (low) intensity. When the field of interest is perpendicular to the light polarization, an oscillation at $2\omega_L$ is imprinted onto the transmitted light power. The photocurrent is amplified and digitized and an off-line analysis is used to infer the magnetic field magnitude $B \cong \gamma_F \omega_L$, where $\gamma_F \approx 3.5 \text{ Hz/nT}$. We will present our current progress, results and prospects of the FAP magnetometer.

REFERENCES

[1] J. M. Pendlebury et al., Phys. Rev. D 92, 092003 (2015).

[2] Z. D. Grujić, P. A. Koss, G. Bison, and A. Weis, Eur. Phys. J. D 69:135 (2015).

Europium and Samarium dopant ions as luminescent sensors of Y_2O_3 phase transitions under high pressure

Ana Vlašić¹, Mihailo Rabasović¹, Branka Murić¹, Vladan Čelebonović¹ and Marko G. Nikolić¹

¹*Institute of Physics,*

Belgrade, Serbia

e-mail:vlasic.ana88@gmail.com

Rare earth ions (RE^{3+}) are highly sensitive to local symmetry. Any change in the symmetry is observable in their luminescence spectra [1]. In this work we investigated the photoluminescence properties of cubic and monoclinic Y_2O_3 matrix, doped with either Eu^{3+} or Sm^{3+} ions, under high pressure. Photoluminescence emission measurements for cubic Y_2O_3 were recorded in the pressure range from 0 to 20 GPa for $Y_2O_3:Sm^{3+}$, and from 0 to 15 GPa for $Y_2O_3:Eu^{3+}$. Measurements for the monoclinic matrix were recorded from 0 to 8 GPa for $Y_2O_3:Eu^{3+}$.

With varying pressure the intensity ratio of ${}^4G_{5/2} \rightarrow {}^6H_{7/2}$ and ${}^4F_{3/2} \rightarrow {}^6H_{7/2}Sm^{3+}$ emission lines has three distinct regions. In the pressure range from 9.2 GPa to 13.1 GPa it has a steep pressure dependence and could be used for detecting a pressure induced phase transition in the Y_2O_3 matrix from cubic to monoclinic crystal structure. Furthermore, the intensity ratio of ${}^5D_0 \rightarrow {}^7F_1$ and ${}^5D_0 \rightarrow {}^7F_2Eu^{3+}$ emission lines in the cubic matrix has a similar pressure dependence to the intensity ratio of these Sm^{3+} emission lines. It matches the behavior of the pressure sensitive Sm^{3+} dependence in the range from 9.1 GPa to 11.6 GPa, and is proven to contain a phase transition around 11 GPa [2].

The monoclinic $Y_2O_3:Eu^{3+}$ also has a pressure-sensitive intensity ratio of ${}^5D_0 \rightarrow {}^7F_1$ and ${}^5D_0 \rightarrow {}^7F_2$ emission lines. The dependence is unambiguous, without phase transitions in the measured region. The definitive nature and high sensitivity suggests that this dependence can be used as an efficient high pressure sensor.

REFERENCES

[1] G. Blasse, B. C. Grabmaier, Luminescent Materials, Berlin, Springer Verlag (1994).

[2] J. Zhang, H. Cui, P. Zhu, C. Ma, X. Wu, H. Zhu, Y. Ma, Q. Cui, J. Appl. Phys. 115, 023502 (2014).

Excitation transfer from the Second to the First resonance line of Potassium observed in a hot atomic vapor

C. Andreeva¹, A. Krasteva¹, A. Markovski², S. Tsvetkov¹, S. Gateva¹, S. Gozzini³, S. Cartaleva¹

¹*Institute of Electronics, Bulgarian Academy of Sciences, boul. Tzarigradsko shosse 72, Sofia, Bulgaria*

²*Faculty of Automatics, Technical University of Sofia, Sofia, Bulgaria*

³*Istituto Nazionale di Ottica, CNR., S.S. \A. Gozzini " di Pisa, via Moruzzi 1, 56124 Pisa, Italy*
e-mail: chr.at.iebas@gmail.com

Potassium vapor contained in coated optical cells has been used for very effective preparation of sub-natural width coherent resonances on the first resonance line [1-3].

In this communication, we present experimental study of the fluorescence profiles of the second resonance line of potassium ($4s^2S_{1/2} \rightarrow 5p^2P_{3/2}$), with a wavelength of 404.4 nm, and their dependence on the atomic density. Excitation by violet tunable single frequency laser light leads not only to 404.4 nm fluorescence decay to the ground state, but also to a partial transfer of the $5p^2P_{3/2}$ atomic population to the excited $4p^2P_{1/2}$ and $4p^2P_{3/2}$ states of the first resonance line, due to cascade transitions. The second type of population transfer is evidenced by registration of the fluorescence profiles at the 770nm infrared $4s^2S_{1/2} \rightarrow 4p^2P_{1/2}$ transition.

The experiment is performed by exciting pure potassium vapor by means of a single-frequency laser light at 404.4 nm. The fluorescence profiles of the atomic fluorescence at 404.4 nm and 770 nm are registered separately. For this, two appropriate filters are used for discrimination and measurements are taken for the violet (404.4 nm) or infrared (770.1 nm) fluorescence. The cells are shielded against stray magnetic fields. Increasing the potassium source temperature, the violet fluorescence profile starts to exhibit a well expressed self-absorption dip, while such behavior is not observed for the infrared fluorescence profile. In addition, the infrared fluorescence registration demonstrates a significantly higher signal-to-noise ratio. In order to analyze the observed differences, simple modeling describing the atomic population transfer between the relevant potassium levels will be presented.

Further development is foreseen related to magneto optical resonances registration using the reported experimental approach.

The authors would like to acknowledge the support of the National Science Fund of Bulgaria (Contract N_DN 08-19 /14.12.2016).

REFERENCES

- [1] S. Gozzini, S. Cartaleva, A. Lucchesini, C. Marinelli, L. Marmugi, D. Slavov, T. Karaulanov, Eur. Phys. J. D 53, 153-161 (2009).
- [2] K. Nasyrov, S. Gozzini, A. Lucchesini, C. Marinelli, S. Gateva, S. Cartaleva, L. Marmugi, Phys. Rev. A 92 (4), art. no. 043803, (2015).
- [3] A. Lampis, R. Culver, B. Megyeri, J. Goldwin, Opt. Express 24, 15494-15505 (2016).

H-alpha line broadening in diagnostics of pulsed laser plasma in aqueous aerosol

M. Momčilović, J. Ciganović, J. Savović, M. Stoilković
Vinca Institute of Nuclear Sciences,
Belgrade, Serbia
 e-mail:missa@vinca.rs

Measurements and analysis of broadened profiles of the H-alpha line following laser-induced optical breakdown are presented. A primary goal of this work is to weigh the feasibility of pulsed CO₂ laser to produce analytically useful plasma in aqueous aerosol at open atmosphere.

Transversally Excited Atmospheric pressure (TEA) CO₂ laser lasing at 10.6 μm was used to generate atmospheric pressure breakdown plasma. Plasma was created by striking the laser pulses over the solid metal interface through which aqueous aerosol drifts carried by a current of argon [1]. Laser pulse duration was about 100 ns and energy of 160 mJ. Emission spectra were recorded by time-integrated space-resolved measurement technique using a 2-m spectrograph equipped with a CCD camera. The applied experimental setup gives the spectral resolution of 0.0086 nm/pix and instrumental line width of 0.02 nm.

H-alpha line was recorded at successive distances from the surface of the metal interface. H-alpha line profiles were analyzed using Full-widths at half-maximum (FWHM) parameter.

The pseudo-Voigt function consisting of a weighted sum of a Gaussian function and a Lorentzian function has been found to fit the H-alpha line profile successfully [2, 3]. On the very surface of the interface the Lorentz width was found to be 1.5 nm and gradually increases to about 1.8 nm at distances of 3-5 mm above the surface. This corresponds to the electron density range $1.5-2 \times 10^{23} \text{ m}^{-3}$. Thereafter, the line profile width steeply declines to distances of 7 mm that is the diameter of the stream of the aerosol. The Gauss width has more complex spatial shape. In the range of 0 mm to 3 mm from the surface the Gauss width was about 0.25 nm and then reaches maxima of about 0.4 nm at distances 4-5 mm from the surface.

The appropriate red shift of the H-alpha line was also recorded. Maximum shift of about 0.06 nm was recorded at distances of 4-5 mm from the surface. The spatial position of the maximal red shift corresponds to the position of the maximal Gauss width meaning the maximal gas temperature, i.e. speed of the plasma.

REFERENCES

- [1] M. Matijević, M. Stoilković, M. Momčilović, J. Savović, J. Ciganović and M. Kuzmanović, Laser-Induced Breakdown Spectroscopy at a Solid-Aqueous Aerosol Interface, 28th Summer School and International Symposium on the Physics of Ionized Gases, S P I G 2016, CONTRIBUTED PAPERS & ABSTRACTS OF INVITED LECTURES, Belgrade, Serbia, 348-351 (2016).
- [2] Lin Yang et al, JOURNAL OF APPLIED PHYSICS 115, 163106 (2014).
- [3] J. Torres et al., J. Phys. D: Appl. Phys. 40, 5929–5936(2007).

Frequency-doubled laser sources stabilized to Rb-cell references

N. Almat, W. Moreno, M. Pellaton, F. Gruet, C. Affolderbachand G. Mileti
Laboratoire Temps-Fréquence, Institut de Physique, Université de Neuchâtel
Neuchâtel, Switzerland
 e-mail: nil.almat@unine.ch

We have developed several frequency-stabilized optical sources that are based on frequency-doubling of commercial laser diodes emitting in the telecommunication C-band (1560 nm) in view of their use in Rubidium (Rb) vapor-cell based atomic clocks. In such clock, the laser light at 780 nm serves, first, to create a population polarization in the two hyperfine levels, $|5S_{1/2}, F=1\rangle$ and $|5S_{1/2}, F=2\rangle$, of Rb through the optical pumping process. And also, it is used to optically detect the clock signal whose frequency corresponds to the hyperfine energy level difference and strongly depends on the laser's frequency and intensity due to the light-shift (LS) effects [1]. To reduce the impact of the LS on the Rb atomic clock's stability, optical sources with high frequency ($< 10^{-11}$) and intensity ($< 10^{-3}$) stability are required. Here, we present a compact and modular four-laser system to evaluate such optical sources. The modular aspect of our four-laser scheme allows not only identifying the stability limits at all timescales for each system, but also determining the contribution of individual components to the system's overall instability. In addition, we evaluate the impact of the lasers' frequency and optical power fluctuations on our pulsed optically pumped (POP) Rb atomic clock [2] stability.

Our experimental setup is composed of two largely identical arms based on fiber-optics, and of two free-space and compact laser heads [3] used as optical frequency reference sources. Each of the two fibered arms consists of a fiber-pigtailed laser diode emitting at 1560 nm, one is a DFB laser (Emcore) and the other one an external cavity laser (Rio) with linewidths of the order of 2 MHz and of 2 kHz, respectively. The output light of the lasers is frequency-doubled by second harmonic generation (SHG) in a periodically poled lithium niobate waveguide. Finally, the laser frequency is stabilized to one of the ^{87}Rb D2 transition line using a frequency reference unit of 0.81 dm³ volume, which consists of a Rb vapor cell ($< 2\text{ cm}^3$) in Doppler-free spectroscopy scheme and two photodetectors with their pre-amplification electronics.

The frequency stabilities of the fibered laser sources are measured via two simultaneous heterodyne beat-notes established at 780 nm with the reference laser heads and at 1560 nm before the SHG with each other. The frequency-doubled lasers are stabilized to the cross-over (CO) signal $|5S_{1/2}, F=2\rangle \leftrightarrow |5P_{3/2}, F=1, 3\rangle$ and the reference laser heads to CO $|5S_{1/2}, F=2\rangle \leftrightarrow |5P_{3/2}, F=2, 3\rangle$. For all the lasers, the frequency stability in terms of overlapping Allan deviation, is better than $4 \cdot 10^{-12}$ at 1 s and $< 10^{-11}$ up to 10^4 s. The measured frequency stability for the Rio laser is currently limited by the instability of the reference laser head. The relative optical power stability at 780 nm is slightly better than 10^{-2} up to 10^4 s for the frequency-doubled fiber lasers. This currently presents a serious limitation for their use in high-performance Rb atomic clocks. The contribution of the frequency and optical power instabilities of the frequency-stabilized lasers is estimated using the LS coefficients determined on our POP Rb clock. The estimated total contribution to the clock instability is less than $1.5 \cdot 10^{-15}$ for the laser heads, $< 10^{-13}$ for the frequency-doubled Emcore laser and $< 5 \cdot 10^{-14}$ for Rio laser. Both frequency-doubled lasers provide a compact optical source at two different wavelengths, 780 nm and 1560 nm, with high frequency stability $< 10^{-11}$ up to 10^4 s. Concerning their implementation in our POP clock, an active optical power stabilization of the frequency-doubled lasers could further reduce the impact of the laser intensity fluctuations on the Rb atomic clock stability.

REFERENCES

- [1] B. S. Mathur, H. Tang and W. Happer, Phys. Rev. 171 1 (1968).
- [2] M. Gharavipour, C. Affolderbach, S. Kang, T. Bandi, F. Gruet, M. Pellaton and G. Mileti, J. of Phys. Conf. Ser. 723 012006 (2016).
- [3] F. Gruet, M. Pellaton, C. Affolderbach, T. Bandi, R. Matthey and G. Mileti, Proc. of the Int. Conf. on Space Optics (2012).

Retrieval of group refractive index in a dense atomic vapor helped by buffer gas-assisted radiation channeling

A. Papoyan¹, S. Shmavonyan¹, Davit Khachatryan¹ and G. Grigoryan¹

¹*Institute for Physical Research, NAS of Armenia,
Ashtarak, Armenia*

khachatryandavit333@gmail.com

Precise determination of dispersion and absorption properties of medium, notably on far wings of atomic resonance remains a challenge. We report on direct retrieval of the group refractive index in the spectral region of ~30 GHz covering hyperfine structure of Rb D₂ line, exploiting reflection spectrum from the optical cell where rubidium atoms are buffered by a high-density cesium vapor [1].

In our experiment we use a vapor cell with non-parallel windows, which does not exhibit interference effects associated with multiply reflected light from cell's boundaries outside the resonance. Nevertheless, in the vicinity of resonance line the vapor cell behaves as a low-finesse Fabry–Perot cavity. We attribute this behavior to fiber-type radiation channeling built up because of buffer gas-imprisonment of resonant atoms inside the laser beam. Group refractive index across the studied spectral region was determined from the frequency positions of interference oscillations of the reflected beam intensity.

The experimental results were compared with theoretical calculations based on the model presented in [2]. In this theory we consider one-dimensional problem with parallel boundaries, considering multiple reflection regime. The obtained results are fully consistent with experimental reflection spectra taken at different temperature conditions.

The presented technique can be used for dispersion measurements in dense buffered gases, quantitative studies of transition from dipole-dipole binary to multiparticle collisional regime, as well as for realization of optical effects in coherently driven hot atomic gases [3].

REFERENCES

- [1] A. Papoyan, S. Shmavonyan, D. Khachatryan, and G. Grigoryan, *J. Opt. Soc. Am. B* 34, 877 (2017).
- [2] A. Badalyan, V. Chaltykyan, G. Grigoryan, et al., *Eur. Phys. J. D* 37, 157 (2006).
- [3] D.J. Whiting, J. Keaveney, C.S. Adams, and I.G. Hughes, *Phys. Rev. A* 93, 043854 (2016).

Application of virtual instrumentation into the metrology system for optical thermometer calibration

Boban Zarkov, Slavica Simic
*Directorate of Measures and Precious Metals,
Belgrade, Serbia
e-mail:zarkov@dmdm.rs*

In this paper we describe a new acquisition system in National Metrology Institute of Republic of Serbia which is used to calibrate optical thermometers in the temperature range from 250 ° C to 1 650 ° C. The system is based on a virtual instrument made using the LabView software package. By measuring the voltage from the standard thermocouples and optical thermometers, through high-precision digital multimeters, we connect the temperature and the optical radiation of the body. It is possible to determine the calibration of the optical thermometer based on data obtained using Planck's law (the range above the temperatures of fixed points of silver, gold or copper based on ITS-90) or based on the Sakuma-Hattori equation for temperatures below the mentioned fixed point's temperatures.

The acquisition process of the signal from thermocouples and optical pyrometer (which is standardized), statistic processing, recording and storage of data are carried out automatically. By using a virtual instrument, the calibration process of thermometer is significantly faster and simpler, while the use of real-time graphic display provides better control over the process.

As a result of the optimization process and the usage of the acquisition system, the precision and accuracy of the measurement are increased and also the significant decrease in measurement of uncertainty type A have been noted, as well as the total measurement uncertainty in the process of optical thermometer calibration.

Second order optical autocorrelator for measuring ultra short laser pulses duration

Andreja Vladković¹, Mihailo Rabasović¹, Torsten Golz², Nikola Stojanović², Dejan Pantelić¹, Branislav Jelenković¹, Aleksandar Krmpot¹

¹*Institute of physics Belgrade, University of Belgrade,
Pregrevica 118,
11080 Belgrade, Serbia*

²*Deutsches Elektronensynchrotron (DESY),
Notkestrasse 85,
22607 Hamburg, Germany
e-mail: andrejav@ipb.ac.rs*

Second order, i.e. intensity, optical autocorrelation is well established and commonly used technique for ultrashort laser pulse duration measurements [1]. More advanced technique that combines autocorrelation and spectral measurements provides even exact temporal shape of the pulse [2]. We report on development of an intensity autocorrelator for measuring femtosecond pulses duration using a nonlinear crystal. Autocorrelator setup is based on Michelson interferometer with BBO (β Barium Borate) crystal in the detection arm for second harmonic generation. Corner cube prism on a motorised stage provides variable delay line. Photodiode with spectral filter was used for signal detection. Data acquisition, the stage driving and the autocorrelation traces display is performed by computer, acquisition card and specially developed software. The software performs simple data processing: filtering and calculation of the pulse duration as Full Width at Half Maximum (FWHM) of autocorrelation curve. Autocorrelator was used to measure duration of ultrashort pulses from a modelocked lasers. We have tested the set-up and the software for various pulse duration and wave lengths from two ultrafast lasers: Coherent Mira 900 (160fs, 700-1000nm) and Timebandwidth products, Yb GLX (200fs, 1040nm). For the longer pulse duration (150fs-5ps) regenerative amplifier Coherent RegA with external pulse compressor/stretcher was used.

Acknowledgments: This work is supported by bilateral project 451-03-01038/2015-09/1 between Ministry of Education, Science and Technological Development -MESTD of Republic of Serbia and German Academic Exchange Service-DAAD and by projects III45016 and OI 171038 of MESTD of Republic of Serbia.

REFERENCES

- [1] W. Demtroeder, Laser Spectroscopy, Springer (1996).
- [2] Rick Trebino, Frequency-Resolved Optical Gating: The Measurement of Ultrashort Laser Pulses, Springer (2002).

Origin of Space-separated Charges in Photoexcited Organic Heterojunctions on Subpicosecond Time Scales

Veljko Janković and Nenad Vukmirović

Scientific Computing Laboratory, Centre for the Study of Complex Systems, Institute of Physics Belgrade, University of Belgrade, Pregrevica 118, 11080 Belgrade, Serbia

e-mail: veljko.jankovic@ipb.ac.rs

The promise of economically viable and environmentally friendly conversion of sunlight into electrical energy has driven vigorous and interdisciplinary research on donor/acceptor heterojunction organic photovoltaics. However, the actual mechanism of the emergence of free charges on subpicosecond (<100-fs) time scales following the excitation of a heterojunction remains elusive.

We investigate subpicosecond exciton dynamics in the lattice model of an all-organic heterojunction. Exciton generation by means of a photoexcitation, exciton dissociation, and further charge separation are treated on equal footing and on a fully quantum level using the density matrix formalism combined with the dynamics controlled truncation scheme [1]. Our results indicate that the space-separated charges appearing on <100-fs time scales following the photoexcitation are predominantly directly optically generated [2], in contrast to the usual viewpoint that they originate from ultrafast population transfer from initially generated excitons in the donor material. The space-separated states acquire nonzero oscillator strengths from donor excitons thanks to the strong resonant mixing between these two groups of exciton states. The results of ultrafast pump-probe experiments are commonly interpreted in terms of exciton populations only. Our theoretical insights into the ultrafast pump-probe spectroscopy highlight the importance of coherences, which cannot be disregarded on such short time scales, in the interpretation of pump-probe spectra [2].

REFERENCES

- [1] V. Janković and N. Vukmirović, Phys. Rev. B 92, 235208 (2015).
- [2] V. Janković and N. Vukmirović, Phys. Rev. B 95, 075308 (2017).

High-harmonic generation in bulk diamond irradiated by intense ultrashort laser pulse

Tzveta Apostolova and Boyan Obreshkov

*Institute for Nuclear Research and Nuclear Energy, Bulgarian Academy of Sciences,
Tsarigradsko chaussee 72, Sofia 1784, Bulgaria
email:tzveta.apostolova@gmail.com*

We theoretically and numerically investigate the high-harmonic generation (HHG) from bulk diamond driven by a linearly polarized intense pulsed laser irradiation of wavelength 800 nm and time duration 15 fs [1]. For laser intensity in the range $1 \leq I \leq 50 \text{ TW/cm}^2$ we find that HHG spectrum consists of two plateaus with dominant odd-order harmonics extending beyond the 50th harmonic order. Consistently with experimental observations [2,3], we find that the cutoff energy of the two plateau region scales linearly with the laser electric field. Depending on the electric field, we distinguish three regimes of HHG spectrum: I) perturbative regime ($F \leq 1 \text{ V/nm}$) in which the intensity of different harmonics scales as I^n , where n is the harmonic order and I is the peak intensity of the laser pulse, II) intermediate regime ($1 \text{ V/nm} \leq F \leq 5 \text{ V/nm}$) in which the spectral intensity of different harmonic orders are comparable and scale as I^3 regardless of the harmonic order and III) non-perturbative regime ($F \geq 5 \text{ V/nm}$) in which HHG spectrum is composed of two plateaus with indistinguishable intensities of individual harmonics whose magnitudes are orders of magnitude lower in the second plateau. We find similarities of HHG in solids and HHG in gas phase [4] namely a few step process – i) hybridization of substrate orbitals creates a transiently conducting state of virtual electron-hole pairs ii) the electric field accelerates these virtual dipole pairs producing real electron-hole pairs, iii) the carriers experience an AC Stark shift, which widens the diamond bandgaps and iv) some fraction of electrons recombine with their holes resulting in the emission of a single energetic photon. The sensitivity of the HHG process to the finite pulse duration and the time lag in the emission of high harmonics is discussed. The obtained results prove the feasibility of diamond for attosecond pulse generation.

[1] T. Apostolova and B. Obreshkov, *arXiv preprint arXiv:1611.00805* (2016).

[2] G. Ndabashimiye et al., *Nature* 534, 520 (2016).

[3] S. Ghimire et al, *Nature Phys.* 3, 381 (2011).

[4] G. Vampa et al., *Nature* 522, 462 (2016).

En route: single-shot THz characterization technique for THz beamline at FLASH1

R. Pan¹, E. Zapolnova¹, T. Golz¹, M. Rabasovic², A. Krmpot², A. Vladkovic², J. Petrovic³, N. Stojanovic¹

¹ *Deutsches Elektronen-Synchrotron (DESY),*

Hamburg, Germany

² *Institute of Physics,*

Belgrade, Serbia

³ *Vinca Institute of Nuclear Sciences,*

Belgrade, Serbia

e-mail: rui.pan@desy.de

High-field THz radiation is a fascinating tool to study the interaction of electromagnetic waves with matter, such as demagnetization dynamics [1], tracking the ultrafast motion of a signal molecule [2], resonant control of states of matter [3] and et al. THz beamline at FLASH1 provides both tunable narrow bandwidth (1-30THz) and broad bandwidth intense THz pulses for user's experiment.

Recently we have developed a THz characterization tool, optimized for FLASH's THz spectral range. It is based on THz electro-optic (EO) sampling, in combination of EO spectral decoding for THz pulse arrival timing jitter correction. It enables characterization of THz pulse, as a statistical average used in the experiment, with high temporal and spectral resolution.

Because of the highly fluctuating nature of the THz generation process at FLASH, for certain class of experiments, knowledge of the individual THz pulse properties is essential. Thus a fast diagnostic of THz parameters is required and single-shot method offers clear advantages. The EO spectral decoding subsystem in the THz pulse characterization tool can be used as independent setup at performing single-shot measurements. However, due to the frequency interference in a long chirped laser pulse, the measured THz temporal profile is almost always distorted [4], particularly when characterizing ultra-broadband THz pulses with realistic probing laser.

In order to study this single-shot technique, the broad bandwidth THz dump radiation is measured by EO spectral decoding setup. The distortion is analyzed in details and the measured profiles show agreement with our calculations.

The measurements can help us to study possible retrieval strategies of the original THz electric field from the distorted measured one. This as a final goal has a single shot characterization of THz pulses for FLASH user experiments.

Authors acknowledge financial support from German Academic Exchange Service (DAAD Grant Number 57219839) and Federal Ministry for Education and Research (BMBF Grant Number 05K12CH4).

REFERENCES

- [1] B. Pfau, et al., Nature communications 3: 1100, (2012).
- [2] Cocker L.Tyler, et al., Nature 539.7628: 263-267 (2016).
- [3] Kampfrath Tobias, et al., Nature Photonics 7.9: 680-690(2013).
- [4] S. P. Jamison, et al., In proceedings of EPAC08.

Tunable High- field THz source at FLASH: Spectral and spatial characterization.

E. Zapolnova¹, T. Golz¹, R. Pan¹, A. Vladkovic².

M. Rabasovic², A. Krmpot², J. Petrovic³ and N. Stojanovic¹

¹*Deutsches Elektronen-Synchrotron DESY,
Hamburg, Germany*

²*Institute of Physics,
Belgrade, Serbia*

³*Vinca Institute of Nuclear Sciences,
Belgrade, Serbia*

Email: ekaterina.zapolnova@desy.de

4th generation X-ray light sources have attracted enormous attention of scientists from various fields, allowing conducting pump-probe experiments, which can reveal the mechanisms of chemical reactions and processes, occurring on the molecular and atomic level and on the time-scale of few femtoseconds.

FLASH (Free Electron Laser in Hamburg) has a world-wide unique ability to generate tunable, broadband, high-field THz pulses, which are synchronized with XUV pulses on the order of few femtoseconds [1, 2]. It opens the door to new exiting THz pump X-ray probe experiments, such as THz driven magnetization and ion dynamics, coherent spin control, etc. For such experiments it's extremely important to know the properties of the radiation, which is delivered to the experiment; therefore suitable tools for characterization are required.

We are presenting a custom made ultra-broadband FTIR Spectrometer (Fourier Transform Infrared), optimised for THz source at FLASH and a 2D beam-profiler, both optimized to detect high-field, broadband THz radiation (0.6 μm to 600 μm) and which are used as a part of the THz characterization tool, developed at THz beamline at FLASH. THz characterization tool also includes the Electro-optic Sampling (EOS) set up and Spectral Decoding (EOSD) set up, developed together in collaboration with the Institute of Physics and Vinca Institute of Nuclear Sciences in Belgrade, Serbia. We will also present the experiments, which have been conducted in THz beamline during last couple of years to give an overview on the exiting opportunities for light-matter interaction experiments with such an intense and broadband THz source.

Authors acknowledge financial support from German Academic Exchange Service (DAAD Grant Number 57219839) and Federal Ministry for Education and Research (BMBF Grant Number 05K12CH4).

REFERENCES

- [1] M. Gensch et. al., *Infrared Phys. Technol.* 51, 423(2008).
- [2] F. Tavella, N. Stojanovic, G. Geloni, M. Gensch, *Nat. Photon.* 5, 162(2011).

Multiphoton imaging with blue-diode-pumped SESAM-modelocked Ti:Sapphire oscillator

B. Resan^{1*}, A. Rohrbacher², O. E. Olarte³, and P. Loza-Alvarez³

¹*School of Engineering, University of Applied Sciences and Arts Northwestern Switzerland, Windisch*

²*Lumentum Switzerland AG, Schlieren, Switzerland*

³*ICFO-Institut de Ciències Fòtoniques, The Barcelona Institute of Science and Technology, Castelldefels (Barcelona), Spain*

e-mail: bojan.resan@fhnw.ch

More than any other gain media, titanium doped sapphire (Ti:Al₂O₃) is used as an ultrabroadband solid-state laser material for ultrashort pulse generation. Over the past decades, many pumping schemes were developed in the green region near the absorption maximum [1], but they all included complex and expensive solutions, typically a frequency converted solid-state laser. The complex pump laser adds to the cost, complexity and footprint of the whole Ti:Sapphire system and limits wider scale applications for everyday use in industrial, medical or scientific environments. Owing to the developments in the laser-projection technology, low-cost laser diodes emitting over 3 W in the blue region around 450 nm became available. Beside much lower cost and smaller footprint, direct diode pumping provides better reliability, higher efficiency and better pointing stability. Although having its challenges, direct blue diode pumping showed that Ti:Sapphire laser performance is feasible and ultrashort pulses can be achieved in the wide tunable spectral region [2,3]. However, the average power and pulse energy reported so far were rather low for most applications.

Our new developed laser is pumped by two Nichia laser diodes in a counterpropagating scheme. Each diode is driven at a current of 2.3 A and emits 2.9 W average power at wavelength around 450 nm. We used 4 mm long Brewster angle cut Ti:Sapphire crystal with 0.25 % doping. The group velocity dispersion introduced in the crystal is compensated by group delay dispersion (GDD) mirrors placed in one cavity arm. In the same arm the 7 % output coupler is used as an end mirror. The modelocking is obtained by focusing the beam onto a SESAM placed at the end of the other cavity arm. The laser generated 460 mW average power, i.e. 5 nJ pulse energy, at 92 MHz pulse repetition rate, wavelength was centered at 784.5 nm, and pulse duration was 82 fs with -900 fs² GDD compensation [4]. The calculated peak power was 61 kW. To our knowledge, this is the highest pulse energy achieved, about 5 times higher than previously published, and the highest peak power reported for direct diode pumped Ti:Sapphire lasers.

Such a laser is ideally suited for biomedical imaging and nanostructuring applications. We demonstrate its application in three color two-photon excitation fluorescence (TPEF) imaging [5] of a section of mouse intestine and BPAE cells; and 3D SHG microscopy images of collagen type-I from a commercial tendon sample.

REFERENCES

- [1] P. F. Moulton, *Opt. Soc. Am. B* 3(1), 125-133 (1986).
- [2] C. G. Durfee, T. Storz, J. Garlick, S. Hill, J. A. Squier, M. Kirchner, G. Taft, K. Shea, H. Kapteyn, M. Murnane, and S. Backus, *Opt. Express* 20, 13677-13683 (2012).
- [3] P. W. Roth, D. Burns, and A. J. Kemp, *Opt. Express* 20, 20630-20634 (2012).
- [4] A. Rohrbacher, O. E. Olarte, P. Loza-Alvarez, B. Resan, *Opt. Express* 25, 10667-10684 (2017).
- [5] C. Xu, W. Zipfel, J. B. Shear, R. M. Williams, and W. W. Webb, *Proc. Natl. Acad. Sci. U.S.A.* 93(20), 10763–10768 (1996).

One Approach to Laser Scanning Problems for Improving Road Condition Diagnostics

N.Slavkovic¹, D.Mamula Tartalja¹ and M.Bjelica²

¹ICT College, Belgrade, Serbia

²School of Electrical Engineering,
University of Belgrade, Serbia

e-mail:nikola.slavkovic@ict.edu.rs

Laser surface scanning is one of the diagnostic techniques based on processes of coherent light reflection. In the sense of road surface and undersurface inspection, it is one the most important technique directly contributing the road safety concept.

The laser beam reflection and transparenance in multilayer environments has been already considered in the various thin films theory approximations. Another technique that is closely connected to the surface scanning is geo diagnostics by geopenetrating radars (GPR). The overall road conditions inspection technology is analyzed in the various ranges of electromagnetic radiation, using different approximations, with the main theoretic support that is based on detecting material properties.

Based on the previous studies on interaction of light with non-metallic materials, optical, thermal, acoustic and other material properties were connected. For the given problem of road condition diagnostics, the characteristics of the signal reflected from the material can be evaluated and sent to the receiving multisensor platform. At the moment, the existing laser survey scanning techniques, with sophisticated devices for checking the road conditions, and their precision, are strongly dependent on meteorological conditions, sensing distance, laser induced and reflected beam angles, as well as conditions and structure of different concrete and asphalt road mixtures.

Moreover, the road can also be naturally covered with spilled oil, a slash of ice or the so-called black ice, water, snow, etc. These circumstances require the special knowledge of spectral optical properties, which depend on the type of incident beam used for road condition diagnostics, as well as its intensity. All the mentioned conditions in which the propagation and reflection of the laser diagnostic beam is performed, will inevitably affect the measurement errors, and in signal processing, conclusions can be made that do not show the authentic conditions of the roads, which can later lead to problems in road safety management. For this reason, we propose to model the laser light in interaction with the assumed layers.

This paper proposes the improvement of the complete signal processing procedure of the laser survey scanning method for road conditions, in terms of correction the above-mentioned errors, and the estimation of the measurement uncertainty of both types, A and B. This will be done by engaging the existing models, as well as forming new ones, where the diagnostic laser equipment will be interacted with the appropriate road surface material, which would increase the accuracy and the precision of the system itself.

REFERENCES

- [1] D.W. Law, L. Holden, and D. Silcock, *Australian Journ. of Civ. Eng.*, Vol. 13, Iss. 1, (2015).
- [2] T. Yamada, T. Muramatsu, Research on interaction of laser light and non-metals - Evaluation of laser irradiation behavior to concrete, JAEA-Research 2014-026, Japan Atomic Energy Agency, (2015).
- [3] S. C. Radopoulou, and I. Brilakis, *Automation in Construction*, 53, 95–104 (2015).
- [4] M Rabah, A. Elhattab, and A. Fayad. Automatic Concrete Cracks Detection and Mapping of Terrestrial Laser Scan Data. *NRIAG Journal of Astronomy and Geophysics* 2: 250–255 (2013).
- [5] G. Bitelli, A. Simone, F. Girardi, C. Lantieri, *Laser Scanning on Road Pavements: A New Approach for Characterizing Surface Texture*, *Sensors (Basel)*, 12(7): 9110–9128, (2012).

Photophoresis-based laser trapping with a line optical trap

A. Porfirev and S. Fomchenkov
Samara National Research University
Samara, Russia
e-mail:porfirev.alexey@gmail.com

It is known that laser trapping of light-absorbing nano- and microobjects in air occurs through the action of photophoretic forces [1]. In some cases, the photophoretic forces are several orders of magnitude greater than radiation pressure. Vortex beams [2], optical bottle beams [3] and single Gaussian beams [4] were used for such laser trapping. Use of Gaussian beams also makes it possible to perform three-dimensional manipulation of objects, but only if they have a non-spherical shape. In [5], a robust method to trap and manipulate ensembles of light-absorbing particles in air by using a three-dimensional (3D) optical lattice formed by overlapping coherent beams was proposed. The photophoretically trapped particles are attached to the nodes of the lattice and could be rotated and translated by moving the grating. In this paper, we propose a line optical trap generated by a cylindrical lens. This technique can be used to rotate and translate the trapped light-absorbing particles by turning the lens.

To generate the line optical trap, we used combination of the cylindrical lens and a microobjective. The cylindrical lens was mounted on the aperture rotation stage that allows us to rotate the generated line trap through 360 degrees. To demonstrate the optical trapping and rotation of light-absorbing particles in air, we used carbon nanoparticle agglomeration. These particles have a non-spherical shape, and therefore ideally suited for experiments of this kind that has been shown in previous experiments. The typical size of the agglomerations ranged up to tens of micrometers.

To spray the microparticles into the generated line optical trap, a syringe with an outlet diameter of approximately 700 μm was utilized. Particles emitted from a syringe rushed into the interior of the cell by the action of the initial external force and the gravity force. After falling into the region near the line optical trap, light-absorbing particles began to absorb the laser radiation, which led to their heating. The resulting photophoretic forces led to trapping particles inside the line optical trap. In experiments, we rotated the cylindrical lens around the axis, which led to the rotation of the particles, which were trapped inside the line optical trap at a distance from its central part. At the same time, the particles trapped in the line optical trap on the beam axis did not rotate.

REFERENCES

- [1] V.G. Shvedov, A.S. Desyatnikov, A.V. Rode, W. Krolikowski, Y.S. Kivshar, *Opt. Express* 17, 5743 (2009).
- [2] V.G. Shvedov, A.V. Rode, Y.V. Izdebskaya, A.S. Desyatnikov, W. Krolikowski, Y.S. Kivshar, *Phys. Rev. Lett.* 105, 118103 (2010).
- [3] V.G. Shvedov, C. Hnatovsky, A. Rode, and W. Krolikowski, *Opt. Express* 19, 17350 (2011).
- [4] Z. Zhang, D. Cannan, J. Liu, P. Zhang, D.N. Christodoulides, Z. Chen, *Opt. Express* 20, 16212 (2012).
- [5] V.G. Shvedov, C. Hnatovsky, N. Shostka, A.V. Rode, W. Krolikowski, *Opt. Lett.* 37, 1934 (2012).

Gold chloride cluster ions generated by vacuum laser ablation

Boris Rajčić¹, Silvana B. Dimitrijević², Marijana Petković¹, Marija Nišavić¹, Mario Cindrić³, Filip Veljković¹
and Suzana Veličković¹

¹University of Belgrade, Vinča Institute of Nuclear Sciences, Belgrade, Serbia

²Mining and Metallurgy Institute Bor, Bor, Serbia

³Ruđer Bošković Institute, Zagreb, Croatia

e-mail: boris@vin.bg.ac.rs

In this work we have studied the vapor species which are generated by pulsed Nd:YAG laser ablation of chloroauric acid (HAuCl₄) in the absence of a buffer or reactive atmosphere and without postablation supersonic expansion. The laser ablation of HAuCl₄ into vacuum generates significant yields of gold chloride cluster ions, the compositions of which were analyzed by time-of-flight mass spectrometry with a commercial matrix assisted laser desorption/ionization (MALDI) instrument.

Pulsed laser ablation and vaporization of solids have found wide application in the deposition of thin films of a wide variety of materials for various purposes such as producing a high-quality semiconductor films for electronic and optoelectronic devices [1]. For this reason many laser ablation studies have been focused on the properties and performance of such deposited materials. Also, a large efforts have aimed at characterizing laser-solid interactions and ablation vapor plume [2]. On the other side, the laser ablation it has been successfully applied for generating novel and large vapor cluster species such as homogenous and heterogeneous metal clusters [3]. Earlier results have shown that the ablation of laser-gold nanofilm (Au NF) under irradiation with a nanosecond pulsed laser probably follows a photothermal evaporation mechanism, in which absorption of laser energy by the Au NF leads to formation of Au-nanoparticles via spinodal dewetting, followed by surface melting, and eventually a decrease in size or splitting, due to evaporation from surface atoms or the entire particle. The formation of Au cluster ions during the evaporation of Au NFs is accompanied by electron ejection [4]. Gold halide clusters have significant applications in catalysis, optics, medicaments, and environmental sciences.

This work shows the possible formation of gold chloride cluster ions by the laser ablation. A small volume (0.5 μl) of HAuCl₄ solution was applied onto the stainless-steel sample plate and left to dry at room temperature. Different concentration of HAuCl₄ solution were analyzed, such as: 2,5 g Au/dm³ (initial solution), 0,25 g Au/dm³, and 0,025 g Au/dm³. The laser intensity was varied between 4000-5000 a.u. and the average of 1800 laser shots were taken for each spectrum. Preliminary results shows the formation of negative gold chloride cluster ions, such as: AuCl(HCl)(H₂O), AuCl₂, AuCl₂(HCl)₂H₂O, AuCl₂(HCl)₂(H₂O)₃, AuCl₂(HCl)₂(H₂O)₄, AuCl₂(HCl)₃(H₂O)₃, AuCl₂(HCl)₃(H₂O)₄, AuCl₃(HCl)₂(H₂O)₅, AuCl₄(HCl)₄, Au₂Cl(HCl)₃H₂O, Au₂Cl(HCl)₃(H₂O)₃, Au₂Cl(HCl)₅H₂O, Au₂Cl(HCl)₆H₂O, Au₂Cl(HCl)₅(H₂O)₂, Au₂Cl₂(HCl)₆(H₂O)₅. Concerning different concentrations, the spectra have shown that the intensities of these complex composition clusters, [Au_xCl_y(HCl)_m(H₂O)_n], formed from the HAuCl₄ increase with decreasing the concentration of HAuCl₄ solution.

Acknowledgement

This work was supported by the Ministry of Education, Science and Technological development of the Republic of Serbia (Project No. 172019).

REFERENCES

- [1] Cheung, J. T.; Horwitz, J. S., MRS Bull. 17(2), 30 (1992).
- [2] Leuchtner, R. E.; Horwitz, J. S.; Chrisey, D. B., In Laser Ablation in Materials Processing: Fundamentals and Applications, Materials Research Society Symposium Proceedings, Vol. 285, Braren, B., Dubowski, J. J., Norton, D. P., Eds.; MRS: Pittsburgh, 87-92 (1993).
- [3] Shuichi H.; Daniel W.; Takayuki U., Journal of Photochemistry and Photobiology C: Photochemistry Reviews 13, 28-54 (2012).
- [4] Hohlfeld J.; Wellershoff S. S.; Gudde J.; Conrad U.; Jahnke V.; Matthias E., Chem. Phys. 251, 237-258 (2000).

Effect of the Corrected Ionization Potential on the High-Harmonic Generation transition rate in a linearly polarized laser field

Violeta Petrović, Hristina Delibašić, Kristina Isaković
*Department of Physics, Faculty of Science,
University of Kragujevac, Serbia
e-mail: violeta.petrovickg@gmail.com*

Abstract: In this paper we theoretically described the influence of the ponderomotive and the Stark shift [1,2] on the high-order harmonic generation's transition rate (HHG rate) for the cases of noble and alkali atoms. To describe harmonic generation we used the analytical formula by Frolov et al. [3] which is derived for a weakly bound electron in the tunneling limit and modified it in way to include mentioned effects. Firstly, we assumed the general beam shape in nonrelativistic, linearly polarized laser field. We showed that the inclusion of these effects affects the HHG rate. For the same conditions, the intensity of the alkali harmonics were considerably weaker compared to the intensity of noble harmonics [4]. Also, the Stark shift for the alkali atoms induces not only decrease of the peak heights i.e. decrease of the ionization yield, but also the peak broadening. At the end, we analyzed the influence of the beam shape on the behavior of obtained theoretical curves. We considered two types of profiles of laser radiation, Gaussian and Lorentzian [5,6]. It is shown that the HHG rate depends on the spatial distribution of laser beam profiles.

REFERENCES

- [1] E. A. Volkova, A. M. Popov, O. V. Tikhonova, *J. Exp. Theor. Phys.* 113, 394 (2011).
- [2] K. Yamanouchi, M. Nisoli, W.T. Hill, *Progress in Ultrafast Intense Laser Science VIII*, (2012).
- [3] M. V. Frolov, N. L. Manakov, T. S. Sarantseva, A. F. Starace, *J. Phys. B: At. Mol. Opt. Phys.* 42, 035601 (2009).
- [4] A. D. Shiner, B. E. Schmidt, C. Trallero-Herrero, H. J. Wörner, S. Patchkovskii, P. B. Corkum, J-C. Kieffer, F. Légaré, D. M. Villeneuve, *Nature Physics* 7, 464 (2011).
- [5] I. I. Bondar, V. V. Suran, D. I. Bondar, *Phys. Rev. A* 88, 023407 (2013).
- [6] V. M Petrović, T. B. Miladinović, *Journal of Experimental and Theoretical Physics*, 119, 651 (2014).

Laser ablation of nickel/palladium multilayer thin films by nanosecond pulses

B. Salatić¹, S. Petrović², D. Peruško², I. Bogdanović-Radović³, M. Čekada⁴, P. Panjan⁴, D. Pantelić¹ and B. Jelenković¹

¹*Institute of Physics, University of Belgrade, Belgrade, Serbia*

²*Vinca Institute of Nuclear Sciences, University of Belgrade, P.O.Box 522, 11001 Belgrade, Serbia*

³*Ruđer Bošković Institute, P.O.Box 180, 10002 Zagreb, Croatia*

⁴*Jožef Stefan Institute, Jamova 39, 1000 Ljubljana, Slovenia*

e-mail:banes@ipb.ac.rs

Metallic thin films, based on nickel (Ni) and palladium (Pd) are promising material for a wide range of application, as catalytic components [1], optical devices [2], photovoltaic gas sensors [3], dye sensitized solar cells [4], and especially for environmental purposes [5]. The potential of nanosecond laser micro-processing for surface modification of nickel-palladium (Ni/Pd) multilayer thin film deposited on n-type (100) silicon wafer was studied. The multilayer structure composed of five bilayer (Pd/Ni) was deposited by d.c.sputtering from a pure Ni and Pd targets, using Ar ions, to a total thickness of about 180 nm. These multilayer thin films were then exposed to various number of pulses of Er:Glass laser, operating at 1540 nm wavelength with pulse duration of 44 ns. Multi-pulse laser irradiations were done at an incidence angle of 90° in an ambient air environment. The changes of the composition and surface morphology in the 5x(Pd/Ni)/Si system were monitored by Particle Induced X-Ray Emission (PIXE), by Rutherford backscattering spectrometry (RBS), by scanning electron microscopy (SEM) and by profilometry. The main part of the absorbed laser energy was rapidly transformed into heat, producing intensive modifications of composition and morphology on the multilayer surface. The results show an increase in surface roughness, formation of a specific surface topography, appearance of hydrodynamic features and ablation of surface material without shallow or deep crater like characteristics. RBS analysis revealed that laser modification was induced intermixing between the individual Ni and Pd layers, but also with silicon substrate. During the laser processing of 5x(Pd/Ni)/Si system delivered energy was probably sufficient to cause solid-state reactions, the formation of intermetallic compounds and silicides with Ni and Pd. An interesting finding is the 5x(Pd/Ni)/Si thin film has undergone some changes in the chemical composition and structure in the irradiated areas, indicating better crystallinity with an increase of the number of applied pulses.

REFERENCES

- [1] C. Qiu, R. Shang, Y. Xie, Y. Bu, C. Li, H. Ma, *Mater. Chem. Phys.* 120, 323–330 (2010).
- [2] K. Yoshimura, Y. Yamada, M. Okada, *Appl. Phys. Lett.* 81, 4709 (2002).
- [3] E. Lee, J.M. Lee, E. Lee, J.S. Noh, J.H. Joe, B. Jung, W. Lee, *Thin Solid Films* 519, 880–884 (2010).
- [4] P. Yang, Q. Tang, *Electrochem. Acta* 182, 827–833 (2015).
- [5] W.-C. Li, T.J. Balk, *Scripta Materialia* 62, 167–169 (2010).

Effects of nanosecond laser pulses at 248 nm wavelength on multilayer CrN/(Cr,V)N coatings

B. Gaković¹, Suzana Petrović¹, P. Panjan², J. Kovač², V. Lazović³, C. Ristoscu⁴, I. Negut⁴
and I. N. Mihailescu⁴

¹*Vinca Institute of Nuclear Sciences, University of Belgrade, Serbia*

²*Jožef Stefan Institute, Ljubljana, Slovenia*

³*Institute of Physics, University of Belgrade, Serbia*

⁴*National Institute for Lasers, Plasma and Radiation Physics, Magurele, Romania*
e-mail: biljagak@vinca.rs

The effects of UV nanosecond laser pulses on multilayer CrN/(Cr,V)N coatings were studied. In the experiment laser irradiation was performed in air at 248 nm wavelength and pulse duration of 25 ns. The surface composition and microstructure was analyzed depending on the initial content of vanadium in the coatings and number of accumulated laser pulses at a fluence of 0.17 Jcm^{-2} . Most of the absorbed laser energy was rapidly transformed into heat, producing intensive modifications of the composition and morphology of the multilayer structure. The result has shown that concentration of metallic components was homogeneously distributed inside the coatings. However, on the surface and in the sub-surface regions the contents of Cr and V were decreased due to oxidation. The composition and thickness of created mixture of oxides Cr_2O_3 and V_2O_5 depend on the number of laser pulses and initial V content. Laser induced surface morphology changes of the multilayer CrN/(Cr,V)N coatings were registered at the irradiation areas: (i) grainy structures at peripheries, (ii) cracks and (iii) irregular closed shapes in the center.

A Laser-based Fabrication Method of Carbonized Polyimide Surfaces for Flexible Devices

Yong-Won Ma¹ and Bo Sung Shin^{1,2}

¹*Engineering Research Center for Net Shape and Die Manufacturing, Pusan National University, Korea*

²*Department of Cogno-Mechatronics Engineering, Pusan National University, Korea,*

e-mail: bosung@pusan.ac.kr

In this research, we demonstrate the fabrication of carbonized polyimide (PI) film for flexible devices based on laser irradiation. PI has been studied extensively for flexible devices which required various excellent properties, including flexibility, low dielectric constant, good biocompatibility [1]. Focused laser beam induced high heat can selectively convert thermoset polymer PI into conductive porous carbon micro-nano structures [2]. In this experiment, we used 355 nm nanosecond pulsed laser which had a high absorption rate of 20,000 cm^{-1} at PI, which is advantageous for carbonization of the 355 nm wavelength at low laser power. We changed the number of the irradiation, processing time and scanning speed. This study will include various features such as optical microscopy, SEM, XPS and electric conductivity. Future application of the carbonized PI film is flexible electronics such as micro-supercapacitors, sensors, and photonic components.

REFERENCES

- [1] M. Ghosh, Polyimides: Fundamentals and Applications, CRC Press, New York (1996).
- [2] J. B. In, B. Hsia, J. H. Yoo, S. Hyun, C. Carraro, R. Maboudian, C. P. Grigoropoulos, Carbon. 83, 144 (2015).

Tungsten modification induced by femtosecond laser with 10^{14} W/cm² intensity in vacuum

M. Trtica¹, J. Stasic¹, J. Limpouch², P. Gavrilov²,

¹*Vinca Institute of Nuclear Sciences, P.O. Box 522, 11001 Belgrade, Serbia*

²*Czech Technical University in Prague, Faculty of Nuclear Sciences and Physical Engineering,*

CZ-115 19 Praha, Czech Republic

e-mail: etrtica@vinca.rs

Irradiation of refractory metals including tungsten (W) by high intensity laser radiation possesses fundamental as well as applied significance. Due to extraordinary characteristics, tungsten is nowadays an interesting metal which can be used in wide range of applications, from electronic to nuclear field. In the latter area, it is well known that tungsten can be used as plasma-facing material in fusion device/reactor [1] where high fluxes are present. Behavior/modification of tungsten surface under the action of high intensity laser radiation is scarce in literature and the goal of this research is focused in that direction.

Tungsten modification in this study was done by pulsed, femtosecond laser [2,3] with the following parameters: output pulse energy up to 12 mJ; emission wavelength 800 nm; laser pulse duration 60 fs; repetition rate up to 10 Hz; fluence and intensity 16.2 J/cm² and 2.7 10¹⁴ W/cm², respectively (focusing regime), etc. Irradiation was carried out in vacuum, helium and air ambience.

Generally, surface modification of the tungsten depends on the laser output parameters - pulse energy density (fluence), intensity, wavelength, laser pulse duration, number of accumulated laser pulses, etc., as well as the sample characteristics, for example absorptivity, and used environmental conditions (e.g. vacuum or gas (helium, air, etc.)). Surface changes and phenomena at W-target, in vacuum ambience, can be summarized as follows: (i) crater shaped damages with depth increasing with higher number of accumulated laser pulses; (ii) formation of solid droplets at near and further periphery; (iii) vast rim surrounding craters, and (iv) appearance of intensive plasma.

REFERENCES

- [1] O.V. Ogorodnikova, V.V. Gann, M.S. Zibrov, Yu.M. Gasparyan, Phys. Proc. 71, 41 (2015).
- [2] M. Trtica, D. Batani, R. Redaelli, J. Limpouch, V. Kmetik, J. Ciganovic, J. Stasic, B. Gakovic, M. Momcilovic, Laser and Particle Beams 31, 29 (2013).
- [3] M. Trtica, J. Limpouch, P. Gavrilov, L. Gemini, P. Panjan, J. Stasic, D. Milovanovic, G. Brankovic, Laser and Particle Beams 33, 551 (2015).

Laser-induced periodic structure on Ti and Ti/Al thin films for photocatalytic application

D. Pjević¹, D. Peruško¹, E. Skoulas², E. Stratakis², Z. Siketić³, I. Bogdanović-Radović³, T. Savić¹, M. Čomor¹, S. Petrović¹

¹*Institute of Nuclear Sciences "Vinča", University of Belgrade, P.O. Box 522, 11001 Belgrade, Serbia*

²*Institute of Electronic Structure and Laser (IESL), Foundation for Research and Technology (FORTH), N. Plastira 100, Vassilika Vouton, 70013 Heraklion, Crete, Greece*

³*Ruđer Bošković Institute, P.O. Box 180, 10002 Zagreb, Croatia*

Email: dejanp@vin.bg.ac.rs

Modification of single titanium and complex titanium-aluminium samples by laser processing in the femtosecond time domain is unexplored field. This work included a study of the effects caused by changes in the composition and morphology of the compact Ti thin film and multilayer Ti/5x(Al/Ti) structure. Titanium and its oxides have specific physical, chemical and mechanical properties, such as high corrosion resistance, good stability, high strength and porosity. Titanium-oxide materials in different types and forms have shown great potential as ideal and powerful photocatalysts for various significant reactions due to their chemical stability, nontoxicity, and high reactivity. Laser surface modification allows production of active surface with formation of the desired oxide, creation of nano/micro textures and change wettability of the surface.

The samples were processed by focused an Yb:KGW laser beam with 1026 nm central wavelength, 170 fs pulse duration and repetition rate of 1 kHz. The laser-induced morphological and composition modifications have shown dependence on applied intensities and number of laser pulses. The formed surface nanostructures on the Ti and Ti/Al thin film surface (5x5 mm) are obtained in scanning regime. The results show an increase in surface roughness, formation of parallel periodic surface structures, appearance of hydrodynamic features and ablation of surface material. At low pulse energies range (not over 0.01 mJ) and effective 50 pulses, the two types of LIPSS can be observed: low and high spatial frequency LIPSS (HSFL and LSFL). The low spatial frequency LIPSS (LSFL), oriented perpendicular to the laser polarization with periods slightly lower than the irradiation wavelength, was typically formed. The laser-induced surface oxidation was analysed by Elastic Recoil Detection Analysis (ERDA) in the subsurface part of the investigated samples, which indicates formation Ti-oxide and mixture of Al- and Ti-oxide in the case of multilayer structure. Photocatalytic degradation rate on the laser irradiated surface of Ti and Ti/Al thin films was compared with unmodified samples. The rate of photo-degradation was associated with changes in structure of Ti-oxide and in increasing of surface roughness with formation of periodic structure.

Calculation of populations of energy levels of sodium interacting with an intense laser pulse and estimation of the resonant dynamic Stark shift

A. Bunjac¹, D. B. Popović¹ and N. S. Simonović¹
Institute of Physics, University of Belgrade, Serbia
e-mail:simonovic@ipb.ac.rs

Populations of energy levels of sodium interacting with a linearly polarized intense (up to 10^{13} W/cm²) laser pulse of a few femtoseconds duration with wavelengths in the visible and near infrared domain are determined by solving the time-dependent Schrödinger equation (TDSE) for the valence (active) electron which is considered as moving in an effective potential of the atomic core and the external electromagnetic field [1]. To solve the TDSE we used two different methods: (i) the method of time-dependent coefficients (TDC) and (ii) the wave-packet propagation (WPP) method. In the TDC method the total wave-function is expanded in a finite basis of unperturbed atomic (bound) states and their populations at the end of the pulse are determined from the values of expansion coefficients at that time. In the WPP method the total wave function is discretized on a coordinate grid and its evolution is calculated using the second-order-difference scheme [1, 2]. Compared to the TDC method the WPP method is more time-consuming but also more accurate because in this case there is no restriction to a finite basis and the continuum states are taken into account. For the TDC calculations here we used a basis set consisting of the lowest 14 sodium states (s, p, d, f states from 3s to 6d). It is found that the calculated populations of low lying levels as functions of the laser frequency ω agree well with the results obtained by the PPT method in the range of laser peak intensities up to few TW/cm². The peaks in the population of excited states (nl) occurring when $K\omega = \omega_{nl,3s} \equiv E_{nl}(F,\omega) - E_{3s}(F,\omega)$ (multi(K)-photon resonance condition) are used to determine the field strength dependence of the resonant dynamic Stark shift for separations of levels.

REFERENCES

- [1] A. Bunjac, D. B. Popović and N. Simonović, *Eur. Phys. J. D* (2017), accepted for publication.
- [2] A. Askar and A. S. Cakmak, *J. Chem. Phys.* 68, 2794 (1978).

Inducing periodic structures on multilayers of Ti and Ta by femtosecond laser beam

Aleksander G. Kovačević¹, Suzana M. Petrović², Davor Peruško², Vladimir Lazović¹, Iva Bogdanović-Radović³, Vladimir Pavlović⁴, Dejan Pantelić¹, Branislav M. Jelenković¹

¹*Institute of Physics, University of Belgrade, Pregrevica 118, 11080 Belgrade, Serbia*

²*Institute of Nuclear Sciences „Vinča“, University of Belgrade, Po Box 522, 1000 Belgrade, Serbia*

³*Institute “Ruđer Bošković”, Bijenička cesta 54, 10000 Zagreb, Croatia*

⁴*Faculty of Agriculture, University of Belgrade, Nemanjina 6, 11080 Belgrade, Serbia*

e-mail: Aleksander.Kovacevic@ipb.ac.rs

Nanostructuring of surfaces by femtosecond (fs) laser beam interaction is the topic of research for some time [1]. The emergence of the laser-induced periodic surface structures (LIPSS) on metal-dielectric surfaces is of interest from fundamental and application points of view. The interaction of fs beam with thin films can also generate LIPSS, with the arrangement of thin films in multi-layer structure being important for the quality of the LIPSS [2]. Excellent properties of titanium (Ti) and tantalum (Ta), like corrosion resistance, heat transfer properties and workability, recommend them as useful materials for a wide range of applications - heat exchangers, reactors, and others exposed to extremely corrosive fluids. Combining Ti and Ta could be attractive for applications, but challenging, as they have great difference in melting point and density, therefore, TiTa alloys are still not widely adopted in applications [3].

We have performed the interaction of fs laser beam with multilayer Ti/Ta samples in order to investigate the effects of interaction with ultra-short pulses to surface morphology and to both surface and bulk chemistry of newly generated compounds. Each layer of the sample was 17 nm thick. The interactions were in two regimes: dynamic and static, depending whether the beam scanned over the sample surface or not. SEM and PIXE RBS analyses have shown the LIPSS formed with or without ablation depending on the beam fluence. The LIPSS orientation is dependent on the input beam polarization. Both types of LIPSS were formed, low- and high-spatial frequency LIPSS, with periods being as low as 120 nm.

REFERENCES

- [1] A. Y. Vorobyev, C. Guo, Laser Photon. Rev. 7, 385-407 (2013), and the references within.
- [2] A. G. Kovačević, S. Petrović, B. Bokić, B. Gaković, M. T. Bokorov, B. Vasić, et al., Appl. Surf. Sci. 326, 91-98 (2015).
- [3] S. L. Sing, W. Y. Yeong, F. E. Wiria, J. Alloy. Compd. 660, 461-470 (2016).

Micro-structured biopolymer scaffolds fabricated by femtosecond laser ablation

A. Daskalova¹, I. Bliznakova¹, P. Loukakos², A. Zhelyazkova¹, E. Kijeńska³ and C. Fotakis²

¹*Institute of Electronics, Bulgarian Academy of Sciences, Sofia, Bulgaria*

²*Institute of Electronic Structure and Laser Foundation for Research & Technology – Hellas, Belgrade, Serbia*

³*Faculty of Materials Science and Engineering, Warsaw University of Technology Warsaw, Poland*

e-mail:albdaskalova@gmail.com

Surface properties of biomedical implants are one of the most important parameters when tissue engineered scaffolds are designed. It is discovered that cells- surface interaction like adhesion, proliferation, and differentiation depends strongly on surface characteristics such as wettability, chemistry and roughness [1].

In this study, pulse shaping technique was employed for femtosecond laser irradiation of biopolymer thin films. This method permits a gradual energy delivery into the sample due to the possibility of temporal redistribution of energy in the laser pulse. The influence of different delay times between consecutive pulses was examined with regard to evolution of surface morphology via field emission scanning electron microscopy (FESEM).

The thin biofilms were exposed to ultra-short laser irradiation with laser pulses of 30fs duration established in a CPA Ti:Sapphire laser system (Femtopower – Compact Pro) at 800nm central wavelength and 1kHz repetition. We discovered delay time dependence of material morphologies and modification thresholds. We have used pulse delay times (t_d) varying from 0 to 1ps and number of applied laser pulses (N) from 1-1000.

The ability to modify surface characteristics of the biopolymer thin films, by changing their roughness thus influencing wettability properties, permits manipulation of the cell dynamics.

The analysis of cell culture studies demonstrate that cells are completely repelled from the areas where a new structured zone is reported. MG63 cells cytoskeletons can be seen aligning along the groove direction. Phenomena like cell trapping, directional cell growth are monitored.

It was demonstrated that surface topography has an important effect on cells mobility and that cells are able to reorganize themselves in relation to surface features.

REFERENCES

- [1] A. Wilson, I. Jones, F. Salamat-Zadeh, J.F. Watts, International Journal of Adhesion & Adhesives 62 69–7770 (2015).
- [2] N. Sanner, N. Huot, E. Audouard, C. Larat, J.-P. Huignard, Optics and Lasers in Engineering 45 737–741 (2007).

Laser parameters optimization for the artifacts silver coated surfaces cleaning

B. Radojkovic¹, S. Ristic², S. Polic², B. Jegdic³ and M. Janicijevic^{4,5}

¹*Innovation center Faculty of Mechanical Engineering, University of Belgrade, Serbia*

²*Central Institute for Conservation in Belgrade, Belgrade, Serbia*

³*Institute of Chemistry, Technology and Metallurgy, Belgrade, Serbia*

⁴*Faculty of Electrical Engineering, University of Belgrade, Serbia*

⁵*Metalac A.D. Gornji Milanovac, Serbia*

e-mail:bojana52@yahoo.com

In recent decades, lasers have become the devices that came out of research laboratories and are widely used in industry, engineering, medicine, arts, etc. Among the many applications, lasers have found a place in the conservation of cultural heritage as a source of radiation in the modern diagnostic techniques, cleaning and scanning objects of priceless value [1]. Their importance in cleaning of cultural heritage objects is based on the properties of these techniques, such as high sensitivity, nondestructivity, selectivity, flexibility, on-site applicability and others.

Laser techniques application in metal artifacts cleaning has to be carefully evaluated due to complex phenomena in laser–metal interaction and specificity of every artifact item. There is a large variety of metal materials and their combinations in cultural heritage. Also, the different organic and inorganic encrustations and corrosion products in different progression stage can be found on artifacts surfaces [2,3].

Therefore, the optimization of laser parameters for safe and effective metal artifacts cleaning process is important step in order to avoid unwanted side-effects such as changes in the color or grater surface damages.

A specific field of the metal surface laser cleaning is the cleaning of thin metal foils and coated surfaces. In cultural heritage such examples are metal yarns on the textile embroidery [4, 5]. Often, these yarns are coated with some precious metal as are silver or gold.

This paper presents a study of laser cleaning parameters for safe and effective cleaning of silver coated copper metal yarns. In that purpose the preliminary investigation are performed on silver coated copper plate. That investigation involve numerical modeling of laser– silver coated copper plate interaction and experimental irradiation of real sample surface with pulsed nanosecond Nd:YAG laser by changing laser parameters as are wavelength, laser beam energy and number of pulses. The numerical 3D model of the generated heat on the silver coated copper plate was obtained using the COMSOL Multiphysics software package and was carried out with the aim to define the temperature distribution around the irradiated zone and the maximum temperatures.

Optical microscopy, SEM and EDX analysis are used for the diagnosis of the morphological and chemical effects of laser irradiation on real sample surface. Obtained results are compared with results of laser irradiation analyses on naturally tarnished metal yarns embroidery from museum sample.

This investigation confirms that Nd:YAG lasers can be successfully used for metal yarns cleaning. Application of adequate numerical model can provide an opportunity for a faster and cheaper determination of the cleaning process optimum values range. Some parameters for successfully and safely cleaning of silver coated copper surface were determined.

REFERENCES

- [1] C. Fotakis, D. Anglos, V. Zafirooulos, S. Georgiou, V. Tornari, CRC Press, 336 pages (2006).
- [2] J. Cronyn, The Elements of Archaeological Conservation, Taylor & Francis e-Library, 326 pages (2004).
- [3] J. Lee, J. Yu, Y. Koh, J Cult Herit, 4, 157s (2003).
- [4] B. Radojkovic, S. Ristic, S. Polic, R. Jancic-Heinemann, D. Radovanovic, J. Cult. Herit. 23, 128 (2017).
- [5] C. Degriigny, E. Tanguy, R. Le Gall, V. Zafirooulos, G. Marakis, J. Cult. Herit. 4, 152s (2003).

Laser induced mixing in multilayered Ti/Ta thin film structures

Marko Obradović¹, Janez Kovač², Suzana Petrović¹, Vladimir Lazović³, Branislav Salatić³, Jovan Ciganović¹, Dejan Pjević¹, Momir Milosavljević¹, Davor Peruško¹

¹VINČA Institute of Nuclear Sciences, University of Belgrade, P.O. Box 522, 11001 Belgrade, Serbia

²Jožef Stefan Institute, Jamova 39, 1000 Ljubljana, Slovenia

³Institute of Physics Belgrade, University of Belgrade, Pregrevica 118, 11080 Zemun, Serbia
e-mail:mobradovic@vin.bg.ac.rs

Metallic biomaterials should exhibit excellent biocompatibility, high corrosion resistance and low elastic modulus which are close to that of human bones. It was shown that in this sense Ti-Ta alloys have considerably better mechanical properties compared to pure titanium or tantalum [1, 2].

The main purpose of these experiments was investigation of possibility to induce interlayer mixing in an Ti/Ta immiscible multilayer system by laser irradiation. The absence of interlayer mixing was previously shown on this system during the Ar⁺ ion irradiation up to relatively high fluence of 2×10^{16} ions cm⁻² [3].

The system consisted of ten alternate Ti and Ta thin films (~18 nm each) and covered by slightly thicker Ti layer (~27 nm) on the top with the purpose of creating an appropriate porous structure very important for potential biocompatibility [4]. Structure was deposited on Si (100) wafers to a total thickness of 205 nm.

Laser irradiation was performed in air by picoseconds Nd: YAG laser. Defocused laser pulses had a laser spot on the sample surface of 3 mm in diameter and fluences of 0.057 and 0.11 J cm⁻². Laser beam was scanned over the 5x5 mm² surface area with different steps along y-axes to provide a variation in deposited energy density.

For structural and compositional characterisation following methods were used: Auger electron spectroscopy, X-ray photoelectron spectroscopy, atomic force microscopy and scanning electron microscopy.

The obtained results show that laser processing at a lower fluence causes only oxidation of the top Ti layer, invariable to the number of applied laser pulses and no interlayer mixing was observed. Application of laser pulses at fluence of 0.11 J cm⁻², on the other hand, caused significant increase of surface roughness and partial and/or complete ablation of deposited layers, but in partially ablated regions considerable mixing between Ti and Ta films was registered.

These experiments indicate that the use of picoseconds laser pulses with fluences in interval (0.057 – 0.11) J cm⁻² could be very useful for mixing of titanium and tantalum layers and fabrication of a new material for medical implants. Suitable choice of films thicknesses would lead to the desired composition of this alloy.

REFERENCES

- [1] J. Breme, V. Wadewitz, Int. J. Oral. Maxillofac. Imp. 4, 113 (1989).
- [2] Y.-L. Zhou, M. Niinomi, J. Alloys. Compd. 466, 535 (2008).
- [3] M. Milosavljević, V. Milinović, D. Peruško, A. Grce, M. Stojanović, D. Pjević, M. Mitrić, J. Kovač, K.P. Homewood, Nucl. Instrum. Meth. B 269, 2090 (2011).
- [4] W.E. Yang, H.H. Huang, Thin Solid Films 518, 7545 (2010).

Energy distribution of ejected photoelectrons in $K^{-2}V$ process

Kristina Isaković, Violeta Petrović, Hristina Delibašić

Department of Physics, Faculty of Sciences,

Kragujevac University, Serbia

e-mail: kristina_isakovic@yahoo.com

Abstract: In the last few years, a great deal of attention has been devoted to Double-Core-Hole states, and especially those involving K-shells, K^{-2} states, as well as, $K^{-2}V$ states, which consider simultaneous core ionization and core-excitation [1]. In this paper we have given a theoretical framework that enables prediction of the energy distribution of ejected photoelectrons in $K^{-2}V$ process. In order to achieve this, we obtained a formula for the transition rate taking into account the channels of sequential and nonsequential ionization, and ionization with ionic core excitation, i.e. we treated the ionization rate as a cumulative contribution of simultaneous processes, ionization and excitation [2,3]. We assumed a non-relativistic domain and linearly polarized laser field. We started with the $K^{-2}V$ process in helium like atoms and showed that inclusion of additional processes significantly influences the transition rate and at the same time the energy distribution of the ejected photoelectrons, especially in the energy range of the ejected photoelectrons bringing us to the energy range of low energy electrons which have a significant role in bio damage [4].

REFERENCES

- [1] S. Carniato, P. Selles, L. Andric, J. Palaudoux, F. Penent, M. Žitnik, K. Bučar, M. Nakano, Y. Hikosaka, K. Ito, P. Lablanquie, *The Journal of Chemical Physics* 142, 014308 (2015).
- [2] S. Y. Sun, X. F. Jia, *Chin. J. Chem. Phys.* 26, 576 (2013).
- [3] G. Goldsztejn, T. Marchenko, R. Püttner, L. Journel, R. Guillemin, S. Carniato, P. Selles, O. Travnikova, D. Céolin, A. F. Lago, R. Feifel, P. Lablanquie, M. N. Piancastelli, F. Penent, and M. Simon, *Phys. Rev. Lett.* 117, 133001 (2016).
- [4] I. Baccarelli, I. Bald, F. A. Gianturco, E. Illenberger, J. Kopyra, *Phys. Rep.* 508, 1 (2011).

Extending useful spectrum of solar radiation in dye-sensitized solar cells using stochastic surface reliefs in plasmonic materials

K. Cvetanović Zobenica¹, Z. Jakšić¹, M. Obradov¹, D. Vasiljević Radović¹, D. Stanisavljev²

¹*Center of Microelectronic Technologies, Institute of Chemistry, Technology and Metallurgy, University of Belgrade, Serbia*

²*Faculty of Physical Chemistry, University of Belgrade, Serbia*
e-mail:jaksa@nanosys.ihtm.bg.ac.rs

Dye-sensitized solar cells (DSSC) attract increasing attention due to their relatively low production costs and wider choice of materials compared to other photovoltaic devices for solar harvesting [1]. Since their introduction in 1989 [2] their performance has been steadily improving [3]. Extending the useful range of irradiation frequencies of the DSSC is desirable in order to collect as much electromagnetic energy from the solar spectrum as possible. One possible method proposed to further increase the quantum efficiency of the DSSC and of solar cells generally is plasmonic enhancement [4,5]. To this purpose either noble metal nanoparticles or core shell metal-on-semiconductor nanoparticles interspersed with dye-sensitized titanium dioxide were used in the photoanode. Localized plasmons on the nanoparticles and increased scattering cross section enabled to decrease the thickness of the solar cells, while varying size of the plasmonic particles helped to extend the usable radiation band. Another route for enhancement is the use of rough gold films serving as plasmonic nanoantennas coupled with titanium dioxide film [6]. In this contribution we propose the use of alternative plasmonic material, doped transparent conductive oxide (TCO), as the stochastically roughened structure at the surface of the DSSC. Such oxides (e.g. tin oxide, zinc oxide) are typically already used as the conductive part of the photoanode immediately above the dye-sensitized mesoporous titanium dioxide [1]. If roughened, TCO surface features can be regarded as a collection of diffractive scatterers with different sizes. As a consequence, this ensures enhanced coupling between the propagating and the plasmonic modes in an extended range of frequencies, dependent on the range and distribution of the subwavelength surface features. At the same time, the incident waves that were not coupled will be randomly scattered by the roughened surface, effectively further extending the optical path through the medium. We used finite element simulations and analytical treatment to assess the properties of the novel DSSC structure with a roughened TCO electrode. The use of the additional broadband plasmonic coupler ensures thinning of the photoanode without compromising the optical response, which on the other hand results in smaller amounts of necessary sensitizer dyes, leading to the possibility to use more expensive dyes at the same cost and ultimately extending the available choice of sensitizers. At the same time, the textured surface, being a collection of subwavelength scatterers with different sizes, effectively widens the frequency range in which the solar radiation can be coupled into the plasmonic modes. The plasmonic response of the TCO material itself can be tuned by design, using different doping levels, thus ensuring further tailoring of the response [5]. Obviously, different older schemes for the DSSC improvement, like e.g. the use of additional plasmonic nanoparticle scatterers within the titanium dioxide mesoporous matrix, can still be used with the proposed layout.

REFERENCES

- [1] J. Gong, K. Sumathy, Q. Qiao, Zh. Zhou, *Renew. Sust. Energy Rev.* 68, 234 (2017).
- [2] B. O'regan, M. Grätzel, *Nature* 353, 737 (1991).
- [3] N. T. R. N. Kumara, L. Andery, C. M. Lim, M. I. Petra, P. Ekanayake, *Renew. Sust. Energy Rev.* 78, 301 (2017).
- [4] H. A. Atwater, A. Polman. *Nature mat.* 9, 205 (2010).
- [5] Z. Jakšić, *Micro and Nanophotonics for Semiconductor Infrared Detectors*, Springer (2014).
- [5] D. N. Joshi, S. Mandal, R. Kothandraman, R. A. Prasath. *Mat. Lett.* 193, 288 (2017).
- [6] F. Tan, T. Li, N. Wang, S. K. Lai, C. C. Tsoi, W. Yu, X. Zhang. *Scient. Rep.* 6, 33049 (2016).

Influence of graphene and two-dimensional materials on electromagnetic enhancement in silver nanoparticle clusters

U. Ralević¹, A. Panarin² and G. Isić¹

¹*Graphene Laboratory of Center for Solid State Physics and New Materials, Institute of Physics Belgrade, University of Belgrade, Belgrade, Serbia*

²*B. I. Stepanov Institute of Physics, National academy of sciences of Belarus, Minsk, Belarus*
e-mail: isicg@ipb.ac.rs

Since its discovery in the 1970s, surface-enhanced Raman scattering (SERS) has become indispensable in analytic applications of Raman spectroscopy involving trace concentrations of analyte. It is well established that SERS enhancement factors above 10^{10} can be reached if the analyte molecules are deposited into the electromagnetic "hotspots" formed in metal nanoparticle gaps or crevices, allowing single-molecule detection. While several mechanisms are known to contribute to the overall enhancement, the dominant contribution to large enhancement factors is known to be of the electromagnetic nature, scaling approximately as the fourth degree of the local electric field enhancement.

Silver nanoparticles deposited on appropriately chosen substrates are amongst most frequently used SERS substrates because the plasmonic properties of silver at visible frequencies are superior to other metals. However, silver is prone to oxidation in ambient conditions, especially when illuminated by a strong laser beam, leading to stability issues when attempting to use it in SERS substrates [1]. In addition to improved stability, a passivation of the silver surface by ultrathin dielectric layers has been shown [2] to be beneficial as a way to functionalize the surface. Recent studies [3,4] have indicated that graphene, as a two-dimensional material which combines atomic thickness with mechanical robustness, might be an ideal protection layer for silver nanoparticle SERS substrates.

Here we employ rigorous finite-element based numerical simulations of light scattering on silver nanoparticle clusters deposited on a substrate, in order to determine the electromagnetic SERS enhancement factor provided by the nanoparticle cluster. While it is evident that graphene or a similar absorbing two-dimensional cover layer [5] reduces this factor, our aim is to determine and understand the magnitude of this reduction, in order to help optimize the use of graphene in novel silver nanoparticle SERS substrates.

REFERENCES

- [1] A. Yu. Panarin, I. A. Khodasevich, O. L. Gladkova, S. N. Terekhov, *Appl. Spectrosc.* 68, 297 (2014).
- [2] X. Zhang, J. Zhao, A. V. Whitney, J. W. Elam, R. P. Van Duyne, *J. Am. Chem. Soc.* 128, 10304 (2006).
- [3] W. Xu, J. Xiao, Y. Chen, Y. Chen, X. Ling, J. Zhang, *Adv. Mater.* 25, 928 (2013).
- [4] W. G. Xu, X. Ling, J. Q. Xiao, M. S. Dresselhaus, J. Kong, H. X. Xu, Z. F. Liu, J. Zhang, *Proc. Natl. Acad. Sci. USA* 109, 9281 (2012).
- [5] U. Ralević, G. Isić, B. Vasić, R. Gajić, *J. Phys. D: Appl. Phys.* 47, 335101 (2014).

Analysis of layer interactions between stacked metasurfaces

J. Sperrhake¹, M. Falkner¹, S. Fasold¹ and T. Pertsch¹

¹*Institute of Applied Physics, Abbe Center of Photonics,*

Friedrich-Schiller-Universität Jena, Germany

e-mail: jan.sperrhake@uni-jena.de

Light interaction with nano-particles has been a matter of research since the beginning of the century [1]. In more recent years, different geometries and arrangements were studied while trying to achieve different optical properties such as dichroism or asymmetric transmission [2]. Despite all the effort these nano-structured photonic surfaces, often termed metasurfaces, are still challenging to model and even more challenging to fabricate. One road to simplify the problem is choosing flat geometries in periodic arrangements. Unfortunately, this implies fewer possibilities in their optical design. Especially when trying to control the full state of polarization of transmitted or reflected light the restriction to planar symmetries can be a hindrance. It would therefore be desirable to have a way of easily combining multiple metasurfaces to a multifunctional system. The question is then how to describe a stack of metasurfaces and what kind of issues this imposes on fabrication.

Metasurfaces are characteristic for their structure sizes and particle separations in a subwavelength regime. As a result, higher diffraction orders emerge that couple to adjacent layers. Usually, due to the complexity of this interaction, rigorous numerical methods have to be applied in order to describe these stacked systems. However, depending on period, layer separation and the wavelength of the incident light a condition can be found for a reduction of the layer interaction to the zeroth diffraction order only. If transmission and reflection coefficients for each single layer are known, the entire stack can then be described analytically [3]. Mainly, this implies two things. First, simulation time and effort decreases tremendously. Second, a zeroth order model is equivalent to assuming that the metasurfaces are infinitely thin homogeneous layers which do not have to be aligned laterally [4]. This means the major issue of layer alignment can be ignored during fabrication, decreasing the possibility for errors and allowing for faster procedures.

Moreover, applying a scattering matrix (S-matrix) formalism to this approach yields additional physical information [3]. S-matrices can be combined using Redheffer's starproduct [5], a more involved matrix product connecting the ports of consecutive S-matrices. The starproduct can be decomposed in an infinite geometric series accounting for all the possible interactions as light passes through the layers. This allows us to separate leading order interactions from interferometric, i.e. Fabry-Perot-like, terms, which is crucial to fully understand the emerging optical properties of stacked systems.

In our contribution, we will derive an approximation for a zeroth order description of stacked metasurfaces and demonstrate its versatility both numerically and experimentally. For the latter, a system of two nano-structured layers separated by a dielectric spacer was fabricated and characterized. Being comprised of both gold nano-wires and patches it demonstrates the combination of resonant and polarization sensitive features.

Furthermore, we will show how to analyze stacked systems using a new formalism of decomposed S-matrix coupling. For that, we will derive the necessary equations which govern the interaction between layers and apply them to a system of numerically derived single layers.

REFERENCES

- [1] D. Smith, W. Padilla, D. C. Vier, S. C. Nemat-Nasser, S. Schultz, *Phys. Rev. Lett.* 84, 4184 (2000).
- [2] C. Menzel, C. Helgert, R. Rockstuhl, E.-B. Kley, A. Tünnermann, T. Pertsch, F. Lederer, *Phys. Rev. Lett.* 104, 253902 (2010).
- [3] C. Menzel, J. Sperrhake, T. Pertsch, *Phys. Rev. A* 99, 063832 (2016).
- [4] A. Andryieuski, C. Menzel, C. Rockstuhl, R. Malureanu, F. Lederer, and A. Lavrinenko, *Phys. Rev. B* 82, 235107 (2010).
- [5] R. Redheffer, *Journal of Mathematics and Physics* 39, 269 (1960).

Spontaneous emission into Tamm plasmon modes on semi-infinite metallodielectric superlattices

G. Isić¹, Z. Jakšić², S. Vuković²

¹*Center for Solid State Physics and New Materials, Institute of Physics Belgrade,
University of Belgrade, Belgrade, Serbia*

²*Center of Microelectronic Technologies, Institute of Chemistry, Technology and Metallurgy,
University of Belgrade, Serbia
e-mail: isicg@ipb.ac.rs*

An optical medium is said to be hyperbolic if the principal values of its dielectric permittivity tensor differ in sign, implying a hyperboloid equifrequency surface. As the photonic density of states (PDOS) and the associated spontaneous emission rate of quantum emitters are known to be proportional to the area of the equifrequency surface, hyperboloid media exhibit very large Purcell factors, infinite in the local approximation. In nature, a hyperboloid behavior occurs in certain crystals at mid and far infrared frequencies and is usually associated with vibrational resonances.

In recent years [1], periodic stacks of ultrathin metal and dielectric layers, here referred to as metallodielectric superlattices, have been considered as artificial media exhibiting a hyperboloid behavior up to visible frequencies. As visible and infrared wavelengths are many times longer than the period, the main optical properties of a superlattice can be understood by approximating it by a uniaxial homogeneous medium. A more rigorous microscopic picture [2] shows that the unusual properties are a consequence of the transparency of individual layers which allows a hybridization of surface plasmon polaritons (SPPs), supported by each metal-dielectric interface, and the formation of Bloch SPPs delocalized across the superlattice.

Here we consider the spectral characteristics of PDOS at the interface between a semi-infinite metallodielectric superlattice and a homogeneous medium. We discuss the conditions leading to the appearance of surface modes referred to as Tamm plasmons and their contribution to the surface PDOS, aiming to discriminate the efficiency of a quantum emitter placed near the surface. Coupling of the emitted radiation with Tamm and Bloch plasmons improves the interpretation of recent experiments by Krishnamoorthy et al. [3]. We show how the classical results for emission into surface plasmons [4] are modified in case of Tamm plasmons, explain the factors influencing the magnitude of the relative contribution of Tamm plasmons to the total PDOS and its critical behavior in the vicinity of the topological transition frequency between hyperbolic and elliptical regime.

REFERENCES

- [1] A. Poddubny, I. Iorsh et al., *Nat. Photon.* 7, 958-967 (2013).
- [2] G. Isić, R. Gajić, S. Vuković, *Phys. Rev. B* 89, 165427 (2014).
- [3] H. N. S. Krishnamoorthy, Z. Jacob et al., *Science* 336, 205-209 (2012).
- [4] G. W. Ford, W. H. Weber, *Phys. Rep.* 113, 195-287 (1984).

Influence of a resonance on delay times in terahertz chiral metamaterial slab

D. B. Stojanović^{1,2}, P. P. Beličev¹, G. Gligorić¹, J. Radovanović², V. Milanović², Lj. Hadžievski¹

¹ *Vinča Institute of Nuclear Sciences,
University of Belgrade, Serbia*

² *School of Electrical Engineering,
University of Belgrade, Serbia*

e-mail:petrab@vin.bg.ac.rs

The advantage of metamaterials made of resonant particles is that, in the interaction with THz waves, they can generate enhanced response which enables diverse functionalities in THz frequency range. In view of that, it was pointed out that the control of delay times of THz pulses can be used for a variety of THz applications [1, 2]. On the other hand, during the interaction with light, chiral metamaterials exhibit optical activity and circular dichroism as a consequence of different propagation of right (RCP) and left (LCP) circularly polarised waves [3]. Here, we consider the delay times that characterize the interaction of THz wave with a chiral metamaterial slab consisting of resonant Ω particles embedded in dielectric material.

We observe the interaction of RCP and LCP waves with the slab and focus on the analysis of various effects that occur due to the different polarisation of incident waves. It follows that the RCP wave has much stronger coupling with the resonant particles than the LCP wave. Results show that the energy density, absorption and hence, the dwell time of RCP wave have higher values at the resonant frequency comparing to the case when LCP wave interacts with the slab. Calculations were done performing numerical simulations of the resonant Ω particles, as well as by using the effective parameters extracted through parameter retrieval procedure considering a homogenous chiral slab. To the best of our knowledge, this is the first analysis of delay times in chiral metamaterial [4] and obtained results can be used for circular polarisation characterization in THz spectral region.

Additionally, we analyse the impact of incident field intensity on delay times for the case of homogenous nonlinear chiral slab presuming that the chiral particles are immersed in nonlinear dielectric of Kerr type. Due to the presence of nonlinearity, common features of metamaterials can be significantly altered [5]. We present our analyses on the nonlinear effects related to resonant behaviour of circularly polarised waves which will affect the corresponding delay times.

REFERENCES

- [1] H-T Chen et al., Nature 444, 597 (2006).
- [2] F. Miyamaru et al., Sci. Rep. 4, 4346 (2014).
- [3] J. Gansel et al., Science 325, 1513 (2009).
- [4] D. B. Stojanović, J. Radovanović, V. Milanović, Phys. Rev. A 94, 023848 (2016).
- [5] P. P. Beličev, I. Ilić, V. Milanović, J. Radovanović, Lj. Hadžievski, Phys. Rev. A 80, 023821 (2009).

Photoemission Electron Microscopy of Airy Surface Plasmon Polaritons

A. V. Singh, M. Falkner, M. Steinert, C. Menzel and T. Pertsch

Institute of Applied Physics, Abbe Center of Photonics, Friedrich-Schiller-Universität Jena, Germany

e-mail: Matthias.Falkner@uni-jena.de

The generation of non-diffracting beams that are suitable for flat land photonics has always been of interest, not only from a photonic device point of view but for fundamental research as well. A metal-dielectric interface serves as the best companion of Airy beams in planar systems. These interfaces are known to support surface plasmon polaritons (SPPs). Surface plasmons can confine the wave to an interface decaying exponentially in the direction normal to the surface. Airy SPPs are propagating surface plasmon excitations that are confined to the metal-dielectric interface, containing the properties of Airy beams. This unique combination enables one to tailor the flow of energy at the metal surface. This opens up new capabilities in prominent device application e.g. optical traps and tweezers, biosensors, selective on-chip manipulation of nanoparticles [1, 2].

The generation of Airy SPPs has basically two requirements. First, the free space k-vector should match with the SPP k-vector. Second, the generated surface plasmon should have Airy wave profile. Many methods have been proposed to generate these non-diffracting beams [3, 4]. The generated Airy SPPs have been investigated using experimental methods like leakage radiation microscopy [3] or scanning near-field microscopy (SNOM) [4]. In SNOM the presence of a scanning probe perturbs the field being measured, so the measurement may not be a true representation of the field properties. This limitation can be overcome by using more sophisticated experimental tools.

Here, we report a versatile method of investigation of Airy SPPs on a metallic surface by PhotoEmission Electron Microscopy (PEEM). It can provide unprecedented spatial resolution of the order of 20nm. PEEM allows direct visualization of the plasmon field through photoemission [5], where the photo-emitted electrons provide a map of electromagnetic fields at the surface. Our sample design is inspired by Minovich *et al.* [4] and was realized by focused ion beam milling into a 200 nm thick gold film. This specially designed diffraction grating can generate the Airy beam profile and simultaneously can couple free space propagating waves to surface plasmons. For the illumination, we used a home-built tunable optical parametric chirped pulse amplifier. The central wavelength was varied between 690 and 840 nm. The emitted photoelectrons were imaged by a PEEM from Focus GmbH. Large scale 3D finite difference time domain simulations were performed to optimize and theoretically verify the design.

Both theory and experiment show an excellent agreement. On the air-gold interface, the Airy SPP is launched at the grating edge and simultaneously interferes with the incident laser pulse. The photo-emitted electrons provide the direct visualization of the total field. The area of constructive and destructive interference leads to higher and lower nonlinear photoemission yield. This result clearly shows surface plasmon generation containing all the properties of Airy beams. The main lobe of the Airy SPP propagates along a curved trajectory for more than 25 μ m.

In conclusion, we have experimentally investigated the Airy plasmons with high spatial resolution, and their propagation along the curved trajectory has been visualized. The experimental results not only match with theoretical results but also contain deeper insight into the structure.

REFERENCES

- [1] M. Righini, A. S. Zelenina, C. Girard and R. Quidant, *Nat. Phys.* 3, 477 (2007).
- [2] A. E. Klein, A. Minovich, M. Steinert, N. Janunts, A. Tünnermann, D. N. Neshev, Y. S. Kivshar, and T. Pertsch, *Opt. Lett.* 37, 3402 (2012).
- [3] P. Zhang, S. Wang, Y. Liu, X. Yin, C. Lu, Z. Chen, and X. Zhang, *Opt. Lett.* 36, 3191 (2011).
- [4] A. Minovich, A. E. Klein, N. Janunts, T. Pertsch, D. N. Neshev, and Y. S. Kivshar, *Phys. Rev. Lett.*, 107, 116802 (2011).
- [5] O. Schmidt, M. Bauer, C. Wiemann, R. Porath, M. Scharte, O. Andreyev, G. Schöhense, M. Aeschlimann, *Appl. Phys. B74*, 223 (2002).

Electromagnetic wave propagation through chiral metamaterials composed of twisted closed ring resonators

D. B. Stojanović^{1,2}, P. P. Beličev¹, G. Gligorić¹, Lj. Hadžievski¹

¹ *Vinča Institute of Nuclear Sciences,*

University of Belgrade, Serbia

² *School of Electrical Engineering,*

University of Belgrade, Serbia

e-mail:dankas@vin.bg.ac.rs

Chiral metamaterial consists of periodically placed resonant elements exhibiting chiral effects such as circular dichroism and optical activity. They appear due to the coupling of electric and magnetic fields which is result of an interaction of electromagnetic wave and chiral metamaterial. Numerous designs of chiral resonant elements are proposed providing applications for polarization conversion, filtering and absorption in THz frequency range [1, 2].

Here, we analyze propagation of electromagnetic waves through chiral metamaterial composed of twisted closed ring resonators (TCRR). The proposed chiral metamaterial is ultrathin structure which makes this design easy to fabricate and, at the same time, maintains effects which can be observed in conventional chiral 3D metamaterial structures. Dimensions of chiral elements are chosen to provide resonances within THz frequency range. Different geometrical parameters are varied in order to determine their influence on resonant frequency and losses [3].

For our TCRR chiral metamaterial structure, the analysis is made from microscopic as well as from macroscopic point of view. Through numerical simulations, we calculate electromagnetic field distribution, scattering coefficients, absorption and consequently, circular dichroism. Additionally, we examine losses in our chiral structure in terms of radiative and non-radiative ones [4] and explore its influence on the circular dichroism.

REFERENCES

- [1] G. Kenanakis, E. N. Economou, C. M. Soukoulis, M. Kafesaki, EPJ Appl. Metamat. 2, 1-12 (2016).
- [2] T. Kan et al., Nat. Commun. 6, 8422 (2015).
- [3] L. Solymar, E. Shamonina, Waves in metamaterials, Oxford (2009).
- [4] A. B. Khanikaev et al., Nat. Commun. 7, 12045 (2016).

Metal layers with subwavelength texturing for broadband enhancement of processes in photocatalytic microreactors

M. Rašljčić¹, Z. Jakšić¹, Ž. Lazić¹, M. Obradov¹, D. Vasiljević Radović¹, Ž. Čupić², D. Stanisavljev³

¹ *Center of Microelectronic Technologies, Institute of Chemistry, Technology and Metallurgy, University of Belgrade, Serbia*

² *Center of Catalysis and Chemical Engineering, Institute of Chemistry, Technology and Metallurgy, University of Belgrade, Serbia*

³ *Faculty of Physical Chemistry, University of Belgrade, Serbia*

e-mail: jaksa@nanosys.ihtm.bg.ac.rs

Plasmonics offers the possibility to tailor the frequency dispersion and concentrate electromagnetic fields into spaces much smaller than a single wavelength, with radiation intensities being proportionally increased compared to the incident beam, often for a several orders of magnitude [1]. Such extreme localizations obtained by means of surface plasmons polaritons (SPP) are useful for numerous practical applications including ultrasensitive chemical sensing, enhancement of photodetector sensitivity and many others [2]. One of the fields of use of plasmonics is the enhancement of photocatalytic efficiency under the irradiation by visible light [3]. More specifically, a wide class of reactions in photocatalysis can be enhanced by the use of solar radiation [4].

In order to convert as much optical radiation as possible into electrochemical energy one needs to ensure coupling between the propagating modes of solar radiation and the surface-bound modes of a SPP. Since wave vectors of the surface modes obviously must be much larger than those of the propagating beams in order to ensure field concentration, this is not a trivial task, and there is a need for an coupler structure to impart additional momentum to the propagating beam. A possible solution is to use nanoparticles of good plasmonic materials, usually gold or silver, which serve simultaneously as couplers and field concentrators owing to the formation of localized SPP. This approach is actually used in vast majority of plasmonic photocatalytic systems [3, 4]. Another approach is to use rough metal films [5,6]. A stochastic surface profile can be represented as a superposition of a number of different sinusoidal diffractive gratings, effectively behaving similarly to a collection of metal nanoparticles with different sizes and ensuring a broadband coupling.

Here we consider the use of subwavelength texturing of plasmonic films for microreactors. To this purpose the bottom of the microchannel is roughened, ensuring SPP localization and field enhancement. Since the height of microchannels is small, practically the whole volume of the microchannel can coincide with the region of enhanced evanescent field, thus ensuring high efficiency. We consider single crystalline silicon, polycarbonate and quartz glass as the materials for the microreactors. Standard chemical bulk micromachining is used as the means to generate stochastic reliefs both at the subwavelength and at the macroscopic scale, while different profiles are obtained by varying the etching parameters and the microreactor building materials. Standard photolithography is used to define microchannels, and radiofrequent sputtering is applied to deposit a gold film over the roughened surface. The same approach can be used for different photocatalytic processes. A useful trait of this method is that SPP-based chemical sensors can be conveniently integrated into such microreactors, being based on the same mechanism, thus ensuring a possibility for in situ characterization and real-time control of the reactor products.

REFERENCES

- [1] J. Schuller, E. Barnard, W. Cai, Y. Jun, J. White, M. Brongersma, *Nature Mater.* 9, 193 (2010).
- [2] W. L. Barnes, A. Dereux, T. W. Ebbesen, *Nature*, 424, 824 (2003).
- [3] S. Linic, P. Christopher, D. B. Ingram, *Nature Mater.* 10, 911 (2011).
- [4] X. Zhang, Y. L. Chen, R. S. Liu, D. P. Tsai, *Rep. Prog. in Phys.* 76, 046401, (2013).
- [5] M. Rašljčić, Z. Jakšić, M. M. Smiljanić, Ž. Lazić, K. Cvetanović, D. Vasiljević Radović, *Proc. IcETRAN 2016, MOI2.3.1-5* (2016).
- [6] F. Tan, T. Li, N. Wang, S. K. Lai, C. C. Tsoi, W. Yu, X. Zhang. *Sci. Rep.* 6, 33049 (2016).

Optical modulation using gain-assisted metasurfaces

B. Vasić¹ and R. Gajić¹

¹*Graphene Laboratory (GLAB) of Center for Solid State Physics and New Materials, Institute of Physics Belgrade, University of Belgrade, Belgrade, Serbia*
e-mail: bvasic@ipb.ac.rs

Tunable metasurfaces are planar arrays of metallic or dielectric resonators coupled with appropriate tunable elements [1]. They enable design of very compact and efficient optical modulators, with deep subwavelength thickness, fast operation, and low power consumption. Previous modulators were based on passive tunable elements, where the tuning was achieved by controlling either their refractive index or losses. Still, a perfect optical modulation providing both states with zero and unit reflection/transmission has not been achieved so far. Here we investigate gain-assisted metasurfaces in order to achieve perfect reflection modulation from zero to one. So far, optical gain was mainly used to compensate losses [2] and achieve lasing in metamaterial and plasmonic structures [3, 4, 5].

The considered structure [6] is metal-insulator-metal (MIM) plasmonic cavity, while the insulating layer is doped with dye molecules in order to provide an optical gain. When dye molecules are not excited, the insulating layer is purely absorbing, so the MIM cavity acts as a perfect plasmonic absorber thus giving zero reflection and OFF state. When the dye-doped film is inverted (the emission of dye molecules dominates over absorption), losses in metallic parts can be compensated. In this case, at the emission frequency of dye molecules, the MIM cavity behaves as a perfect mirror with unit reflection in ON state.

Gain-assisted metasurfaces are studied using numerical simulations based on rigorous coupled wave analysis. First we discuss design of MIM cavities, the optimization of their geometry, and required level of the optical gain. The modulator operation is analyzed in terms of its radiative and non-radiative decay rates, and their evolution with the degree of inversion of dye-doped layer. It is shown how the optical gain can be used for adjusting both OFF and ON states. Finally, we discuss possible lasing from these structures.

This work is supported by the Serbian Ministry of Education, Science and Technological Development under Project No. OI171005.

REFERENCES

- [1] N. I. Zheludev and Y. S. Kivshar, *Nat. Mater.* 11, 917 (2012).
- [2] S. Xiao, V. P. Drachev, A. V. Kildishev, X. Ni, U. K. Chettiar, H.-K. Yuan, and V. M. Shalaev, *Nature* 466, 735 (2010).
- [3] N. I. Zheludev, S. L. Prosvirnin, N. Papasimakis, and V. A. Fedotov, *Nat. Photonics* 2, 351 (2008).
- [4] M. A. Noginov, G. Zhu, A.M. Belgrave, R. Bakker, V.M. Shalaev, E. E. Narimanov, S. Stout, E. Herz, T. Suteewong, and U. Wiesner, *Nature* 460, 1110 (2009).
- [5] W. Zhou, M. Dridi, J. Y. Suh, C. H. Kim, D. T. Co, M. R. Wasielewski, G. C. Schatz, and T. W. Odom, *Nat. Nanotechnol.* 8, 506 (2013).
- [6] B. Vasić and R. Gajić, *Opt. Lett.* 42, 2181 (2017).

Film-coupled silver nanoparticles on flat and periodically corrugated aluminium substrates

G. Isić¹, U. Ralević¹, S. Aškračić^{1a}, S. Graovac¹, S. Savić-Šević², A. Mikhailov³, A. Antanovich³, A. Prudnikau³, M. Artemyev³, I. Fabijanić⁴, V. Janicki⁴, B. Okorn⁴, J. Sancho-Parramon⁴ and R. Gajić¹

¹Graphene Laboratory of^aCenter for Solid State Physics and New Materials, Institute of Physics Belgrade, University of Belgrade, Belgrade, Serbia

²Photonics Center, Institute of Physics Belgrade, University of Belgrade, Belgrade, Serbia

³Research Institute for Physical Chemical Problems, Belarusian State University, Minsk, Belarus

⁴Ruđer Bošković Institute, Zagreb, Croatia

e-mail: isicg@ipb.ac.rs

The strong scattering of light by noble metal nanoparticles has, since ancient times, been utilized in various ways, from Roman stained glass to modern day hCG pregnancy tests. At optical frequencies, both the "lightning rod effect" associated with nanometer geometric features and the excitation of collective charge oscillations known as localized surface plasmons (LSPs) contribute to the formation of strong and highly localized electric field "hotspots" at the nanoparticle surface. Understanding the "hotspot" formation mechanism and its attributes such as resonant wavelength, excitation efficiency or spatial confinement, as well as mastering the technology to efficiently produce LSP systems with desired properties, has been at the focus of plasmonics and nanooptics in the past decade and motivated by the perspective of producing a new generation of ultrasensitive spectroscopic sensors [1] or controlling the photon generation by quantum emitters [2]. A significant recent development has been realized by the use of the layer-by-layer polyelectrolyte deposition technique [2,3], providing cheap means to produce dielectric layers the thickness of which can be controlled with subnanometer precision.

Here we report on a comprehensive study of optical properties of silver nanospheres or nanocubes separated from a flat or periodically corrugated aluminium substrate by a few nanometer thick layer of oxide and several polyelectrolyte layers. Combining theoretical methods based on the mixed representation of the Dyadic Green function for the electric field, numerical simulations employing the finite element method, various colloidal synthesis protocols for silver nanoparticle generation, holographic generation of periodically corrugated surfaces, electron beam deposition of aluminium films, layer-by-layer polyelectrolyte deposition, spectrophotometry, spectroscopic ellipsometry, Raman spectroscopy and atomic force microscopy, we investigate the properties of surface plasmon polaritons of the aluminum surface [4] and their role in the formation of LSPs highly localized in tiny gaps between the nanoparticle and aluminium substrate.

REFERENCES

- [1] L. Rodriguez-Lorenzo, R. A. Alvarez-Puebla, I. Pastoriza-Santos, S. Mazzucco, O. Stephan, M. Kociak, L. M. Liz-Marzan, F. J. Garcia de Abajo, *J. Am. Chem. Soc.* 131, 4616 (2009).
- [2] O. Kulakovich, N. Strekal, A. Yaroshevich, S. Maskevich, S. Gaponenko, I. Nabiev, U. Woggon, M. Artemyev, *Nano Lett.* 2, 1449 (2002).
- [3] J. J. Mock, R. T. Hill, A. Degiron, S. Zauscher, A. Chilkoti, D. R. Smith, *Nano Lett.* 8, 2245 (2008).
- [4] D. Gerard, S. K. Gray, *J. Phys. D: Appl. Phys.* 48, 184001 (2015).

Refractive index fluctuations due to multianalyte adsorption in chemical and biological plasmonic sensors of ultralow analyte concentrations

O. Jakšić, I. Jokić, Z. Jakšić, M. Frantlović, M. Rašljić and K. Cvetanović Zobenica
*University of Belgrade, Institute of Chemistry, Technology and Metallurgy – Center of Microelectronic Technologies,
Belgrade, Serbia*
e-mail: ijokic@nanosys.ihm.bg.ac.rs

The principle of operation of optical affinity-based chemical and biological sensors relies on adsorption-desorption (AD) process of target substance particles on the sensing surface, leading to the change of the surface layer composition, and consequently its optical parameters, thus altering the properties of light that interacts with the sensing element [1]. A well known group of such sensors are refractometric sensors, in which the refractive index of the sensing area depends on the amount of the adsorbed substance (i.e. of the number of adsorbed target particles), and is therefore used as a measurement parameter. Since AD process is random in nature, the number of adsorbed particles on the sensing surface fluctuates, resulting in refractive index fluctuations, which are known as AD noise. This fundamental noise can limit the sensor ultimate performance regarding its total noise and minimal detectable concentration. AD noise analysis is therefore important for the design, optimization, and characterization of practical adsorption-based refractometric sensors.

Plasmonic sensors belong to refractometric sensors, and are known for highly sensitive label-free detection [2]. However, as in all adsorption sensors, there is the problem of selectivity. Although methods for sensing surface functionalization are used in order to promote binding of target analyte particles, adsorption of other substances from the environment is inevitable. Such substances often have much higher concentrations than the target substance, so the interfering signal caused by their unwanted adsorption can dominate and produce a false measurement result. Adsorption of multiple substances therefore must be taken into account in the analysis of the sensor response and its fluctuations.

Equilibrium response fluctuations of adsorption-based sensors have been analyzed in the cases of single and multianalyte adsorption in which it is justified to neglect the influence of AD process on the change of analyte concentration in the sensor reaction chamber [3, 4], so that a linear adsorption model can be used. Fluctuations in microfluidic sensors that have constant influx of analyte particles due to mass transfer have also been modeled [5, 6]. In plasmonic sensors, refractive index fluctuations are considered by taking into account the depletion of particles in the reaction chamber due to adsorption of one analyte, assuming ideal sensor selectivity [7, 8]. In this paper we present a model of sensor response fluctuations that corresponds to a more realistic practical situation of both multianalyte adsorption on the sensing surface and the varying analyte concentration of the adsorbing species in a closed reaction chamber. By discussing an example of two adsorbed substances, we analyze the influence of unwanted adsorption on the refractive index fluctuations depending on the analyte concentrations. Subsequently, we compare the results of the analysis with those obtained by using the linear adsorption model for multiple substances. Finally, we determine the conditions in which the application of the presented model becomes necessary, having in mind that the new generation of plasmonic sensor is intended for detection of ultralow analyte concentrations.

REFERENCES

- [1] Z. Jakšić, Proc. X Int. Symp. Industrial Electronics INDEL 2014 pp. 16-31, Banja Luka, Nov. 6-8 (2014).
- [2] J. Homola, ed., Surface plasmon resonance based sensors, Springer (2006).
- [3] Z. Djurić, I. Jokić, M. Frantlović, O. Jakšić, Sens. Actuators B 127, 625 (2007).
- [4] O. Jakšić, Z. Jakšić, Ž. Čupić, D. Randjelović, L. Kolar-Anić, Sens. Actuators B 190, 419 (2014).
- [5] I. Jokić, Z. Djurić, M. Frantlović, K. Radulović, P. Krstajić, Z. Jokić, Sens. Actuators B 166-7, 535 (2012).
- [6] M. Frantlović, I. Jokić, Z. Djurić, K. Radulović, Sens. Actuators B 189, 71 (2013).
- [7] O. Jakšić, I. Jokić, Z. Jakšić, Ž. Čupić, L. Kolar-Anić, Phys. Scr. T162, 014047 (2014).
- [8] I. Jokić, O. Jakšić, Opt. Quant. Electron. 48, 353 (2016).

Controlling silver nanoparticle production by ion-reduction process for tailoring of plasmonic properties

I. Fabijanić¹, V. Janicki¹, B. Okorn¹, J. Sancho Parramon¹

¹*Ruđer Bošković Institute,*

Zagreb, Croatia

e-mail: ifabijan@irb.hr

For the last few decades, scientists have been focused on the production of metal nanoparticles due to their electronic, optical, magnetic and other specific properties. The potential application of metal nanoparticles is indeed broad; they have already been used in catalysis, photonics, optoelectronics, surface-enhanced Raman scattering (SERS) [1], anticancer therapy, drug delivery, cell labeling, non-invasive diagnostics (bioimaging and NMR imaging), etc. [2,3]. Silver nanoparticles are of particular importance because of their physical and chemical properties, which can be broadly tailored by controlling their size and morphology. Although a wide variety of silver nanoparticle synthesis methods have been published [1], one of them is especially important because it allows us to tailor the process to obtain nanoparticles of the desired shape and/or size – the chemical reduction of silver precursor in a solution, usually in the presence of a stabilizing agent. Because of a delicate interplay of kinetics and thermodynamics, it is quite difficult to control both size and shape simultaneously [4], but with the choice of silver precursor, reducing agent, solvent, stabilizing agent, reaction temperature, reaction time, molar ratio of precursor/ solvent, molar ratio of nucleating agent/metallic silver, weight ratio of stabilizing agent/silver precursor [5], the precursor injection rate [1] as well as the precursor/ reducing agent/ stabilizing agent/ adding sequence it is possible to synthesize specifically-shaped silver nanoparticles with a relatively narrow size distribution [6]. Still, the production of nanoparticles should be simple, reproducible and relatively cheap, which is sometimes hard to achieve.

Here, the silver nanoparticle production by the reduction of silver ions is presented. The influence of temperature, solvent selection, precursor injection rate and reactants adding sequence on the morphology and size of silver nanoparticles is investigated. The reproducibility of the process under the same experimental conditions has also been examined. The synthesized nanoparticles have been characterized by scanning electron microscopy and UV-Vis spectrometry. The experimentally determined plasmonic properties of nanoparticles are compared with the theoretical prediction of electrodynamic simulations. Some of the ongoing results will be presented at this conference.

REFERENCES

- [1] D. Kim, S. Jeong, J. Moon, *Nanotechnology* 17, 4019 (2006).
- [2] M. Iv, N. Telischak, D. Feng, S. J. Holdsworth, K. W. Yeom, H. E. Daldrup-Link, *Nanomedicine (Lond)*. 10, 993 (2015).
- [3] N. Khlebtsov, L. Dykman, *Chem. Soc. Rev.* 40, 1647 (2011).
- [4] A. Callegari, D. Tonti, M. Chergui, *NanoLett.* 3, 1565 (2003).
- [5] C. Ducamp-Sanguesa, R. Herrera-Urbina, M. Figlarz, *J. Solid State Chem.* 100, 272 (1992).
- [6] B. Wiley, Y. Sun, B. Mayers, Y. Xia, *Chem. Eur. J.* 11, 454 (2005).

Resonant absorption and extrinsic chirality in GaAs-based nanowires

E. Petronijevic¹, G. Leahu¹, A. Belardini¹, M. Centini¹, R. Li Voti¹, T. Hakkarainen², E. Koivusalo², M. Rizzo Piton^{2,3}, S. Suomalainen², M. Guina² and C. Sibilial¹

¹*La Sapienza University of Rome, Rome, Italy*

²*Optoelectronics Research Centre,*

Tampere University of Technology, Finland

³*Departamento de Física,*

Universidade Federal de São Carlos, Brazil

e-mail: emilija.petronijevic@uniroma1.it

Semiconductor nanowires (NWs) have stimulated great interest due to their ability to confine optical fields, and enhance the electrical and optical response in nano-scale dimensions. High quality ensembles of GaAs-AlGaAs-GaAs core-shell-supershell NWs with hexagonal cross-section were fabricated by low cost, self-catalyzed, lithography-free growth on Si substrates [1]. The sample geometries (length $\sim 5\mu\text{m}$, diameter $\sim 140\text{-}150\text{nm}$) and material properties lead to the resonant absorption due to the excitation of NW modes in the visible and near-IR part of the spectrum. The absorption properties in similar NWs have been so far characterized indirectly, by measuring the photocurrent, reflectance or photoluminescence. Here we first demonstrate that scattering-free photo-acoustic spectroscopy (PAS) can be applied to directly measure such absorption [2]. The experimental results are in great agreement with the numerical analysis of these modes, simulated in both single NW and interacting NWs whose distribution was taken from SEM distribution analysis. The work therefore proves the new application of PAS as a low-cost, sensitive characterization tool for NW ensembles.

We further investigate the hybridization of GaAs-based NWs with Au; we cover three out of six sidewalls of the samples by 10-20nm of gold, thus inducing a symmetry breaking which leads to an “extrinsic” chiral response under a proper experimental set-up. We apply PAS to measure the circular dichroism at 532nm and 980nm incident wavelength under many sample and angle configurations [3]. The experimental results are in good agreement with simulations, showing that the optimization of NW geometry could lead to chiral light applications.

The resonant modes lead to the chiral field formation in the vicinity of GaAs-based NWs; the overall symmetry can again be broken by the asymmetric golden layer [4]. We show that the chiral field maps can be manipulated by changing the incident angle of the linearly polarized light. Our work is here inspired by the actual samples from [1-3], and we optimize the NW dimensions for the maximum enhancement of the chiral field. Finally, we underline the possible experimental configuration for the enantioselective spectroscopy application.

REFERENCES

- [1] T. V. Hakkarainen, A. Schramm, J. Mäkelä, P. Laukkanen, M. Guina, *Nanotechnology* 26, 275301 (2015).
- [2] G. Leahu, E. Petronijevic, A. Belardini, M. Centini, R. Li Voti, T. Hakkarainen, E. Koivusalo, M. Guina, C. Sibilial, *Sci. Rep.* 7, 2833 (2017).
- [3] G. Leahu, E. Petronijevic, A. Belardini, M. Centini, C. Sibilial, T. Hakkarainen, E. Koivusalo, M. Rizzo Piton, S. Suomalainen, and M. Guina, *Adv. Opt. Mater.* 2017, 1601063 (2017).
- [4] E. Petronijevic, M. Centini, A. Belardini, G. Leahu, T. Hakkarainen, C. Sibilial, *Opt. Express* 25(13), 14148 (2017).

Open Triangular Ring Cavity Resonator Integrating a Nanograting Mirror

G. Ehrlich¹, M. Zohar², M. Auslender¹ and S. Hava¹

¹Department of Electrical and Computer Engineering, Ben Gurion University, Beer-Sheva 84105, Israel

²Department of Electrical Engineering, Sami Shamoon College of Engineering, Beer Sheva 8410, Israel
e-mail: ehrlichg@bgu.ac.il

We analyzed the optical properties of an open FP cavity ring resonator based on a nanograting mirror (NGM) and two identical tilted flat mirrors, M1(2), where the first diffracted order is coupled to the zero order to obtain the resonance in the cavity.

Grating structures are well known meta-surface devices [1] capable of performing functions for nonconventional optics. Open cavity standing-wave Fabry–Perot interferometers based on grating beam splitters, have been proposed and implemented [2] for overcoming the problems of transmission optics posed by the high-power light. A ring FP cavity embedding similar constituents was later proposed [3]. No theory was elaborated in the open case [2], and only schematic treatment was presented in the ring case [3], however the grating was not optimized for the best cavity gain. Our study aims at filling this gap, and this paper is devoted to the ring FP cavity.

The analyzed structure is based on an NGM and M1(2) arranged at a height H above the grating and a distance L from each other. Let coherent light of a wavelength λ impinges NGM at an angle θ_i , then properly relating the cavity dimensions (L, H), the mirror tilts and the grating period (Λ), the initially diffracted -1^{st} order beam can be forced to launch the light circulation, so that after the first round trip the circulation proceeds infinitely with the secondary 0^{th} order beam. Simultaneously, the secondary out-of-cavity $+1^{\text{st}}$ order beams diffracted from the NGM and combined with the initial 0^{th} order beam, as they propagate under the same angle, and continues to the light read out at the detector port (D). The light recirculation gives rise to an intracavity light power gain if the cavity is tuned and *viceversa* if it is detuned, as can be distinguished at the D-readout.

At $H, L \gg \lambda$ the travelling-wave nature of the ring resonator enables using ray tracing. Then, for the circulating resonant light maximum power gain, we obtain

$$G_{\text{res}} = \frac{|\rho_{-1}(\theta_i)|^2}{(1 - |\rho_0(\theta'_i)|R)^2}, \quad \sin \theta'_i = \sin \theta_{-1} = \sin \theta_i - \lambda/\Lambda, \quad (1)$$

where $\rho_m(\vartheta)$ is the complex reflection amplitude of m^{th} diffracted order at an incidence angle ϑ , and R is the reflectance of the mirrors M1(2). Finally, the ray-tracing results are plausibly combined with the rigorous electromagnetic simulation of the amplitudes $\rho_m(\vartheta)$ using our in-house software described in detail elsewhere [4]. Furthermore, we optimized G_{res} given by Eq.1 for an NGM of TiO₂-air grating-patterned surface on a SiO₂/Si multilayer stack. The procedure results in an extremely narrow Fano-like spectrum of $|\rho_0(\theta_{-1})|^2$ peaked at ~98%. The intra-cavity power gain and the carrier combined throughput light power buildup show high sensitivity to the cavity dimensions with a high finesse and throughput signal contrast.

To summarize, we studied novel arrangement of two flat mirrors and nanograting mirror to couple -1^{st} diffracted order into cavity circulation. The intra-cavity and combined throughput light power buildup show high sensitivity to the cavity dimensions. Thus, the considered optomechanical meta-device resonator can serve as a highly sensitive position detector, mode cleaner or mode combiner.

REFERENCES

- [1] N.I. Zheludev and Yu.S. Kivshar, Nature Mater. 11, 917 (2012).
- [2] K.-X. Sun and R. L. Byer, Opt. Lett., 23, 567 (1998).
- [3] R. Schnabel, A. Bunkowski, O. Burmeister and K. Danzmann, Opt. Lett. 31, 658 (2006).
- [4] M. Zohar, M. Auslender, L. Faraone, and S. Hava, J. Nanophotonics 5, 051824 (2011).

All-dielectric metamaterials based on water. Experimental confirmation of the toroidal response

Ivan Stenishchev^{1,2}, Alexey Basharin^{1,2}

¹National University of Science and Technology (MISiS), The Laboratory of Superconducting metamaterials, 119049 Moscow, Russia

²National University of Science and Technology (MISiS), Department of Theoretical Physics and Quantum Technologies, 119049 Moscow, Russia
e-mail: iv.steni@yandex.ru

Static toroidal dipole moment was firstly predicted by Zel'dovich in 1958 for parity violation explanation in the atomic nucleus [1], but its "second birth" was due to the dynamic toroidal response demonstration in metamaterials.

In this paper, we experimentally demonstrate toroidal response of *all*-dielectric metamaterials in microwave. We propose two simplest for fabrication configurations based on *all*-dielectric clusters called metamolecules. The clusters of first metamaterial consist of four high-index dielectric particles. This metamaterial was investigated earlier, and theoretically demonstrated the toroidal excitation in LiTaO₃ particle clusters in the terahertz frequency range [2]. However, for our microwave study, the water exhibits dielectric properties in microwave with low losses [3]. At the same time, water was proved to be a candidate for dielectric metamaterials due to its convenience for metaatoms fabrication. Clusters of the second metamaterial are the inverted version of the first one, that is the high index dielectric slab with perforated identical cylindrical holes. Such a structure is distinguished by the simplicity for fabrications in the nanoscale (visible optics) using the Focus Ion Beam method [4].

To evaluate the role of multipoles in forming the resonant response we compare the powers scattered by 5 strongest multipoles. We calculate the multipole moments induced in metamolecules based on density of displacement currents in the dielectric inclusions obtained from simulations. As result we observe the dominating toroidal dipole moment on the frequency 2.55 GHz for the first structure and 0.97 GHz for the second case.

For experimental confirmation we use the two horn antennas methods in an anechoic chamber. We demonstrate at the first time the transmission spectra which are corresponds to toroidal peak for both types of metamaterials.

In addition, in this work we discuss how we can exploit our ideas for metamaterial "birth" of a toroidal moment in optics by using nanoparticles and nano-holes in low-index dielectrics like *Si*. We show the behavior of multipoles in dielectric media with different permittivity. Our findings are promising in low-index nanophotonics, metamaterials and especially in metamaterials with anapole and toroidal response.

REFERENCES

- [1] Y. B. Zel'dovich, Sov. Phys. JETP 6, 1184 (1958).
- [2] A. Basharin, M. Kafesaki, E. Economou, C. Soukoulis, V. Fedotov, V. Savinov, and N. Zheludev, Phys. Rev. X 5, 011036 (2015).
- [3] M. Rybin, D. Filonov, K. Samusev, P. Belov, Y. Kivshar & M. Limonov, Nature Communications 6, 10102 (2015).
- [4] I. Stenishchev, A. Basharin "All-dielectric toroidal metamaterials. Water experiments" Scientific Reports

Subwavelength nickel-copper multilayers as an alternative plasmonic material

Ivana Mladenović¹, Zoran Jakšić¹, Marko Obradov¹, Slobodan Vuković¹,

Goran Isić², Dragan Tanasković¹, Jelena Lamovec¹

¹ *Center of Microelectronic Technologies, Institute of Chemistry, Technology and Metallurgy,
University of Belgrade, Serbia*

² *Institute of Physics,*

University of Belgrade, Serbia

e-mail: jaksa@nanosys.ihtm.bg.ac.rs

Plasmonic materials ensure extreme concentrations and localizations of electromagnetic fields as a consequence of the appearance of evanescent waves (surface plasmons polaritons) in the range of negative values of relative dielectric permittivity near the plasma frequency [1]. The many applications of plasmonics include ultrasensitive chemical sensors, advanced all-optical devices, enhanced photodetectors, energy harvesting devices and many others [2].

Among hurdles to a more widespread use of plasmonics are a rather limited range of available plasmonic materials (usually good metals like gold and silver) and their high absorption losses in the range of interest. This is why alternative plasmonic materials are of large interest [3]. Besides using materials like transparent conductive oxides, highly doped semiconductors, intermetallic and similar, a possible approach is to combine a plasmonic material with lossless dielectric into mesoscopic or subwavelength nanocomposites (plasmonic crystals) [4], thus allowing almost arbitrary tailoring of frequency dispersion in a spectral range defined by the plasma frequency.

In this contribution we consider numerically and experimentally the use of bimetallic superlattices, i.e. all-metal plasmonic crystals consisting of two alternating materials with negative values of their relative dielectric permittivities. We use the copper-nickel multilayers. Copper is a good plasmonic material, but not widely used due to surface oxidation impairing its electromagnetic properties over time. The layers of nickel, also a plasmonic material, serve a dual purpose of being a protection against copper oxidation and ensuring formation of surface waves at the alternating interfaces between the two materials. At the same time, the multilayers serve as couplers between the propagating and the surface waves.

We simulated the electromagnetic properties of subwavelength Cu-Ni multilayers by the 2D finite element method using realistic material parameters. We adjusted the response by simply varying Cu to Ni thickness ratio. A rich optical behavior was obtained, as governed by the electromagnetic properties of the multilayers. Experimentally, we fabricated 1D plasmonic crystals consisting of alternately stacked nanocrystalline Ni and Cu layers by electrodeposition on a cold-rolled copper substrate [5]. We obtained highly parallel interfaces with thin individual strata and excellent morphology. We made use of beneficial structural properties of both Cu and Ni, while suppressing the undesirable ones. The approach offers high quality, large area, compact and low cost structures, while retaining a compatibility with the standard microfabrication and microelectronic processes.

REFERENCES

- [1] S. A. Maier, *Plasmonics: Fundamentals and Applications*, Springer New York, NY, (2007).
- [2] W. L. Barnes, A. Dereux, T. W. Ebbesen, *Nature* 424, 824 (2003).
- [3] P. West, S. Ishii, G. Naik, N. Emani, V. Shalaev, A. Boltasseva, *Laser & Photon. Rev.* 1 (2010).
- [4] S. M. Vuković, Z. Jakšić, I. V. Shadrivov, Y. S. Kivshar, *Appl. Phys. A*, 103, 615 (2011).
- [5] J. Lamovec, V. Jović, D. Randjelović, R. Aleksić, V. Radojević, *Thin Solid Films*, 516, 8646 (2008).

Nontrivial nonradiating all-dielectric anapole sources

Nikita A. Nemkov^{1,2}, Ivan V. Stenishchev^{1,2}, Alexey A Basharin^{1,2}

¹*National University of Science and Technology (MISIS), The Laboratory of Superconducting metamaterials,
Moscow, Russia*

²*National University of Science and Technology (MISIS), Department of Theoretical Physics and
Quantum Technologies,
Moscow, Russia*

e-mail: alexey.basharin@misis.ru

Dynamic anapole is a promising element for future nonradiating devices, such as cloaked sources and sensors, quantum emitters, and especially the ingredients for observing dynamic Aharonov-Bohm effect [1, 2]. However, the anapole response can be damped by the Joule losses. In this paper we theoretically propose and experimentally demonstrate a novel type of active all-dielectric sources, which are in some sense, realizes the elementary anapole of Afanasiev, and study its radiative/nonradiative regimes in microwave and optics.

Dynamic toroidal dipole can be defined in terms of the the time-dependent poloidal torus currents. The sources defined by the dynamic toroidal dipole moment radiates with the same angular momentum and the far-field properties as electric dipole source. Therefore, the toroidal and electric dipole moments are indistinguishable for any distant observers. Obviously, the point dynamic anapole may be viewed as the basic building block out of which an arbitrary nonradiating source can be composed. Dynamic anapole modes are relevant to many phenomena in metamaterials, nanophotonics and beyond. For instance, their existence proves that the inverse scattering problem of the electrodynamics is unsolved without additional assumptions about the source structure [1].

Here, we propose experimentally the novel class of all-dielectric nonradiating sources exhibiting a resonant anapole response [3]. Our metamolecule is based on subwavelength high-index dielectric cylinders operating in the regime of resonant Mie scattering and excited by electric dipole antenna. We show that the near-field coupling between the individual Mie- modes of the cylinders is capable of suppressing all standard multipoles besides the toroidal and electric dipole excitations. The proposed metamolecule can be readily fabricated from low-loss dielectric material SrTiO₃ and produces a unique field topology at the Mie resonance. Moreover, we demonstrate at the first time radiating/nonradiating nature of toroidal and anapole active modes. Our findings can be useful for future design of nonradiating sources, as a ground for Aharonov-Bohm demonstrations and promising invisible structures for nanophotonics [4].

REFERENCES

- [1] N. Papasimakis, V. A. Fedotov, V. Savinov, T. A. Raybould & N. I. Zheludev, *Nature Materials* 15, 263–271 (2016).
- [2] Andrey E. Miroshnichenko et al., *Nature Communications* 6, 8069 (2015).
- [3] Nikita A. Nemkov, Ivan V. Stenishchev, Alexey A. Basharin, *Scientific Reports* 7, 1064 (2017).
- [4] N.A. Nemkov, A.A. Basharin and V.A. Fedotov, *Physical Review B* 95, 165134 (2017).

Metamaterials with broken symmetry: general approach, experiment and multipolar decomposition

Anar K. Ospanova^{1,2} and Alexey A. Basharin^{1,2}

¹*National University of Science and Technology (MISiS), The Laboratory of Superconducting metamaterials, Moscow, Russia*

²*National University of Science and Technology (MISiS), Department of Theoretical Physics and Quantum Technologies, Moscow, Russia*

e-mail: anar.k.ospanova@gmail.com

We introduce the general approach with describing all the EIT effects as the contribution of toroidal and electric dipoles called us anapole. We demonstrate experimentally that broken symmetry in metamaterials is always defined anapole excitation that is fundamental origin of EIT. In this paper, we propose to study the effects associated with broken symmetry in metamaterials. Some are going to be explained from the point of view of multipolar decomposition.

EIT (Electromagnetic Induced Transparency) is an effect of appearance of narrow transmission gap in the spectrum of absorption of optically opaque system, which is called “transparency window”. This effect is due to dipole allowed transitions in three-level atomic system [1]. Classically, effect of EIT was shown in planar metamaterials. All investigated metamolecules have peculiarities of broken symmetry. Asymmetry of these elements brought to such phenomena like “trapped modes”, Fano-resonance – classical analogues of EIT [2, 3]. In this paper, we introduce the general approach that the resonances of these systems are accompanied by existence of anapole mode [4]. Anapole mode is the consequence of destructive interference between electric and toroidal dipole moments, which have almost the same intensity and radiation pattern and illuminated at the same frequency. Due to this effect, we observe full transparency window and metamaterial becomes invisible for external observer [5].

For this aim, we demonstrate such an effect on the base of simple system, we carried out experiment by means of breaking symmetry of square. We broke metallic particle in the form of square into the two C-shaped splitting resonators (SRR) directed up and down, and started to move them with respect to each other. The “transparency window” became broader by increasing the distance between SRR. At the same time, all states with emergence of “transparency window” are accompanied by existence of anapole mode. Such fact leads to hypothesis, that all mentioned effects of transparency like “trapped modes” and Fano-resonance are dictated by existence of anapole mode.

The main promising result here, that all EIT effects are destructive interference of anapole. Our general approach will be interesting for the invisibility theory, nanophotonics and metamaterials.

REFERENCES

- [1] N. Papanikolaou and N.I. Zheludev, *Optics and Photonics News* 20, 10, (2009).
- [2] V.A. Fedotov, M. Rose, S. L. Prosvirnin, N. Papanikolaou and N.I. Zheludev, *PRL* 99, 147401 (2007).
- [3] Shuang Zhang, Dentcho A. Genov, Yuan Wang, Ming Liu, and Xiang Zhang, *PRL* 101, 047401 (2008).
- [4] A.A. Basharin, V. Chuguevsky, N. Volsky, M. Kafesaki and E.N. Economou// *PHYSICAL REVIEW B* 95, 035104 (2017) .
- [5] N.A. Nemkov, A.A. Basharin and V.A. Fedotov, *PHYSICAL REVIEW B* 95, 165134 (2017).

Titanium nitride plasmonic resonator Fabry-Perot for Raman lasing on nanoscale

A. V. Kharitonov^{1,2}, S. S. Kharintsev^{1,3} and M. Kh. Salakhov^{1,3}

¹*Department of Optics and Nanophotonics, Kazan Federal University, Russia*

²*Kazan National Research Technical University, Kazan, Russia*

³*Institute of Perspective Technologies, Tatarstan Academy of Sciences, Russia*

e-mail: AntVHaritonov@kpfu.ru

Novel plasmonic materials play a crucial role for development of innovative photonic devices as well as for improvement of their performance. Transition metal nitrides, being refractory metals with tuneable optical properties, are prominent representatives of alternative plasmonic materials [1,2]. These nanocompounds, also known as conductive ceramics, lift the restrictions imposed by noble metals on operational intensity and temperature ranges of plasmon-assisted devices. Recent intensive examination of linear and nonlinear optical parameters of metal nitrides has revealed TiN to be a promising media for nonlinear plasmonics – metal-based nonlinear optics [3,4].

This work focused on another distinctive feature of TiN – Raman activity. Surface plasmon wave (pump wave) excited at interface between TiN and some dielectric experience inelastic scattering on lattice phonons within TiN. This leads to emergence of plasmonic wave at Stokes and anti-Stokes frequencies (signal wave). In nonlinear optical regime pump wave and signal wave can interact through third-order Raman susceptibility. Thus, in contrast to Raman-silent metals, TiN-based structures enable nonlinear light frequency conversion not only to second- and third harmonics, but also to Raman-shifted modes. Moreover, the threshold of the underlying stimulated Raman scattering effect in these structures could be greatly reduced by appropriate geometry and material design. Using planar plasmonic resonator Fabry-Perot [5] made of TiN we have observed the nonlinear Raman response at continuous wave modest power laser illumination. Here we provide insight into the physics behind high-efficient nonlinear Raman scattering within media acting both as Raman-active and plasmonic. A special attention is given to synthesis and characterization of TiN thin films suitable for plasmon-induced Raman amplification.

This work paves the ways to development of nano-sized Raman lasers [6] and highly sensitive biosensors [7].

REFERENCES

- [1] G. V. Naik, V. M. Shalaev, A. Boltasseva, *Adv. Mater.* 25, 3264 (2013).
- [2] U. Guller, A. Boltasseva, V. M. Shalaev, *Science* 344, 263 (2014).
- [3] N. Kinsey, A. A. Syed, D. Courtwright, C. DeVault, C. E. Bonner, V. I. Gavrilenko, V. M. Shalaev, D. J. Hagan, E. W. Van Stryland, A. Boltasseva, *Opt. Mater. Express* 5, 2395 (2015).
- [4] M. Kauranen, A. V. Zayats, *Nat. Photonics* 6, 737 (2012).
- [5] S. I. Bozhevolnyi, T. Sondergard, *Opt. Express* 15, 10869 (2007).
- [6] H. S. Rong, S. B. Xu, Y. H. Kuo, V. Sih, O. Cohen, O. Raday, M. Paniccia, *Nat. Photonics* 1, 232 (2007).
- [7] J. Homola, *Chem. Rev.* 180, 494 (2008).

Phase and amplitude tunability in planar THz metamaterials with toroidal response

Maria V. Cojocari^{1,2}, Kristina Schegoleva^{1,2}, Alexey A. Basharin^{1,2}

¹*National University of Science and Technology (MISiS), The Laboratory of Superconducting metamaterials, Moscow, Russia*

²*National University of Science and Technology (MISiS), Department of Theoretical Physics and Quantum Technologies, Moscow, Russia*

e-mail: masha_cojokari@mail.ru

For filling the terahertz frequency gap, where no practical technologies for generating, detecting and modulating the radiation exist, some unusual medium is required. Metamaterials, as structures with properties unattainable in Nature, are capable of resolving this issue [1]. We suggest a design of planar metamaterial, supporting toroidal dipole excitation, as tunable THz modulator [2].

The basis of proposed metamolecule was discussed earlier in [3]. It consists of two metallic split parts, resembling epsilon letters, looking at each other. Incident plane electromagnetic wave, polarized along central strips, excites asymmetrical currents on the surface of the metamolecule. As a result, magnetic field vectors are organized head to tail, which causes toroidal moment excitation. It interferes destructively with electric dipole, which also is arose, forming an anapole [4]. Far-fields in such structure are reduced, meanwhile fields in metamolecule origin are described by δ -function. This determines formation of a metamaterial with strong electric field localization and high Q-factor.

For terahertz frequencies metamolecule's basis is simulated as gold. To support tunable regime we introduce silicon inclusions with pump-power-dependent conductivity. They are repeating central strips and are located on both sides of them. The idea is to control the distribution of currents on the metamolecule surface by transiting the silicon from dielectric to metallic state. This leads to the blueshift of resonance frequency originated by currents flowing along silicon strips instead of the external ones, reducing electrical size of the metamolecule. The results of simulation show 50% tunability. With smaller periodicity of unit cells proposed metamaterial can exhibit phase tunability up to 2 rad. The switch from amplitude blueshift to phase tunability can be explained from multipole expansion. While for bigger periodicity of metamolecules the difference between electrical and toroidal dipoles' intensities varies, for smaller one it remains constant. Meantime, anapole mode of the structure is defined by the interaction between electrical and toroidal dipoles - the stronger is similarity, the higher is Q-factor. Thus, resonance of structure with bigger periodicity remains unchanged.

To conclude, we hope that proposed metamaterial, due to its properties, will be a platform for realization of THz modulators: extremely strong electric field localization in such metamaterial can reduce the impact of actual losses of metals in terahertz frequencies and the fact that we need to manipulate only with small silicon strips, makes us expect that conductivity switch would not require high power sources.

REFERENCES

- [1] Padilla, W. J., Taylor, A. J., Highstrete, C., Lee, M. & Averitt, R. D. Phys. Rev. Lett. 96, 107401 (2006).
- [2] Maria V. Cojocari, Kristina Schegoleva, Alexey A. Basharin, Optics Letters 42, (2017).
- [3] Alexey A. Basharin et al., Phys. Rev. B 95, 035104 (2017).
- [4] T. Kaelberer, V. A. Fedotov, N. Papasimakis, D. P. Tsai, N. I. Zheludev, Science 330, 1510 (2010).

Laser induced ultrafast switching processes in diamond

T. Apostolova¹ and B. Obreshkov¹

¹*Institute for Nuclear Research and Nuclear Energy, Bulgarian Academy of Sciences,
Tsarigradsko chaussee 72, Sofia 1784, Bulgaria
e-mail: obreshkov.boyan@gmail.com*

The electron dynamics in diamond irradiated by linearly-polarized intense ultrashort laser pulses is studied theoretically for a wide range of pulse energies ($1-10^3 \text{ mJ/cm}^2$) and laser wavelengths. Calculations based on the three-dimensional time-dependent Schrodinger equation incorporating a realistic band structure of bulk diamond predicts generation of ultrafast polarization currents, which are completely reversible, i.e. the laser pulse reversibly increases (free from breakdown) the AC conductivity of diamond within a femtosecond, which allows electric currents to be controlled and switched by the light pulse. As the laser intensity is increased, a DC current in direction of the laser field is generated after the end of the pulse and is considered as a precursor of optical breakdown on a femtosecond timescale [1]. Above this threshold, we model the linear response of the photoexcited plasma of electron-hole pairs and the change of optical properties in terms of transient dielectric function revealing the gradual transformation of diamond bulk into virtual plasmonic material supporting photoexcitation and propagation of surface plasmon-polaritons (SPPs) [2]. In the context of efficacy factor theory [3], these transient SPP waves have a potential to imprint sub-wavelength polarization-dependent laser-induced periodic surface structure into the surface relief via laser ablation. This study may also allow to predict and potentially extend the capabilities of the dielectric nano-optical meta devices and the photo-modulated meta surfaces based on them and to uncover ultimate limits of diamond as high-index dielectric materials for potential applications in ultrafast optical switching, electronic signal manipulation into the petahertz time domain, spatial phase modulation and saturable absorption.

REFERENCES

- [1] S. Lagomarsino et al., Phys. Rev. B **93**, 085128 (2016).
- [2] T. Apostolova et al., *arXiv preprint arXiv:1701.04650* (2017).
- [3] J. E. Sipe et al., Phys. Rev. B **27**, 1141 (1983).

Plasmonic Transmission Gratings for biosensors and atomic physics

A. Sierant¹, B. Jany¹, D. Bartoszek-Bober¹, J. Fiutowski², J. Adam² and T. Kawalec¹

¹*Marian Smoluchowski Institute of Physics, Łojasiewicza 11, 30-348 Cracow, Poland*

²*NanoSyd, Mads Clausen Institute, University of Southern Denmark, Alsion 2, DK-6400 Sønderborg, Denmark*
e-mail:aleksandra.plawecka@doctoral.uj.edu.pl

Surface plasmon polaritons (SPPs) are electromagnetic excitations, which travel along a boundary of dielectric and a conductor, exponentially decaying in the perpendicular direction in both media. Such excitations generate a strong potential for cold atoms, which can be used for manipulation and guiding of ultracold atomic gases. To excite SPPs one can use metallic diffraction grating, which parameters strongly affect the shape of the potential [1]. This phenomenon has a variety of applications, including biosensors [2] and optical dipole mirrors for cold atoms [3].

Here, we introduce metallic transmission gratings, processed onto a glass substrate with focused ion beam (FIB) technique of numerically found grating parameters. We investigate the proposed transmission gratings by means of near-field scanning optical microscope (NSOM) and far field measurements. Subsequently, the results are compared with numerical calculations implemented with rigorous coupled wave analysis (RCWA) and finite-difference in time-domain (FDTD) methods.

REFERENCES

- [1] Barnes WL, Dereux A, Ebbesen TW, Nature 424, 824–830 (2003).
- [2] X.D. Hoa, A.G. Kirk, M. Tabrizian, Biosensors and Bioelectronics, Volume 23, 2, 151-160 (2007).
- [3] T. Kawalec, et al., Opt. Lett. 39, 2932 (2014).

Flat lenses with continuously graded metamaterials designed using transformation optics: An exact analytical solution of field equations

M. Dalarsson¹, R. Mittra² and Z. Jakšić³

¹*Department of Physics and Electrical Engineering, Linnaeus University, 351 95Växjö, Sweden*

²*Department of Electrical Engineering, The Pennsylvania State University, University Park, PA, USA*

³*Institute of Chemistry, Technology and Metallurgy, University of Belgrade, Serbia*

e-mail:mariana.dalarsson@lnu.se

We present an exact analytical solution for electric and magnetic fields in continuously graded flat metamaterial lenses. Such lenses are usually designed as a number of metamaterial layers with the refractive index graded both in radial and in longitudinal direction. In the present contribution we model such lenses as compact cylindrical composites with continuous relative permittivity and permeability functions that approach unity asymptotically far from the composite center. In order to illustrate the method, we derive an exact analytical solution for electric and magnetic fields in one particular class of composite designs with permittivity graded in both radial and longitudinal directions, and with permeability graded in the radial direction only.

Flat lenses designed using Transformation Optics (TO) have been studied in a number of publications (e.g. [1-2]). A plano-concave metamaterial-based lens designed to obtain a gain above 13 dB in the frequency band 10–12 GHz has been presented in [3]. Such a lens has a narrow bandwidth typical for the metamaterial-based designs exhibiting resonant dispersion. In [3-4] the field manipulation (FM) method was used, where the relative permeability was set to unity and only the relative permittivity was graded to create the desired refractive index. Such an approach, however, decreases the efficiency of the composite lenses [3]. The mentioned studies of the flat-lenses designs generally require direct numerical solving of the field equations. Contrary to that, an analytical approach to modeling flat lenses with continuously graded profiles using FM method has been reported in [4]. The availability of exact analytical solutions for FM models is, however, limited by the need to have an effective permittivity equal to unity [3].

In this contribution we extend the analytical approach outlined in [4] to a case where we allow radial dependence of relative permeability. Thus we obtain an exact analytical solution for electric and magnetic fields for one particular class of composite designs with permittivity graded in both radial and longitudinal directions and with permeability graded in radial direction only. At the same time the model applied here is convenient to describe a much wider class of graded geometries, while at the same time avoiding unnatural singularity points in spatial dependence of refractive index that were typical for earlier solutions. The approach we use is analogous to the one applied for planar [6] and cylindrical [6] metamaterial structures.

The main reason to analytically study the continuous models of the fields in flat lenses is that this may provide additional insight helping to improve the existing or suggest entirely new flat lens designs.

REFERENCES

- [1] D. A. Roberts, N. Kundtz, D. R. Smith, *Opt. Express*, 17, 16535 (2009).
- [2] S. Jain, M. Abdel-Mageed, R. Mittra, *IEEE Ant. Wireless Propagation Lett.*, 12, 777 (2013).
- [3] T. Driscoll, G. Lipworth, J. Hunt, N. Landy, N. Kundtz, D. N. Basov, D. R. Smith, *Optics Express*, 20, 13264 (2012).
- [4] M. Dalarsson, R. Mittra, *IEEE Internat. Symp. on Antennas and Propagation and North American Radio Science Meeting*, WE-UB.1A.2, Vancouver, BC, Canada, 19-24 July 2015.
- [5] M. Dalarsson, P. Tassin, *Opt. Express*, 17, 6747 (2009).
- [6] M. Dalarsson, M. Norgren, Z. Jaksic, *PIER*, 151, 109 (2015).

Fresnel diffraction of a Laguerre-Gaussian $LG(l,n)$ laser beam by a combination of a fork-shaped grating and an axicon

S. Topuzoski

Institute of Physics, Faculty of Natural Sciences and Mathematics

Arhimedova 3, 1000 Skopje, R. Macedonia

e-mail: suzana_topuzoski@yahoo.com

In this work we present a theoretical analysis about the Fresnel diffraction of a Laguerre Gaussian (LG) laser beam with radial mode number n and azimuthal mode number l by a combination of an axicon and a fork-shaped grating with a phase singularity of integer order p .

The diffracted wave field amplitudes and intensities in the zeroth and higher diffraction orders are calculated through sums of hypergeometric Kummer functions. They are vortex beams, except for the beam in the higher negative m_0 -th diffraction order for which $l - m_0 p = 0$ is satisfied. Usually, the LG beam with zeroth radial mode number is taken into consideration in similar problems [1], but, having on mind the latest discovering of the role of the radial mode number, as a hidden quantum number connected to "intrinsic hyperbolic momentum charge" [2], we investigate its influence on the diffracted intensity distributions.

The results obtained are further being specialized for particular cases:

For diffraction of a Laguerre-Gaussian $LG(l,n=0)$ and a Gaussian laser beam by a combination of axicon and a fork-shaped grating;

For diffraction of $LG(l,n)$ beam by a fork-shaped grating (i.e. the axicon is absent). By comparing the results from this and the previous case we make conclusions about the influence of the axicon on the diffraction patterns;

For the simplest case, when a Gaussian beam is diffracted by a fork-shaped grating (arriving to the well-known results from [3]).

REFERENCES

- [1] S. Topuzoski, *Opt. Commun.* 330, 184 (2014).
- [2] W. N. Plick, M. Krenn, *Phys. Rev. A* 92, 063841 (2015).
- [3] Lj. Janicijevic, S. Topuzoski, *J. Opt. Soc. Am. A* 25, 2659 (2008).

Manipulation of the topological charges of vortices within large optical vortex lattices: Far-field beam reshaping

L. Stoyanov, G. Maleshkov, I. Stefanov, A. Dreischuh

*Department of Quantum Electronics, Faculty of Physics, Sofia University "St. Kliment Ohridski"
Sofia, Bulgaria*

e-mail: l.stoyanov@phys.uni-sofia.bg

Optical vortices (OVs) are intriguing phenomena in nature that attract much attention in many areas of physics, ranging from micro-manipulation of trapped particles to strong-field physics, just to mention a few. The OVs have characteristic spiral phase profiles and point phase singularities in their wavefronts that determine also the intensity structures of the beams [1]. Such beams carry photon angular momenta, which can be transferred to matter [2]. The topological charge (TC) l of an OV corresponds to the total phase change $2\pi l$ over the azimuthal coordinate φ . The basic interactions between two OVs are rather simple. If two OVs with equal charges are placed on a common background beam, they repel and rotate. If the TCs are opposite, the OVs attract and translate in transverse direction.

While interacting with each other by phase and intensity gradients, multiple (or multiple-charged) vortices can arrange themselves in regular patterns (vortex lattices) [3]. Depending on the signs of the TCs the vortex lattices can exhibit rotation or rigid propagation. Previous experiments on the generation and non-linear propagation of square and hexagonal optical vortex lattices showed that if the TCs of the vortices have identical signs, the lattice exhibits rotation. If their signs are alternative, stable propagation of the OV lattice has to be expected [4].

Recently it was shown that the TC of an optical vortex beam can be "erased" when the vortex beam diffracts from computer-generated holograms encoded with the same TC but with the opposite sing. As a result a well formed Gaussian bright peak is observed in the (artificial) far-field [5]. Here we extend this approach and investigate the far-field diffraction of a large square-shaped optical vortex lattice with hundreds of OVs generated by a spatial light modulator (SLM) from second identical lattice produced by a second SLM. As an initial step, for calibration purposes only, we created an OV with TC=-1 on the first SLM which subsequently diffracts from another OV with TC=+1 created on the second SLM. As expected, the TC of the vortex beam was erased and a well formed single peak was seen in the beam waist. Then we studied the far-field diffraction of a single OV from a square-shaped optical vortex lattice with alternating TCs and the case when smaller OV array (again with alternating TCs) diffracts from the same square-shaped optical vortex lattice. Finally we observed the erasure of whole OV lattice when two identical OV lattices were encoded on both SLMs but with opposite charges with respect to one another. On-site and off-site alignments of both OV lattices are also investigated and will be discussed.

In our view the observed spectacular beam reshaping near the focus of a lens (artificial far-field) is paving the way for further analyses e.g. all-optical guiding, switching and coupling applications.

This work was supported by National Science Fund (Bulgaria) project No. DFNI-T02/10-2014.

REFERENCES

- [1] A. S. Desyatnikov, Yu. S. Kivshar, L. Torner, *Progress in Optics* 47, 291 (2005).
- [2] H. He, M. E. J. Friese, N. R. Heckenberg, H. Rubinsztein-Dunlop, *Phys. Rev. Lett.* 75, 826 (1995).
- [3] D. Neshev, A. Dreischuh, M. Assa, S. Dinev, *Opt. Commun.* 151, 413 (1998).
- [4] A. Dreischuh, S. Chervenkov, D. Neshev, G.G. Paulus, H. Walther, *J. Opt. Soc. Am. B* 19, 550 (2002).
- [5] L. Stoyanov, S. Topuzoski, I. Stefanov, L. Janicijevic, A. Dreischuh, *Opt. Commun.* 350, 301 (2015).

Characterization of liquid-phase epitaxy grown thick GaInAs(Sb)N layers

V Donchev¹, I Asenova^{1,3}, M Milanova², D Alonso-Álvarez³, K Kirilov¹,
N Shtinkov⁴, I G Ivanov⁵, S Georgiev¹, E Valcheva¹ and N Ekins-Daukes³

¹Faculty of Physics, University of Sofia, Bulgaria

²Central Laboratory of Applied Physics, Plovdiv, Bulgaria

³Department of Physics, Imperial College London, UK

⁴Department of Physics, University of Ottawa, Canada

⁵Department of Physics, Chemistry & Biology, Linköping University, Sweden
e-mail: vtd@phys.uni-sofia.bg

We present an experimental and theoretical study of GaInAs(Sb)N layers with thickness around 2 μm , grown by liquid-phase epitaxy (LPE) on n-type GaAs substrates. The samples are studied by surface photovoltage (SPV) spectroscopy and by photoluminescence spectroscopy. A theoretical model for the band structure of Sb-containing dilute nitrides is developed within the semi-empirical tight-binding approach in the $sp^3d^5s_N$ parameterization [1] and is used to calculate the electronic structure for different alloy compositions. The SPV spectra measured at room temperature clearly show a red shift of the absorption edge with respect to the absorption of the GaAs substrate. The shifts are in agreement with theoretical calculations results obtained for In, Sb and N concentrations corresponding to the experimentally determined ones. Photoluminescence measurements performed at 300 K and 2 K show a smaller red shift of the emission energy with respect to GaAs as compared to the SPV results. The differences are explained by a tail of slow defect states below the conduction band edge, which are probed by SPV, but are less active in the PL experiment.

REFERENCES

[1] N. Shtinkov, P. Desjardins and R. Masut, *Phys. Rev. B.* 67081202 (2003).

Vertical Raman LIDAR profiling of atmospheric aerosol optical properties over Belgrade

Z. Mijić, L. Ilić and M. Kuzmanoski
Institute of Physics, Belgrade, Serbia
 e-mail: luka.ilic@ipb.ac.rs

The direct radiative effect due to aerosol–radiation interactions is the change in radiative flux caused by the combined scattering and absorption of radiation by anthropogenic and natural aerosols. Due to their short lifetime and the large variability in space and time atmospheric aerosols are considered one of the major uncertainties in climate forcing and atmospheric processes [1]. For radiative studies it is necessary to measure aerosol optical properties, size, morphology and composition as a function of time and space, with a high resolution in both domains to account for the large variability. Lidar (Light Detection And Ranging), an active remote sensing technique, represents the optimal tool to provide range-resolved aerosol optical parameters. Large observational networks such as the European Aerosol Research Lidar Network (EARLINET) [2], the Aerosol Robotic Network (AERONET), provide the long-term measurement series needed to build a climatology of aerosol optical properties at the continental and global scales.

In order to assess the origin and type of aerosols which travel over Balkan region, having an impact on modification of the regional radiative budget, case studies combining measurements at the EARLINET joining lidar station in Belgrade with atmospheric modeling have been analyzed. For vertical profiling and remote sensing of atmospheric aerosol layers the Raman lidar system at the Institute of Physics Belgrade (44.860 N, 20.390 E) has been used. It is bi-axial system with combined elastic and Raman detection designed to perform continuous measurements of aerosols in the planetary boundary layer and the lower free troposphere. It is based on the third harmonic frequency of a compact, pulsed Nd:YAG laser, emitting pulses of 65 mJ output energy at 355 nm with a 20 Hz repetition rate. The optical receiver is a Cassegrain reflecting telescope with a primary mirror of 250 mm diameter and a focal length of 1250 mm. Photomultiplier tubes are used to detect elastic backscatter lidar signal at 355 nm and Raman signal at 387 nm. The detectors are operated both in the analog and photon-counting mode and the spatial raw resolution of the detected signals is 7.5 m. Averaging time of the lidar profiles is of the order of 1 min corresponding to 1200 laser shots. Lidar measurements can be used in synergy with numerical models in order to validate and compare information about aerosols. In this paper DREAM (Dust Regional Atmospheric Model) model, designed to simulate and/or predict the atmospheric cycle of mineral dust aerosol [3], will be used to analyze dust transport. The capability of the lidar technique to derive range-resolved vertical profiles of aerosol optical parameters (backscatter and extinction coefficient) with very high spatial and temporal resolution will be used to identify the altitude of layers and the temporal evolution of intrusions. Using these altitudes as inputs in air mass trajectory model, the source of aerosols can be identified. The additional techniques (satellite remote sensing) will be also discussed for selected case-studies.

REFERENCES

- [1] IPCC: The Physical Science Basis, Contribution of Working Group I to the Fifth Assessment Report of the Intergovernmental Panel on Climate Change, edited by: Stocker, T. F., Qin, D., Plattner, G.-K., Tignor, M., Allen, S. K., Boschung, J., Nauels, A., Xia, Y., Bex, V., and Midgley, P. M., Cambridge University Press, Cambridge, United Kingdom and New York, NY, USA, (2013).
- [2] G. Pappalardo, A. Amodeo, A. Apituley, A. Comeron, V. Freudenthaler, H. Linné, A. Ansmann, J. Bösenberg, G. D'Amico, I. Mattis, L. Mona, U. Wandinger, V. Amiridis, L. Alados Arboledas, D. Nicolae, and M. Wiegner.: EARLINET: towards an advanced sustainable European aerosol lidar network, *Atmos. Meas. Tech.* 7, 2389 (2014).
- [3] S. Nickovic, G. Kallos, A. Papadopoulos, O. Kakaliagou, *J. Geophys. Res.* 106, 1813 (2001).

Planar versus three-dimensional growth of metal nanostructures at 2D heterostructures

S. Stavrić¹, M. Belić², Ž. Šljivančanin^{1,2}

¹*Vinca Institute of Nuclear Sciences,
Belgrade, Serbia*

²*Texas A&M University at Qatar,
Education City, Doha, Qatar
e-mail: stavric@vinca.rs*

Graphene (G) and other recently synthesized two-dimensional (2D) crystals show diverse structural and electronic properties. A novel class of materials with unique features can be manufactured by assembling individual layers of these 2D materials. For example G/MoS₂ heterostructures combine excellent conductivity and transparency of G with high optical activity in visible light of MoS₂. Understanding interaction of 2D materials and their heterostructures with metals is of critical importance for their technological applications.

Employing density functional theory we studied microscopic mechanisms governing initial stages of growth of three selected metals (Li, Ti and Ca) on G. Tendency towards planar or 3D growth is rationalized based on description of the interaction between metal adatoms, as well as adsorption geometries of their trimers and tetramers.

In addition to this we investigated G/MoS₂ intercalation with Au and found strong tendency of gold intercalants to form planar structures.

REFERENCES

- [1] S. Stavrić, M. Belić and Ž. Šljivančanin, Carbon 96, 216 (2016).
- [2] Ž. Šljivančanin and M. Belić, submitted to Phys. Rev. Mater.

***Ab initio* study of superconducting properties of $NbSe_2$ monolayer in the DFPT formalism using Wannier interpolation**

Tatjana Agatonović Jovin¹ and Radoš Gajić²

¹*Institute of Chemistry, Technology and Metallurgy, University of Belgrade, Njegoševa 12, 11000 Belgrade, Serbia*

²*Graphene Laboratory (GLAB) of Center for Solid State Physics and New Materials, Institute of Physics, University of Belgrade, Pregrevica 118, 11080 Belgrade, Serbia*

e-mail: tatjanaj@ipb.ac.rs

Low-dimensional transition metal dichalcogenides present a benchmark and model systems for studying the incidence and nature of superconductivity at mesoscopic scales. These two-dimensional (2D) superconductors are typically characterized by highly expressed anisotropic properties.

Here we present a study of the superconducting properties in a single (2D) layer of $NbSe_2$, representing a true 2D superconductor and a well-suited candidate for probing the multi-band model [1]. Parameters for superconductivity, anisotropic superconducting gaps, strength of the electron-phonon coupling, spectral function and critical temperature were extracted using the anisotropic Migdal-Eliashberg theory [2] with electron-phonon interpolation based on maximally localized Wannier functions [3,4]. We also present the electronic band structure and charge density wave order in a $NbSe_2$ monolayer using the density functional theory.

The additional study in bulk three-dimensional (3D) $NbSe_2$ system is performed, where the effects of dimensionality on correlated electronic phases such as charge density wave order and superconductivity were investigated.

REFERENCES:

- [1] M. M. Ugeda et al., Nat. Phys. 12, 92-97 (2016).
- [2] E. R. Margine and F. Giustino, Phys. Rev. B 87, 024505 (2013).
- [3] N. Marzari et al., Rev. Mod. Phys. 84, 1419 (2012).
- [4] F. Giustino, Rev. Mod. Phys. 89, 015003 (2017).

Characterization of magnetron sputtered transparent hole conducting layers for organic solar cells

M. Sendova-Vassileva¹, R. Gergova¹, Hr. Dikov¹, G. Popkirov¹, V. Gancheva² and G. Grancharov²

¹*Central Laboratory of Solar Energy and New Energy Sources, Bulgarian Academy of Sciences, 72 Tzarigradsko Chaussee, 1784 Sofia, Bulgaria*

²*Laboratory of Structure and Properties of Polymers, Institute of Polymers, Bulgarian Academy of Sciences, Acad. G. Bonchev St., Block 103-A, 1113 Sofia, Bulgaria*
e-mail:marushka@phys.bas.bg

Organic solar cells (OSC) are still the subject of intensive research and recently efficiencies of 13.2% have been reported for multijunction OSCs [1]. One of the main perspectives for their application is printing on inexpensive flexible substrates. The role of the transparent hole transport layer (HTL) is of major importance for their function, however the widely used organic layer PEDOT:PSS has shown a number of deficiencies connected with the stability of the cells.

Molybdenum oxide (MoOx) usually obtained by thermal evaporation is widely used as a substitute for PEDOT:PSS. It was recently shown that MoOx deposited by magnetron sputtering from an oxide matrix in argon only atmosphere can successfully be used for the same purpose [2]. The deposition by magnetron sputtering guarantees reliable and repeatable HTLs and covering big areas is also possible. In this study an alternative high work function material for HTL is investigated, namely, tungsten oxide (WOx), deposited by magnetron sputtering from an oxide matrix in argon only atmosphere. The optical and structural properties of the films and the oxidation state of the metal ions are studied by optical transmission, Raman and XPS spectra.

The performance of WOx, applied as a hole transport layer in polymer solar cells with a bulk heterojunction active layer, deposited by spin coating is compared with that of PEDOT:PSS and MoOx. The current-voltage characteristics of solar cells with the structure glass/ITO/HTL/PCDTBT:PC70BM/Al using the three different HTLs are measured and the test solar cells are characterized by quantum efficiency spectra and impedance spectroscopy.

REFERENCES

[1] <http://optics.org/news/7/2/15>

[2] M. Sendova-Vassileva, Hr. Dikov, P. Vitanov, G. Popkirov, R. Gergova, G. Grancharov and V. Gancheva, *Journal of Physics: Conference Series* 764, 012022 (2016).

Post-processing synchronization and characterization of generated signals by a repetitive Marx generator

A. Redjimi¹ · Z. Nikolić² · D. Knežević^{3,4} · D. Vasiljević⁵

¹University of Defense, Military Academy, Generala Pavla Jurišića Šturma 33, 11000 Belgrade, Serbia

²University of Belgrade, Faculty of Physics, Studentski trg 12, 11000 Belgrade, Serbia

³Military Technical Institute (VTI), Ratka Resanovića 1, 11132 Belgrade, Serbia

⁴University of Belgrade, School of Electrical Engineering, Bulevar kralja Aleksandra 73 11000 Belgrade Serbia

⁵University of Belgrade, Institute of Physics, Photonics Center, Pregrevica 118, 11080 Belgrade, Serbia

e-mail: darko@ipb.ac.rs

A new approach was developed for solving the problem of time synchronization of a set of signals obtained by different measurement techniques without a common trigger. The recorded signals were the result of sparks and bursts generated by a repetitive Marx generator. The repetitive Marx generator consists of ten 7nF, 30kV capacitors, eighteen 1mH inductivities, one 1k Ω resistor and nine spark gap switches [1]. A thermal imaging camera FLIR SC7200 (set at 1180 frames per second), a high speed camera Casio Exilem EX-FH25 (set at 1000 frames per second) and an audio recorder Zoom H6 ($F_s = 96\text{KHz}$, 24 bit) were used to obtain the necessary data for synchronization and characterization. Moreover, a piezoelectric sensor (Murata, 7BB-20-6L0, resonant frequency 6kHz), was applied for shock waves characterization during the early stages of bursts. In the first place, different data with evident time shifts were acquired. Then, a set of simple operations such as maximum selection and localization, threshold comparison, Euclidean distance calculation and minimization were employed for signal analysis and pattern matching to ensure a good data synchronization, which allowed a detailed analysis of the phenomenon in the end.

REFERENCES

[1] G.B. Sretenović, B.M. Obradović, V.V. Kovačević, M.M. Kuraica, Current applied physics 13 121-129 (2013).

Cryogenic slab CO laser with RF discharge pumping: sealed-off plasma chemistry of the active medium

A.A. Ionin¹, I.V. Kochetov², A.Yu. Kozlov¹, A.K. Kurnosov², A.P. Napartovich^{1,2}, L.V. Seleznev¹, D.V. Sinitsyn¹

¹ *P.N. Lebedev Physical Institute of the Russian Academy of Sciences, Moscow, Russia*

² *Troitsk Institute for Innovation and Fusion Research, Troitsk, Moscow region, Russia*

e-mail: akozlov@sci.lebedev.ru

Long time dynamics of output power of cryogenically cooled slab CO laser pumped by a repetitively pulsed RF discharge [1], operating in the sealed-off mode on transitions of first overtone ($\lambda = 2.6\text{-}3.9$ microns) vibrational band was studied. It was shown that the addition of oxygen to the initial gas mixture CO:He=1:10 in abnormally large quantities - up to 50% with respect to the CO concentration - resulted in multiple increasing of the duration of the laser operating cycle (until cessation of lasing due to degradation of the active gas mixture). Earlier experimental studies and theoretical calculations [2-4] have shown that even a small addition of oxygen to the active medium of a CO laser prevent lasing at high transitions (between CO molecule levels with the numbers of the vibrational quantum number $V > 20$) due to the vibrational-vibrational exchange between the excited CO molecules and unexcited oxygen.

To explain the contradictions, the study including the measurement of the dynamics of the luminescence spectra of the laser active medium in visible and UV spectral regions was carried out. Also samples of the gas mixture from the ballast volume of the laser were extracted at various moments of the operating cycle to record their IR absorption spectra and to define concentrations of detected components. Besides, time dynamics of ozone concentration in active gas mixture was measured by absorption of the UV radiation of a mercury lamp in the ballast volume of the laser (O_3 is produced by RF discharge in oxygen containing gas mixtures).

Theoretical calculations of parameters and characteristics of the laser were carried out. Special attention was paid to the influence of plasma-chemical processes involving molecular oxygen on the laser action under real experimental conditions. In particular the dynamics of the active medium temperature and the dynamics of the small signal gain on transitions of first-overtone vibrational bands were calculated for different oxygen concentrations X in the active gas mixtures $O_2:CO:He=X:1:10$. The influence of addition of molecular oxygen to the active medium on the lasing threshold conditions was determined. The calculations were compared with the experimental results.

Regularities in the dynamics of variations of CO molecules concentrations and concentrations of plasma chemical reactions products were determined. Analysis of correlation in time between the composition of the active gas medium and laser power allowed to make a phenomenological description of the set of chemical and plasma chemical reactions, gas dynamic and diffusion processes defining the behavior of the laser output characteristics over the entire operating cycle of the laser.

The study was supported by the Russian Foundation for Basic Research (Grant #15-02-01378).

REFERENCES

- [1] A.A. Ionin, A.Yu. Kozlov, O.A. Rulev, et al., *Appl. Phys. B: Lasers and Optics*, 122:183, (2016).
- [2] E. Plönjes, P. Palm, I. Adamovich, W. Rich, *J. Phys. D.: Appl. Phys.*, 33, p.2049, (2000).
- [3] A.A. Ionin, Yu.M. Klimachev, A.Yu. Kozlov, *Quantum Electronics*, 38, p.833, (2008).
- [4] Grigoryan G. M. Kochetov I.V., Kurnosov A.K., *J. Phys. D: Appl. Phys.*, 43, p.085201, (2010).

Organic Nanocrystals for Quantum Nanophotonic Applications

S.Pazzagli^{1,2}, P. Lombardi^{2,3}, F. S. Cataliotti^{1,3}, C. Toninelli^{2,3}

¹*Dipartimento di Fisica e Astronomia, via Sansone 1, 50019 Sesto Fiorentino, Italy*

²*INO-CNR, Largo Fermi 6, 50125 Firenze, Italy*

³*LENS-Università di Firenze, via Nello Carrara 1, 50019 Sesto Fiorentino, Italy*

e-mail: sofia.pazzagli@unifi.it

Dibenzoterrylene (DBT) molecules embedded in Anthracene (Ac) crystals combines a bright and stable emission in the near-infrared, both at room and low temperature, with a narrow lifetime-limited emission (~40MHz) around 785nm at cryogenic temperature [1]. To date, DBT:Ac system has been successfully integrated in nanophotonics layered structures thanks to the 50nm-thickness of Ac spin-coated crystals, covering several hundreds μm^2 of the substrate [2]. However, to fully exploit this molecule-based solid state system as a single photon source to e.g. deliver photons into a nearby waveguide, precise positioning method and/or controllable size of the emitter is indeed desirable.

In this work we present a novel method to grow DBT-doped anthracene crystals with average size of few-hundreds nanometers and controllable DBT concentration. Optical investigations demonstrate that the optical properties of the bulky DBT:Ac system at both room and cryogenic temperature are preserved. Preliminary results on the integration of the nanocrystals in different polymeric matrices are discussed, as possible writable system for applications in integrated optics and nanophotonics.

REFERENCES

- [1] J. B. Trebbia et al., Opt. Express, 23986–23991 (2009).
- [2] C. Toninelli et al., Opt. Express 18, 6577–6582 (2010).

Density Matrix Superoperator for Terahertz Quantum Cascade Lasers

A. Demić¹, A. Grier¹, Z. Ikonić¹, A. Valavanis¹, R. Mohandas¹, L. Li¹,
E. Linfield¹, A. G. Davies¹ and D. Indjin¹

¹ *School of Electronic and Electrical Engineering,
University of Leeds, U.K.
e-mail:elade@leeds.ac.uk*

Terahertz-frequency quantum cascade lasers (THz QCLs) require very small energy difference between the lasing states (~ 10 meV), and modelling of these devices can be challenging. Various models for transport in QCLs exist [1]; most commonly employing semi-classical approaches such as self-consistent rate-equation (RE) modelling, which considers non-radiative transitions of carriers due to various scattering mechanisms. Although these models provide insight into the scattering behaviour, they are unable to correctly describe transport between adjacent periods of a QCL structure [2] because they do not take injection barrier thickness into account in transport calculations. This leads to the prediction of instantaneous transport between the periods, whereas the actual transport that occurs is based on resonant tunnelling. Alternative approaches, based on density matrix (DM) modelling include quantum transport effects and are able to overcome known shortcomings of RE models. In this work, we present a DM approach that extends the model presented in [3], applicable for arbitrary number of states per module. This model has proved successful for a variety of QCL simulations [4-8].

The time evolution of the density matrix is described by the Liouville equation. We consider periodic QCL structure with infinite number of periods, which implies infinite-sized matrices, but due to the nearest neighbour approximation and symmetry of QCL structure Liouville equation folds into the system of $mN \times mN$ block equations (where N is the number of states in the single module and m is the number of considered periods (in general $m = 2x + 1$, x – number of neighbours, in our case (the nearest neighbour approximation) $m = 3$). We show that commonly known form of the Lindblad superoperator $L = H \otimes I - I \otimes H^T + i\hbar D$ where H is the Hamiltonian of the entire system, I is the identity matrix, D is the dissipater of the system and \otimes is the Kronecker tensor product, can be formulated for periodic system as $L_{per} = H_{per} \boxtimes I_{per} - I_{per} \boxtimes H_{per}^T + i\hbar D_{per}$ where H_{per} is block-partitioned Hamiltonian of $mN \times mN$ size (in our case three-diagonal block matrix), I_{per} is a matrix filled with m^2 identity matrices (each of size $N \times N$), D_{per} is the corresponding dissipater form for periodic system and \boxtimes is Khatri-Rao product. This formulation of Lindblad superoperator enables simple numerical implementation and provides a system of equations that can be intuitively interpreted. The dissipater in our model has similar form as in RE and we can formulate the density matrix formalism in similar intuitive manner as in RE.

We apply our model to 2 THz bound-to-continuum structure and compare our results with RE model [8]. We obtained smooth results (contrary to RE) and managed to reconstruct the entire $L - I - V$ characteristic of the experimental result in pulsed operation at 20K.

REFERENCES

- [1] C. Jirauschek, T. Kubis, *Appl. Phys. Rev.*, 1, 011307 (2014).
- [2] H. Callebaut, Q. Hu, *J. App. Phys.*, 98, 104505 (2005).
- [3] T. Dinh, A. Valavanis, L. Lever, Z. Ikonić, R. Kelsall, *Phys. Rev. B*, vol. 85, 235427 (2012).
- [4] A. Grier, PhD thesis, University of Leeds (2015).
- [5] B. Burnett, B. Williams, *Phys. Rev. B*, 90, 155309 (2014).
- [6] B. Burnett, B. Williams, *Phys. Rev. App.* 5, 034013 (2016).
- [7] A. Grier *et al.*, *Opt. Express*, 24, 21948 (2016).
- [8] A. Demić, A. Grier, Z. Ikonić, A. Valavanis, R. Mohandas, L. Li, E. Linfield, A. Davies, D. Indjin. *IEEE Transactions on Terahertz Science and Technology*, 7, 1, (2017).

Fluorescence of bio-molecules a simple and quick method: What honey emission speaks about bee society and honey quality

M. Stanković¹, D. Bartolić¹, B. Šikoparija², D. Spasojević¹, D. Mutavdžić¹, M. Natić³ and K. Radotić¹

¹*Institute for Multidisciplinary Research, University of Belgrade, Belgrade, Serbia*

²*BioSense Institute, Novi Sad*

³*Faculty of Chemistry, University of Belgrade, Belgrade, Serbia*

³*Institute of Physics,*

Belgrade, Serbia

e-mail: mira.mutavdzic@imsi.rs

Fluorescence is non-destructive, sensitive, simple and fast method for analysis of fluorescent compounds contained in very low amounts (nanomolar concentrations) in the samples. It can be used for structural or concentration studies, in analytical or diagnostic purposes [1]. The fluorescence spectra, in combination with appropriate statistical methods, may provide useful fingerprints in food analysis [2].

Various methods for study of honey quality and adulteration have been in research focus [3]. Over the last years, in different geographic areas a notable loss of honey bee (*Apis mellifera* L.) colonies has been reported. A number of stressors affecting honey bees, including diseases, parasites, pesticides and poor nutrition have been identified [4]. Therefore fast and reliable methods are required for screening bee products both as a tool for assessing quality and to identify risks for colony state.

We used fluorescence spectroscopy combined with advanced statistical analysis in order to identify variability in Fruska Gora lime tree (*Tilia* L.) honey collected at different locations in 2015. Since homogenization of the honey before packing in jars is considered as critical procedure from the Quality Control point of view, we have explored to what extent the ratio of the two main fluorophores in honey, originating from proteins and phenolic compounds change between extraction stage to packaging.

Steady state fluorescence spectroscopy in combination with Multivariate Curve Resolution Alternating Least Squares (MCR-ALS) for spectral analysis has been applied to differentiate samples of honey. The three-dimensional excitation–emission matrix (EEM) is a rapid, selective and sensitive method: by changing excitation and the emission wavelength simultaneously, information regarding the fluorescence characteristics of the different compounds contained in the sample of interest can be obtained [5].

Proteins in honey mainly originate from bees and their quantity depends on bee society [6]. Phenolic compounds come from plant sources. In our study the source was the same – lime from close localities on Fruska Gora. As a control experiment we quantified proteins and phenols in the honey samples.

Changed fluorophore ratio between extraction and packaging stage may indicate that analysed sample was not representative for the particular apiary, or honey homogenization was non-adequate before packaging. This reflects variation in properties of the bee colonies. The contribution of plant source to the honey emission spectra was estimated by comparing emission spectra of lime pollen and honey.

REFERENCES

- [1] B. Valeur, *Molecular fluorescence: Principles and applications* 63 (2001).
- [2] J. Sádecká, J. Tóthová, *Czech, J. Food Sci.* 25, 159-173 (2007).
- [3] K. Ruoff, W. Luginbuhl, R. Kunzli, S. Bogdanov, J. Oliver Bosset, K. von der Ohe, W. von der Ohe, R. Amadoa, *J. Agric. Food Chem.* 54, 6858–6866 (2006).
- [4] N. Even, J.M. Devaud, A. B. Barron, *Insects* 3, 1271-1298 (2012).
- [5] B. B. Campos, D. Mutavdžić, M. Stanković, K. Radotić, M. Algarra et al., *New J. Chem.* 41, 4835-4842 (2017).
- [6] H. Nazarian, R. Taghavizad, A. Majid, *Pak. J. Bot.* 42, 3221-3228 (2010).

Tuning exciton and trion population in MoS₂ with photodoping

V. Jadriško¹, N. Vujičić¹, D. Čapeta² and M. Kralj¹

¹ *Institute of Physics,
Zagreb, Croatia*

² *Faculty of Science – Physics department,
University of Zagreb, Croatia
e-mail: vjadrisko@ifs.hr*

Monolayer transition metal dichalcogenides (TMDs) are promising materials for future 2D nanoelectronic systems. Monolayer molybdenum disulfide (MoS₂) as a representative of 2D TMDs, is one of the most stable layered materials and has been widely studied. Monolayer MoS₂ is a atomically thin semiconductor with direct bandgap in the visible spectral range, which holds great potential in many application including high-performance electronics, light emitters, photodetectors and sensors.[1]

Optical response of undoped atomically thin MoS₂ is dominated by excitonic effects. Optical spectrum is characterized by two exciton peaks (A and B excitons) which are signature of vertical transitions from a spin-orbit split valence band to conduction band at the K point of the Brillouin zone. With doping additional carriers are introduced into the system and the optical spectra of such doped system consists of emission from both neutral excitons and charged excitons, called trions. [2]

Here we report photoinduced doping of CVD grown monolayers and bilayers of MoS₂ on SiO₂/Si substrate. Additionally, we investigated optical response under photodoping of monolayer MoS₂ transferred on clean SiO₂/Si substrate. Photodoping of atomically thin MoS₂ with continuous wave laser introduces red-shift in photoluminescence spectra. This red-shift is caused by growing trion population with increasing the laser power. Under large photodoping of MoS₂ samples dominance of trion emission in photoluminescence spectra is observed. Trion population grows 4 times with respect to exciton A population in as-grown MoS₂ monolayer with laser power increase from 1 μW to 500 μW. For bilayer MoS₂ the exciton A and trion A⁻ population ratio is constant around $A/A^- = 3$. In the case of transferred monolayer MoS₂, trion population grows 42 times with respect to exciton A population. Rapid growth of trion population in transferred sample is caused by adding additional donor impurities during transfer process.

REFERENCES

- [1] M. Currie, A. T. Hanbicki, G. Kioseoglu, B. T. Jonker, Appl. Phys. Lett. 106, 201907 (2015).
- [2] C. Qin, Y. Gao, Z. Qiao, L. Xiao, S. Jia, Adv. Optical Mater. (2016).

Trajectory based interpretation of the laser light diffraction on a sharp edge

Milena D Davidović¹, Miloš D Davidović², Angel S Sanz³, Mirjana Božić⁴, Darko Vasiljević⁴

¹ Faculty of Civil Engineering, University of Belgrade, Serbia

² Vinca Institute, University of Belgrade, Serbia

³ Department of Optics, Universidad Complutense de Madrid, Spain

⁴ Institute of Physics, University of Belgrade, Serbia

e-mail: milena@grf.bg.ac.rs

Bohmian mechanics enables visualization and interpretation of quantum mechanical behavior of massive particles through trajectories connected to the probability current density [1]. Electromagnetic field also admits hydrodynamic formulation when the existence of suitably defined photon wave function is assumed [2]. This formulation gives possibility to interpret the optical phenomena in a picturesque way through photon trajectories which describe the evolution of the electromagnetic energy density behind an obstacle.

This approach, based on the trajectories, was used in the analysis of modified Young's double slit diffraction [3], in the context of the Arago-Fresnel laws [4], as well as in the analysis of the modes in the optical and microwave waveguides [5]. A group of scientists from the University of Toronto under the guidance of professor Steinberg, has been able to experimentally determine the mean paths of single photons in the Young's experiment [6]. The measured trajectories show good agreement with theoretically anticipated trajectories presented in [2, 3]. The achievement of Steinberg's group was selected by the Physics World as the top breakthrough in physics for the year 2011, as the discovery that is 'shifting the moral of quantum measurement' [7].

Theoretical solution for the diffraction of plane wave by the edge of the perfectly conducting plane was given by Sommerfeld in 1896 [8], and this solution became the starting point in solving the diffraction problems for various two dimensional obstacles [9, 10]. Diffraction of Gaussian beam by the edge was studied since the sixties of the last century [11] but more attention was given to the central part of the diffraction image, while the less pronounced side trails were analyzed much later [12]. In this paper we use photon trajectories approach to analyze the diffraction pattern obtained on the screen put behind the laser beam partially covered by a sharp edge, such as a razor blade.

REFERENCES

- [1] Bohm D., Hiley B.J., The Undivided Universe, New York: Routledge (1993).
- [2] Davidović M.D., Sanz A. S., Arsenović D., Božić M., Miret-Artes S., Phys. Scr. T135, 014009 (2009). [3] Sanz A. S., Davidović M. D., Božić M., Miret-Artes S., Ann. Phys. 325, 4, 763 (2010).
- [4] Davidović M. D., Sanz A. S., Božić M., Arsenović D., Dimić D., Phys.Scr. T153, 014015(2013).
- [5] Davidović Miloš D., Davidović Milena D., Acta Phys. Pol. A 116, 4, 672 (2009).
- [6] Kocsis S., Braverman B., Ravets S., Stevens M. J., Mirin R. P., Shalm L. K., Steinberg, A. M. Science 332, 1170 (2011).
- [7] <http://physicsworld.com/cws/article/news/2011/dec/16/physics-world-reveals-its-top-10-breakthroughs-for-2011>
- [8] Sommerfeld, A., Mathematische Annalen 47, 134 (1896).
- [9] Sommerfeld, A., Optics, New York: Academic Press, 249-266 (1969)
- [10] Born M., Wolf E., Principles of Optics, New York: Pergamon Press, 428-435 (1986)
- [11] Pearson J. E., McGill T. C., Kurtin S., Yariv, A. J. Opt. Soc. Am. 59 1440 (1969).
- [12] Anakhov S. P., Lymarenko R. A., Khizhnyak A. E. Radiophys. Quant. El. 47, 926 (2004).

Index

A

Abedini M.	125
Abramovic D.	128, 138
Adam J.	205
Adhikari S.K.	14,49
Affolderbach C.	19, 155, 160
Agatonovic Jovin	212
Agdarov S.	6
Ahmadi M.	125
Aillerie M.	77
Akram J.	56
Aleksic N.B.	60, 79
Alic N.	4
Almat N.	160
Altonyan V.	100
Álvarez D.A.	209
Ambrosius H.	135
Andjus P.R.	110,114
Andreev V.A.	59
Andreeva C.	158
Antanovich A.	193
Antic S.D.	114, 118
Apostolova T.	165, 204
Arsenovic D.	48, 62
Arsoski V.V.	98
Arsov Z.	26
Artemyev M.	29,193
Asenova I.	209
Ashour O.A.	12,79
Aškrabic S.	109, 193
Atanasoski V.	121
Aumiler D.	39
Auslender M.	197
Avrahamy R.	129
Avramov L.	107
Avramovic V.	126
Avtzi S.	115

B

Bajic J.	38
Bajic J.S.	40
Balashev K.	144
Balaž A.	49, 51, 52, 55
Ban T.	39
Baronio F.	21,63
Barry L.P.	10
Bartolic D.	218
Bartoszek-Bober D.	205
Basharin A.A.	198,200,201,203

Batinic B.	40
Beccherelli R.	136
Beiderman Yaf.	6
Beiderman Yev.	6
Beinyk T.H.	95
Belardini A.	196
Belic M.R.	12, 60, 79, 211
Belicev	133
Belicev P.	188, 190
Berberova N.	99
Binet G.	135
Bjelica M.	169
Blache F.	143
Blagoeva B.	153
Blažic L.	116
Bliznakova I.	180
Bogdanovic U.	46
Bogdanovic-Radovic I.	173, 177, 179
Boiko D.L.	130
Bojinov N.	92
Bojovic B.	112
Bonifazi M.	16
Borisova E.	105
Borzsonyi A.	36
Boukhachem A.	100
Božić M.	220
Bradley T.	32
Brkic M.	126
Browning C.	10
Bugarški B.M.	104
Bugay A.N.	73
Buljan H.	52
Bunjac A.	178
Busuladžic M.	65

C

Calin B.	28
Calin Bogdan S.	140
Calò C.	10
Canalias C.	35
Capeta D.	219
Caputo R.	136
Cartaleva S.	158
Caruso F.	53
Cataliotti F.S.	53, 216
Cekada M.	173
Celebonovic V.	157
Centini M.	196
Cerkic A.	65
Chernysheva M.	41

Index

Chichkov B.....	3	Djukic-Vukovic A.....	81
Chin S.A.....	79	Do H.V.....	53
Chiou C.C.....	139	Dohcevic-Mitrovic Z.....	109
Chrafihi Y.....	50	Dolgovskiy V.....	156
Chung I.S.....	147	Donchev V.....	209
Ciganovic J.....	159,182	Dreischuh A.....	208
Cindric M.....	171	Dreischuh T.....	107
Cipriš A.....	39	Drvenica I.T.....	104
Cirkovic S.T.....	120	Ducic T.....	34, 110
Cojocari M.V.....	203	Dukarov S.V.....	95
Colombo S.....	156		
Comor M.....	177	E	
Crnjanski J.....	146, 149	Eggeling C.....	26
Cubrovic M.....	74	Ehrlich G.....	197
Cuk V.M.....	120	Ekins-Daukes N.....	209
Cukaric N.A.....	98		
Cupic Ž.....	191	F	
Curcic M.M.....	48, 62	Fabijanac I.....	193, 195
Cvetanovic -Zobenica K.....	84, 194	Falkner M.....	186, 189
		Fasold S.....	186
D		Ferraro A.....	136
Dakova A.....	68, 72	Filipovic N.....	58
Dakova D.....	68, 72	Fiutowski J.....	205
Dalarsson M.....	206	Fomchenkov S.....	170
Damljanovic V.....	82, 90, 93	Fotakis C.....	180
Daskalova A.....	180	Frantlovic M.....	194
Davidovic M.D.....	59,220	Fralalocchi A.....	16
Davidovic D.M.....	59		
Davidovic Lj.D.....	59	G	
Davidovic M.D.....	59,220	Gajic R.....	46,80,88,93,94,193,212
Davies A.G.....	217	Gakovic B.....	174
Debregeas H.....	143	Galiani S.....	26
Decobert J.....	135	Galovic S.....	42
Delibašić H.....	172, 183	Gancheva V.....	213
DeLuka S.R.....	120	Garvas M.....	26
Demic A.....	217	Gateva S.....	158
Demoli N.....	128, 138	Gavrilov P.....	176
Deneva M.....	141	Gazibegovic-Busuladžić A.....	65
Denz C.....	70	Genova Ts.....	105
Despotovic S.....	117	Georgiev S.....	209
Dikic G.....	82	Geiss R.....	66
Dikov Ch.....	139	Georgieva D.....	72
Dikov Hr.....	213	Gergova R.....	213
Dimitrijevic S.B.....	171	Gerhardt I.....	24
Dimitrov D.....	139	Gharavipour M.....	19, 151, 155
Dimitrov D.Z.....	92, 97	Ghavanini A.A.....	123
Dinic I.....	81	Gherardini S.....	53
Diziain S.....	66	Gilic M.....	86
Djordjevic M.....	109	GIvanov I.....	209
Djordjevich A.....	78, 150		

Index

Gligoric G.....64, 188, 190
Golz T.....163, 166, 167
Gorin D.....105
Gozzini S.....158
Grancharov G.....213
Graovac S.....193
Grier A.....217
Grigoryan G.....161
Gruet F.....19, 155, 160
Grujic Z.D.....138,154, 156
Guina M.....196
Gurdev L.....107
Guven K.....119
Gvozdic D.....146,149

H

Habibovic D.....65
Hadžic B.....86
Hadžievski Lj.....63, 121, 188, 190
Hakkarainen T.....196
Hasovic E.....65
Hava S.....129, 197
Hingerl K.....9
Hofstetter W.....52
Homewood K.P.....83, 84
Hudomal A.....52

I

Ikonc Z.....217
Ilic L.....210
Ilic V.Lj.....104
Indjin D.....217
Ionin A.A.....69, 71, 215
Isakovic K.....172, 183
Isic G.....46, 185,187,193,199
Ivanov O.....144
Ivanov D.....99
Ivanovic M.....121
Ivanovic M.D.....112

J

Jadriško V.....219
Jakovceviski I.....23
Jakšic O.....194
Jakšic Z.....184,187,191,194,199,206
Janicijevic M.....181
Janicki V.....193, 195
Jankovic V.....164

Jany B.....205
Jegdic B.....181
Jelenkovic B.M
.....48,62,87,90,103,104,106,116,151,163,173,179
Jiipa F.....28, 140
Jokanovic B.....134
Jokic I.....194
Jovanic S.....103, 104, 117
Jovanovic Đ.....80
Jovanovic S.....61
Jovic M.....103, 126
Jovic Savic D.M.....70
Joža A.....40
Juloski J.T.....120

K

Kamalian M.....76
Kanazir S.....103, 126
Kang H.J.....153
Kasarov R.....85
Kasarova S.....85
Kawalec T.....205
Khachatryan D.....161
Khalifa T.....62
Kharintsev S.S.....202
Kharitonov A.V.....202
Kijenska E.....180
Kim Y. M.....153
Kinyaevskiy I.....69
Kirilov K.....209
Klimachev Yu.....69
Knežević D.....137, 214
Kochetkov Yu.....69
Kochetov I.V.....215
Kocovic D.....114
Koivusalo E.....196
Kokanyan E.....77
Koklic T.....26
Kokot B.....26
Kosek E.....123
Koss P.A.....156
Kostic R.....86, 96
Kostritskii S.M.....77
Kovac J.....174, 182
Kovacevic A.G.....67,179
Kovacevic M.S.....78,150
Kovachev L.....68, 72
Kovachev K.....68
Kozlov A.....69
Kozlov A.Yu.....215

Index

- Kralj M.....11, 219
Krasteva A.....158
Krešic I.....39
Krizan J.....101
Krmpot A.....48,62,81,103,106,113,116,117,166
Krolikowski W.....5
Krsic J.....127
Krstic M.....146, 149
Kurnosov A.K.....215
Kuzmanoski M.....210
Kuzmanovic Lj.....78, 150
- L
- Laban B.....46
Lagay N.....135
Lai B.....110
Lainovic T.....116
Lakovic N.....40
Lalic I.....117
Lalovic M.....146
Lamovec J.....199
Lazarevic Z.....86
Lazic Ž.....191
Lazovic V.....106,113,116,174,179,182
Lazovic V.M.....46
Leahu G.....196
Lebedev V.....154, 156
Leijtens X.....143
Leisher P.O.....30
Lekic M.....67
Lemaître F.....135
Li L.....217
Limpouch J.....176
Lin S.H.....139
Linfield E.....217
Litvinova K.S.....108
LiVoti R.....196
Lombardi P.....216
Loncar V.....49
Loncarevic N.....103
Loncarevic-Vasiljkovic N.....126
Loukakos P.....180
Lourenço M.A.....83, 84
Lovecchio C.....53
Löw R.....33
Loza-Alvarez P.....168
Lukic D.....142
Luning J.....25
- M
- Ma Y.W.....175
Majaron H.....26
Maleshkov G.....208
Maluckov A.....63, 64
Mamula T. D.....169
Mancic A.....61, 63
Mancic L.....81
Marinkovic B.P.....101, 122
Marinova V.....92, 139
Markova S.....144
Markovski A.....158
Markushev D.....42
Marlinez A.....10
Mata vulj P.....137, 145,148
Matijevic M.....111
Matkovic A.....80
Matveevskaya N.A.....95
Maucher F.....5
Mazzone V.....16
Menzel C.....189
Merghem K.....10
Mertelj A.....26
Micevic A.....146
Mihailescu I.N.....174
Mijic Z.....210
Mikhailov A.....193
Milanova M.....209
Milanovic B.....82
Milanovic D.....126
Milanovic V.....130,132, 188
Mileti G.....19, 151, 155, 160
Miletic M.....109,112
Milgrom B.....129
Milicevic N.....117
Milicevic Ž.....117
Miljkovic N.....145
Milosavljevic M.....182
Milosevic V.....134
Milošević D.B.....65
Milosevic O.....81
Mitric J.....128, 138
Mittra R.....206
Mladenovic I.....199
Mladenovic M.....43
Mohammadpour R.....125
Mohandas R.....217
Mojovic L.....81
Mokrousova D.V.....71
Momcilovic M.....159
Moreno W.....19, 155, 160

Index

- Moudou L.....50
Mrdovic I.....109
Muller M.....53
Muric B.....87, 157
Mušević I.....26
Mutavdžic D.....218
- N
- Napartovich A.P.....215
Natic M.....218
Nazarova D.....99, 153
Nedelchev L.....99, 153
Negut I.....174
Nemkov N.A.....200
Nenchev M.....141
Nešic M.....42, 111
Nestorovic Z.....102
Nicoara I.....89
Nikitovic Z.....48
Nikolic Z.....157, 214
Nikolic M.G.....81, 101, 122, 137,142
Nikolic S.N.....12, 79
Nikolov I.....85
Nikova T.....153
Nišavic M.....171
NumkamFokoua E.....32
- O
- Obradov M.....32, 44, 191, 199
Obradovic M.....182
Obreshkov B.....165, 204
Odžak S.....65
Okorn B.....193, 195
Olarte.....168
Onal E.D.....119
Oosten D.....20
Opacak N.....132
Ospanova A.K.....201
Ottaviano L.....147
- P
- Pajcin B.....148
Pajic T.....106
Pan R.....166, 167
Panarin A.....185
Panjan P.....173, 174
Pantelic D.V.
.....87,90,104,106,113,116,117,138,163,173,179
- Papoyan A.....161
Park G.C.....147
Pashev K.....144
Pasiskevicius V.....35
Paun I.....28
Paunovic N.....120
Pavlovic V.....58, 179
Pavlovic D.....113
Pazzagli S.....216
Peeters F.M.....98
Pellaton M.....19, 155, 160
Pelster A.....17, 51, 54
Perego A.M.....45, 76
Pérez-Díaz J.L.....144
Pernice W.....13
Pertsch T.....66, 186, 189
Peruško D.....173, 177, 179, 182
Pešic J.....80, 88, 94
Petkova P.....100
Petkovic M.....111, 171
Petricevic S.....82
Petronijevic E.....196
Petrov S.....139
Petrovic J.....121,127,166
Petrovic M.....74
Petrovic M.S.....60
Petrovic N.Z.....75
Petrovic S.....173, 174, 177, 182
Petrovic S.M.....179
Petrovic V.....172, 183
Petrovich M.N.....32
Piller J.....156
Piterimov D.A.....71
Pjevic D.....177, 182
Poh T.....5
Poletti F.....32
Polic S.....181
Pommereau F.....135
Popkirov G.....213
Popovic D.....109
Popovic D.B.....178
Popovic I.....111
Popovic M.N.....42
Popovic Maneski L.....112
Porfirev A.....170
Preda L.....140
Prilepsky J.....76
Prudnikau A.....193
- R

Index

Rabasovic M.D.....		Sazonov S.V.....	73
.81,101,103,104,106,113,116,117,122,157,163,166		Schegoleva K.....	203
Rabasovic M.S.....	101, 122	Schneider F.....	26
Radic S.....	4	Scholtes T.....	154, 156
Radivojevic M.....	148	Seleznev L.V.....	69, 71, 215
Radjenovic B.....	131, 133	Semyachkina-Glushkovskaya O.....	105
Radmilovic-Radjenovic M.....	131, 133	Sendova-Vassileva M.....	213
Radoi V.....	123	Setzpfandt F.....	22
Radoicic M.....	111	Sevostyanov O.G.....	77
Radojicic I. S.....	48, 62, 151	Shi Y.....	156
Radojkovic B.....	181	Shin B.S.....	175
Radonjic M.....	57	Shmavonyan S.....	161
Radotic K.....	218	Shtinkov N.....	209
Radovanovic J.....	130, 132, 188	Shutov A.V.....	71
Rafailov E.U.....	108	Sibilia C.....	196
Rahi A.....	124	Sierant A.....	205
Rahmani K.....	50	Siketec Z.....	177
Rajcic B.....	171	Simic S.....	152, 162
Rakich P.....	31	Simonovic N.S.....	178
Ralev Y.....	144	Singh A.V.....	189
Ralev Y.....	144	Singh M.B.....	114, 118
Ralevic U.....	185	Sinitsyn.....	215
Ralevic U.....	46, 193	Sinitsyn D.....	69
Ramdane A.....	10	Skarka V.....	67
Ramos R.V.....	145	Skoulas E.....	177
Rašljic M.....	191, 194	Skupin S.....	5
Redjimi A.....	214	Slavchev V.....	68, 72
Resan B.....	168	Slavik R.....	32
Rezai M.....	24	Slavkovic N.....	169
Richardson D.J.....	32	Sokolovski S.G.....	108
Ristic S.....	181	Spasenovic M.....	80, 94, 128, 138
Ristic-Djurovic J.L.....	86, 120	Spasojevic D.....	218
Ristoscu C.....	174	Sperrhake J.....	186
RizzoPiton M.....	196	Stamenkovic S.....	110
Rohrbacher.....	168	Stancic A.....	104
Romcevic M.....	86, 120	Stanciu G.....	105
Romcevic N.Z.....	67, 86, 120	Stanisavljev D.....	184, 191
Rüegg J.....	123	Stankovic M.....	218
		Stankovic V.....	152
S		Stasic J.....	176
Salakhov M.Kh.....	202	Stavric S.....	211
Salasnich L.....	27	Stef M.....	89
Salatic B.....	173, 182	Stefanov I.....	208
Sancho-Parramon J.....	193, 195	Stein E.....	54
Sanz A.....	220	Steinert M.....	66, 189
Sasanpour P.....	124, 125	Stenishchev I.....	198, 200
Savic T.....	177	Stepic M.....	61, 111
Savic-Ševic S.....	90, 101, 193	Stevanovic K.....	106
Savovic J.....	159	Stevanovic Lj.....	58
		Stoiljkovic M.....	159
		Stojadinovic B.....	102

Index

Stojanovic D.B.	188, 190
Stojanovic A.	145
Stojanovic D.	86, 96
Stojanovic-Krasic M.	61
Stojanovic N.	121, 163, 166
Stoyanov D.	107
Stoyanov L.	208
Stoykova E.	141, 153
Stratakis E.	177
Strinic A.	60
Stupar D.Z.	38, 40
Su Y.C.	139
Sultanova N.	85
Sunchugasheva E.S.	71
Suomalainen S.	196

Š

Šantic N.	39
Šaponjić Z.	111
Šetrajcic J.P.	91
Šetrajcic–Tomic A.J.	91
Ševic D.	101, 122
Šikoparija B.	218
Škarabot M.	26
Šljivancanin Ž.	211
Šolajic A.	88
Štrancar J.	26

T

Tadic J.	114
Tadic M.Ž.	98
Tanaskovic D.	199
Tandukar S.	147
Tarasov N.	45
Teichert C.	18
Tekieh T.	124
Terziev I.	105
Timotijevic D.V.	70
Todorov P.	144
Todorovic D.	128, 138
Todorovic N.	106
Tomaševic-Ilic T.	80, 94
Tomic Lj.	82
Toncheva E.	107
Toninelli C.	216
Topalovic D.B.	98
Topic V.	147
Topuzoski S.	207
Totovic A.	146, 149

Trajic J.	86
Trajkovic M.	143
Tranca D.	105
Trbovich A.M.	120
Trtica M.	176
Tserevelakis G.J.	115
Tsilimbaris M.K.	115
Tsvetkov S.	158
Turitsyn S.K.	45, 76

U

Umek P.	26
Urbancic I.	26
Curčić S.	113
Ustinovskii N.N.	71

V

Valavanis A.	217
Valcheva E.	209
Vankov O.	107
VanVeldhoven R.	135
Vasic Anicijevic D.	46
Vasic B.	192
Vasic I.	52, 55
Vasic V.	46
Vasilev P.	100
Vasiljevic D.	87, 214, 220
Vasiljevic J.M.	70
Vasiljevic-Radovic D.	184, 191
Veerman P.	127
Velickovic S.	171
Veljic V.	51
Veljkovic F.	171
Vladkovic A.	163, 166, 167
Vlašic A.	101, 142, 157
Vodnik V.	46
Vojnovic M.	91
Vrbica M.	113
Vrzic-Petronijevic S.	114
Vucenovic S.M.	91
Vudragovic D.	49
Vujicic N.	219
Vujicic V.	10
Vujin J.	94
Vukmirovic N.	43, 164
Vukojevic V.	123
Vukovic N.	130
Vukovic S.	187, 199

Index

W

Wabnitz S.....	21, 63
Walther P.....	57
Weis A.....	2, 154, 156
Wheeler N.V.....	32
White J.A.....	118
Widengren J.....	8
Williams K.....	135, 143
Wrachtrup J.....	24

Z

Zacharakis G.....	115
Zalevsky Z.....	6
Zamfirescu M.....	28, 140
Zannotti A.....	70
Zapolnova E.....	166, 167
Zarkov B.....	67, 152, 162
Zemtsov D.....	69
Zhang Y.Q.....	12
Zhelyazkova A.....	180
Zivic M.....	106
Zlatkovic B.....	48, 62
Zografopoulos D.C.....	136
Zohar M.....	197
Zorkani I.....	50
Zukauskas A.....	35
Zvorykin V.D.....	71

Ž

Žikic D.....	102
Zivanov M.....	38, 42
Živanov M.B.....	40